

# **Development of Rationally Designed Polymer for Extraction and Purification of physiologically active components from Vegetable Oils**

Thesis submitted for the degree

of Doctor of Philosophy at University of Leicester

By

**Eman Mohammed Alghamdi**

**Department of Chemistry**

Supervisors

Dr Elena Piletska

Prof Sergey Piletsky

September 2018



UNIVERSITY OF  
**LEICESTER**

# **Development of Rationally Designed Polymer for Extraction and Purification of physiologically active components from Vegetable Oils**

Eman Alghamdi

## **Abstract**

Vegetable oils are among the most common topics of many recent studies. This is because they are important constituents of the human diet and a major source of edible lipids. Moreover, vegetable oils such as soybean, sunflower and palm oils are typical raw materials used for the production of biodiesel.

Chapter 1 presents an introduction to the physiologically-active compounds in some vegetable oils in terms of their importance and their available extraction methods from edible oils.

Chapter 2 displays a development of a rationally designed polymer (RDP) that had an affinity towards a group of minor components. RDP has several advantages over commercial sorbents that make it suitable for analytical and industrial applications. It has a low cost, potential group-specificity towards the compounds that share some common functionalities, and compatibility with mass-manufacturing and high stability.

Chapter 3 shows a study to develop the rationally designed polymer (RDP) for the extraction and purification of a group of minor components including free fatty acids,  $\alpha$ -tocopherol and some phytosterols, from a range of oils including sunflower oil, palm oil, wheat germ oil, olive oil, sesame oil and soybean oil in a single step without any additional pre-treatment with an environmentally-friendly process.

Chapter 4 includes a comparison of the developed RDP and several commercially available resins in relation to the retention and recovery of the compounds of interest. The comparison has shown the superiority of RDP to extract the group of minor components from 20% sunflower oil in heptane with the minimum use of organic solvents.

Chapter 5 also includes a comparison between the RDP and tocopherol-specific MIPs and magnetic molecularly imprinted nanoparticles (MIP NPs), in terms of the advantages of each material for particular separation and purification. MIP and MIP NP have shown an affinity towards  $\alpha$ -tocopherol; however, the RDP extracted not only  $\alpha$ -tocopherol but also other minor compounds in a higher concentration under the mild conditions of SPE.

## **Acknowledgments**

I would like to express my deepest gratitude to my supervisor, Dr Elena Piletska, for her patience, valuable guidance and enthusiastic encouragement throughout my research degree during the past four years. I also would like to thank my second supervisor Prof. Sergey Piletsky for his inspiring guidance, knowledge, expertise and critical comments on the thesis.

I would also like to extend my thanks to all the past and present members of the Biotechnology Group at University of Leicester. Special thanks to Dr Michael Whitcombe, Dr Kal Karim, Dr Antonio Guerreiro, Dr Francesco Canfarotta, Dr Katarzyna Smolinska-Kempisty and Dr Joanna Czulak for their help, support and allowing me the opportunity to work with them to learn more. I would also like to extend my thanks to the technician Michael Lee for his help in the instrumental programs used for measurements in this thesis. A sincerely thank to all friends in the Biotechnology Group and in the chemistry department at University of Leicester for their continuous supporting.

I would like to express my heartfelt gratitude to my father, mother, mother in law, sisters and brother for their emotional support and their constant encouragement and motivation throughout my studies. My immeasurable appreciation and thanks is for my family, my husband, my son and my daughters for encouragement and for being so proud of my efforts. Your love and excitement have helped me believe in myself. Thank you very much, I could not have done it without you.

Finally, thanks to King Abdul-Aziz University who has provided the opportunity and the scholarship which has made this research possible.

## Contents

<b>Abstract</b> .....	<b>ii</b>
<b>Acknowledgments</b> .....	<b>iii</b>
<b>Contents</b> .....	<b>iv</b>
<b>List of Figures</b> .....	<b>xi</b>
<b>List of Tables</b> .....	<b>xv</b>
<b>List of Equations</b> .....	<b>xv</b>
<b>Publications</b> .....	<b>xviii</b>
<b>Abbreviations</b> .....	<b>xix</b>
<b>Chapter One</b> .....	<b>1</b>
Literature review .....	<b>2</b>
<b>1.1 Vegetable oils</b> .....	<b>2</b>
<b>1.2 Phytochemical composition of the vegetable oils</b> .....	<b>3</b>
<i>1.2.1 Fatty acids</i> .....	<b>4</b>
<i>1.2.2 Vitamin E</i> .....	<b>6</b>
<i>1.2.3 Phytosterol</i> .....	<b>12</b>
<b>1.3 Solid phase extraction (SPE)</b> .....	<b>15</b>
<b>1.4 Commercial sorbents used for SPE of minor components from vegetable oils</b> .....	<b>17</b>
<b>1.5 Molecularly imprinted polymer MIP</b> .....	<b>19</b>
<i>1.5.1 Synthesis of Molecularly Imprinted Polymer</i> .....	<b>20</b>
<i>1.5.2 Types of molecular imprinting</i> .....	<b>22</b>
<i>1.5.2.1 Covalent imprinting</i> .....	<b>22</b>
<i>1.5.2.2 Non-covalent imprinting</i> .....	<b>22</b>
<i>1.5.2.3 Semi-covalent imprinting</i> .....	<b>22</b>

<b>1.6 Applications of Molecularly Imprinting Polymers .....</b>	<b>23</b>
1.6.1 <i>Molecularly Imprinted-Solid Phase Extraction (MISPE)</i> .....	23
1.6.2 <i>Sensors</i> .....	25
1.6.3 <i>Catalysis</i> .....	25
1.6.4 <i>Drug delivery</i> .....	26
<b>1.7 Computational design of MIPs.....</b>	<b>27</b>
<b>1.8 Comparison of Molecularly Imprinted Polymer (MIP) and Non-Imprinted Polymer (NIP) .....</b>	<b>28</b>
<b>1.9 Rationally-designed polymers RDPs.....</b>	<b>29</b>
<b>1.10 Aims and objectives .....</b>	<b>31</b>
<b>References.....</b>	<b>32</b>
<b>Chapter Two .....</b>	<b>44</b>
Development of RDP resin and SPE protocol for extraction of $\alpha$ -tocopherol and other physiologically-active components from sunflower oil .....	45
<b>2.1 Introduction .....</b>	<b>45</b>
2.1.1 <i>Multi-target adsorbents</i> .....	45
2.1.2 <i>Sample clean-up using MIPs</i> .....	48
2.1.3 <i>RDP versus MIP</i> .....	488
<b>2.2 Materials and methods .....</b>	<b>49</b>
2.2.1 <i>Chemicals and reagents</i> .....	49
2.2.2 <i>Equipment and analysis techniques</i> .....	49
2.2.3 <i>Molecular modelling of the <math>\alpha</math>-tocopherol-specific polymers</i> .....	50
2.2.4 <i>Synthesis of RDP</i> .....	51
2.2.5 <i>Evaluation of the <math>\alpha</math>-tocopherol binding ability</i> .....	51
2.2.6 <i>Choosing the cross-linker</i> .....	53
2.2.7 <i>Polymer synthesis and optimisation of the monomer cross-linker ratio</i> .....	54
2.2.8 <i>Quantification of <math>\alpha</math>-tocopherol</i> .....	55
2.2.9 <i>Characterisation of RDP</i> .....	56

2.2.9.1 Measuring the surface area of RDPs .....	56
2.2.9.2 Calculation of the breakthrough volume .....	56
2.2.9.3 Calculation of the binding capacity .....	56
2.2.9.4 Calculation of the $\alpha$ -tocopherol recovery .....	57
2.2.9.5 The reusability of the polymer .....	57
2.2.10 Optimisation of SPE protocol for $\alpha$ -tocopherol solution .....	57
2.2.11 Application of optimised conditions for the extraction of $\alpha$ -tocopherol from sunflower oil.....	58
2.2.11.1 Development of the ratio between the oil and loading solvent .....	58
<b>2.3 Results and discussion .....</b>	<b>59</b>
<b>2.3.1 Molecular modelling .....</b>	<b>59</b>
2.3.2 Composition of the RDP .....	62
2.3.2.1 The functional monomer .....	63
2.3.2.2 The cross-linker .....	65
2.3.2.3 Choosing the optimal monomer: cross-linker ratio .....	67
2.3.2.4 Characterisation of the developed polymers .....	68
2.3.2.5 Measurement of the breakthrough volume and binding capacity.....	68
2.3.2.6 Evaluation of reusability and measurement of the surface area .....	70
2.3.3 Calibration curve of $\alpha$ -tocopherol.....	70
2.3.4 Optimisation of the SPE protocol using the model solution of $\alpha$ -tocopherol.....	72
2.3.5 Application of the SPE conditions for the extraction of $\alpha$ -tocopherol and other minor compounds from sunflower oil.....	77
<b>2.4 Conclusions .....</b>	<b>79</b>
<b>References .....</b>	<b>80</b>
<b>Chapter Three .....</b>	<b>86</b>
Applications of the optimised SPE protocols to extract selected physiologically-active compounds from the vegetable oils .....	87
<b>3.1 Introduction .....</b>	<b>87</b>
<b>3.2 Materials and methods .....</b>	<b>90</b>
3.2.1 Chemicals and reagents .....	90

3.2.2 Equipment and analysis techniques .....	90
3.2.3 Investigation the affinity of RDP towards minor components .....	91
3.2.4 Applications of the optimised SPE protocol to the vegetable oils .....	91
3.2.4.1 Preparation of oil sample .....	91
3.2.4.2 The SPE protocol conditions .....	92
3.2.4.3 Calibration curves .....	92
3.2.5 Saponification the fatty acids.....	93
3.2.6 Method validation .....	93
<b>3.3 Results and discussion .....</b>	<b>94</b>
3.3.1 Molecular modelling: .....	94
3.3.1.1 Study the molecular modelling of fatty acids .....	96
3.3.1.2 Study the molecular modelling of phytosterols .....	101
3.3.2 Quantification of the minor components in the vegetable oils.....	104
3.3.2.1 Calibration curves .....	104
3.3.3 Investigation the minor components .....	105
3.3.3.1 Extraction and analysis of palmitic acid (16:0) .....	107
3.3.3.2 Extraction and analysis of oleic (18:1) and linoleic (18:2) acids .....	112
3.3.3.3 Extraction and analysis of $\alpha$ -tocopherol .....	118
3.3.3.4 Extraction and study of phytosterols .....	121
Campesterol .....	121
Stigmasterol .....	123
$\beta$ -sitosterol .....	125
3.3.3.5 Further minor components extraction .....	127
Sesamin.....	127
3.3.4 Method validation .....	129
<b>3.5 Conclusions .....</b>	<b>131</b>
<b>References .....</b>	<b>132</b>
<b>Chapter Four .....</b>	<b>139</b>
Comparison between the developed RDP and commercial SPE adsorbents for the extraction of minor compounds from sunflower oil .....	140
<b>4.1 Introduction .....</b>	<b>140</b>

4.1.1 SPE definition.....	140
4.1.2 Main steps of SPE.....	143
4.1.2.1 Condition.....	143
4.1.2.2 Loading (retention).....	144
Mechanisms of retention on SPE stationary phases.....	144
4.1.2.3 Washing .....	146
4.1.2.4 Elution .....	147
<b>4.2 Materials and methods.....</b>	<b>148</b>
4.2.1 Chemicals and reagents .....	148
4.2.2 Equipment and analysis techniques .....	149
<b>4.3 Results and discussion .....</b>	<b>150</b>
4.3.1 After loading.....	150
4.3.2 After washing .....	154
4.3.3 After elution .....	157
<b>4.4 Conclusion:.....</b>	<b>160</b>
<b>References .....</b>	<b>161</b>
<b>Chapter Five.....</b>	<b>165</b>
Comparison of the selectivity and capacity of the three different formats of molecularly imprinted polymers.....	166
<b>5.1 Introduction .....</b>	<b>166</b>
<b>5.2 Materials and methods .....</b>	<b>168</b>
5.2.1 Chemicals and reagents.....	168
5.2.2 Equipment and analysis techniques.....	168
5.2.3 Synthesis of the microparticles of bulk polymers RDPs and MIP.....	169
5.2.4 Preparation of the bulk MIP.....	169
5.2.5 Characterisation of the MIP particles .....	170
Surface area .....	170
5.2.6 Recognition of MIP towards $\alpha$ -tocopherol .....	170

5.2.7 Comparison between the microparticles MIP and RDP.....	170
5.2.8 Application of the optimised SPE protocol to sunflower oil solution to MIP.....	171
5.2.9 Exploration the Selectivity and capacity of MIP NPs.....	171
Synthesis of MIP NPs.....	171
5.2.9.1 Functionalisation of the glass beads (GB) .....	171
5.2.9.2 Silanisation of the glass beads.....	172
5.2.9.3 Immobilisation of $\alpha$ -tocopherol on the surface of the glass beads.....	173
5.2.9.4 Salinisation the iron oxide nanoparticles .....	174
5.2.9.5 Solid-phase synthesis of MIP NPs in organic solvent .....	174
5.2.9.6 The elution of MIP NPs .....	175
5.2.10 Physical characterisation of magnetic nanoparticles.....	175
5.2.10.1 Dynamic Light Scattering (DLS) size analysis .....	175
5.2.10.2 Investigating the sorption property of MIP NPs.....	176
<b>5.3 Results and discussion .....</b>	<b>177</b>
5.3.1 Synthesis of microparticles MIP.....	178
5.3.1.1 Characterisation of the MIP.....	178
5.3.1.2 Rebinding of $\alpha$ -tocopherol towards the MIP .....	178
5.3.2 MIP vs. RDP.....	179
5.3.2.1 Physical characteristic of polymers .....	179
5.3.2.2 Loading capacity .....	180
5.3.2.3 Recovery of $\alpha$ -tocopherol.....	182
5.3.2.4 SPE from 20% sunflower using bulk MIP and RDP .....	183
5.3.3 Synthesis of MIP NPs.....	185
5.3.4 The affinity properties of MIP NPs.....	195
<b>5.4 Conclusion.....</b>	<b>198</b>
<b>References.....</b>	<b>200</b>
<b>Chapter Six .....</b>	<b>204</b>
Conclusions and future work .....	205
<b>6.1 Conclusions .....</b>	<b>205</b>
<b>6.2 Future work.....</b>	<b>207</b>

<b>Appendix 1 .....</b>	<b>208</b>
<b>Appendix 2 .....</b>	<b>212</b>
<b>Appendix 3 .....</b>	<b>213</b>

## List of Figures

Figure 1.1: The major and minor components of vegetable oils.....	3
Figure 1.2: Structure of the eight forms of tocopherols and tocoterienols.....	7
Figure 1.3: Stereoisomers of $\alpha$ -tocopherol.....	10
Figure 1.4: The most common phytosterols available in vegetable oils.....	13
Figure 1.5: Main steps of SPE.....	16
Figure 1.6: Typical SPE apparatus.....	17
Figure 1.7: Molecular imprinting approach.....	20
Figure 2.1: Chemical structures of some pharmaceuticals extracted using group-specificity MIP.....	47
Figure 2.2: The library of functional monomers used in LEAPFROG screening.....	52
Figure 2.3: Solid phase extraction tools.....	53
Figure 2.4: The chiral centres in the 2D molecular structure (a), 3D molecular structure of $\alpha$ -tocopherol minimised using the SYBYL software (b).....	60
Figure 2.5: Molecular complexes between $\alpha$ -tocopherol and the functional monomers: EGMP (1), MAA (-) (2), UA (-), (3) AMPSA (4), IA (5) and EGDMA (as a cross-linker) (6), the hydrogen bonds are shown as dotted lines.....	63
Figure 2.6: Regeneration cycles of the RDP loaded with $\alpha$ -tocopherol in heptane standard solution. Standard deviations were represented as error bars (n=5).....	70
Figure 2.7: The calibration curve of $\alpha$ -tocopherol hexane using UV.....	71
Figure 2.8: The relationship between concentration and absorbance of $\alpha$ -tocopherol solution in hexane.....	71
Figure 2.9: The calibration curve of $\alpha$ -tocopherol using GC/MS.....	72
Figure 2.10: The optimised conditions for SPE of $\alpha$ -tocopherol using RDP.....	74
Figure 2.11: The statistical demonstration of candidate solvents for the optimisation of SPE conditions. (1) Condition and loading, (2) washing, (3) elution.....	75
Figure 2.12: The GC/MS chromatogram of a standard solution of $\alpha$ -tocopherol.....	76

Figure 2.13: The similarity between the mass-spectrum of extracted $\alpha$ -tocopherol (upper) and the spectrum of $\alpha$ -tocopherol from the spectral library (lower). .....	76
Figure 2.14: The GC/MS chromatogram for the eluted samples. ....	78
Figure 3.1: The equation of esterification (biofuel production). ....	88
Figure 3.2: The formation of soap during the esterification (undesirable interference by free fatty acids in the reactants). ....	88
Figure 3.3: The relative binding energy of common functional monomers towards minor components. ....	96
Figure 3.4: The 3D structures of palmitic acid (1), the hydrogen bonds between palmitic acid and the functional monomers: MAA (-) (2), EGDMA(cross-linker) (3), AMPSA (4), EGMP (-) (5), UA (-) (6) and IA (-) (7). ....	98
Figure 3.5: The 3D structures of oleic acid (1), the hydrogen bonds between palmitic acid and the functional monomers: MAA (-) (2), EGDMA(cross-linker) (3), EGMP (-) (4), AMPSA (5), IA (-) (6) and UA (-) (7). ....	99
Figure 3.6: The 3D structures of linoleic acid (1), the hydrogen bonds between palmitic acid and the functional monomers: MAA (-) (2), EGDMA(cross-linker) (3), EGMP (-) (4), AMPSA (5), IA (-) (6) and UA (-) (7). ....	100
Figure 3.7: The 3D structures of campesterol (1) and the hydrogen bonds between campesterol and the functional monomers: MAA (2), EGDMA(cross-linker) (3), EGMP (-) (4), AMPSA (5), IA (-) (6) and UA (-) (7). ....	102
Figure 3.8: The 3D structures of stigmasterol (1) and the hydrogen bonds between stigmasterol and the functional monomers: MAA (2), EGDMA (cross-linker) (3), EGMP (-) (4), AMPSA (5), IA (-) (6) and UA (-) (7). ....	103
Figure 3.9: The 3D structures of $\beta$ -sitosterol (1) and the hydrogen bonds between $\beta$ -sitosterol and the functional monomers: MAA (2), EGDMA(cross-linker) (3), EGMP (-) (4), AMPSA (5), IA (-) (6) and UA (-) (7). ....	104
Figure 3.10: GC chromatograms of the eluted samples from the six different vegetable oils spiked with the seven standards (this experiment was repeated three times). ....	106
Figure 3.11: GC chromatogram for (a) palmitic acid and (b) methyl palmate solutions in hexane. ....	108

Figure 3.12: Mass spectrum of (a) palmitic acid and (b) methyl palmate. ....	109
Figure 3.13: IR spectrum for (a) palmitic acid and (b) methyl palmate .....	110
Figure 3.14: The relative quantities of palmitic acid in different vegetable oils. ....	111
Figure 3.15: GC chromatogram for (a) oleic acid and (b) methyl oleate solutions in hexane. ....	113
Figure 3.16: GC chromatogram for (a) linoleic acid and (b) methyl linoleate solutions in hexane. ....	113
Figure 3.17: Mass spectrum of oleic acid (a) and methyl oleate (b). ....	114
Figure 3.18: IR spectrum for (a) oleic acid and (b) methyl oleate. ....	115
Figure 3.19: Mass spectrum of (a) linoleic acid and (b) methyl linoleate. ....	116
Figure 3.20: IR spectrum of linoleic acid (a) and methyl linoleate (b). ....	117
Figure 3.21: The relative quantities of oleic and linoleic acids together in different vegetable oils. ....	118
Figure 3.22: Mass spectrum of extracted $\alpha$ -tocopherol (upward) and NIST mass spectrum (down). ....	119
Figure 3.23: The relative quantities of $\alpha$ -tocopherol in different vegetable oils. ....	120
Figure 3.24: The mass spectrum of campesterol. ....	122
Figure 3.25: The relative quantities of campesterol in different vegetable oils. ....	123
Figure 3.26: Mass spectrum of stigmasterol. ....	124
Figure 3.27: The relevant concentrations of stigmasterol in different vegetable oil. ....	125
Figure 3.28: The mass spectrum of $\beta$ -sitosterol. ....	126
Figure 3.29 : The relative concentrations of $\beta$ -sitosterol in different vegetable oils. ....	127
Figure 3.30: The mass spectrum of sesamin. ....	128
Figure 4.1: Illustration of the possible intermolecular interactions between the analyte and surface of the stationary phase in SPE. ....	145
Figure 4.2: Binding energy of different types of intermolecular interactions. ....	146

Figure 4.3: The relationships between the main elements of SPE. ....	148
Figure 4.4: Statistical demonstration of the concentration of the compounds which were not absorbed during loading. ....	153
Figure 4.5: Statistical demonstration of the concentration of the compounds which were lost during washing. ....	156
Figure 4.6: Statistical demonstration of the concentration of the eluted compounds. ....	159
Figure 5.1: The chemical structure of $\alpha$ -tocopherol (a), the mechanism for breaking the epoxy ring under basic conditions (b). ....	172
Figure 5.2: Chemical structure of GOPTS used in the immobilisation. ....	173
Figure 5.3: The steps of solid phase synthesis (deoxygenate the polymerisation mixture by purging with a stream of $N_2$ (a), addition of the polymerisation mixture to the solid phase (b), UV polymerisation (c), cooled washing (d), hot washing (e) and colour of glass beads after last hot wash (f). ....	174
Figure 5.4: GC/MS chromatograms with the integration of the peaks. ....	182
5.5: Statistical analysis of the concentrations of non-adsorption of the minor components to MIP and RDP particles after the incubation with 20% sunflower oil in heptane. ....	185
Figure 5.6: Salinisation with epoxy derivative for the activated glass beads. ....	187
Figure 5.7: The immobilisation of $\alpha$ -tocopherol on the modified glass beads. ....	188
Figure 5.8: The polymerisation of magnet MIP NPs specific to $\alpha$ -tocopherol. ....	189
Figure 5.9: The process of collection of MIP NPs. ....	191
Figure 5.10: The image of the eluted MIP NPs obtained in one synthesis cycle. ....	192
Figure 5.11: The method of separating magnetic MIP NPs from solution using the magnet. ....	192
Figure 5.12: The DLS graphs for three different concentrations of MIP NPs solutions. ....	194
Figure 5.13: The steps of the optimised protocol of separation of $\alpha$ -tocopherol by incubation with MIP NPs. ....	196
Figure 5.14: The calibration curve $\alpha$ -tocopherol using UHPLC/DAD/MS. ....	197

## List of Tables

Table 1.1: Some fatty acids present in natural oils.....	5
Table 1.2: Relative Fatty Acid (%) in different vegetable oils. ....	6
Table 1.3: Tocopherol content in some vegetable oils (mg kg <sup>-1</sup> ). ....	7
Table 1.4: Relative biological activities of $\alpha$ -tocopherol derivatives and synthetic derivatives of $\alpha$ -tocopherol acetate (determined by the foetal resorption-gestation test of rat) .....	9
Table 1.5: The content of common phytosterols of some vegetable oils (mg kg <sup>-1</sup> ).....	14
Table 1.6: Examples of commonly-used initiators, functional monomers and cross-linkers in MIP synthesis. ....	21
Table 2.1: The different polymers composition using different functional monomers. ....	53
Table 2.2: The polymer composition (g) of two MAA-based polymers with different cross-linkers. ....	54
Table 2.3: The polymer composition with different monomer: cross-linker ratio. ....	55
Table 2.4: The candidate solvents used for optimisation SPE conditions. ....	58
Table 2.5: The list of functional monomers suggested by SYBYL software based on the template structure ( $\alpha$ -tocopherol). ....	61
Table 2.6: The percentage of recovery of the different polymers synthesised with different functional monomers and EGDMA (cross-linker). ....	65
Table 2.7: Percentage of recovery for two MAA-based polymers with two different cross-linkers. ....	66
Table 2.8: Different features of the different polymers with different monomer: cross-linker ratios. ....	67
Table 2.9: The breakthrough volume of MD polymer. ....	69
Table 2.10: Breakthrough volume of ME polymer. ....	69
Table 2.11: Quantities of minor components extracted from sunflower oil in heptane. ....	77
Table 3.1: Summarised the calibration curve equations and R-squared values were produced from calibration curves (Appendix 2) for all the minor compounds. ....	105
Table 3.2: The concentrations of palmitic acid in different vegetable oils. ....	107

Table 3.3: The concentrations of oleic and linoleic acid in different vegetable oils. ....	112
Table 3.4: The concentrations of $\alpha$ -tocopherol in different vegetable oils.....	119
Table 3.5: The concentrations of campesterol in different vegetable oils.....	122
Table 3.6: The concentrations of stigmasterol in different vegetable oils. ....	124
Table 3.7: The concentrations of $\beta$ -sitosterol in different vegetable oils. ....	126
Table 3.8: The matrix effects of spiking 1 mL heptane with standards solutions at known concentrations. (percentage of recovery is average of triplicates $\pm$ SD). ....	130
Table 4.1: Characteristics of the main chromatographic separation approaches. ....	142
Table 4.2: Concentration of the minor components in the samples lost during loading (mg g <sup>-1</sup> ). ....	151
Table 4.3: Concentration of the minor components in the samples after washing (mg g <sup>-1</sup> ). ....	155
Table 4.4: Concentration of the minor components in the samples after elution (mg g <sup>-1</sup> ). ....	158
Table 5.1: The percentage of adsorbed $\alpha$ -tocopherol on MIP particles.....	179
Table 5.2: The physical characteristics (surface area and pore size) of MIP and RDP particles.....	180
Table 5.3: The loading capacity of MIP and RDP calculated from the recovery percentage of $\alpha$ -tocopherol. ....	181
Table 5.4: The percentage of recovery $\pm$ standard deviation from RDP and MIP.....	183
Table 5.5: Concentration (mg mL <sup>-1</sup> ) of the non-adsorption minor components to MIP and RDP after incubating overnight with 20% sunflower oil in heptane. ....	184
Table 5.6: The physical characterisations of MIP NPs. ....	193
Table 5.7: The concentration and percentage of $\alpha$ -tocopherol bound by the MIP NPs from different concentration of standard solution.....	197
Table 5.8: The concentration and percentage of eluted $\alpha$ -tocopherol from the MIP NPs from different concentration of standard solution.....	198

## List of Equations

<b>Equation 1.1:</b> Gibbs free energy equation.....	28
<b>Equation 2.1:</b> The polymer capacity .....	57
<b>Equation 2.2:</b> Beer-Lambert law.....	71
<b>Equation 5.1:</b> Stokes-Einstein equation. ....	176

## **Publications**

### **Conference**

1- Alghamdi Eman, Piletska Elena. Development of rationally-designed polymers for  $\alpha$ -tocopherol extraction and purification using solid phase extraction. The 9th Saudi Students Conference, 13th-14th February, 2016, Birmingham, UK.

2- Alghamdi Eman, Piletska Elena. Development of rationally-designed polymers for  $\alpha$ -tocopherol extraction and purification using solid phase extraction. The 5th Global Chemistry Congress, 04-06 September, 2017, London, UK.

### **Papers**

1- Alghamdi E.; Whitcombe M.; Piletsky S.; Piletska E. Solid phase extraction of  $\alpha$ -tocopherol and other physiologically active components from sunflower oil using rationally designed polymers. *Anal. Methods* 2018, *10*, 1–8.

2) Alghamdi E.; Piletsky S.; Piletska E. Application of the bespoke solid-phase extraction protocol for extraction of physiologically-active compounds from vegetable oils. *Talanta* 2018, *189*, 157–165.

## Abbreviations

ACN	Acetonitrile
AIBN	Azobisisobutyronitrile
AMPSA	Acrylamido-2-methyl-1-propanesulfonic acid
AOAC	Association of Official Analytical Chemists
$\alpha$ -TTP	$\alpha$ -tocopherol transfer protein
DIPEA	Di-isopropylethylamine
DLS	Dynamic light scattering
DMF	Dimethylformamide
DVB	Divinylbenzene
dh	Hydrodynamic diameter
DRD	Diode array detector
EIPA	Ethyl-di-isopropylamine
EGDMA	Ethylene glycol methacrylate
EtOH	Ethanol
FFAs	Free fatty acids
FID	Flame ionization detection
IR	Infrared spectroscopy
IUPAC	International Union of Pure and Applied Chemistry
IA	Itaconic acid
GB	Glass beads
GC	Gas chromatography
GOPTS	Glycidyloxypropyl trimetoxysilane
H <sub>2</sub> SO <sub>4</sub>	Sulfuric acid
HPLC	High performance liquid chromatography
LDL	Low-density lipoprotein
MAA	Methacrylic acid
MIT	Molecularly imprinted technology
MIP	Molecularly imprinted polymers
MS	Mass spectrometry
NIP	Non-imprinted polymers
NaCl	Sodium chloride
NaOH	Sodium hydroxide
NPs	Nanoparticles
NP	Normal phase
PDI	Polydispersity index
PBS	Phosphate buffered saline
RDP	Rationally designed polymer

RP	Reverse phase
SD	Standard deviation
SPE	Solid phase extraction
TLC	Thin layer chromatography
TRIM	Tri-methylolpropane tri-methacrylate
UA	Urocanic acid
UV	Ultra-violet spectrophotometry
UHPLC	Ultra-high performance liquid chromatography
v/v	Volume by volume
wt.	Weight

# Chapter one

# Literature review

## 1.1 Vegetable oils

Vegetable oil is an essential component of the human diet and a major source of edible lipids, which supplies more than 75% of the total world consumption of the lipids.<sup>1</sup> Vegetable oils provide an important medium used in cooking, a source for energy, to protect body tissues, to maintain the normal body temperature, to carry the essential lipid-soluble vitamins in the human body and many other vital functions. Moreover, vegetable oils are the main source of many necessary nutrients such as the essential fatty acids, vitamins and some phenolic compounds.<sup>2,3</sup>

Oils, in general, are an important renewable material for biofuel production.<sup>4</sup> The growth in population and development of industry around the world has caused an increase in the demand for energy. This, in turn, has led to more attention being given to renewable energy sources. Although 80% of world energy consumption is still derived from fossil fuels, significant research has been conducted and great improvements have been made in the use of biofuels derived from biomass.<sup>5,6</sup> Biomass is defined as any matter of biologic origin that can be converted into biofuel.<sup>7</sup> When biofuel is produced from biomass that is based on vegetable oil, corn or sugar, it is called 'first-generation fuel'. If the biomass is part of other parts of the plants, including the leaves, bark, fruit and seeds, it is named 'second-generation fuel'.<sup>8</sup>

Vegetable oils are considered as an important resource for the first generation of biofuel. These oils contain useful secondary metabolites such as tocopherols, tocoterienols, sterols and other phenolic compounds which could be extracted prior or through the biofuel production procedures. These valuable compounds, which have various industrial and pharmaceutical applications can be extracted from the oil during pre-treatment or other biofuel-producing processes and by doing that, it simplifies the biomass to the its basic components of fermentation or esterification used to produce ethanol or biodiesel.<sup>5,8</sup> Therefore, some of the valuable components will be recovered and will add extra value to the biofuel production, which will reduce the cost of the biofuel. The goal of this study was to prepare efficient and cheap polymers that possess a high affinity towards some physiologically-active compounds in the vegetable oils. These were

used as an adsorbent for optimised solid phase extraction (SPE) in order to extract valuable components from vegetable oil.

## 1.2 Phytochemical composition of the vegetable oils

Vegetable oils are commonly produced from fruits or plant seeds such as sunflower, olive, sesame, corn, etc. Oils are obtained in different ways such as pressing or solvent extraction.<sup>3,9</sup> The method of oil extraction is an important factor determining the nature and the quantity of produced oil.

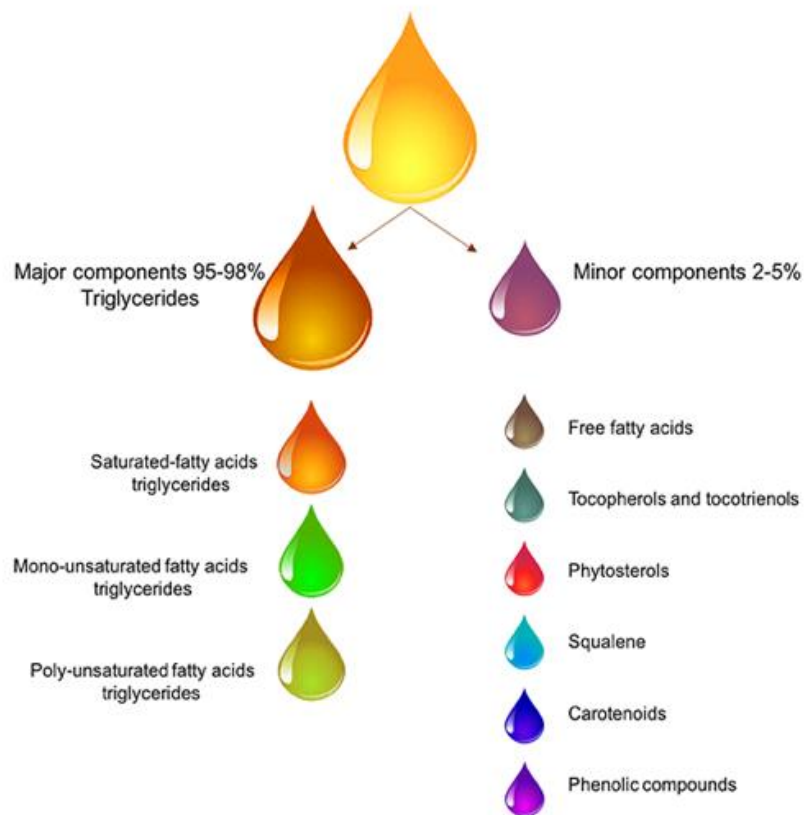


Figure 1.1: The major and minor components of vegetable oils.

Vegetable oils are considered as a non-polar and lipophilic matrixes that consist of variable and complex components, depending on their origin, quality and extraction methods.<sup>10</sup> Triacylglycerols are the main components of the oils, making up to 95-98%. Triglycerides consist of three fatty acid molecules ester-linked with the OH groups of one glycerol molecule. The fatty acids that bound to the glycerol are determining the characteristics of the oil. Triglycerides are generally classified according to the saturation degree of fatty acids into saturated, mono- and poly-unsaturated fatty acids, which may result in different physical and chemical properties.<sup>1,3</sup> The remaining oil (2-5%) (non-glyceridic fraction) comprises different compound groups such as hydrocarbons, tocopherols and phytosterols, as demonstrated in Figure 1.1. The analyses of these components indicated different information about the origin and the quality of vegetable oils.<sup>3,11-13</sup>

### **1.2.1 Fatty acids**

Free fatty acids are one of the minor components of the vegetable oils. Free fatty acids are generally formed during the hydrolysis of triglycerides. They are undesirable in the vegetable oils and should be eliminated during refining processes since they impact negatively on edible oils. In addition, unfavourable features of edible oils such as the low smoke point of oil and increasing the foam-making properties of the oil are caused by the higher free fatty acids in the vegetable oil.<sup>14,13</sup>

In terms of producing biofuel from vegetable oils, removal of free fatty acids is essential to make the biodiesel production more effective, which preventing the reverse reaction with the alkali catalyst during transesterification reaction. This usually requires a great amount of alcohol to maintain the equilibrium of the reaction and produce more methyl esters.<sup>15,16</sup> The negative impact of free fatty acids was observed through the production of soap and water, thus hindering the separation and purification procedures of the biodiesel production.<sup>16,17</sup>

Table 1.1: Some fatty acids present in natural oils.<sup>18</sup>

Name	Chemical formula	Molecular weight	Chemical structure
Myristic acid	C <sub>14</sub> H <sub>28</sub> O <sub>2</sub>	228	CH <sub>3</sub> (CH <sub>2</sub> ) <sub>12</sub> COOH
Palmitic acid	C <sub>16</sub> H <sub>32</sub> O <sub>2</sub>	256	CH <sub>3</sub> (CH <sub>2</sub> ) <sub>14</sub> COOH
Palmitoleic acid	C <sub>16</sub> H <sub>30</sub> O <sub>2</sub>	254	CH <sub>3</sub> (CH <sub>2</sub> ) <sub>5</sub> CH=CH(CH <sub>2</sub> ) <sub>7</sub> COOH
Stearic acid	C <sub>18</sub> H <sub>36</sub> O <sub>2</sub>	284	CH <sub>3</sub> (CH <sub>2</sub> ) <sub>16</sub> COOH
Oleic acid	C <sub>18</sub> H <sub>34</sub> O <sub>2</sub>	282	CH <sub>3</sub> (CH <sub>2</sub> ) <sub>7</sub> CH=CH(CH <sub>2</sub> ) <sub>7</sub> COOH
Linoleic acid	C <sub>18</sub> H <sub>32</sub> O <sub>2</sub>	280	CH <sub>3</sub> (CH <sub>2</sub> ) <sub>4</sub> CH=CH-CH <sub>2</sub> -CH=CH(CH <sub>2</sub> ) <sub>7</sub> COOH
Linolenic acid	C <sub>18</sub> H <sub>30</sub> O <sub>2</sub>	278	CH <sub>3</sub> -CH <sub>2</sub> -CH=CH-CH <sub>2</sub> -CH=CH-CH <sub>2</sub> -CH=CH(CH <sub>2</sub> ) <sub>7</sub> COOH
α-Eleostearic acid	C <sub>18</sub> H <sub>30</sub> O <sub>2</sub>	278	CH <sub>3</sub> -(CH <sub>2</sub> ) <sub>3</sub> -CH=CH-CH=CH-CH=CH(CH <sub>2</sub> ) <sub>7</sub> COOH
Ricinoleic acid	C <sub>18</sub> H <sub>33</sub> O <sub>3</sub>	298	CH <sub>3</sub> (CH <sub>2</sub> ) <sub>4</sub> CH-CH-CH <sub>2</sub> -CH=CH(CH <sub>2</sub> ) <sub>7</sub> (OH)COOH

Most fatty acids of natural origin have an alkyl chain comprising between 4 and 22 carbon atoms. Table 1.1 shows examples of some fatty acids. The most common unsaturated fatty acid is palmitic acid, which is an important constituent of such widely-used products as ice cream, toothpaste, candles and cosmetic products.<sup>17</sup> Oleic acid, which is a mono-unsaturated fatty acid, is known for its reducing effect on the blood sugar levels and protection of the heart.<sup>19</sup> It was shown that linoleic acid, which is one of the main di-unsaturated fatty acids, can lower the triglyceride and cholesterol content of the cells, which leads to a reduction of the incidence of cardiovascular diseases.<sup>20</sup>

The method for determination of the fatty acid in the oil samples, which was standardised by IUPAC<sup>21</sup> and AOAC<sup>22</sup>, is based on using a silica gel column to separate the oil sample into two fractions, the first fraction contains triacylglycerols. The second fraction involves the more polar compounds such as polymers of triacylglycerols, oxidised triacylglycerols monomers, diacylglycerols, monoacylglycerols, free fatty acids (FFAs), and other polar minor constituents. The elution is conducted in two steps: the first fraction

is eluted with a mixture of hexane and diethyl ether (87:13), the second more polar fraction requires a relatively polar solvent for elution, i.e. diethyl ether. Different authors suggested using aminopropyl SPE cartridge to separate polar lipids, such as free fatty acids, using low polarity solvents.<sup>12, 23</sup>

Table 1.2: Relative fatty acid (%) in different vegetable oils.<sup>18, 24</sup>

Fatty acids	Sesame oil	Sunflower oil	Palm oil	Soybean oil	Corn oil	Peanut oil	Rapeseed oil
Myristic acid	nd	nd	1.1	nd	nd	nd	nd
Palmitic acid	9.5	6.4	46.3	11.0	13.2	11.6	4.4
Stearic acid	5.7	nd	nd	nd	nd	nd	0.2
Oleic acid	38.5	22.9	38.0	22.2	31.1	39.3	60.9
Linoleic acid	44.8	64.7	9.3	54.7	52.4	38.3	20.7
Linolenic acid	nd	nd	nd	0.7	nd	nd	0.3

\* nd: not detected

The usual method of expressing the content of free fatty acids was in using the percentage of each type of fatty acid towards the total fatty acids as shown in Table 1.2 that have been published in several studies.<sup>18,24</sup> The most common determination and separation of free fatty acids was started by converting the free fatty acids to methyl ester, then using the GC/MS for separation and quantitation.<sup>3,12,23–25</sup>

### 1.2.2 Vitamin E

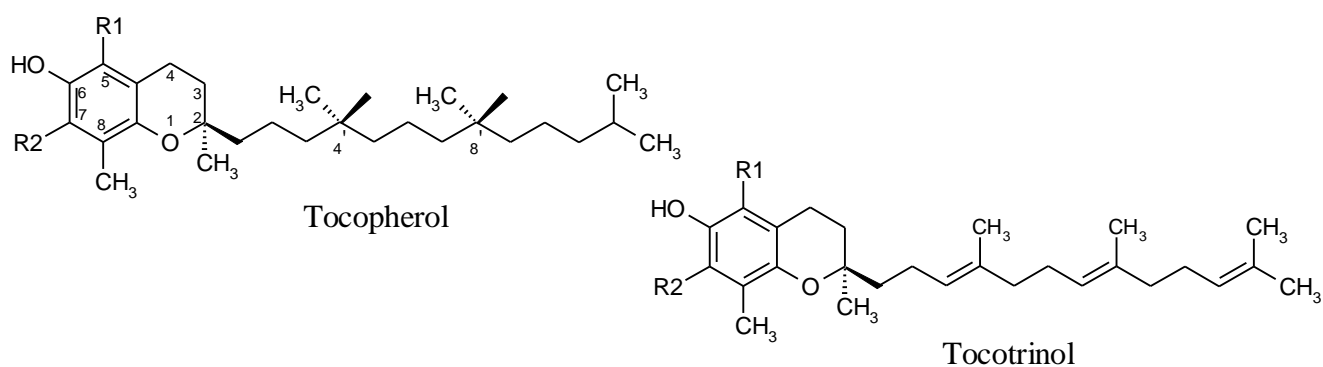
Tocopherols and tocotrienols form the vitamin E group. The vitamin E compounds are lipid-soluble, and they are abundant in most vegetable oils in varying amounts (70–1900 mg/kg).<sup>12</sup> The common tocopherol in most vegetable oils is  $\alpha$ -tocopherol which is associated with antioxidant activity in the human body.<sup>10,11,26</sup> Recent studies have also indicated the importance of another member of the vitamin E family,  $\gamma$ -tocopherol. It is known that the main role of vitamin E in the human body is to reduce the hydroperoxyl radicals. It was also proven that the presence of  $\alpha$ -tocopherol increases the bioavailability

of  $\gamma$ -tocopherol.<sup>27</sup> Individual amounts of tocopherol components in some vegetable oils are given in Table 1.3.

Table 1.3: Tocopherol content in some vegetable oils (mg kg<sup>-1</sup>).<sup>28</sup>

Tocopherol	Sesame oil	Soybean oil	Olive oil	Argan oil	Wheat germ oil	Sunflower oil
$\alpha$ -tocopherol	9.8	190	310	59	1330	678.4
$\gamma$ -tocopherol	403.6	1040	15	531	6	127.6
$\delta$ -tocopherol	32.5	640	2	51	27	26.3
total tocopherol	446.0	1870	330	675	1363	712.2

The vitamin E group include eight compounds,  $\delta$ -,  $\beta$ -,  $\gamma$ -, and  $\alpha$ -tocopherol and the corresponding tocotrienols. All of these compounds share a chromanol ring and a hydrophobic chain, as shown in the Figure 1.2. The chain is phytyl in tocopherols and isoprenyl in tocotrienols.<sup>29,30</sup>



	R <sub>1</sub>	R <sub>2</sub>	Molecular weight
$\alpha$ -tocopherol and tocotrinol	CH <sub>3</sub>	CH <sub>3</sub>	430
$\gamma$ - tocopherol and tocotrinol	H	CH <sub>3</sub>	416
$\beta$ -tocopherol and tocotrinol	CH <sub>3</sub>	H	416
$\delta$ -tocopherol and tocotrinol	H	H	402

Figure 1.2: Structure of the eight forms of tocopherols and tocotrienols.<sup>31, 32</sup>

Vitamin E is a fat-soluble antioxidant that has promising properties in preventing and curing Alzheimer's disease, cancer and cardiovascular diseases.<sup>33,34,35</sup> Vitamin E is not synthesised in the human body,<sup>30</sup> therefore, we are required to obtain it from nutritional sources such as vegetable and seed oils. Vitamin E deficiency can cause muscular diseases, foetal death and neuropathy.<sup>30,36,37</sup> Vitamin E is only present as  $\alpha$ -tocopherol in the human body. The evidence for this comes from the fact that there is only one receptor available in the plasma,  $\alpha$ -tocopherol transfer protein ( $\alpha$ -TTP), which is responsible for its metabolism and biological activity in the human body.<sup>30,38,39</sup>

There is an increasing interest in the extraction of tocopherol from their natural resources such as wheat germ oil,<sup>30</sup> vegetable oils and vegetables.<sup>30,36</sup>  $\alpha$ -tocopherol and  $\delta$ -tocopherol are more readily available in the human diet than the other forms of tocopherol.<sup>36</sup> Though anti-oxidative activity has been displayed by all types of tocopherols, it has been proven that  $\gamma$ - and  $\delta$ -tocopherols possess the highest anti-oxidative potential.<sup>37,26,38</sup> The role of  $\alpha$ -tocopherol in the human body has been investigated.<sup>37,38,39</sup>  $\alpha$ -tocopherol is associated with the inhibition of undesirable oxidative processes by preventing free radical formation from unsaturated fatty acids. This was reported as a direct cause of certain types of cancer.<sup>38,39</sup> In addition,  $\alpha$ -tocopherol was regarded as an important industrial constituent, e.g. it has been used in the additive formulation for food,<sup>37</sup> cosmetics and drugs<sup>36</sup>. In terms of industrial or therapeutic applications, it is preferable to obtain tocopherols from natural sources. This research focuses on sunflower oil, soybean oil, sesame oil, olive oil, wheat germ oil and palm oil.

In 1937, Emerson and his co-workers discovered that the compounds such as  $\alpha$ -,  $\beta$ -,  $\delta$ -,  $\gamma$ -tocopherols prevented vitamin E deficiency in the human body.<sup>30</sup> Over the last 70 years, many attempts have been made to develop economically viable and accurate procedures to determine, extract and purify  $\alpha$ -tocopherol, which was reported to have the highest significant biological effect compared with the other forms of tocopherol and the synthetic  $\alpha$ -tocopherol. One possible reason for this superior physiological effect is the specific stereochemistry of  $\alpha$ -tocopherol.<sup>36</sup> It is known that all tocopherol isomers that are present naturally in the human diet have three chiral centres in the phytyl chain; all three are in the RRR diastereoisomers, while the synthetic  $\alpha$ -tocopherol occurs as a racemic mixture of all the eight configurations. It is very difficult, almost impossible to make the

physiologically active molecule with such complex stereo configuration using organic synthesis, therefore, the extraction from natural sources is the only option.

Table 1.4: Relative biological activities of  $\alpha$ -tocopherol derivatives and synthetic derivatives of  $\alpha$ -tocopherol acetate (determined by the foetal resorption-gestation test of rat).<sup>37</sup>

<b>Tocopherol</b>	<b>Activity (%)</b>	<b>Tocopherol</b>	<b>Activity (%)</b>
Natural derivatives		Synthetic derivatives	
RRR- $\alpha$ -tocopherol	100	RRR- $\alpha$ -tocopherol acetate	100
RRR- $\beta$ -tocopherol	57	RRS- $\alpha$ -tocopherol acetate	90
RRR- $\gamma$ -tocopherol	37	RSS- $\alpha$ -tocopherol acetate	73
RRR- $\delta$ -tocopherol	1.4	SSS- $\alpha$ -tocopherol acetate	60
		RSR- $\alpha$ -tocopherol acetate	57
		SRS- $\alpha$ -tocopherol acetate	37
		SRR- $\alpha$ -tocopherol acetate	31
		SSR- $\alpha$ -tocopherol acetate	21

Azzi and Stocker presented a study on the different isomers of tocopherol comparing synthesised  $\alpha$ -tocopherol acetate with different configurations of the three chiral centres.<sup>37</sup> All of the isomers of the tocopherol have been investigated in terms of their biological activity and the comparison is shown in Table 1.4.

As mentioned above, only the RRR isomer of  $\alpha$ -tocopherol is recognised in the human body, while the other seven configurations (Figure 1.3) are not maintained in the human body and are metabolised differently from  $\alpha$ -tocopherol.<sup>36,38,39</sup>

Tocopherols have hydrophobic nature, thus the most widely used method for extraction of tocopherols from vegetable is was extraction with ethanol followed by hot saponification using potassium hydroxide. Although solvent extraction is time-consuming and requires organic solvents, still it is a simple method and effectively eliminates the impurities and interferences during chromatographic analysis and requires mild conditions of temperature and pressure.<sup>24,40</sup>

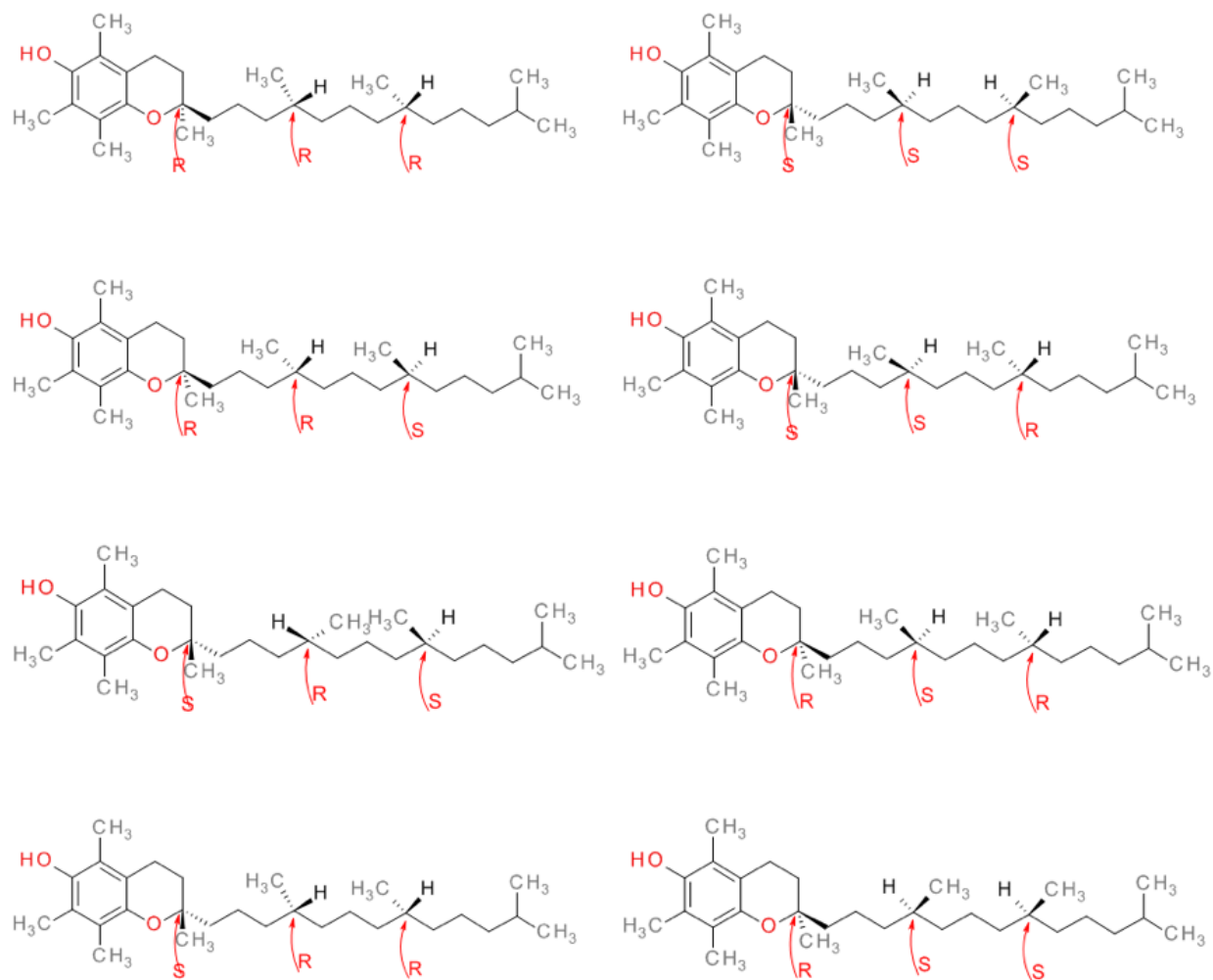


Figure 1.3: Stereoisomers of  $\alpha$ -tocopherol.<sup>24</sup>

There is an extensive list of publications that reported the attempts to develop efficient methods to extract tocopherol from different sources.<sup>1-3</sup> For example, Ofori-Boateng and Lee developed an ultrasonic-assisted extraction of  $\alpha$ -tocopherol from palm oil. The extraction efficiency was compared with the commonly used methods such as Soxhlet extraction or saponification. The highest recovery of tocopherols was observed in the case of ultrasonic-assisted extraction.<sup>41</sup> The advantage of this method includes the possibility to perform the extraction at a low temperature, which is useful in case of extraction of tocopherol, as it is usually unstable at high temperatures and might decompose. In addition, the ultrasound helped to improve penetration of the solvent into the cell allowing development of an inexpensive, simple, fast, a low-sample and solvent-required method which is an efficient alternative to conventional techniques. Nevertheless, this method was criticised in terms of low experimental reproducibility because of a lack of uniformity of the distribution of ultrasound energy and cooling of the sonication vessel was required due to a large amount of heat generation.<sup>42</sup>

Super-critical fluid extraction is a method that shows promise due to the relatively low consumption of time and organic solvents, accuracy and economic viability.<sup>43,44</sup> Several studies were conducted on tocopherols using this method for extraction. However, it is still generally unavailable for practical applications due to the high cost of the equipment.<sup>11,45,46</sup>

Solid phase extraction (SPE) is one of the most effective and popular extraction methods in terms of its relatively low cost and high resistance to environmental and other physical and chemical conditions.<sup>40,47</sup> It was used widely in industry as an effective clean-up method for bio-recovery of natural compounds from various biomasses. Typically, SPE is conducted using several types of stationary phases packed commercially in glass or plastic columns. However, the most common criticisms levelled at these commercial stationary phases are their poor stability, inadequate selectivity, limited reusability and restricted binding capacity, especially for polar compounds.<sup>48,49</sup> Bartosińska reported solid phase extraction (SPE) as an effective extraction method for small-scale study purposes.<sup>47</sup> In addition, among the most commonly used SPE sorbents were C18, silica gel and aminopropyl-functionalised silica.<sup>12</sup>

Regarding the detection methods, there are different methods to detect tocopherol after extraction from vegetable oils. The method standardised by IUPAC and AOAC is based on direct injection into the HPLC system with UV or fluorescence detector.<sup>12,40</sup> Reverse phase and normal phase HPLC were reported to separate tocopherols and different methods such as TLC or using a silica gel column were stated to separate tocopherols from sterols or triacylglycerols. GC/MS has been used effectively for the determination and quantification studies of tocopherols, which was required for the derivatised tocopherol with the saponification process.<sup>10,11,24,50</sup>

### **1.2.3 Phytosterol**

Sterols are an important phytochemical group of compounds because they possess a wide range of biological properties. Plant sterols, which are called phytosterols, are important for health as antioxidative agents and decrease serum low-density lipoprotein (LDL) cholesterol levels, thus protecting against cardiovascular diseases.<sup>42,51</sup> Phytosterols are applicable in the nutrition industries as steroidal intermediates and precursors to produce hormone pharmaceuticals.<sup>52,53</sup>

Phytosterols are 28- or 29-carbon alcohols with a steroid nucleus, a  $3\beta$ -hydroxyl group, and a 5, 6 double bond. Phytosterols vary by containing an extra methyl or ethyl group, or double bond. Moreover, most phytosterol side chains contain 9–10 carbon atoms, instead of the 8 carbon atom side chain in cholesterol.<sup>42</sup> The most important natural sources of phytosterols in human diets are oils and margarine. Phytosterols are found in vegetable oils in either free form or as conjugates through esterification of the  $3\beta$ -hydroxyl group with a fatty acid or hydroxycinnamic acid.<sup>13,50</sup> The esterified sterol content and free sterol have different physiological effects and their composition of vegetable oils has been used to measure adulteration of oil. Figure 1.4 show examples of the most common phytosterols available in vegetable oils.

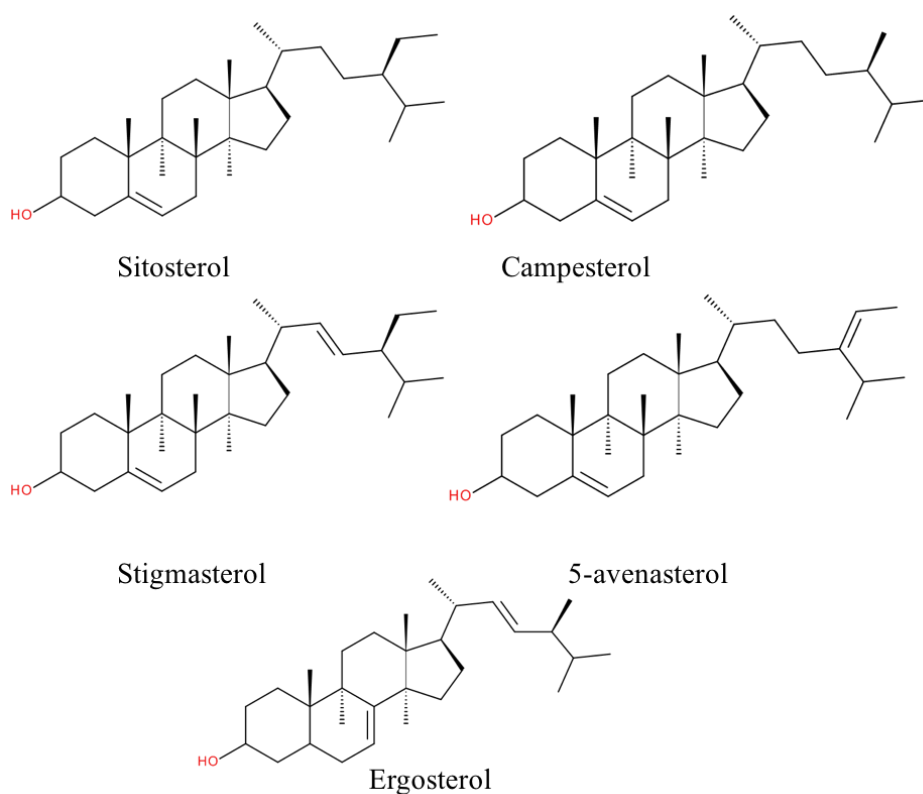


Figure 1.4: The most common phytosterols available in vegetable oils.<sup>42</sup>

Typical analytical methods for identification or quantification of phytosterols involve saponification and conversion of the sterols to trimethylsilyl ether derivatives to reduce the hydroxyl group polarity prior to separation of phytosterols individually using gas-chromatographic analysis coupled with either mass spectroscopy (MS) or flame ionization detection (FID) for identification.<sup>51,53</sup> A standardised protocol for total phytosterol analysis included acidic hydrolysis for the esterified phytosterol prior to the saponification of the phytosterol content as it has been developed by the American Oil Chemists' Society, and Association of Official Analytical Chemists.<sup>53</sup> Then, derivatised to trimethylsilyl ether is analysed by GC after clean up and separation the phytosterols from another organic phase using SPE or TLC. TLC can be used to fractionate lipid or non-specifiable lipid extracts and visualized with a UV lamp on a silica gel plate.<sup>24,26,50</sup> Moreover, common effective method of separation and purification of phytosterols were SPE using different SPE sorbents, such as neutral alumina or silica SPE cartridges. In addition, NP and RP-HPLC systems have been used for the analysis of phytosterols in vegetable oils. RP-HPLC has been the more commonly used than NP-HPLC for the

separation of individual sterols due to the possibility to use less volatile polar organic solvents in water, and offers quick equilibration in a bonded silica stationary phase with the mobile phase solvents.<sup>42,54</sup>

In the case of the separation of free phytosterols, the direct saponification methods have been applied to the oil sample for the determination of free phytosterols. It was reported that phytosterols represented the highest portion of the unsaponifiable fraction of vegetable oils.<sup>51</sup> Corn oil, rapeseed oil and wheat germ oil typically have the highest total phytosterol contents of individual sterols and this does not include the esterified phytosterols in the original oil. Table 1.5 shows examples of some vegetable oil content of phytosterols.

Table 1.5: The content of common phytosterols of some vegetable oils (mg kg<sup>-1</sup>).<sup>51</sup>

<b>Phytosterol</b>	<b>Sunflower oil</b>	<b>Sesame oil</b>	<b>Olive oil</b>	<b>Soybean oil</b>	<b>Palm oil</b>
Campesterol	210	360	34	48	100
Stigmasterol	280	3.3	5.9	560	60
$\beta$ -sitosterol	1450	2170	1050	1170	280
Total phytosterols	3400	4920	1620	2850	660

To analyse certain environmental, food or bio-samples, direct injections of the original sample matrixes are not recommended, since simple matrix components can affect the instrument. For example, using the selective detection provided by MS the crude sample extracts may inhibit or enhance the analyte ionisation, hindering the quality of the quantification.<sup>55</sup> Therefore, it is important to consider choosing the appropriate preparation method that suits the sample and the applied analytical method to remove the potential interferences. The traditional process for this objective was liquid-liquid extraction. Liquid-liquid extraction is hindered by some defects such as being generally labour-intensive, time-consuming, and requiring a large amount of expensive, toxic and environmentally unfriendly organic solvents, often combined with environmental and health hazards. However, during the last few years, new goals have been set to improve eco-friendly laboratory work such as using smaller initial analyte sizes, enhancement of selectivity in extraction, to enable the automation, and to reduce the amount of glassware

used and organic solvent consumption. Taking into consideration the current requirements for improving the work in the laboratories to be eco-friendlier, liquid-liquid extraction should be replaced with preparation and clean-up methods that fulfil these features. Solid phase extraction (SPE) is one of the available options that could be the suitable replacements.

### **1.3 Solid phase extraction (SPE)**

The solid phase extraction (SPE) technique has become one of the most preferred and applicable procedure for sample preparation and clean-up in green analytical chemistry. SPE has been supplemented by using beside various instrumental analytical procedures, especially HPLC and GC to determine analytes from samples. SPE has many advantages compared to conventional methods, such as being able to remove undesirable interferences, to carry out clean-up and enable concentration processes in one run before chromatographic analysis, reducing the consumption of organic solvents, and increasing the selectivity of extraction.

Using SPE as a pre-treatment method is determined by several factors:

1- The analysis technique that is going to be used to detect and quantify the analyte. For example, GC/MS is a sensitive technique and more suitable for the vaporised samples with lower molecular weight. HPLC could be an alternative for the samples with high molecular weight. LC/MS is another available analysis method for a wide range of samples that requires fewer preparation and clean-up steps.

2- The type of intermolecular interactions between the target and the SPE sorbent (mechanism of interaction). The retention of the analyte on the surface of the SPE sorbent is performed by bonds formed between the analyte and the sorbent particles. These bonds formed by intermolecular interactions that have been classified based on the nature of the sample solution. There are three main types of interactions, 1) polar interactions that occur between the analyte in organic solvent and sorbent with polar moieties; 2) hydrophobic interactions that happen between analyte in aqueous solvent and non-polar SPE sorbent; 3) cationic or anionic exchange between analytes carrying permanent negative or positive charges respectively and charged functional groups bounded to silica surface. The main retention mechanism of the compound is performed mainly by the electrostatic attraction

of the charged functional group on the compound to the charged group that is bonded to the SPE sorbents.

3- The solvent system used in the SPE protocol. The SPE process is conducted in four steps which are demonstrated in Figure 1.5. First, the cartridge is conditioned with solvent A. Then, a solution of the sample in liquid B is loaded onto the sorbent in the cartridge. The interfering compounds co-adsorbed with interest are washed out from the cartridge with solvent C. Finally, the purified compound is eluted from the cartridge using solvent D which is optimised to disrupt the molecular interactions which participate in the binding of target compound/s to the SPE sorbent. Examples will be mentioned in the next subtitle. An SPE manifold equipped with a vacuum pump is used during all steps of the SPE.

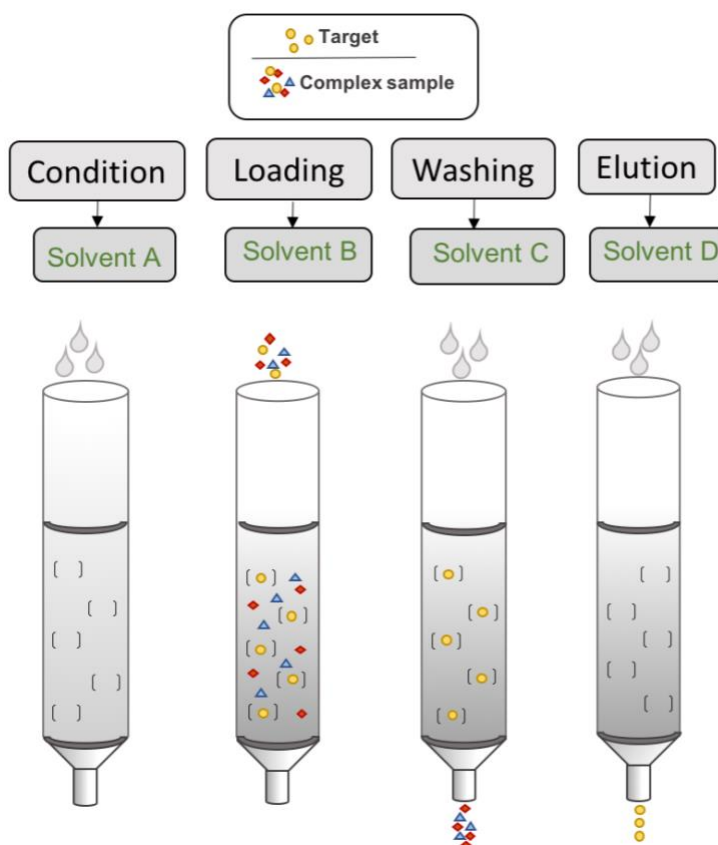


Figure 1.5: Main steps of SPE.

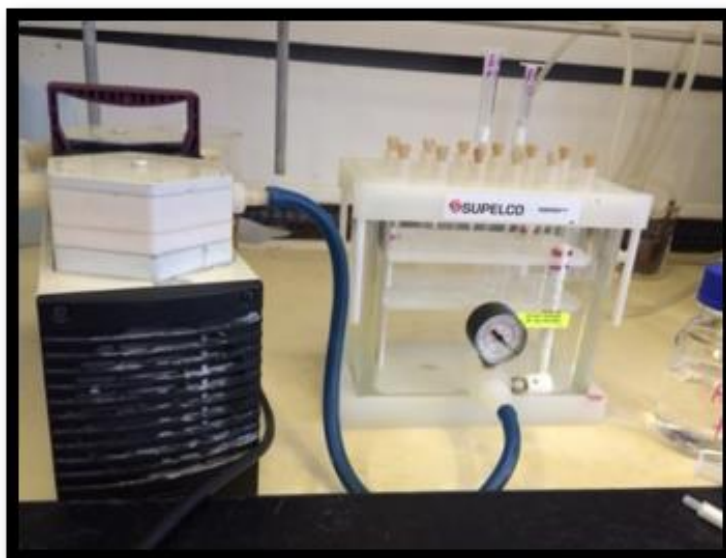


Figure 1.6: Typical SPE apparatus.

#### 1.4 Commercial sorbents used for SPE of minor components from vegetable oils

Typically, SPE is performed using a stationary phase prepared and packed in glass or plastic columns named as cartridge.<sup>56,57</sup> There are several types of stationary phases that are commercially available to be used for SPE analytical research. The extraction of the target compound/s from SPE cartridge can be conducted using one of two strategies; a washing step with an appropriate solvent can be carried out before target compound elution to remove the interferences.<sup>58,59</sup> Otherwise, analytes can be eluted first leaving the interfering matrix components retained by the sorbent.

Stationary phases are classified based on the methods of the distribution of substances in the solid material which, in turn, depends on the intermolecular interactions with the bound phase and solid support, with dispersed sample matrix components, and with the eluting solvents, as well as on molecular size. The types of SPE sorbent are reversed phase, normal phase, ion exchange phase and adsorbent phase.<sup>56,60,61</sup>

There were several studies of extraction, purification or clean-up the minor components from vegetable oils using different types of SPE sorbents. For example, the analysis of free fatty acids from natural materials usually included these steps, 1) separation of lipids; 2) extraction of free fatty acids; 3) esterification of free fatty acids to

methyl esters; 4) analysis of fatty acid methyl esters using GC/FID, GC/MS or HPLC or any other suitable analysis techniques.<sup>60-62</sup> Silica cartridge was used by Correia and co-workers to extract tocopherol and fatty acids from different vegetable oils prior to analysis with HPTLC. Vegetable oils included peanut, sunflower and soybean oils.<sup>62</sup> The elution process started with a less polar eluting solvent mixture (petroleum ether/diethyl ether 92:8) to extract the non-polar fraction first, followed by polar diethyl ether solvent to elute the polar fraction. The purification of the fatty acids is often performed using SPE columns with a bonded aminopropyl sorbent, to separate the analyte to low-medium polarity lipids, free fatty acids and a phospholipids fraction.<sup>23,63</sup>

$\alpha$ -tocopherol has been purified or extracted from edible oil sources with SPE in several studies.<sup>11,47,64-66</sup> Grigoriadous *et al.* used a silica cartridge for preparing and purifying a fraction involved  $\alpha$ -tocopherol and squalene from olive oil sample. The oil sample was loaded in hexane and the eluting process was conducted in two stages. First, squalene was extracted with 10 mL of hexane and then, extract  $\alpha$ -tocopherol was extracted with hexane/dimethyl ether (99:1), before analysis with HPLC/UV.<sup>64</sup>

In an attempt to develop extraction of minor compounds from edible oils, a study was conducted to optimise a replacement of time and solvent-consuming saponification process with a simple and reliable method to determine and quantify tocopherols and sterols.<sup>11</sup> The study was applied to rapeseed, sunflower, soybean, castor, poppy and cuphea oils. The developed method included using a silica gel cartridge and applying the oil samples to the cartridges after esterifying the targets in hexane/ methyl *tert*-butyl ether (99:1) (v/v). Then, the same solvent was used for elution and GC/MS was used for analysis. The validation study resulted in the good quality of the yield of extraction. Moreover, several studies conducted SPE to purify  $\alpha$ -tocopherol from oil samples effectively using different type of sorbents such as C8, C18,<sup>47</sup> aminopropyl<sup>65</sup> and silica cartridge<sup>66</sup>.

Phytosterols are another example of minor components in edible oils. The purification of phytosterols was described by Toivo *et al.* as a general process which started with saponification, adding internal standard, adjusting the pH between 2 and 5 and applying the sample to a C18 reverse phase. Then, the sample was derivatised before analysing with GC/MS.<sup>66</sup>

Neutral alumina cartridge for SPE was used for clean-up and purification of eight free and esterified phytosterols from 31 samples of vegetable oils by Phillips and co-workers. The extraction was conducted using hexane for conditioning, followed by loading using 20:80 diethyl ether: hexane. Then, the esterified phytosterols were eluted with 20:80 diethyl ether/hexane, and free phytosterols with ethanol/ hexane/ diethyl ether (50:25:25). The eluted samples were saponified with potassium hydroxide before separation and analysed with GC/MS.<sup>51</sup>

According to Lagarade *et al.*,<sup>42</sup> phytosterols have been separated successfully from the non-saponified fraction of edible oils with several types of SPE sorbent such as reverse-phase sorbent (C18)<sup>67</sup>, normal-phase (neutral alumina)<sup>51</sup> and silica SPE cartridge and eluted with hexane containing 20% *tert*-butyl methyl ether from olive oil.<sup>68-71</sup>

SPE showed simplicity, flexibility, relative selectivity and requirement of mild extraction conditions which led to the diffusion of this method over many classical sample preparation methods. Yet there is a demand for the development of the SPE sorbent to improve their features. One of the most important developments is synthesis the customised porous polymer with specific recognition to specific compounds called molecularly imprinted polymer (MIP). MIPs have many applications in different disciplines which will be presented in this chapter (subtitle 1.6). In the next part of this chapter, will focus only on the achieved applications of MIPs in purification and extraction of the minor component in this study.

### **1.5 Molecularly imprinted polymers (MIPs)**

MIPs are synthetic polymeric materials with specific binding sites to selectively recognise target molecules during rebinding. Recently, there have been extensive reports on the development of Molecularly Imprinted Polymer-based solid phase extraction (MISPE) protocols for the applications in different areas including environmental, food and pharmaceutical analyses.<sup>72</sup>

SPE is preferable as an extraction method compared to other extraction methods in terms of its relatively low cost and high resistance to the environmental and harsh physical and chemical conditions.<sup>73</sup> Before exhibiting the successful application of MIPs in SPE

for extraction of some compounds which are available in minor or trace levels, some features and principles related to MIPs will be presented in the following subsections.

### 1.5.1 Synthesis of Molecularly Imprinted Polymer

Molecular imprinting technology is based on synthesising polymers that have specific recognition to specific compounds (template). The polymer synthesis is relatively simple (as shown in Figure 1.7), and can be made by adding template to the mixture of functional monomers, cross linkers and initiator molecules. Table 1.6 shows examples of some commonly used initiators, cross linkers and functional monomers compounds. Subsequently, the polymerisation starts when monomeric mixture is subjected to the UV light or heat. The molecular complex, which was formed between template molecules and functional monomers, is fixed in the cross-linked network.<sup>74,75</sup> Then, the template was extracted in order to obtain the molecularly imprinted polymer with three-dimensional cavities complementary in shape, size and chemical functionality to the extracted template. These cavities have the ability to rebind with the template or its derivatives using the intermolecular interactions such as hydrogen bonds, van der Waals, dipole-dipole and ionic interactions.<sup>76</sup>

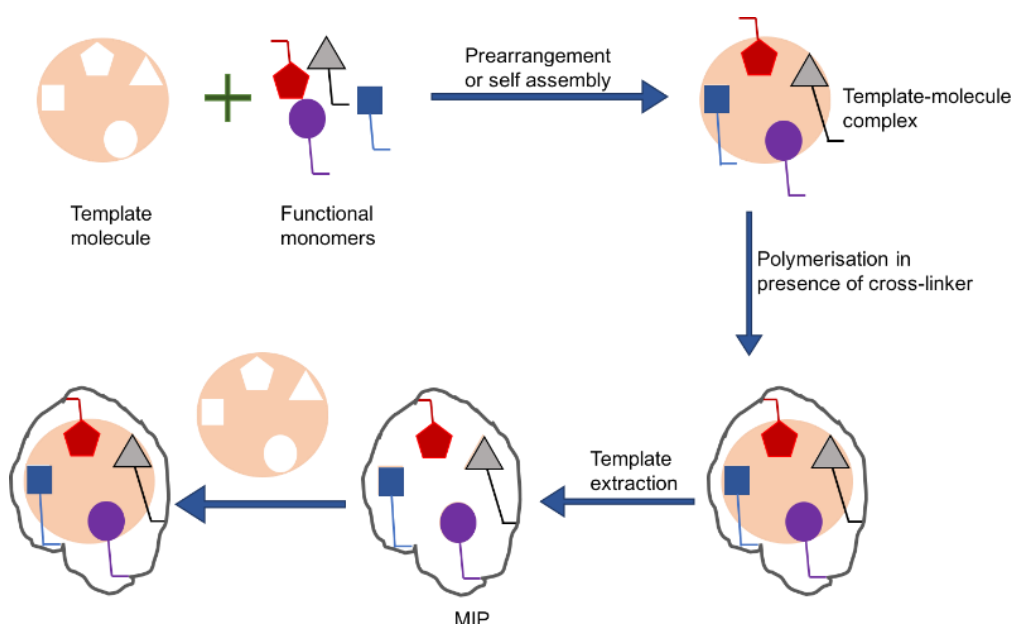
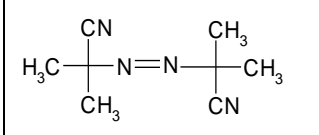
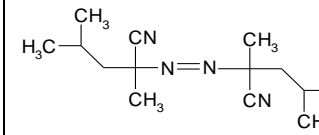
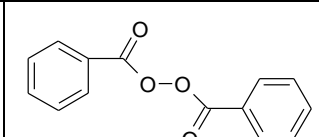
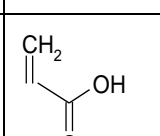
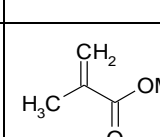
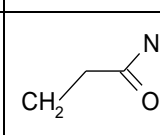
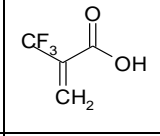
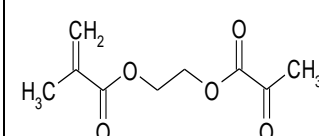
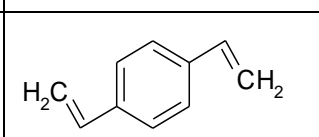


Figure 1.7: Molecular imprinting approach.

Table 1.6: Examples of commonly-used initiators, functional monomers and cross-linkers in MIP synthesis.

Initiators	Chemical structure
Azobisisobutyronitrile	
Azobisdimethylvaleronitrile	
Benzoylperoxide	
Functional monomers	Chemical structure
Acrylic acid	
Methacrylic acid (MAA)	
Acrylamide	
Trifluoromethyl acrylic acid (TFMAA)	
Cross-linkers	Chemical structure
Ethylene glycol dimethacrylate (EGDMA)	
Divinylbenzene (DVB)	

## **1.5.2 Types of molecular imprinting**

In the first step of MIP preparation, template and monomers form the complex functional monomer and cross-linker by one of the three following binding approaches:

### **1.5.2.1 Covalent imprinting**

This approach was first presented by Wulff and Sarhan in 1972.<sup>72</sup> Reversible covalent bonds were formed between the template and monomers prior to polymerisation. The covalent bonds support more homogeneous binding sites on the polymer. This method requires relatively mild conditions to allow cleavage of the formed covalent bonds between template and MIP, which are going to rebind with the same compound or its analogues but from an analyte. The important advantage of this method is the production of stable and well-defined polymers due to the covalent bonds before the polymerisation. Nevertheless, the acid hydrolysis for the cleavage of the reversible covalent interaction that reformed by adding the analyte makes this approach less common than the others.<sup>72,73,77</sup>

### **1.5.2.2 Non-covalent imprinting**

This method was introduced by Mosbach and his co-workers in 1981.<sup>72,77</sup> In this method, the covalent bonds in the previous method were being replaced with rather weaker intermolecular interactions such as hydrogen bonds, van der Waals and hydrophilic reactions between the template and monomers in the first step of MIP preparation. This approach is one of the most adopted in the literature due to its ease of use and the availability of broad choices of suitable monomers. However, this method tends towards polymer formation by adding an excess of free monomers that in turn cause non-selective binding sites compared to the covalent method.<sup>72,73</sup>

### **1.5.2.3 Semi-covalent imprinting**

This method combines elements of the two other methods. It depends on the formation of covalent bonds in the first step of MIP formation. Then, the target binds with the polymer by non-covalent interactions.<sup>72,73,77</sup>

## **1.6 Applications of Molecularly Imprinting Polymers**

The synthesis of MIPs is based on the complex formation between the functional monomer, templates and cross-linker molecules to form polymers with specific recognition properties towards the template. The molecular recognition creates molecular memory that makes complemented cavities in shape, size and chemical functionality, therefore, selectively recognising the imprinted species.<sup>77</sup> MIPs are able to mimic natural antibodies and biological receptors, demonstrating specific molecular recognition phenomena. Moreover, MIPs could be used to separate and analyse mixtures of compounds. MIPs also have considerable robustness and stability under harsh conditions in various environments. All these properties have made MIPs attractive for application in research and analysis.<sup>72,74,78</sup> There are four main areas of research that have been developed using MIPs, including separation science and purification, sensors, catalysis and drug delivery.

### **1.6.1 Molecularly Imprinted-Solid Phase Extraction (MISPE)**

Since SPE has been used as an application of MIPs, it is now called molecularly imprinted solid phase extraction MISPE. MIPs have been applied successfully to extract several compounds from matrices or compounds available in certain samples at very low concentrations.<sup>79</sup> MIPs can be packed in HPLC columns for on-line analysis, or between two frits in cartridges for off-line synthesis.<sup>72</sup>

As mentioned above in subtitle 1.4, although there has been huge development and there exist variety in the commercially available SPE sorbents, there is still demand for improving the sorbent selectivity. In this regard, many studies have been conducted to develop the selectivity during extraction and/or purification of analytes.<sup>80</sup> MIPs are stable polymers with molecular recognition, provided by the presence of a template during their synthesis. Therefore, MIPs are excellent materials providing selectivity to sample preparation.

MIPs were applied successfully in many different types of analytical applications. One of the earlier successful applications was purification of sameridine in biological sample prior to detect with GC/MS. Clean chromatographic traces from plasma samples

were obtained in the sample eluted from synthesised MIP that was synthesised using a sameridine analogue.<sup>81</sup>

Additionally, several studies described the purification of different analytes in environmental samples in aqueous solutions. Generally, the loading step onto the MIP cartridge is performed in a low-polarity solvent, in order to reduce the non-specific interactions, and after the washing step and removal of adsorbed compounds by non-specific bonds from the polymeric matrix, analytes are eluted with a solvent with a suitable degree of polarity to disrupt the non-covalent interactions between the analyte and the imprinted polymer.<sup>80</sup> In order to develop water-compatible MIPs, it is useful to contain hydrophilic surface properties to the polymer to reduce non-specific hydrophobic interactions. This could be attained by using polar porogens,<sup>78</sup> hydrophilic co-monomers (e.g. 2-hydroxyethyl methacrylate, acrylamide) or cross-linkers (e.g. pentaerythritoltriacrylate, methylenebis(acrylamide)),<sup>82</sup> and/or designed monomers capable of stoichiometrically interacting with the template functionalities.<sup>80</sup> Many other examples were demonstrated in the literature about the effective application of MIPs in MISPE, such as extraction and purification of microcystin-LR<sup>83</sup>, cocaine, morphine,<sup>84</sup> biotin,<sup>85</sup> simazine,<sup>86</sup> tarbaryl<sup>87</sup> and triazines<sup>88</sup>.

Although the witnessed achievements were recorded using MIPs in sample preparation, there is a continuous demand for the constant enhancement and for these materials to be able emulate the current development of the scientific research. The traditional polymerisation was the bulk polymerisation which is rapid, simple and does not require a sophisticated or expensive instrumentation. However, MIPs which were synthesised by bulk polymerization have been criticised due to the poor site accessibility to the target molecules. In addition, the thick polymeric network and lower rebinding capacity. Several strategies have been developed to overcome these drawbacks of bulk polymerisation. The different polymerisation methods include suspension polymerisation, emulsion polymerisation, precipitation polymerisation and the most recent method solid-phase synthesis of molecularly imprinted polymer nanoparticles (MIP NPs).<sup>89-92</sup>

### 1.6.2 Sensors

Chemical sensors for clinical diagnostics, environmental and food analyses have been improved using MIPs. MIP technology is applied in sensor research by synthesising antibody-like materials with high selectivity and sensitivity, chemical inertness, long-term stability and insolubility in water and most organic solvents.<sup>78,89</sup> Many studies have been reported for the detection and control of poisonous substances in adulterated foods which are the major challenges in food safety in the world.<sup>93,94</sup> MIP-based immunoassay methods in food safety, and the developed biomimetic immunoassay could be effective alternatives to antibodies which are relatively unstable and costly, resulting in a limitation of their applications and developments.<sup>93</sup> N-methylcarbamate insecticide metolcarb was determined by Wang *et al.*, who developed MIP film as the antibody mimic.<sup>94</sup> The established method was successful to be used in the determination of metolcarb in spiked apple juice, cabbage, and cucumber, with recoveries ranging from 71.5 to 100%. The results suggested that the method was effective for the direct determination of metolcarb in foods. Moreover, vancomycin (antibiotic) was used as a template in molecularly imprinted nanoparticles (MIP NP) prepared by solid-phase syntheses to development of a clinically relevant enzyme-linked assay. The sensitivity of the assay was superior to a previously described enzyme-linked immunosorbent assay based on antibodies.<sup>95</sup>

A sensor to determine atropine concentration in human serum and urine was synthesised by preparing an aniline-*o*-phenylenediamine-atropine MIP layer onto a piezoelectric quartz crystal.<sup>96</sup> In addition, MIPs were successfully used as sensors for enantiomeric separation of compounds like *R* and *S*-propranolol, *D* and *L*-tryptophan and *D* and *L*-serine.<sup>78,97,98</sup>

### 1.6.3 Catalysis

MIPs have been given a lot of importance due to their high selectivity and stability under the harsh conditions of high temperature and pressure, basic or acidic pHs. This explains the interest in them as a replacement for enzymes or catalytic antibodies.<sup>99</sup> For example, Wulff used amidines as monomers to obtain phosphonate ester imprinted polymers with the ability to bind to carboxylic acids and phosphonate esters with very high

affinity. The catalyst was used in the hydrolysis reaction of analogous carboxylate esters. The reaction rate increased 100 times by using the imprinted matrices compared with the un-catalysed reaction.<sup>98</sup>

The specific recognition and catalysis performance of MIP is a result of the conformational complement of imprint-substrates. The shape of the imprint can partially allow molecules that are identical to, or smaller than, the template to enter the interior. Tong *et al.* presented thermodynamic and kinetic surveys on the specific recognition and catalysis by *p*-nitrophenyl phosphate as templates and 1-allylimidazole as functional monomers in MIP.<sup>100</sup> The imprinted polymer catalyst showed a highly specific recognition and catalysis toward the imprint species.

In addition, a catalytic and positively thermosensitive molecularly imprinted polymer was synthesised.<sup>101</sup> At higher temperatures (such as 40 °C), this polymer exhibited significant catalytic activity resulting from the dissociation of the inter-polymer complexes between 1-vinylimidazole and 2-trifluoromethylacrylic acid that facilitated access to the active sites of the imprinted polymer and inflated them.

#### **1.6.4 Drug delivery**

MIPs have ability to bind strongly and selectively to bioactive molecules which could be applied in drug delivery application. Due to the cross-linked nature and affinity properties of MIPs, it was found that they are suitable to be used in the enhancement of the pharmacological therapy by using MIPs to act as reservoirs that are capable to achieve a controlled drug release.<sup>102,103</sup> For example, theophylline-imprinted polymers performed a controlled release of the drug, the obtained polymer showed a slow drug release for several hours in the phosphate buffer, pH 7.0.<sup>104</sup>

MIPs offered some effective applications for improving some drugs, particularly those drugs with a low therapeutic index, which might cause negative effects if their concentration is not kept below a certain threshold value. In addition, MIPs offered selective release of one of the enantiomers of racemic drugs, where the two enantiomers have different activity levels or effects as shown with the template  $\beta$ -adrenergic antagonist.<sup>105,106</sup>

MIPs were capable to simulate the binding characteristics of biological receptors by molecular imprinting. Testosterone was used as a template in preparing a MIP templated with testosterone and using ethylene glycol dimethacrylate as the cross-linker and methacrylic acid as the functional monomer. The resulted MIP recognised the original template as well as shown affinity towards four other related steroids especially estradiol, progesterone, testosterone propionate and estrone.<sup>107</sup>

### **1.7 Computational design of MIPs**

The original use of the molecular modelling system is as a tool to generate and refine the geometry of molecular structures in terms of bond length, bond angles and torsions to represent the lower conformational energy. The molecular modelling was designed for many purposes, one of them is molecules such as drugs, proteins, macromolecules.<sup>108</sup> The Leicester Biotechnology Group improved this system to be used as a computer-aided rational design for the rapid development and optimisation of molecularly imprinted polymers. The developed protocol involved construction of a virtual library of functional monomers that are commercially available at low cost and are easily and commonly used in polymer preparation as adsorbents. The target template is screened against the virtual library to determine a list of the most suitable functional monomers to start within the MIP synthesis. The process of computing and simulating of the physiochemical properties of a molecule relies on the ability to accurately determine the lowest energy conformations of the monomer-template complexation.<sup>74,109,110</sup> The list of monomers is chosen in the molecular modelling process based on the evaluation of interactions between templates and monomers in order to rationalise the choice of the best monomers used for the synthesis of the highest affinity polymeric materials.

The molecular modelling is based on theoretical calculations to determine the intermolecular interactions between the template and monomer in polymerisation mixtures. The calculations are performed using a molecular dynamics approach to calculate the binding interaction in the monomer-template complexation. The amount of this energy is governed by the change in Gibbs free energy of the complexation. The Gibbs free energy of binding can be broken down into individual parameters which has been described as follows:<sup>111</sup>

$$\Delta G_{bind} = \Delta G_{t+r} + \Delta G_r + \Delta G_h + \Delta G_{vib} + \sum \Delta G_p + \Delta G_{conf} + \Delta G_{vdW}$$

**Equation 1.1:** Gibbs free energy equation.

$\Delta G$  is the Gibbs free energy; (bind) shows the Gibbs free energy of complexation. (t+r) are the modes of translation and rotation. (r) is the restriction on rotation when complexed, (h) is the hydrophobic interaction and (vib) is the vibrational modes. (p), (conf) and (vdW) are the polar groups, conformational changes and van der Waals interactions.

In this research, the template structure is refined using the molecular modelling software SYBYL. The computer-aided design is a good starting step for the synthesis of affinity polymers. It minimises the cost and process time of the production of materials possessing high affinity with extra guarantee for their effectiveness without extensive testing or expensive experimental resource consumption.<sup>74</sup> Free energy (equation 1.1) is the theoretical explanation, but to calculate the binding score practically SYBYL software using the LEAPFROG algorithm. The algorithm is applied to identify the binding points on the template molecule. The first binding site points that should be considered are the functional groups of the template. The average electrostatic and steric properties of a monomer are calculated. Then, the polymer is directed to the identified binding site of the monomer. The binding energy is calculated based on the interaction between the monomer and the template which determines a binding score. The LEAPFROG binding score is one of the many different scoring methods by which binding score calculates steric, electrostatic and hydrogen bonding enthalpies.<sup>96,110</sup>

## **1.8 Comparison of Molecularly Imprinted Polymer (MIP) and Non-Imprinted Polymer (NIP)**

It is important to have control polymers for comparison purposes of the MIP performance. Control can be achieved in the form of non-imprinted polymers (NIP). NIPs are synthesised by following exactly the same procedure of molecularly imprinted polymer synthesis. However, the step of adding the template is excluded, thus the resultant polymers consist of functional monomers and cross-linkers organised in rigid polymeric networks without the selectivity generated by adding template molecules.<sup>72</sup> The synthesis

of NIPs accompanies MIP synthesis. The NIP should be subjected similarly to the experiments to compare between them in terms of the selectivity that is absent in NIPs.

However, in some cases NIPs act as MIPs or close to them with a high recovery percentage, for example, nonyphenol was extracted with 99% recovery similarly via MIP and NIP.<sup>112</sup> Another example of successful use of NIP is the effective extraction of kukoamine from potato peel.<sup>76</sup>

The multiple successful examples of NIPs as adsorbents in SPE are a motivation behind using the rationally-designed polymers (RDPs) in the current research. The specificity of RDPs is based on the computational selection of monomers using the same protocol as a design of the MIPs. Generally, the principles of the molecular imprinting are realised in virtual sense (*in silico*) and allow the production of cost effective adsorbents, at scale and possessing the required binding properties.<sup>74</sup>

### **1.9 Rationally-designed polymers RDPs**

Over the years, a number of polymers were designed and applied successfully to extract different compounds from different matrices with high affinity and specificity. In addition, MIPs have demonstrated their superior chemical and thermal stability as compared to traditional stationary phases. Nevertheless, MIPs remain mainly used for analytical applications. However, MIPs are not suitable for the large-scale purification processes due to their cost which is associated with the price of the template and relatively low binding capacity.<sup>74,79</sup>

RDPs developed by Piletsky and co-workers could be an alternative to MIPs as stationary phases in SPE. They were designed computationally using the SYBYL software exactly as for the MIP synthesis. RDPs are synthesised using computationally-selected functional monomers without adding the template to the monomeric mixture. The obtained polymers consist of the rigid polymeric network which contains an excess of functional groups on the polymer surface that are capable to interact with target compound and provide a high binding sites suitable for its extraction and purification. It is possible to highlight that the absence of the specific cavities in the RDP in comparison with MIPs is compensated by the high amount of the functional groups which possess the natural affinity towards the compound of interest.

MIPs, in general, are very selective towards the target, but the small number of binding site could hinder the binding capacity of the polymers. In terms of the industrial purification and extraction, it is necessary to take in consideration what is the maximum amount of the target that could be extracted. In addition, it is preferable to improve the stationary phase to be a multi-purpose SPE resin. It was observed that one of the difficulties associated with MIP synthesis is to achieve complete removal of the template which directly affects the efficiency of the recovery in the extraction step.<sup>74</sup>

In some cases, the difficulty of synthesis of MIPs is related to the fact that the target that is expensive, unavailable in pure standards or unsuitable for use in the research because of its toxic nature. In these cases, the development of the polymer consists of the computational screening of the template against the library of functional monomers and experimental screening of the computer-suggested monomers to make blank imprinted polymers. The advantage of this method is that it increases the chance of success using the virtual imprinting by executing the extraction process under the conditions (pH, solvent, salinity, temperature, etc) which are required in the practical application.<sup>73</sup>

It was found that in some cases the performance of non-imprinted polymers (NIPs) is not distinguished from the performance of MIPs. Consequently, it is apparent that the computer-selected monomers should have an affinity to the corresponding template when it is included into a random polymeric network. This knowledge has been exploited in developing adsorbents (RDPs) which could have natural selectivity for specific target molecules, have lower cost than MIPs, are less selective and can improve extraction from the natural source of the target at the maximum level. High affinity of NIPs was observed in the case of polymers that were computationally designed for nonyphenol with a recovery percentage of 99%, which is similar to the performance of the MIPs made for the same target.<sup>112</sup>

MIPs and the corresponding NIPs were computationally designed to purify the phenolic polyamine kukoamine. The predicted molecular modelling was to match the experimental performance of MIP and NIP with binding capacities of 54 and 45 mg g<sup>-1</sup> respectively. This could suggest that rationally designed polymers broaden the efficiency of extraction process. Further detailed studies could be conducted to extract pure compounds from less complex crude samples.<sup>76</sup>

### **1.10 Aims and objectives**

The main objective of this project is to develop an economical method to extract and purify minor chemical compounds from the essential biomass (vegetable oils), which is one of the common renewable resources used for the production of biofuel. To achieve the aim of this project, a rationally-designed polymer was prepared based on the molecular imprinting principles. It was used as an adsorbent in the optimised SPE protocol in order to extract and purify the selected chemical compounds. In addition, the study aimed to approve the effective performance of the synthesised polymer by comparing the yield of SPE process using the optimised protocol to RDP as well as several commercially available sorbents. Finally, the synthesis of RDP beside MIP from the same components and at the closest conditions was presented to highlight the difference of RDP from the traditional MIP. In addition, the MIP NPs with affinity towards  $\alpha$ -tocopherol was synthesised and optimised the separation conditions.

## References

- 1) Yang, R.; Zhang, L.; Li, P.; Yu, L.; Mao, J.; Wang, X.; Zhang, Q. A Review of Chemical Composition and Nutritional Properties of Minor Vegetable Oils in China. *Trends Food Sci Technol.* **2018**, *74*, 26–32.
- 2) Ballus, C. A.; Meinhart, A. D.; de Souza Campos, F. A.; da Silva, L. F.; de Oliveira, A. F.; Godoy, H. T. A Quantitative Study on the Phenolic Compound, Tocopherol and Fatty Acid Contents of Monovarietal Virgin Olive Oils Produced in the Southeast Region of Brazil. *Food Res. Int.* **2014**, *62*, 74–83.
- 3) Li, C.; Yao, Y.; Zhao, G.; Chen, Y.; Liu, H.; Liu, C.; Shi, Z.; Chen, Y.; Wang, S. Comparison and Analysis of Fatty Acids, Sterols, and Tocopherols in Eight Vegetable Oils. *J. Agric. Food Chem.* **2011**, *59*, 12493–12498.
- 4) Nigam, P. S.; Singh, A. Production of Liquid Biofuels from Renewable Resources. *Prog Energy Combust Sci.* **2011**, *37* (1), 52–68.
- 5) Gunnarsson, I. B.; Svensson, S. E.; Johansson, E.; Karakashev, D.; Angelidaki, I. Potential of Jerusalem Artichoke (*Helianthus Tuberosus* L.) as a Biorefinery Crop. *Ind Crops Prod.* **2014**, *56*, 231–240.
- 6) Chum, H. L.; Overend, R. P. Biomass and Renewable Fuels. *Fuel Process. Technol.* **2001**, *71*, 187–195.
- 7) Yang, Y.; Fang, J.; Ma, W.; Guo, D.; Mohammat, A. Large-Scale Pattern of Biomass Partitioning across China's Grasslands. *J. Biogeogr.* **2010**, *19*, 268–277.
- 8) Naureen R., Tariq M., Yuosoff I., Chowdhury A., A. M. Synthesis, Spectroscopic and Chromatographic Studies of Sunflower Oil Biodiesel Using Optimizes Base Catalyzed Methodlysis. *Saudi J Biol Sci.* **2014**, 1–8.
- 9) Christodouleas, D.; Fotakis, C.; Papadopoulos, K.; Dimotikali, D.; Calokerinos, A. C. Luminescent Methods in the Analysis of Untreated Edible Oils: A Review. *Anal Lett.* **2012**, *5–6*, 625–641.

- 10) Schwartz, H.; Ollilainen, V.; Piironen, V.; Lampi, A. M. Tocopherol, Tocotrienol and Plant Sterol Contents of Vegetable Oils and Industrial Fats. *J Food Compos Anal* **2008**, *21*, 152–161.
- 11) Lechner, M.; Reiter, B.; Lorbeer, E. Determination of Tocopherols and Sterols in Vegetable Oils by Solid-Phase Extraction and Subsequent Capillary Gas Chromatographic Analysis. *J Chromatogr A* **1999**, *857*, 231–238.
- 12) Cert, A.; Moreda, W.; Pérez-Camino, M. Chromatographic Analysis of Minor Constituents in Vegetable Oils. *J Chromatogr A* **2000**, *881*, 131–148.
- 13) Yara-Varón, E.; Li, Y.; Balcells, M.; Canela-Garayoa, R.; Fabiano-Tixier, A. S.; Chemat, F. Vegetable Oils as Alternative Solvents for Green Oleo-Extraction, Purification and Formulation of Food and Natural Products. *Molecules* **2017**, *22*, 1474.
- 14) Tan, C. H.; Ghazali, H. M.; Kuntom, A.; Tan, C. P.; Ariffin, A. Extraction and Physicochemical Properties of Low Free Fatty Acid Crude Palm Oil. *Food Chem.* **2009**, *113*, 645–650.
- 15) Aransiola, E. F.; Ojumu, T. V.; Oyekola, O. O.; Madzimbamuto, T. F.; Ikhu-Omoregbe, D. I. O. A Review of Current Technology for Biodiesel Production: State of the Art. *Biomass Bioenergy* **2014**, *61*, 276–297.
- 16) Freedman, B.; Pryde, E. H.; Mounts, T. L. Variables Affecting the Yields of Fatty Esters from Transesterified Vegetable Oils. *J Am Oil Chem Soc.* **1984**, *61*, 1638–1643.
- 17) Mancini, A.; Mancini, A.; Nigro, E.; Montagnese, C.; Daniele, A.; Orrù, S.; Buono, P. Biological and Nutritional Properties of Palm Oil and Palmitic Acid: Effects on Health. *Molecules* **2015**, *20*, 17339–17361.
- 18) Adekunle, K. F. A Review of Vegetable Oil-Based Polymers: Synthesis and Applications. *OJPChem.* **2015**, *5*, 34–40.
- 19) Kris-Etherton, P. M.; Pearson, T. A.; Wan, Y.; Hargrove, R. L.; Moriarty, K.; Fishell, V.; Etherton T. High Monounsaturated Fatty Acid Diets Lower Both Plasma Cholesterol and Triacylglycerol Concentrations 1 – 3 Experimental Design. *Am J Clin Nutr.* **1999**, *70*, 1009–15.

- 20) Roman, O.; Heyd, B.; Broyart, B.; Castillo, R.; Maillard, M. N. Oxidative Reactivity of Unsaturated Fatty Acids from Sunflower, High Oleic Sunflower and Rapeseed Oils Subjected to Heat Treatment, under Controlled Conditions. *Food Sci. Technol* **2013**, *52*, 49–59.
- 21) Waliking, A. E.; Wessels, H. Chromatographic Separation of Polar and Nonpolar Components of Frying Fats. *J. Assoc. Off. Anal. Chem* **1981**, *64*, 1329–1330.
- 22) AOAC, Official Methods of Analysis, Association of Analytical Chemists, Arlington, VA, 14th Ed., **1984**, Official Method 18.074.
- 23) Kim, H.; Salem, N. Extraction Thermospray LC-MS Analysis. *J. Lipid Res.* **1990**, *31*, 2285–2289.
- 24) Gharby, S.; Harhar, H.; Bouzoubaa, Z.; Asdadi, A.; El Yadini, A.; Charrouf, Z. Chemical Characterization and Oxidative Stability of Seeds and Oil of Sesame Grown in Morocco. *J Saudi Soc. Agricul. S.* **2017**, *16*, 105–111.
- 25) Koushki, M.; Nahidi, M.; Cheraghali, F. Physico-Chemical Properties, Fatty Acid Profile and Nutrition in Palm Oil. *J Paramed Sci.* **2015**, *6*, 117–134.
- 26) Abidi, S. L.; Thiam, S.; Warner, I. M. Elution Behavior of Unsaponifiable Lipids with Various Capillary Electrochromatographic Stationary Phases. *J Chromatogr A* **2002**, *949*, 195–207.
- 27) Moazzami, A. A.; Kamal-Eldin, A. Sesame Seed Is a Rich Source of Dietary Lignans. *JAACS, J Am Oil Chem Soc.* **2006**, *83*, 719–723.
- 28) Galae M., Horga C., C. M. Separation and Determination of Tocopherols in Vegetable Oils by Solid Phase Extraction on Porous Polymers SPE Cartidges and Capillary Gas Chromatography Analysis. *Open Chem.* **2010**, *8*, 1110–1116.
- 29) Monferrere, G. L.; Azcarate, S. M.; Cantarelli, M. Á.; Funes, I. G.; Camiña, J. M.; Monfreere C., Azcarate S., Cantarelli M., Funes I., C. J. Chemometric Characterization of Sunflower Seeds. *Journal of food science* **2012**, *77* (, 1018–1022.

- 30) Murphy P.; Subar F. Vitamin E Intakes and sources in the United States. *Am. J. Clin. Nutr.* **1989**, *52*, 361–367.
- 31) Luo, Z.; Murray, B. S.; Ross, A.-L.; Povey, M. J. W.; Morgan, M. R. A.; Day, A. J. Effects of PH on the Ability of Flavonoids to Act as Pickering Emulsion Stabilizers. *Colloids Surf B Biointerfaces.* **2012**, *92*, 84–90.
- 32) Salgin, U.; Döker, O.; Çalimli, A. Extraction of Sunflower Oil with Supercritical CO<sub>2</sub>: Experiments and Modeling. *J Supercrit Fluids* **2006**, *38*, 326–331.
- 33) Amakura, Y.; Yoshimura, M.; Yamakami, S.; Yoshida, T. Isolation of Phenolic Constituents and Characterization of Antioxidant Markers from Sunflower (*Helianthus Annuus*) Seed Extract. *Phytochem Lett.* **2013**, *6*, 302–305.
- 34) Pająk, P.; Socha, R.; Gałkowska, D.; Rożnowski, J.; Fortuna, T. Phenolic Profile and Antioxidant Activity in Selected Seeds and Sprouts. *Food Chem.* **2014**, *143*, 300–306.
- 35) Puoci F., Cirillo G., Curcio M., Iemma F., Spizzirri U., P. N. Molecular Imprinted SPE of Selective HPLC Determination of A-Tocopherol in Bay Leave. *Anal. Chim. Acta.* **2007**, *593*, 164–170.
- 36) Bramley, P. M.; Elmadfa, I.; Kafatos, a; Kelly, F. J.; Manios, Y.; Roxborough, H. E.; Schuch, W.; Sheehy, P. J. a; Wagner, K. H. Vitamin E. *J. Sci. Food Agric.* **2000**, *80*, 913–938.
- 37) Azzi A., S. A.; Azzi, A.; Stocker, A. Vitamin E: Non-Antioxidant Roles. *Prog. Lipid Res.* **2000**, *39*, 321–255.
- 38) Lemaire-Ewing, S.; Desrumaux, C.; Néel, D.; Lagrost, L. Vitamin E Transport, Membrane Incorporation and Cell Metabolism: Is Alpha-Tocopherol in Lipid Rafts an Oar in the Lifeboat? *Mol Nutr Food Res.* **2010**, *54*, 631–640.
- 39) Atkinson, J.; Epand, R. F.; Epand, R. M. Tocopherols and Tocotrienols in Membranes: A Critical Review. *Free Radic. Biol. Med.* **2008**, *44*, 739–764.

- 40) Saini, R. K.; Keum, Y. Tocopherols and Tocotrienols in Plants and Their Products: A Review on Methods of Extraction, Chromatographic Separation, and Detection; *Food Res Int.*, **2016**, *82*, 59-70.
- 41) Ofori-Boateng, C.; Lee, K. Ultrasonic-Assisted Extraction of  $\alpha$ -Tocopherol Anti-Oxidants from the Fronds of *Elaeis Guineensis* Jacq.: Optimization, Kinetics, and Thermodynamic Studies. *Food Anal Methods* **2013**, *7*, 257–267.
- 42) Lagarda, M. J.; García-Llatas, G.; Farré, R. Analysis of Phytosterols in Foods. *J Pharm Biomed Anal.* **2006**, *41*, 1486–1496.
- 43) Wei, F.; Shen, B.; Chen, M.; Zhou, X.; Zhao, Y. Separation of  $\alpha$ -Tocopherol with a Two-Feed Simulated Moving Bed. *Chin. J. Chem. Eng.* **2012**, *20*, 673–678.
- 44) Victor R.; Ronald R. *The Encyclopedia of Vitamin E*; CABI, **2007**.
- 45) Monferrere, G. L.; Azcarate, S. M.; Cantarelli, M. Á.; Funes, I. G.; Camiña, J. M.; Monfreere C., Azcarate S., Cantarelli M., Funes I., C. J. Chemometric Characterization of Sunflower Seeds. *J. Food Sci.* **2012**, *77*, 1018 –1022.
- 46) Delgado-Zamarreño, M. M.; Fernández-Prieto, C.; Bustamante-Rangel, M.; Pérez-Martín, L. Determination of Tocopherols and Sitosterols in Seeds and Nuts by QuEChERS-Liquid Chromatography. *Food Chem.* **2016**, *192*, 825–830.
- 47) Bartosińska, E.; Buszewska-Forajta, M.; Siluk, D. GC–MS and LC–MS Approaches for Determination of Tocopherols and Tocotrienols in Biological and Food Matrices. *J Pharm Biomed Anal* **2016**, *127*, 156–169.
- 48) Galea M., Horga C., C. M. Separation and Determination of Tocopherols in Vegetable Oil by SPE. *Open Chem.* **2010**, *8*, 110– 116.
- 49) Pyka, A.; Sliwiok, J. Chromatographic Separation of Tocopherols. *J Chromatogr A* **2001**, *935*, 71 – 76.
- 50) Ghafoor, K.; Ozcan, M. M.; Al-Juhaimi, F.; Babiker, E. E.; Sarker, Z. I.; Ahmed, I. A. M.; Ahmed, M. A. Nutritional Composition, Extraction, and Utilization of Wheat Germ Oil: A Review. *Eur J Lipid Sci Technol.* **2017**, *118*, 1–9.

- 51) Phillips, K. M.; Ruggio, D. M.; Toivo, J. I.; Molly, S.; Amy, S. Free and Esterified Sterol Composition of Edible Oils and Fats. *J Food Compost Anal.* **2002**, *15*, 123–142.
- 52) Moreau, R. A.; Whitaker, B. D.; Hicks, K. B. Phytosterols, Phytostanols, and Their Conjugates in Foods: Structural Diversity, Quantitative Analysis, and Health-Promoting Uses. *Prog. Lipid Res.* **2002**, *41*, 457–500.
- 53) Moreau, R. A.; Nyström, L.; Whitaker, B. D.; Winkler-Moser, J. K.; Baer, D. J.; Gebauer, S. K.; Hicks, K. B. Phytosterols and Their Derivatives: Structural Diversity, Distribution, Metabolism, Analysis, and Health-Promoting Uses. *Prog. Lipid Res.* **2018**, *70*, 35-61.
- 54) Villegas, L.; Benavente, F.; Sanz-Nebot, V.; Grases, J. M.; Barbosa, J. A Rapid and Simple Method for the Analysis of Bioactive Compounds in Olive Oil Refining By-Products by Liquid Chromatography with Ultraviolet and Mass Spectrometry Detection. *J Food Compost Anal.* **2018**, *69*, 107–114.
- 55) Luthria D. *Oil Extraction and Analysis*, **2004**, AOCS Press: Maryland, USA.
- 56) Andrade-Eiroa, A.; Canle, M.; Leroy-Cancellieri, V.; Cerdà, V. Solid-Phase Extraction of Organic Compounds: A Critical Review. Part II. *Trends Analyt Chem.* **2016**, *80*, 655–667.
- 57) Andrade-Eiroa, A.; Shahla, R.; Romanías, M. N.; Dagaut, P. An Alternative to Trial and Error Methodology in Solid Phase Extraction: An Original Automated Solid Phase Extraction Procedure for Analysing PAHs and PAH-Derivatives in Soot. *RSC Adv.* **2014**, *4*, 33636–33644.
- 58) Buszewski, B.; Szultka, M. Past, Present, and Future of Solid Phase Extraction: A Review. *Crit Rev Anal Chem.* **2012**, *42*, 198–213.
- 59) Ibrahim, W. A. W.; Ali, L. I. A.; Sulaiman, A.; Sanagi, M. M.; Aboul-Enein, H. Y. Application of Solid-Phase Extraction for Trace Elements in Environmental and Biological Samples: A Review. *Crit Rev Anal Chem.* **2014**, *44*, 233–254.
- 60) Christie W.; HAN X. *Lipid Analysis. Isolation, Separation, Identification and Lipidomic Analysis I*; Woodhead Publishing Limited: Cambridge, **2012**.

- 61) Augusto, F.; Hantao, L. W.; Mogollón, N. G. S.; Braga, S. C. New Materials and Trends in Sorbents for Solid-Phase Extraction. *Trends Analyt Chem.* **2013**, *43*, 14–23.
- 62) Correia, A. C.; Dubreucq, E.; Ferreira-Dias, S.; Lecomte, J. Rapid Quantification of Polar Compounds in Thermo-Oxidized Oils by HPTLC-Densitometry. *Eur J Lipid Sci Technol.* **2015**, *117*, 311–319.
- 63) Russell, J. M.; Werne, J. P. The Use of Solid Phase Extraction Columns in Fatty Acid Purification. *Org. Geochem.* **2007**, *38*, 48–51.
- 64) Grigoriadou, D.; Androulaki, A.; Psomiadou, E.; Tsimidou, M. Z. Solid Phase Extraction in the Analysis of Squalene and Tocopherols in Olive Oil. *Food Chem.* **2007**, *105*, 675–680.
- 65) Košťál, V.; Urban, T.; Řimnáčová, L.; Berková, P.; Šimek, P. Seasonal Changes in Minor Membrane Phospholipid Classes, Sterols and Tocopherols in Overwintering Insect, *Pyrhocoris Apteris*. *J. Insect Physiol.* **2013**, *59*, 934–941.
- 66) Toivo, J.; Piironen, V.; Kalo, P.; Varo, P. Gas Chromatographic Determination of Major Sterols in Edible Oils and Fats Using Solid-Phase Extraction in Sample Preparation. *Chromatographia* **1998**, *48*, 745–750.
- 67) Piironen, V.; Toivo, J.; Lampi, A.-M. Natural Sources of Dietary Plant Sterols. *J Food Compost Anal.* **2000**, *13*, 619–624.
- 68) Breinhölder, P.; Mosca, L.; Lindner, W. Concept of Sequential Analysis of Free and Conjugated Phytosterols in Different Plant Matrices. *J. Chromatogr. B Analyt. Technol. Biomed. Life Sci.* **2002**, *777*, 67–82.
- 69) Mathison, B.; Holstege, D. A Rapid Method To Determine Sterol, Erythrodiol, and Uvaol Concentrations in Olive Oil. *Journal of Agricultural and Food Chemistry* **2013**, *61* (19), 4506–4513.
- (70) Gómez-Coca, R. B.; Pérez-Camino, M. del C.; Moreda, W. On the Glucoside Analysis: Simultaneous Determination of Free and Esterified Steryl Glucosides in Olive Oil. Detailed Analysis of Standards as Compulsory First Step. *Food Chemistry* **2013**, *141* (2), 1273–1280.

- 71) Azadmard-Damirchi S.; Dutta P. Phytosterol Classes in Olive Oils and Their Analysis by Common Chromatographic Methods. In Victor R.; and Ronald R., editor. *Olives and Olive Oil in Health and Disease Prevention*; Elsevier Science & Technology, **2010**; pp 249–257.
- 72) Vaspollo G., Sole R., Mergola L., Lazzoi M., Scorrano S., M. G. Molecularly Imprinted Polymers: Present and Future Prospective. *Int J Mol Sci* **2011**, *12*, 5908 – 5945.
- 73) Qiao, F.; Sun, H.; Yan, H.; Row, K. H. Molecularly Imprinted Polymers for Solid Phase Extraction. *Chromatographia* **2006**, *64*, 625–634.
- 74) Piletska E., Kumir J., Sergeyeva T., Rational Design and Development of Affinity Adsorbents for Analytical and Biopharmaceutical. *JCAM* **2013**, *1*, 229-244.
- 75) Płotka-Wasyłka, J.; Szczepańska, N.; de la Guardia, M.; Namieśnik, J. Miniaturized Solid-Phase Extraction Techniques. *Trends Analyt Chem.* **2015**, *73*, 19–38.
- 76) Piletska, E. V.; Burns, R.; Terry, L.; Piletsky, S. Application of a Molecularly Imprinted Polymer for the Extraction of Kukoamine a from Potato Peels. *J. Agric. Food Chem.* **2012**, *60*, 95–9.
- 77) McEvoy, J. Molecular Recognition Biotechnology, Chemical Engineering and Material Applications, **2011**, Nova Science Publisher: New York, USA.
- (78) Yan, H.; Row, K. H. Characteristic and Synthetic Approach of Molecularly Imprinted Polymer. *Int J Mol Sci.* **2006**, *7*, 155–178.
- 79) Sánchez-Barragán I., Karim K., Costa-Fernández J. M., Piletsky S. A., Molecularly Imprinted Polymer for Carbaryl Determination in Watere. *Sens. Actuators.* **2006**, *123*, 798–804.
- 80) Turiel, E.; Martín-Esteban, A. Molecularly Imprinted Polymers for Sample Preparation: A Review. *Anal. Chim. Acta.* **2010**, *668*, 87–99.
- 81) Andersson, L. I.; Paprica, A.; Arvidsson, T. A Highly Selective Solid Phase Extraction Sorbent for Pre-Concentration of Sameridine Made by Molecular Imprinting. *Chromatographia* **1997**, *46*, 57–62.

- 82) Musile, G.; Cenci, L.; Piletska, E.; Gottardo, R.; Bossi, A. M.; Bortolotti, F. Development of an In-House Mixed-Mode Solid-Phase Extraction for the Determination of 16 Basic Drugs in Urine by High Performance Liquid Chromatography-Ion Trap Mass Spectrometry. *J Chromatogr A* **2018**, *1560*, 10–18.
- 83) Chianella, I, Lotierzo M, Piletsky SA, Tothill I, Chen B, Karim K, Rational Design of a Polymer Specific for Microcystin-LR Using a Computational Approach. *Anal. Chem.* **2002**, *74*, 1288–1293.
- 84) Piletska, E. V, Romero-Guerra M, Chianella I, Karim K, Turner A, Towards the Development of Multisensore for Drugs of Abuse Based on Molecular Imprinted Polymers. *Anal. Chim. Acta.* **2005**, *542*, 111–117.
- 85) Piletska E, Piletsky S, Karim K, Terpetschnig E, Introducing the Biotin-Specific Synthetic Receptors Based on Molecular Imprinted Polymerisation by Photografting from Water. *Anal. Chim. Acta.***2004**, *504*, 179–183.
- 86) Turner, N. W.; Piletska, E. V.; Karim, K.; Whitcombe, M.; Malecha, M.; Magan, N.; Baggiani, C.; Piletsky, S. a. Effect of the Solvent on Recognition Properties of Molecularly Imprinted Polymer Specific for Ochratoxin A. *Biosens Bioelectron.* **2004**, *20*, 1060–1067.
- 87) Brragan I, Karim K, Fernandez J, P. S. A Molecularly Imprinted Polymer for Carbayl Determination in Water. *Sens Actuators B Chem.* **2007**, *123*, 798–804.
- 88) Breton F, Rouillon R, Piletska E, Karim K, Guerreiro A, Chianella I, P. S. Virtual Imprinting as a Tool to Design Efficient MIPs for Photosynthesis-Inhibiting Herbicides. *Biosens Bioelectron* **2005**, *22*, 1948–1954.
- 89) Song, X.; Xu, S.; Chen, L.; Wei, Y.; Xiong, H. Recent Advances in Molecularly Imprinted Polymers in Food Analysis. *J Appl Polym Sci* **2014**, *131*, 1-18 .
- 90) Madikizela, L. M.; Tavengwa, N. T.; Chimuka, L. Applications of Molecularly Imprinted Polymers for Solid-Phase Extraction of Non-Steroidal Anti-Inflammatory Drugs and Analgesics from Environmental Waters and Biological Samples. *J Pharm Biomed Anal.* **2018**, *147*, 624–633.

- 91) Ashleya, Jon; Ali Shahbazia, Mohammad; Kanta, Krishna; Aaydha, Vinayaka; Chidambarab, Wolff, Aanders; , Dang Duong Bangb; Sun, Y. Molecularly Imprinted Polymers for Sample Preparation and Biosensing in Food Analysis: Progress and Perspectives. *Biosens Bioelectron.* **2017**, *91*, 606–615.
- 92) Gilart, N.; Borrull, F.; Fontanals, N.; Marcé, R. M. Selective Materials for Solid-Phase Extraction in Environmental Analysis. *TrEAC* **2014**, *1*, e8–e18.
- 93) Lin, X. H.; Aik, S. X. L.; Angkasa, J.; Le, Q.; Chooi, K. S.; Li, S. F. Y. Selective and Sensitive Sensors Based on Molecularly Imprinted Poly (Vinylidene Fluoride) for Determination of Pesticides and Chemical Threat Agent Simulants. *Sens Actuators B Chem* **2018**, *258*, 228–237.
- 94) Wang, T.; Shannon, C. Electrochemical Sensors Based on Molecularly Imprinted Polymers Grafted onto Gold Electrodes Using Click Chemistry. *Anal. Chim. Acta.* **2011**, *708*, 37–43.
- 95) Chianella, I.; Guerreiro, A.; Moczko, E.; Caygill, J. S.; Piletska, E. V.; De Vargas Sansalvador, I. M. P.; Whitcombe, M. J.; Piletsky, S. A. Direct Replacement of Antibodies with Molecularly Imprinted Polymer Nanoparticles in ELISA—Development of a Novel Assay for Vancomycin. *Anal. Chem.* **2013**, *85*, 8462–8468.
- 96) Chianella, I.; Karim, K.; Piletska, E. V.; Preston, C.; Piletsky, S. a. Computational Design and Synthesis of Molecularly Imprinted Polymers with High Binding Capacity for Pharmaceutical Applications-Model Case: Adsorbent for Abacavir. *Anal. Chim. Acta.* **2006**, *559*, 73–78.
- 97) Fireman-Shoresh, S.; Avnir, D.; Marx, S. General Method for Chiral Imprinting of Sol-Gel Thin Films Exhibiting Enantioselectivity. *Chem. Mater.* **2003**, *15*, 3607–3613.
- 98) Wulff, G. G. Fourty Years of Molecular Imprinting in Synthetic Polymers: Origin, Features and Perspectives. *Mikrochim Acta* **2013**, *180*, 1359–1370.
- 99) Muratsugu S.; Tada M. A Molecular Imprinting polymer as Catalyst in Alvarez-Lorenzo C.; Concheiro A., Editor., *Handbook of Molecularly Imprinted Polymers*. Smithers Rapra Technology Ltd: **2013**pp 259-308.

- 100) Tong, K.; Xiao, S.; Li, S.; Wang, J. Molecular Recognition and Catalysis by Molecularly Imprinted Polymer Catalysts: Thermodynamic and Kinetic Surveys on the Specific Behaviors. *J Inorg Organomet Polym Mater* **2008**, *18*, 426–433.
- 101) Li, S.; Gi, Y.; Turner, F. A Catalytic and Positively Thermosensitive Molecularly Imprinted Polymer. *Adv Funct Mater.* **2011**, *21*, 1194–1200.
- 102) Cunliffe, D.; Kirby, A.; Alexander, C. Molecularly Imprinted Drug Delivery Systems. *Adv. Drug Deliv. Rev.* **2005**, *12*, 1836-1853
- 103) Piletska, E. V.; Abd, B. H.; Krakowiak, A. S.; Parmar, A.; Pink, D. L.; Wall, K. S.; Wharton, L.; Moczko, E.; Whitcombe, M. J.; Karim, K.; Piletsky, S. Magnetic High Throughput Screening System for the Development of Nano-Sized Molecularly Imprinted Polymers for Controlled Delivery of Curcumin. *Analyst* **2015**, *140*, 3113–3120.
- 104) Wu, L.; Li, Y. Study on the Recognition of Templates and Their Analogues on Molecularly Imprinted Polymer Using Computational and Conformational Analysis Approaches. *J. Mol. Recognit.* **2004**, *17*, 567–574.
- 105) Ostrowski, J.; Kjelsberg, M.; Caron, M.; Lefkowitz, R. Mutagenesis of the Beta-Adrenergic Receptor: How Structure Elucidates Function. *Annu. Rev. Pharmacol. Toxicol.* **1993**, *32*, 167–183.
- 106) Luliński, P. Molecularly Imprinted Polymers Based Drug Delivery Devices: A Way to Application in Modern Pharmacotherapy. A Review. *Mater Sci Eng C Mater Biol Appl.* **2017**, *76*, 1344–1353.
- 107) Rathbone, D. Molecularly Imprinted Polymers in the Drug Discovery Process. *Adv. Drug Deliv. Rev.* **2005**, *57*, 1854–1874.
- 108) Brantl V.; Picone D.; Amodeo P.; Temussi P. Solution Structure of Casokefamide. *Biochem. Biophys. Res. Commun.* **1993**, *191*, 853–859.
- 109) Mohamed, R.; Mottier, P.; Treguier, L.; Richoz-Payot, J.; Yilmaz, E.; Tabet, J.-C.; Guy, P. A. Use of Molecularly Imprinted Solid-Phase Extraction Sorbent for the Determination of Four 5-Nitroimidazoles and Three of Their Metabolites from Egg-Based

Samples before Tandem LC–ESIMS/MS Analysis. *J. Agric. Food Chem.* **2008**, *56*, 3500–3508.

110) Karim, K.; Breton, F.; Rouillon, R.; Piletska, E. V.; Guerreiro, A.; Chianella, I.; Piletsky, S. a. How to Find Effective Functional Monomers for Effective Molecularly Imprinted Polymers? *Adv. Drug Deliv. Rev.* **2005**, *57*, 1795–1808.

(111) Nicholls A.; Adbo K.; Andersson H.; Andersson O., Ankarloo J.; Hedin-Dahlström J.; Jokela J. Karlsson G.; Olofsson L.; Rosengren J.P.; Shoravi S.; Can we rationally design molecularly imprinted polymers? *Anal. Chim. Acta.* **2001**, *435*, 9-18.

(112) Guerreiro, A.; Soares, A.; Piletska, E.; Mattiasson, B.; Piletsky, S. Preliminary Evaluation of New Polymer Matrix for Solid-Phase Extraction of Nonylphenol from Water Samples. *Anal. Chim. Acta.* **2008**, *612*, 99–104.

# Chapter two

# **Development of RDP resin and SPE protocol for extraction of $\alpha$ -tocopherol and other physiologically-active components from sunflower oil**

## **2.1 Introduction**

### **2.1.1 Multi-target adsorbents**

In the last few years, particular attention has been given to the development of detecting multiple targets simultaneously in various matrices, such as food and environmental complexes or biological samples, that has encouraged the enhancement of the analytical methodology.<sup>1-8</sup> One of the early trials was reported by Lechner and co-workers using silica gel in SPE cartridge and the eluted samples were analysed by GC/FID.<sup>1</sup> The proposed method performed determination of the quantities of  $\alpha$ -tocopherol,  $\beta$ -tocopherol,  $\gamma$ -tocopherol,  $\delta$ -tocopherol, brassicasterol, stigmasterol, campesterol,  $\beta$ -sitosterol and  $\Delta^5$ -avenasterol simultaneously, in five types of vegetable seed oils including rapeseed, sunflower, soybean, castor and cuphea.<sup>1</sup> The recent studies have shown several feasible protocols for group-specificity molecularly imprinted polymers that demonstrated considerable recognition for a wide range of compounds simultaneously.<sup>2-4</sup> These MIPs have been developed based on chromatographic techniques coupled to one of the standard detecting technologies such as the UV detector, fluorescence, diode array detector or mass spectrometer. Madikizela and co-workers introduced a MIP that has simultaneous selectivity towards three acidic pharmaceutical compounds as templates.<sup>5</sup> The polymer was synthesised using 2-vinyl pyridine as a functional monomer with EGDMA as cross-linker in the presence of diclofenac (3), ibuprofen (1) and naproxen (2) as templates (Figure 2.1). The synthesised polymer was capable of recognising all the three compounds, even in the presence of competitor compound gemfibrozil (4) (Figure 2.1).<sup>5</sup>

Furthermore, Lolic and co-workers optimised an SPE protocol using commercial adsorbent (Strata-X) to extract a group of compounds from seawater at the same time.<sup>6</sup> The eluted compounds from seawater include diclofenac, 1-hydroxyibuprofen (5), carboxyibuprofen (6), acetaminophen (7), acetylsalicylic acid (8), naproxen (2),

nimesulide (9), ketoprofen (10) and ibuprofen (1) (Figure 2.1). These compounds were extracted from several seawater samples collected from different places, some of the seawater samples had all the compounds and were separated, while other samples had only a few of these compounds. The analysis was performed by UHPLC with a C18 column.<sup>6</sup> Another study on similar compounds (1, 2, 3, 4, 10 in Figure 2.1) was reported by Lindqvist *et al.*, using SPE via Oasis MCX commercial cartridge.<sup>7</sup> The compounds were separated from sewage water and were analysed using HPLC/MS. Regarding the biological samples, Stolker and Brinkman reviewed the different types of SPE cartridges which were used for separating various drugs from biological tissues including liver, kidney and meat.<sup>8</sup> The authors reported the most widely used polymeric sorbents including the (poly)styrene-divinylbenzene co-polymers, Oasis-HLB, N-vinylpyrrolidone and divinyl-benzenes.

On the other hand, non-imprinted polymers accompanying synthesis of the imprinted polymer as a control have shown considerable group specificity to some compounds, though it was less than what has demonstrated by MIP. Non-imprinted polymers are synthetic material from functional monomers connected with excess cross-linkers. NIPs have the same chemical characteristics except for the presence of the cavities with specific recognition. However, functional monomers in NIPs serve as binding sites which lead to exhibition of strong non-specific binding to the organic compounds in the analytes.<sup>9-13</sup> For example, Meischl and co-workers extracted acetylsalicylic and salicylic acid simultaneously with the percentage recovery of 98.4% using a NIP synthesised, acrylamide (functional monomer) and EGDMA (cross-linker).<sup>11</sup> Moreover, it was possible to extract 17 $\beta$ -estradiol (harmful compound in water) using NIP at a high level of efficiency (80%).<sup>9</sup> In addition, NIP synthesised by Boulanouar and co-workers used MAA as a functional monomer and EGDMA as a cross-linker. NIP demonstrated specific recognition towards five compounds with the percentage recovery of 75 $\pm$ 13%. These five compounds include: fenthion sulfoxide, malathion, diazinon, fenitrothion and fenthion. In some cases, NIP outperformed MIP and C18 as a material for extraction and concentration of nonylphenol from a water sample.<sup>13</sup>

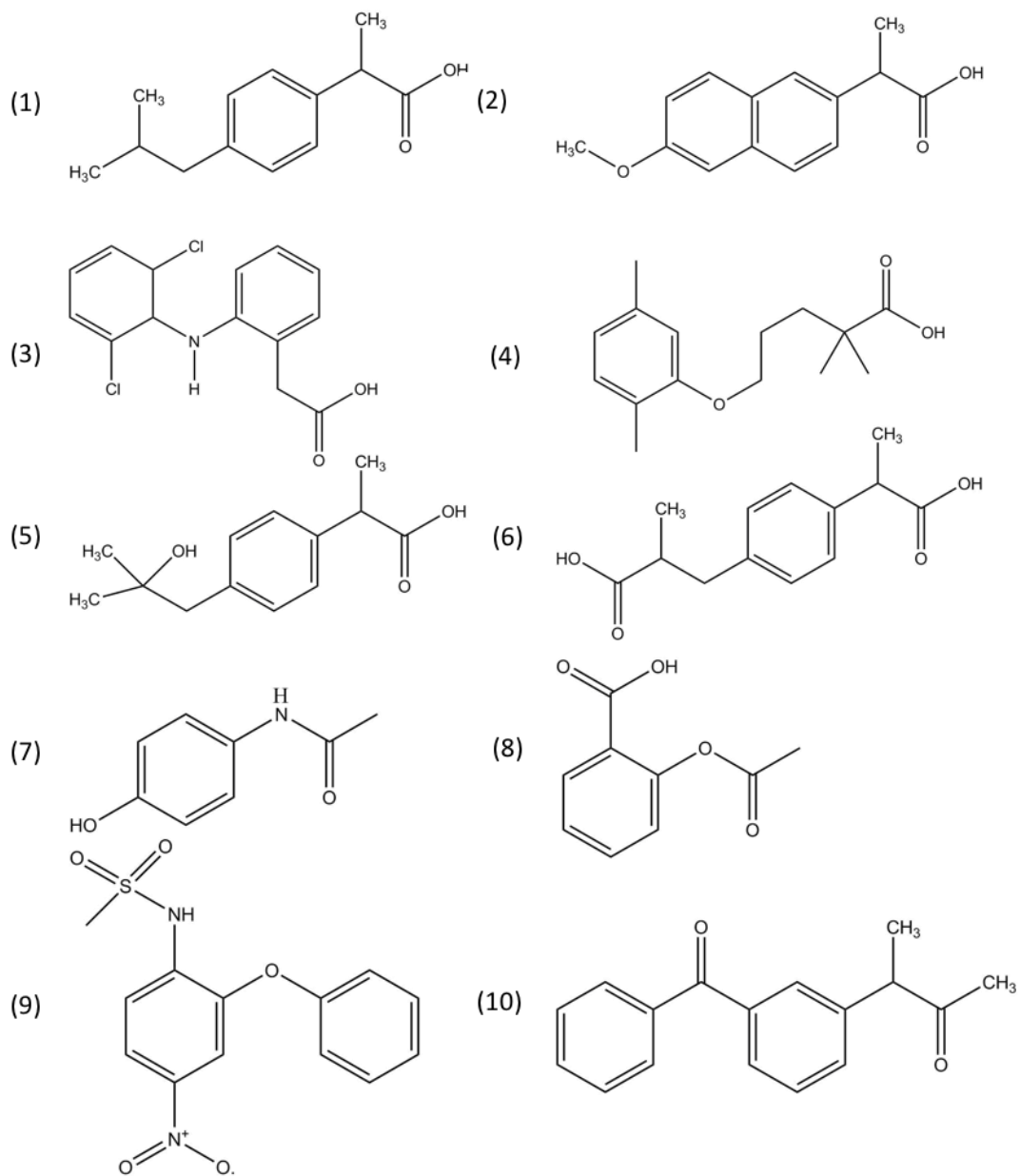


Figure 2.1: Chemical structures of some pharmaceuticals extracted using group-specificity MIP. <sup>5-8</sup>

1) Ibuprofen, 2) naproxen, 3) diclofenac, 4) gemfibrozil, 5) 1-hydroxyibuprofen, 6) carboxyibuprofen, 7) acetaminophen, 8) acetylsalicylic acid, 9) nimesulide and 10) ketoprofen.

### 2.1.2 RDP versus MIP

Regardless the immense attention that MIPs have gained as sorbents employed in classical solid phase extraction for sample preparation, there are some limitations in this methodology demanding more development to overcome such limitation. The most common reported drawback of this technique was the bleeding which occurred in case of incomplete removal of the template (target) molecules from the MIP after the polymerisation. Bleeding led to false positive quantification which is defined as the overestimation of the quantities in the real sample.<sup>3,4</sup> One of the suggested solution was to use the dummy template which was a structural analogue of the template molecule, that was used as a template in synthesis the imprinted polymer. This helped to distinguish between the dummy template and the main target in the real sample in case of leakage from the MIP during the analysis.<sup>3,4,14</sup>

Typically, SPE is performed using stationary phase packed in glass or plastic columns. However, the commercial stationary phases are often blamed for their poor stability, which limits a selection of compatible solvents, for inadequate selectivity, limited reusability and restricted binding capacity, especially for polar compounds.<sup>22,23</sup> Therefore, due to the absence of effective commercial resins for extraction of  $\alpha$ -tocopherol and other secondary metabolites from oil matrices, there is a demand for economical, alternative stationary phase that could be cost-effective and, potentially, be suitable for industrial applications. This chapter includes the development of Rational Designed Polymer (RDP) as a resin for the extraction and purification of a group of minor components including free fatty acids,  $\alpha$ -tocopherol and some phytosterols from such complex and dense matrix like sunflower oil. It is important to highlight that due to the complexity and high viscosity of the oil matrix, the extraction of any compounds from natural oils is a very challenging task. There are very scarce publications that report successful development of the Molecularly Imprinted Polymers as resins for extraction of the oil-soluble pesticides.<sup>12,16-18</sup> Among the advantages of RDPs which could make them suitable for analytical and industrial applications are their low cost, potential group-specificity towards the compounds sharing some common functionalities, and compatibility with mass-manufacturing and high stability.<sup>14,24,25</sup> This chapter demonstrates the development of the protocols and materials, which could effectively be applied for the extraction of minor components of sunflower and other vegetable oils.

## 2.2 Materials and methods

### 2.2.1 Chemicals and reagents

Unrefined sunflower oil was purchased from Activecare through Amazon.com. The vegetable oil-originated  $\alpha$ -tocopherol, a mixture of phytosterols consisting of 46%  $\beta$ -sitosterol, 24% campesterol and 16% stigmasterol were obtained from Santa Cruz Biotechnology (UK). Samples of free fatty acids containing palmitic, oleic and linoleic acids were purchased from Aldrich (UK). Methanol, ethyl acetate, heptane, acetonitrile, n-hexane, dichloromethane and acetic acid were obtained from Fisher Scientific (UK). All solvents were of HPLC-quality grade and used without any purification. 1,1'-azobis(cyclohexane carbonitrile), methacrylic acid (MAA) and ethylene glycol dimethacrylate (EGDMA) were purchased from Aldrich (UK). Dimethylformamide (DMF) was obtained from Acros Organics (UK).

### 2.2.2 Equipment and analysis techniques

The characterisation of the rationally designed polymer was performed using a standard solution of  $\alpha$ -tocopherol (model solution) using UV-Vis spectrophotometer (Shimadzu, UV1800, UK). In the current research, it was found that  $\alpha$ -tocopherol absorbs UV light to give a peak at wavelength  $\lambda_{\max}$  296 nm in direct proportion to its concentration in the sample. Therefore, the UV absorption spectroscopy ( $\lambda_{\max}$  296 nm) was the first analytical technique applied here to quantify the bound  $\alpha$ -tocopherol in hexane and for the evaluation of the binding capacity of the polymer. The optimisation process was applied to SPE extraction from the model solution. One mL SPE columns were packed with 100 mg of the RDP and used in combination with a vacuum manifold (Supelco, UK). All SPE experiments were repeated five times.

The second part of the experiment was applying the optimised protocol to the sunflower oil. The quantification of the eluted  $\alpha$ -tocopherol and other minor components was performed using the Gas Chromatography-Mass-spectrometry (GC/MS) set-up (Perkin Elmer, TurboMass, UK) using a 30 m x 250  $\mu$ m, 0.25 mm I.D., ZB-5 capillary column (Phenomenex, UK). Helium gas was used as mobile phase to carry the sample at a flow-rate of 1 mL min<sup>-1</sup> at 200 °C. After injection of 10  $\mu$ L of the sample at 200 °C, the temperature of the GC oven was raised by 10 °C min<sup>-1</sup> to 350 °C and held for 3 min.

### 2.2.3 Molecular modelling of the $\alpha$ -tocopherol-specific polymers

A computer-aided rational design was used for the optimisation of molecular imprinting procedure. In the current research, molecular modelling was the first step to design the polymer that is going to be the stationary phase in SPE. Molecular modelling was performed using a workstation from Research Machines running the CentOS 5 GNU/Linux operating system. The workstation was configured with a 3.2GHz core 2 duo processor, 4 GB memory and a 350 GB fixed drive. Molecular modelling was executed via the software packages SYBYL 7.0 (Tripos Inc., St. Louis, Missouri, USA). The library of functional monomers was chosen and developed in S. Piletsky group. The functional monomers in this library are available and inexpensive to use rapidly and easily by screening them using the LEAPFROG algorithm. The LEAPFROG algorithm works by screening the library of commonly used functional monomers for their potential interactions with the template ( $\alpha$ -tocopherol) that is either downloaded or drawn. The calculated energies are a combination of (i) a typical monomer-template complexation and (ii) a system of scoring the complementarities between monomer and template where the template is defined by LEAPFROG as the receptor binding site (using additional site-point matching scores, a system of scoring the receptor and ligand interactions).<sup>26</sup>

The monomers were ordered in terms of the strength of their possible interactions with the template ( $\alpha$ -tocopherol). The monomers were ranked by the highest binding score ( $\text{kcal mol}^{-1}$ ) as the best candidates for polymer preparation. The library consists of 22 functional monomers (Figure 2.2 showed some of them) that are commonly used in molecular imprinting due to their ability to interact with a template through ionic and hydrogen bonds, van der Waals' and dipole-dipole interactions.<sup>27</sup> The molecular energy of each monomer from the library was minimised at a value of  $0.01 \text{ kcal mol}^{-1}$  and the charges for each atom were calculated. The structures of the monomers were then refined using molecular mechanical methods. The 2D structures of  $\alpha$ -tocopherol and monomers were minimised, and Gasteiger-Hückel charges were applied to obtain the 3D molecular structure.

#### 2.2.4 Synthesis of RDP

The preparation of the polymer was done by weighing all the components of the polymerisation mixture. Firstly, as shown in Table 2.1, 1 g (10%) of each monomer with 9 g (90%) of EGDMA were dissolved in the equal weight of dimethyl formamide (DMF) 10 g, then, 100 mg (1%) of the initiator 1,1'-azobis (cyclohexane carbonitrile) was added. All the components were dissolved using an ultrasonic bath for 5 min. Subsequently, the monomeric mixture was deoxygenated by purging with nitrogen for 10 min. The vial with monomeric mixture was tightly closed using parafilm and thermo-polymerised at 80 °C for 24 h. On the next day, the polymer was removed from the vial, and ground using electrical mortar. The resulting particles were sieved and polymer fraction with a size between 63 to 125 µm was collected. The prepared polymer fraction was washed overnight using Soxhlet extraction with methanol. The polymer was dried in the oven at 70 °C. Finally, 100 mg of polymer was packed in 1 mL SPE cartridge and used for extraction experiments. 100 mg of each polymer was packed in 1 mL SPE cartridge to evaluate the binding ability of  $\alpha$ -tocopherol to these polymers as a stationary phase in SPE. In this experiment, 1 mL of 0.1 mg mL<sup>-1</sup>  $\alpha$ -tocopherol in hexane was loaded in those cartridges after conditioning them with hexane. The absorption of UV light at wavelength 296 nm was measured for all the samples of  $\alpha$ -tocopherol before loading and after loading. By using calibration curves, the concentrations of these samples were calculated.

#### 2.2.5 Evaluation of the $\alpha$ -tocopherol binding ability

The outcome of the modelling is a list of monomers ordered based on their binding energy. In order to choose one of them, the top 6 monomers in the list were used to prepare rationally-designed polymers (RDPs) with EGDMA (Table 2.2) as a very commonly used cross-linker that gives the polymer the rigidity. In addition, EGDMA as a monomer has been evaluated from the list to assess the potential interaction with the difference in the concentration of  $\alpha$ -tocopherol before and after loading was used to evaluate the binding ability of  $\alpha$ -tocopherol to the polymers then calculated the binding percentage for each polymer as shown in Table 2.3. The evaluation of the polymers was performed using SPE technique. All these steps were repeated three times for each polymer.

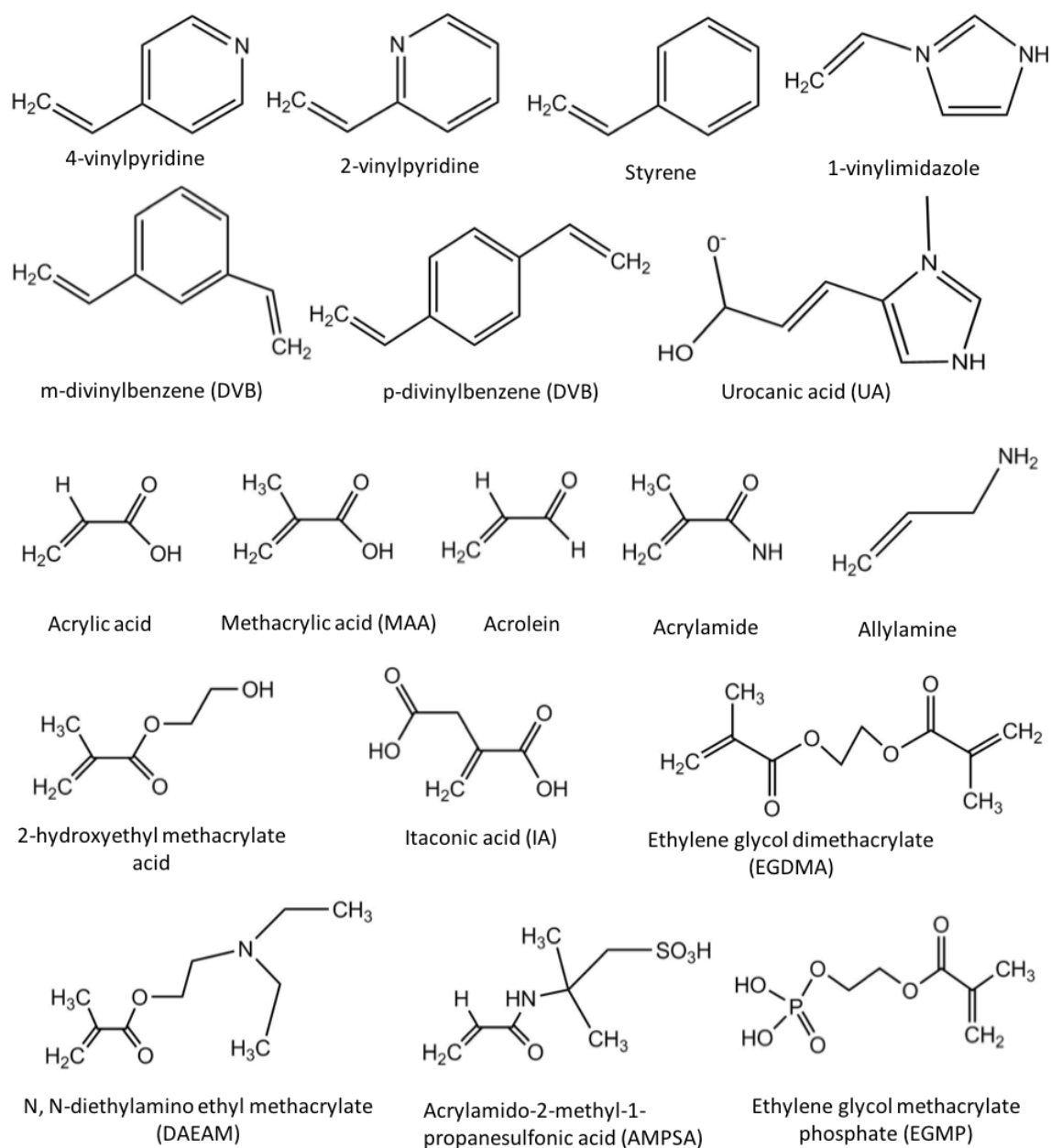


Figure 2.2: The library of functional monomers used in LEAPFROG screening.<sup>44</sup>

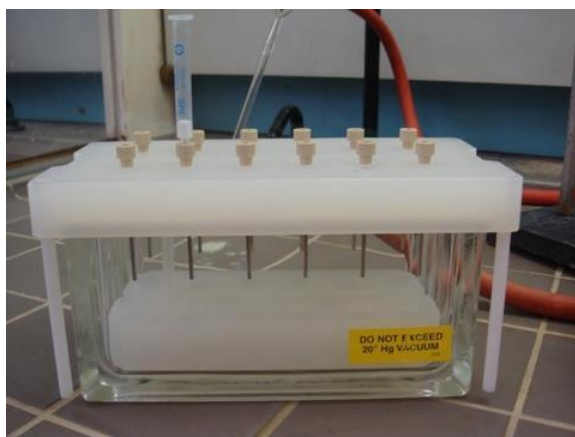


Figure 2.3: Solid phase extraction tools.

Table 2.1: The different polymers composition using different functional monomers.

Compositions	Quantities (g)						
	Pol.1	Pol.2	Pol.3	Pol.4	Pol.5	Pol.6	Pol.7
EGMP	-	-	-	-	-	-	1
MAA	-	-	-	-	-	1	-
AMPSA	-	-	-	-	1	-	-
IA	-	-	-	1	-	-	-
Acrylamide	-	-	1	-	-	-	-
DEAEA	-	1	-	-	-	-	-
EGDMA (cross-linker)	10	9	9	9	9	9	9
DMF (porogen)	10	10	10	10	10	10	10
Initiator	0.1	0.1	0.1	0.1	0.1	0.1	0.1

### 2.2.6 Choosing the cross-linker

In experiment of 2.2.5 the polymers were synthesised using EGDMA as the common cross-linker, in this experiment, DVB was replaced by EGDMA to comparison purpose. Based on the result of the computational modelling, the composition of the polymer has been designed using the functional monomer(s) selected using computational modelling. Based on the outcome of the computational modelling, the composition of the polymer has

been designed using the functional monomer(s) selected using computational modelling. Methacrylic acid (MAA) was selected as the first monomer which demonstrated a high natural binding towards the  $\alpha$ -tocopherol. Two options as cross-linkers, divinyl benzene (DVB) and ethylene glycol dimethacrylate (EGDMA), were selected to choose one of them for the preparation of two MAA-based polymers (MD and MV correspondingly) as shown in Table 2.2.

Table 2.2: The polymer composition (g) of two MAA-based polymers with different cross-linkers.

Composition	MD	MV
Monomer (MAA)	1	1
Cross-linker (DVB)	9	0
Cross-linker (EGDMA)	0	9
Initiator	0.1	0.1
DMF (porogen)	10	10

All the components in Table 2.2 were dissolved using an ultrasonic bath for 5 min. Then, the monomeric mixture was deoxygenated by purging with nitrogen for 10 min. The vial with monomeric mixture was tightly closed using parafilm and thermo-polymerised at 80 °C for 24 h. The polymers MD and MV were grinded, sieved, washed and dried as mentioned in 2.3.4.

### 2.2.7 Polymer synthesis and optimisation of the monomer cross-linker ratio

Several RDPs were prepared with different monomer: cross-linker ratios (0:100 (P1), 1:99 (P2), 10:90 (P3) and 20:80 (P4)) to determine the polymer representing the best performance in the recovery of  $\alpha$ -tocopherol. The composition of the polymerisation mixtures was reported in Table 2.3. All components were dissolved, using an ultrasonic bath for 5 min. Subsequently, the monomeric mixture was deoxygenated by purging with nitrogen for 10 min. The vials containing the monomeric mixtures were tightly closed and allowed to polymerise thermally in a thermostatically-controlled oil bath at 80 °C for 24h.

Table 2.3: The polymer composition with different monomer: cross-linker ratio.

a) MAA, b) EGDMA, c) 1, 1'- azobis (cyclohexane carbonitrile).

Reagents	Quantity (g)			
	P1	P2	P3	P4
Monomer (M) a	0	0.1	1	2
Cross-linker (C) b	10	9.9	9	8
Ratio C:M	1:0	9.9:0.1	9:1	8:2
Initiator c	0.1	0.1	0.1	0.1
DMF	10	10	10	10

After polymerisation, the monolithic polymer was removed from the vial and ground using a ZM200 Ultracentrifuge Mill (Retsch, UK). The obtained polymer powder was sieved using AS200 Sieve Shaker (Retsch, UK) and a fraction of polymer particles with sizes between 63 to 125  $\mu\text{m}$  was collected. The isolated polymer fraction was washed for 12 h using Soxhlet extraction with methanol. The polymer was dried in the oven at 70 °C. Finally, 1 mL SPE cartridges were packed with 100 mg of polymer and used in extraction experiments. All SPE experiments were repeated 5 times.

### 2.2.8 Quantification of $\alpha$ -tocopherol

Since  $\alpha$ -tocopherol was the template that has been used to make the modelling for the RDP, a standard solution of  $\alpha$ -tocopherol was used to evaluate the different polymers. The analytical techniques used to characterise the polymers were UV spectroscopy and GC/MS. Therefore, two calibration curves were prepared by plotting the absorbance (in UV spectroscopy) and the peak integration (in GC/MS) against the different level of concentration of  $\alpha$ -tocopherol solution in hexane.

The calibration curves for UV analysis were made using different concentrations of  $\alpha$ -tocopherol in hexane to calculate the concentration of  $\alpha$ -tocopherol in all samples that were analysed by UV spectroscopy. The chosen range of concentration was determined based on the UV absorbance of  $\alpha$ -tocopherol that gives the linear relationship between

concentration and UV absorbance. The final concentration of  $\alpha$ -tocopherol was calculated using the same calibration curve by evaporating the eluted solvent, and then, analyte was dissolved in hexane before measuring its absorbance.

Since the integration values of the area under the peaks in the GC/MS chromatograms are directly proportional to the concentration of the analysed sample, a calibration curve of  $\alpha$ -tocopherol was made using the integration of the peaks to calculate the concentration of  $\alpha$ -tocopherol in the different fractions of SPE protocol and to calculate the concentration of  $\alpha$ -tocopherol with other minor components from oil samples.

## **2.2.9 Characterisation of RDP**

### **2.2.9.1 Measuring the surface area of RDPs**

The multi-point Brunauer, Emmett and Teller (BET) method was used to evaluate the surface area of the developed RDPs using Surface Area and Pore Size Analyser (Quantachrome, UK).<sup>28,29</sup> The 45-points isotherm curve was used to evaluate the total pore volume and average pore diameter.

### **2.2.9.2 Calculation of the breakthrough volume**

In order to measure the 'breakthrough' volume of the developed polymer a model solution of  $\alpha$ -tocopherol in heptane ( $0.1 \text{ mg mL}^{-1}$ ) was prepared. SPE was carried out using 100 mg of the polymer backed in cartridge that attached to a vacuum manifold at a flow rate  $0.5 \text{ mL min}^{-1}$ . Sequential aliquots of these solutions were passed through the cartridges, and the amount of free  $\alpha$ -tocopherol left in the filtrates was quantified using a UV-Vis spectrophotometer 2100UVPC (Shimadzu, UK) at a wavelength of 296 nm. The breakthrough volume was calculated as the amount of  $\alpha$ -tocopherol adsorbed from the fractions that demonstrated  $\leq 50\%$  adsorption.<sup>26,30</sup> All experiments were conducted in five repeats.

### **2.2.9.3 Calculation of the binding capacity**

The data of the breakthrough volume was used to calculate the binding capacity (B) of the RDP. One millilitre of a model solution of  $\alpha$ -tocopherol in heptane ( $0.1 \text{ mg mL}^{-1}$ )

was filtered through 100 mg of polymer. The polymer capacity was calculated using the equation 2.2:<sup>10,31</sup>

$$B = (C_i - C_f) V m^{-1}$$

**Equation 2.1:** The polymer capacity<sup>11,28</sup>

Where  $C_i$  and  $C_f$  are the initial and final concentration (fraction correspond to 50% adsorption by the polymer) of free analyte,  $V$  is the breakthrough volume and  $m$  is the weight of the polymer.

#### **2.2.9.4 Calculation of the $\alpha$ -tocopherol recovery**

This test was done by filtering 1 mL of heptane spiked with 0.1 mg of  $\alpha$ -tocopherol (model solution) through 100 mg of the developed RDP. Then, 1 mL of methanol containing 5% acetic acid was used to elute the bound  $\alpha$ -tocopherol from the RDP. A comparison between the synthesised polymers and their selection was performed based on the percentages of  $\alpha$ -tocopherol recovered from the polymers after the elution process.

#### **2.2.9.5 The reusability of the polymer**

To assess the possibility of reusing the cartridge for SPE used for a standard solution of  $\alpha$ -tocopherol and 20% sunflower oil, this cartridge was washed with 3 mL of 10% acetic acid-methanol, then 5 to 7 mL of acetonitrile. Then, after drying the polymer, SPE protocol was applied again. The process was repeated 7 times.

#### **2.2.10 Optimisation of SPE protocol for $\alpha$ -tocopherol solution**

The optimisation protocol involved choosing different solvents in each step of the SPE process, such as loading, washing and eluting solvents. The primary selection of solvents was based on literature data that described studies of SPE for  $\alpha$ -tocopherol, as shown in Table 2.4.<sup>14,34,26,33,34</sup> In order to evaluate the extraction process, the highest percentage of  $\alpha$ -tocopherol recovered was used as an indication of the optimal conditions.

Table 2.4: The candidate solvents used for optimisation SPE conditions.<sup>14, 23,26,33,34</sup>

SPE step	Solvents
Conditioning and loading	Hexane, heptane
Wash	Hexane, 50, 60 and 70 % methanol
Elution	Acetonitrile, absolute methanol, methanol with 5% acetic acid

## 2.2.11 Application of optimised conditions for the extraction of $\alpha$ -tocopherol from sunflower oil

### 2.2.11.1 Development of the ratio between the oil and loading solvent

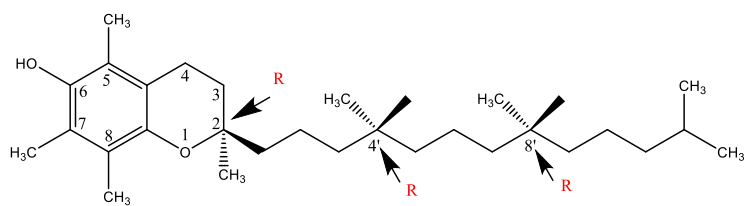
A possibility to use neat oil in combination with RDP was assessed. Unfortunately, due to the high viscosity of oil, it was not possible. Therefore, in order to determine the optimal dilution of sunflower oil in the loading solvent (heptane) 1:9, 1:4, 3:7, 4:6 and 5:5 ratios between oil and heptane were prepared and tested. Sunflower oil samples in heptane were filtered through SPE cartridge packed with 200 mg RDP. The requirements of the washing step were that solvent should remove interfering compounds and impurities without losing the compound of interest ( $\alpha$ -tocopherol).

The loaded oil sample, which consisted of 1 mL of 20% (v/v) sunflower oil in heptane, was spiked with internal standards as follows: 300  $\mu\text{g mL}^{-1}$  of palmitic acid, linoleic acid,  $\alpha$ -tocopherol and a mixture of phytosterols ( $\beta$ -sitosterol, campesterol and stigmasterol). The cartridge was washed with 1 mL of 60% methanol, followed by elution using 3 mL of methanol containing 5% acetic acid. The eluted samples were evaporated and then reconstituted in 1 mL of hexane before GC/MS analysis. The percentage of eluted compounds were calculated using the internal standards and corresponding calibration curves. Each experiment was repeated 5 times.

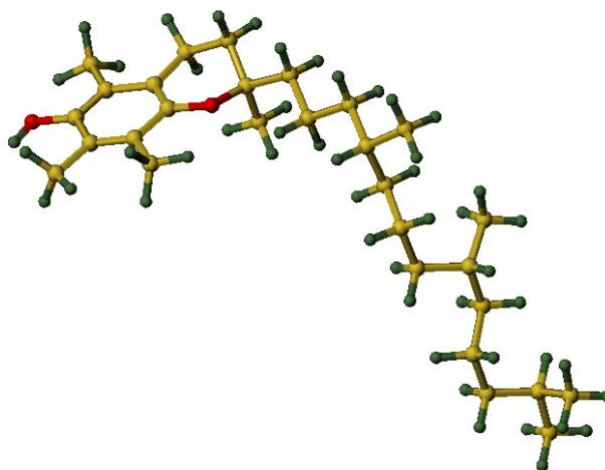
## **2.3 Results and discussion**

### **2.3.1 Molecular modelling**

The design of imprinted polymers for a new template is a multi-step process. It is time-consuming and demands a trial-and-error approach to optimise the polymer components. Different parameters should be considered to design certain polymer such as type and quantity of the functional polymer/s, cross-linker, template and temperature in which the polymerisation performed in the case of using template temperature responsive or temperature sensitive. Several methods have been suggested in the literature to design MIPs instead of experimental methods, including chemometric, molecular modelling and computational methods.<sup>2</sup> Currently, molecular modelling has become an increasingly popular approach that provides reliable data to speculate (computationally) on the strength of the interactions between the target molecule and the functional monomer/s in the synthesis. Madikizela and co-workers described molecular modelling as a trustworthy tool that helps to calculate the binding energy (computationally) before practically evaluating the affinity of the monomers towards specific target molecule.<sup>3</sup> In general, the use of computational chemistry to design the imprinted polymers has proved that it is useful in terms of facilitating the development of synthesising the imprinted polymer with lower consumption of the chemical reagents. Therefore, the aim of this part of the study was production of a list of group of monomers that have affinity towards  $\alpha$ -tocopherol.



(a)



(b)

Figure 2.4: The chiral centres in the 2D molecular structure (a), 3D molecular structure of  $\alpha$ -tocopherol minimised using the SYBYL software (b).

The chemical structure of  $\alpha$ -tocopherol has three chiral centres (Figure 2.4 a). Therefore, there are 8 possible stereoisomers of  $\alpha$ -tocopherol. However, natural  $\alpha$ -tocopherol occurs only in the  $(2R, 4'R, 8'R)$  configuration. A molecular model of  $\alpha$ -tocopherol was drawn in the configuration of  $2R, 4'R, 8'R$  using the SYBYL software, then the chemical structure was minimised (Figure 2.4 b).

Table 2.5: The list of functional monomers suggested by SYBYL software based on the template structure ( $\alpha$ -tocopherol).

Functional monomer	Binding score (kcal mol <sup>-1</sup> )	Functional monomer	Binding score (kcal mol <sup>-1</sup> )
EGMP	-32.41	4-vinylpyridine	-23.05
MAA	-31.65	EGDMA (cross-linker)	-20.28
UA	-29.74	1-vinylimidasole	-18.14
AMPSA	-28.85	o-DVB	-17.09
IA	-27.79	p-DVB	-14.73
Acrylamide	-26.16	Styrene	-13.54
DEAEM	-25.03	m-DVB	-11.65

The minimised structure of  $\alpha$ -tocopherol was used for computational screening of the virtual library of functional monomers using the LEAPFROG algorithm. Each of the monomers was probed for their possible interaction with  $\alpha$ -tocopherol. The results of LEAPFROG are reported in Table 2.5. In the LEAPFROG table, the first five monomers presented the highest binding score (kcal mol<sup>-1</sup>) including ethylene methacrylate phosphate (EGMP), methacrylic acid (MAA), urocanic acid (UA), acrylamido-2-methyl-1-propanesulfonic acid (AMPSA) and itaconic acid (IA). As aforementioned (Section 2.2.3), the imprinted approach in RDP is non-covalent which occur due to interactions such as hydrogen bonds, electronic forces, ionic interactions, van der Waal interactions or hydrophobic interactions.

Using the SYBYL software, it was possible to see only hydrogen bonding between the functional monomers and the template ( $\alpha$ -tocopherol). However, there are other potential types of interaction between the monomer and the template contributing to retaining (adsorption) of the target on the surface of the polymer. Horvath and co-workers reported that the binding of analytes to the imprinted polymers is usually directed by electrostatic driving forces, such as hydrogen bonding,  $\pi$ - $\pi$  bonds or ionic interactions.<sup>3,35</sup>

$\alpha$ -tocopherol was used as a template for the modelling purpose even it has not been added to the components of the polymer. The main aim of the ‘virtual imprinting’ was to select the functional monomers possessing the natural affinity toward the template. Therefore, it was expected that the synthesised polymer might demonstrate some group specificity allowing effective ‘harvesting’ of compounds with similar functionality and properties from the oil matrix.

### **2.3.2 Composition of the RDP**

The main five pre-polymerisation reagents in the synthesis of molecularly imprinted polymers are template, functional monomer, cross-linker, initiator and porogenic solvent. The success of the imprinting technique depends on the accurate selection of these components.<sup>3,4,21,36</sup> In the current research, the template that has been used for the design of the polymer is  $\alpha$ -tocopherol (Figure 2.5). The main difference of synthesising the used polymer here from the classical synthesis of MIP is adding the template to the pre-polymerisation components in the molecular modelling only as mentioned above. Practically in the lab, the polymer was synthesised using the components which have been chosen based on the presence of molecular modelling data with the absence of  $\alpha$ -tocopherol in the mixture.

The composition of the polymer was designed based on the results of the molecular modelling using the functional monomers that demonstrated the highest binding energy towards  $\alpha$ -tocopherol. The molecular modelling reduced the list length of the monomers that underwent the evaluation of the binding ability towards  $\alpha$ -tocopherol.

It was found that the non-covalent binding due to the relatively weak interactions were formed between the target and the functional groups of the monomer molecule. These interactions require relatively milder conditions for the elution. The non-covalent binding method has been desirable in the development of MIPs due to the ease of synthesis with no need of sophisticated instruments and the possibility of controlling the reaction conditions. The bulk polymerisations have been synthesised for development of MIPs sorbents for food sample preparation and clean-up or sample extraction as mentioned in the published work.<sup>2,4</sup> The last component for the successful polymerisation is the porogenic solvent. The porogenic solvents offer the single phase that collects all the

components of pre-polymerisation mixture. It is responsible for creating the pores of the polymeric material which influences performance of the polymer directly.<sup>3,4</sup>

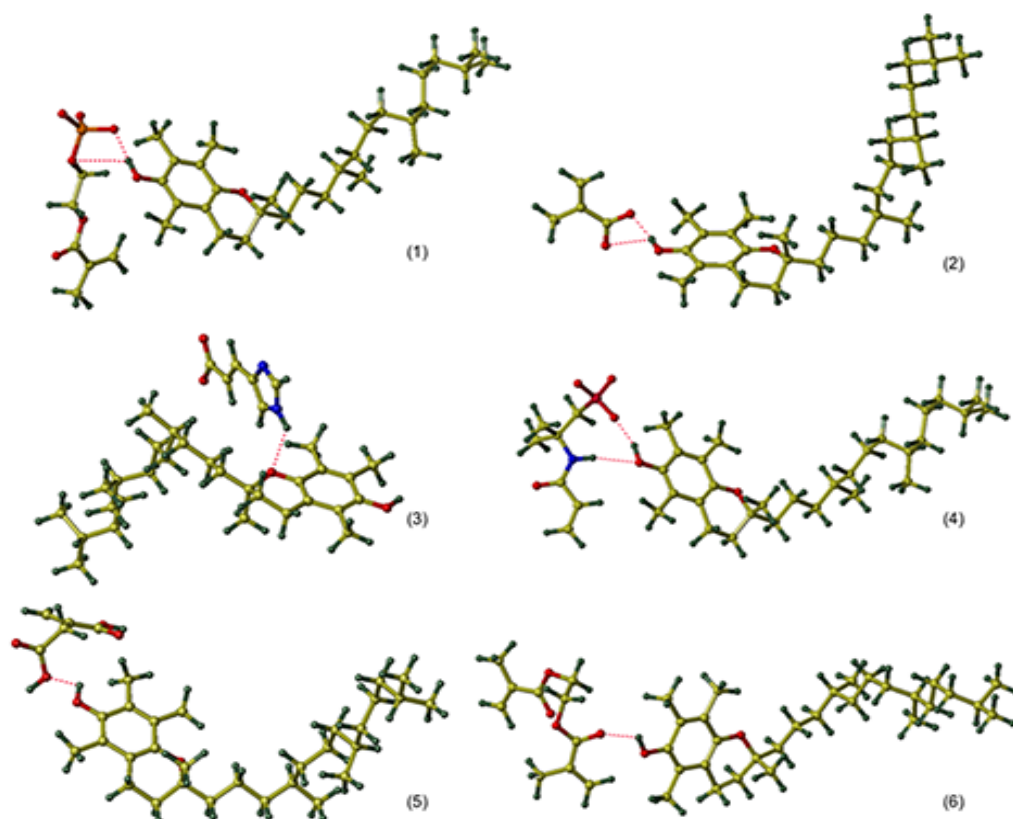


Figure 2.5: Molecular complexes between  $\alpha$ -tocopherol and the functional monomers: EGMP (1), MAA (-) (2), UA (-), (3) AMPSA (4), IA (5) and EGDMA (as a cross-linker) (6), the hydrogen bonds are shown as dotted lines.

### 2.3.2.1 The functional monomer

The monomers polymerise effectively providing functional groups exposed at the surface of the polymer.<sup>20</sup> Therefore, the functional monomers are responsible for determining the types of the interactions in the imprinted sites of the polymer. It has been observed that the appropriate monomer was selected based on its ability to interact with the target compound/s during the synthesis and in the molecular recognition step. The interactions between the functional monomer and the template occurred at the pre-polymerisation step of the MIP synthesis and in the extraction of the targeted compound

from the sample. The selection of the functional monomers was demonstrated with the consideration of matching the functionalities of the template in a complementary fashion. For example, the presence of the unsaturated ring in the monomer such as DVB or 4-vinylpyridine leads to  $\pi$ - $\pi$  interactions with an aromatic ring in the template. In addition, another monomer like methacrylic acid has been observed as an acceptor and donor for hydrogen bonds with template molecules.<sup>3,5</sup> Moreover, it was reported that the acidic monomers (e.g. methacrylic acid) are more suitable for basic analytes, and the basic monomers (such as vinylpyridine) are more appropriate for acidic targets.<sup>2,4</sup>

The molecular modelling of  $\alpha$ -tocopherol resulted in a list of monomers sorted from the highest of binding to the lowest. The first six monomers with EGDMA (cross-linker) were evaluated in terms of their ability of binding with  $\alpha$ -tocopherol. The  $\alpha$ -tocopherol solution in hexane was passed in SPE cartridges that were filled with 100 mg of the RDP polymers, which synthesised with those monomers with EGDMA cross-linker. By measuring the UV absorbance of  $\alpha$ -tocopherol before and after loading, the percentage of bounded  $\alpha$ -tocopherol was calculated for each monomer.

The evaluation of the binding ability of  $\alpha$ -tocopherol to the modelling list of monomer resulted in little different order of affinity towards  $\alpha$ -tocopherol with the molecular modelling calculations. The highest binding ability were binding to AMPSA, MAA, EGMP, IA and EGDMA with little differences in the percentages of binding. Regardless the order of these monomers (as the differences between the percentages were very small Table 2.6) the first functional monomer which was selected for the polymer preparation was MAA. The main reason for starting with MAA monomer was because this monomer has been successfully used to extract  $\alpha$ -tocopherol from other natural sources in published studies.<sup>33,34</sup>

Table 2.6: The percentage of recovery of the different polymers synthesised with different functional monomers and EGDMA (cross-linker).

Polymer	Adsorbed percentage
EGMP	50.2% $\pm$ 2.1
MAA	58% $\pm$ 1.5
AMPSA	65.5% $\pm$ 2
IA	62.7% $\pm$ 2
Acrylamide	42.1% $\pm$ 1.7
DEAEA	39.3% $\pm$ 1.3
EGDMA	61% $\pm$ 1.5

In addition, MAA is a commonly used monomer in MIP synthesis forming non-covalent interactions due to its ability to form hydrogen bonds as being either donor or acceptor through the presence of a carboxylic group with  $\alpha$ -tocopherol that has hydroxyl groups. Therefore, the decision to use MAA as a functional monomer in RDP synthesis was made in order to increase the chance of success of producing an effective RDP which will be capable of extracting the maximum of  $\alpha$ -tocopherol from sunflower oil.<sup>3,20</sup>

### 2.3.2.2 The cross-linker

The cross-linker influence on the binding capacity of the imprinted polymers by offering a balance between the rigidity and flexibility in the imprinted material.<sup>35</sup> The cross-linker that is involved in the polymerisation is responsible for making a robust polymer which should be simultaneously flexible enough to allow the mass access inside the pores. Thus, the vital roles of cross-linkers in the synthesis of the imprinted polymers is to control the morphology for the polymer matrix by providing the stabilisation for the imprinted site in particular, and for the whole polymer matrix in general.<sup>4</sup> The most commonly used cross-linkers in the literature are DVB and EGDMA.<sup>37</sup> Ariffin *et al.* reported that DVB offered lower non-specific interactions compared to EGDMA in the polar analyte.<sup>37</sup> The goal of synthesis of polymer in the current study was to develop a

polymer that has an ability to harvest as much as possible of the minor compounds from oil sample. Thus, the non-specificity was relatively desirable in the current research. The comparative study between the two MAA-based polymers that were synthesised using the DVB once as a cross-linker and EGDMA in the second polymer was in accordance with the previous studies. However, there were small differences between the performances of these polymers when these were applied to extract  $\alpha$ -tocopherol from model solution.

Table 2.7: Percentage of recovery for two MAA-based polymers with two different cross-linkers.

Polymer	Percentage of recovery (%)
MV	93 $\pm$ 2.5
MD	94 $\pm$ 3.7

Based on the percentage in Table 2.7 and the literature studies, the chosen cross-linker was EGDMA. It has been observed that EGDMA surpassed other cross-linkers in contribution to increase the binding capacity of molecularly imprinted polymer by Klejn and co-workers.<sup>36</sup> This was attributed to the presence of methyl groups in the cross-linker which offered reduction of the intramolecular cyclization, thus lengthening the distance between the polymer net, which leads to higher swelling of polymer matrices.<sup>36</sup> Moreover, DVB is relatively hydrophobic and has no functional group comparing to EGDMA that has two carbonyl groups enabling them to participate in the interactions with the template among the polymer. Madikizela and partners reported that the imprinted polymers that have a surface area covered with hydrophilic functional groups are demonstrating better hydrophilic binding associated with decreasing the non-specific hydrophobic interactions.<sup>36</sup> For example, MIPs synthesis with EGDMA as a cross-linker has shown strong potential for extracting the acidic targets due to the hydrogen bonding.<sup>5</sup> In the current study, although the difference in the percentage recovery of  $\alpha$ -tocopherol from the standard solution was very close in the two resulted polymers, the possibility to extract various compounds from the oil sample which has common functional groups with those in  $\alpha$ -tocopherol in the next step of this research is more likely to happen with EGDMA polymer. This is the main motivation for concentrating on them.

### 2.3.2.3 Choosing the optimal monomer: cross-linker ratio

To investigate the effect of the monomer: cross-linker ratio, several polymers were synthesised with different ratios of monomer to cross-linker (0:100 (P1), 1:99 (P2), 10:90 (P3), 20:80 (P4)). A comparison was made between these polymers in terms of breakthrough volume, binding capacity, recovery, surface area and pore volume as was shown in Table 2.8. It was observed that all polymers tested were capable of extracting  $\alpha$ -tocopherol from the model solution, as revealed by examining the breakthrough volumes and the binding capacities. However, although the polymer P1 showed a higher binding capacity than other polymers ( $8.1 \text{ mg g}^{-1}$  of  $\alpha$ -tocopherol, breakthrough volume 9 mL), it was observed that the percentage recovery of  $\alpha$ -tocopherol from this polymer was the lowest among other tested polymers. This was attributed to the fact that the polymer was hydrophobic and, thus, difficult to elute. The data obtained in this experiment are recorded as the average of five replicates determinations and standard deviation (SD).

Table 2.8: Different features of the different polymers with different monomer: cross-linker ratios.

Characteristics	Polymers			
	P1	P2	P3	P4
Breakthrough volume (mL)	9	5	7	4
Binding capacity ( $\text{mg g}^{-1}$ )	$8.1 \pm 0.7$	$3.5 \pm 0.6$	$3.3 \pm 0.8$	$2.4 \pm 1.0$
% recovery	$80 \pm 2.1$	$82.6 \pm 3.3$	$94.5 \pm 5.2$	$79.4 \pm 3.4$
Surface area ( $\text{cm}^2 \text{g}^{-1}$ )	445.05	437.128	276.15	161.20
Pore volume ( $\text{cm}^3 \text{g}^{-1}$ )	0.0302	0.0291	0.349	0.240

It was found that the polymer prepared by using monomer: the cross-linker ratio of 1:9 demonstrated the highest percentage recovery of  $\alpha$ -tocopherol (94%) (Table 2.8). The bound  $\alpha$ -tocopherol was eluted from the polymer using 3 mL of methanol mixed with 5% of acetic acid (the optimised elution solvent). Using the calibration curve, the

concentrations of  $\alpha$ -tocopherol after each step of SPE were calculated to compare the percentage of  $\alpha$ -tocopherol recovery.

#### **2.3.2.4 Characterisation of the developed polymers**

The monomer MAA was chosen for polymer preparation, as it was one of the top candidates from modelling screening and because this monomer has been successfully used in Molecularly Imprinted Polymers (MIPs) employed to extract  $\alpha$ -tocopherol from non-oil sources.<sup>23,33,38</sup> As it was known from previous studies, MAA has the ability to form hydrogen bonds with  $\alpha$ -tocopherol, demonstrated a strong specific binding and also non-specific binding which attributed to long chain moiety and the hydroxyl group in  $\alpha$ -tocopherol molecules.<sup>33</sup> The presence of hydrogen-bonding between the functional monomer and  $\alpha$ -tocopherol was suggested by SYBYL, as shown in Figure 2.5. We believe that these two types of interactions (specific electrostatic and non-specific hydrophobic) attribute to the high capacity and the ability of RDPs to adsorb not only  $\alpha$ -tocopherol but also other minor components present in the sunflower oil.

#### **2.3.2.5 Measurement of the breakthrough volume and binding capacity**

In order to evaluate the binding capacity of the prepared polymers, breakthrough volume has been measured. It allowed comparing the performance of different polymers under required extraction conditions and selecting the polymer which possessed the highest capacity. The data were collected using UV spectroscopy to measure the absorbance of the samples after a pass through the SPE cartridge, then, using the calibration curve to calculate the concentration of breakthrough volume of the two MAA-based polymers with two different cross-linkers were shown in Tables 2.9 and 2.10. The polymer ME has shown a higher capacity of 3.3 mg of  $\alpha$ -tocopherol g<sup>-1</sup> of polymer (breakthrough volume is 7mL) than the polymer MD 0.51mg of  $\alpha$ -tocopherol g<sup>-1</sup> of polymer (breakthrough volume is 2mL). The measurements were repeated 5 times.

Table 2.9: The breakthrough volume of MD polymer.

Cumulative volume (mL)	Concentration of free $\alpha$ -tocopherol (mg mL <sup>-1</sup> )	Percentage of binding %
1	0	100
2	0.0545±0.021	51.8
3	0.0337±0.042	32.4

Table 2.10: Breakthrough volume of ME polymer.

Cumulative volume mL	Concentration of free $\alpha$ -tocopherol (mg mL <sup>-1</sup> )	Percentage of binding (%)
1	0	100
2	0.0082±0.0013	92.8
3	0.0088±0.00043	92.4
4	0.0103±0.024	89.7
5	0.0168±0.011	83.1
6	0.0432±0.0015	56.8
7	0.0522±0.0057	48.9
8	0.0716±0.023	28.5

These results agree with the published findings in Madikizela *et al.* who reported that DVB is hydrophobic in nature with an aromatic ring which could attribute to  $\pi$ - $\pi$  interactions, and has no functional group which makes them less contributing to the hydrophilic interactions between the polymer and the target molecules.<sup>2,3</sup> On the other hand, EGDMA is hydrophilic and has two carbonyl groups that can act as hydrogen bond acceptor. Madikizela also mentioned that the imprinting of the polymer using EGDMA as a cross-linker produced matrix with an outer hydrophilic layer which was associated with the reduction of the non-specific hydrophobic interactions.<sup>3</sup>

### 2.3.2.6 Evaluation of reusability and measurement of the surface area

Molecularly imprinted polymers have been reported in the literature as a material with physical stability and high chemical robustness. There are many reports demonstrated the reusability of MIPs.<sup>11,20,21,28</sup> This type of experiments was based on applying the polymer for SPE for loading followed by elution. Then, wash the polymer with acidic methanol (9:1), thereafter, repeat the loading elution cycle. In each cycle, the loading elution process should measure the efficiency of the extraction by measuring the adsorption capacity or recovery of the target. The possibility to regenerate has been evaluated in the previously published studies for some synthesised MIPs to fifteen times in Dai *et al.*<sup>39</sup> and at least more than 5 times in other different studies.<sup>10,11,40</sup> In the current study, the RDP demonstrated extraction of  $\alpha$ -tocopherol 7 times at the same level of the recovery (94%) of  $\alpha$ -tocopherol in heptane solutions as represented in Figure 2.6.

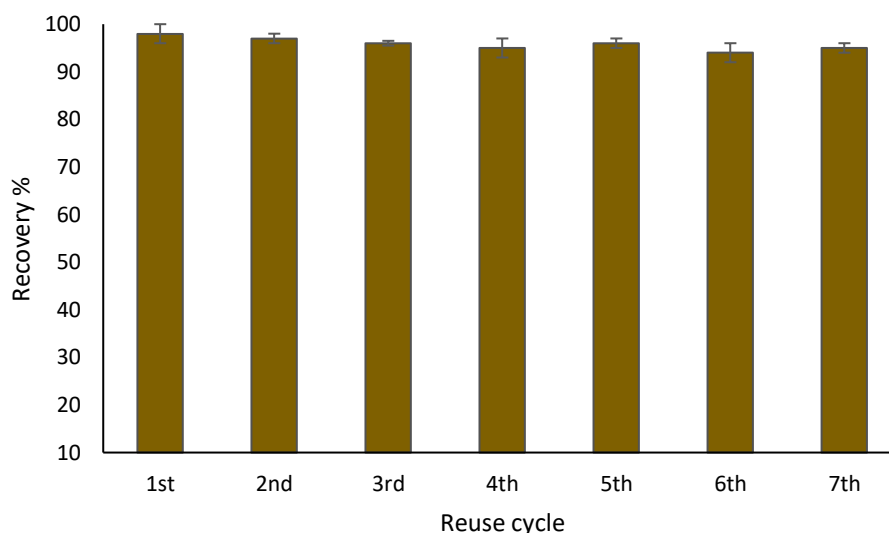


Figure 2.6: Regeneration cycles of the RDP loaded with  $\alpha$ -tocopherol in heptane standard solution. Standard deviations were represented as error bars (n=5).

### 2.3.3 Calibration curve of $\alpha$ -tocopherol

The main purpose of making a calibration curve was to measure the different properties of the synthesised polymer, such as breakthrough volume and binding capacity. A calibration curve using UV spectroscopy was made using very low concentration (less than  $0.2 \text{ mg mL}^{-1}$ ) for a model solution of  $\alpha$ -tocopherol<sup>17</sup> (Figure 2.7).

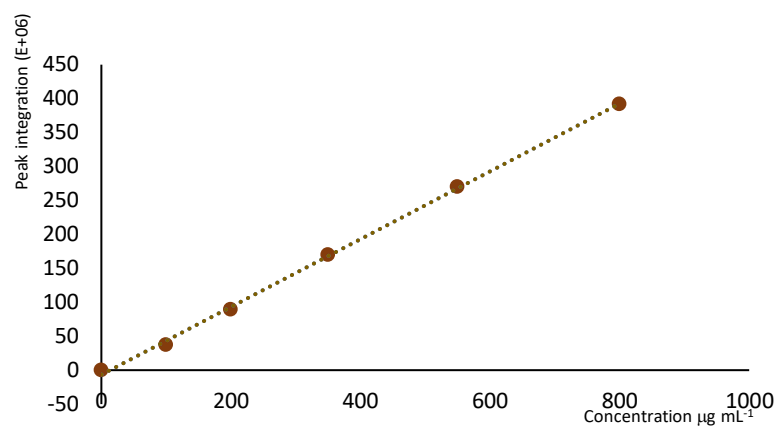


Figure 2.7: The calibration curve of  $\alpha$ -tocopherol hexane using UV,  $Y = 0.499x - 6.702$ ,  $R^2 = 0.999$ .

$$A = \epsilon cl$$

Equation 2.2: Beer-Lambert law.

Equation 2.3 represents Beer-Lambert law where  $A$  is the absorbance,  $\epsilon$  is molar absorption coefficient and  $l$  is the length of the sample. It was found that above  $0.2 \text{ mg mL}^{-1}$ , the relationship between concentration and absorbance deviated from the linear relationship of Beer-Lambert law (Equation 2.3) as shown in Figure 2.8.

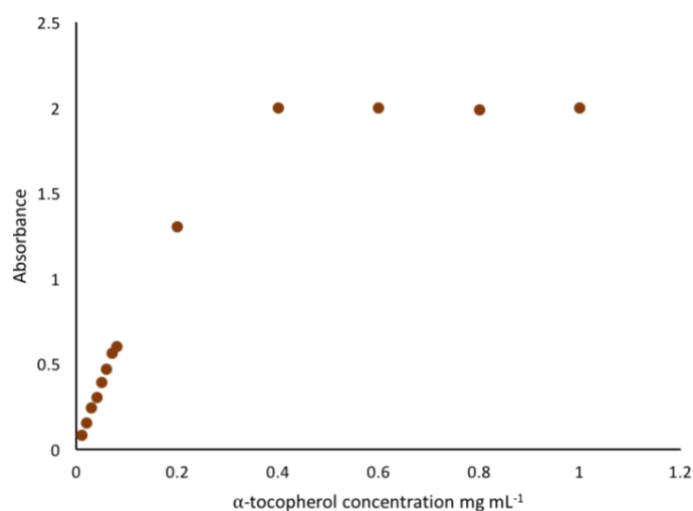


Figure 2.8: The relationship between concentration and absorbance of  $\alpha$ -tocopherol solution in hexane.

In addition, a calibration curve was intended to be used to calculate the concentration of  $\alpha$ -tocopherol in sunflower oil in the different steps of SPE. However, it was not possible to analyse the oils samples using UV spectroscopy due to the presence of interferences.

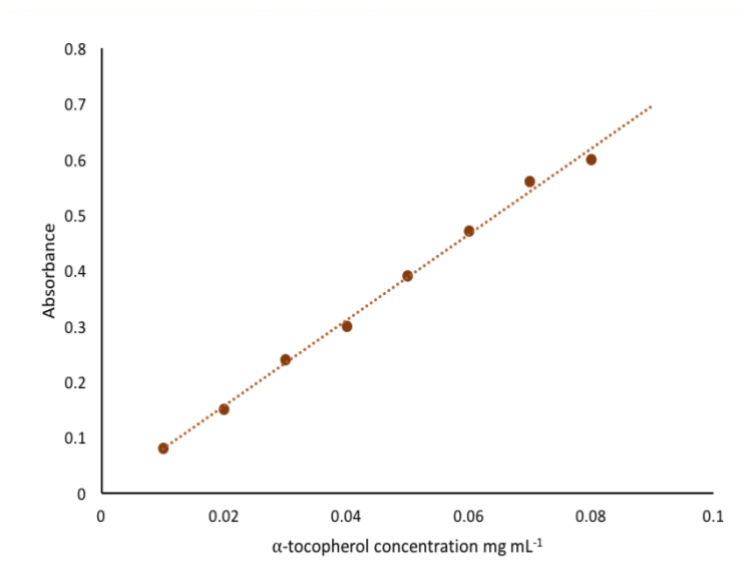


Figure 2.9: The calibration curve of  $\alpha$ -tocopherol using GC/MS,  $Y = 0.7702x + 0.0002$ ,  $R^2 = 0.996$ .

Therefore, the measurements of different samples for the optimisation of SPE of sunflower oil were performed using GC/MS which has been done using a calibration of a standard solution of the target molecules. In this chapter, only the calibration curve of  $\alpha$ -tocopherol using GC/MS (Figure 2.9) were presented. The calibration curves details of other eluted compounds from sunflower oil will be presented in the Chapter 3.

#### 2.3.4 Optimisation of the SPE protocol using the model solution of $\alpha$ -tocopherol

SPE is the most frequently used procedure for clean-up, fractionation, pre-concentration or extraction of a target from different types of samples. The binding capacity of the polymer together with fast desorption of target molecule from the sorbent are marked factors that have an impact on the design of the polymer and the SPE conditions.<sup>36</sup> In this respect, it is essential to develop the SPE protocol in terms of choosing the solvent for each step in SPE process that provide the best yield in diversity and quantity.

The obtained yield from each step of the SPE was influenced by the type of solvent used in loading, washing and elution steps (Figure 2.10). In order to achieve the good retention and recovery of analyte, the protocol of SPE using RDPs as adsorbents to extract  $\alpha$ -tocopherol was optimised based on previous reported studies<sup>13,23,32,33</sup> that allowed to choose the solvents for each step of the SPE and contributed to the highest percentage recovery (94%) of  $\alpha$ -tocopherol from the model solution (0.1 mg mL<sup>-1</sup>  $\alpha$ -tocopherol in loading solvent).

The selected solvents for each SPE step are mentioned earlier in Table 2.4 in the material and method section. The yield of  $\alpha$ -tocopherol was measured by using each of these solvents and the relative concentration of  $\alpha$ -tocopherol produced with each of these solvents and presented statistically in Figure 2.11. From these statistical figures, it can be concluded that the optimised conditions, including the conditioning, loading, washing and eluting solvents in all experiments are as follows:

One mL of the sample in heptane (optimised conditioning and loading solvent) was used for loading, 1 mL of 60% methanol was the optimised solvent for washing, and elution was performed at the best yield of the eluted compound with using 3 mL of methanol acidified with 5% acetic acid. The quantification of  $\alpha$ -tocopherol in the different SPE fractions were conducted using GC/MS set up and a calibration curve.

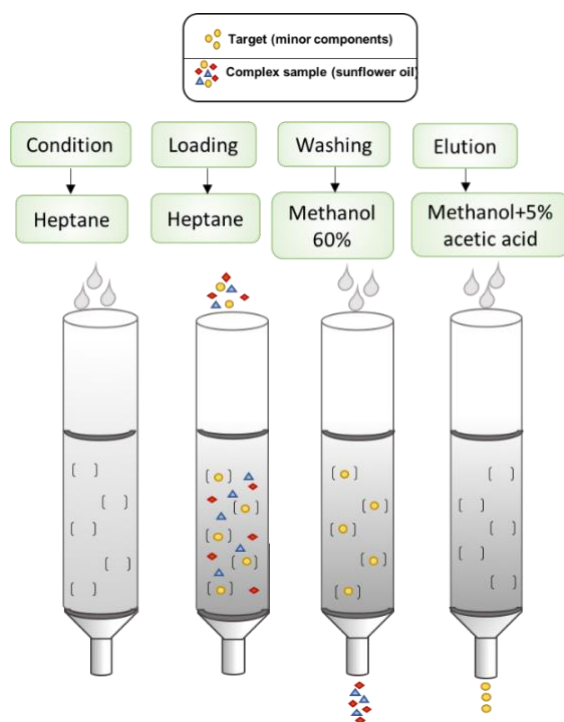


Figure 2.10: The optimised conditions for SPE of  $\alpha$ -tocopherol using RDP.

After loading of the model solution onto the SPE cartridge, it was washed with 60% ethanol in water, which was subsequently evaporated to dryness. Then, the analyte was dissolved in hexane and analysed using GC/MS. Elution of  $\alpha$ -tocopherol from the SPE cartridge was achieved with ethanol containing 5% acetic acid. The eluted sample was evaporated and reconstituted in hexane before analysis by GC. Figure 2.11 summarises these results and these experiments were repeated five times.

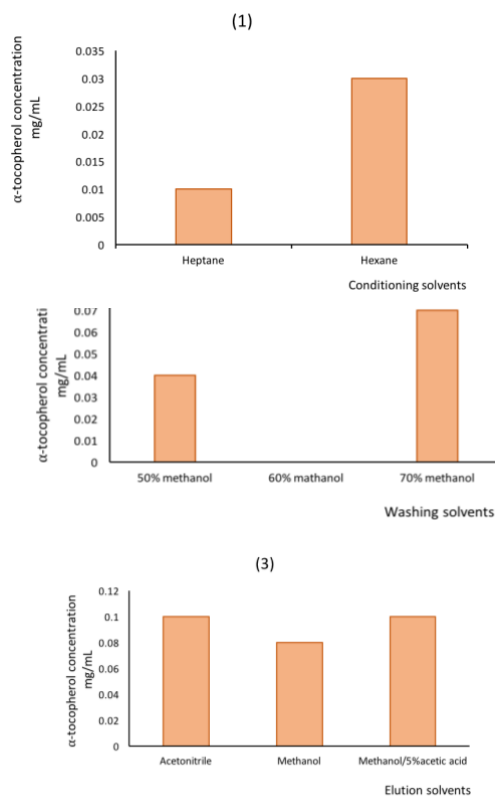


Figure 2.11: The statistical demonstration of candidate solvents for the optimisation of SPE conditions. (1) Condition and loading, (2) washing, (3) elution.

In the GC/MS chromatogram (Figure 2.12), the peak that corresponded to  $\alpha$ -tocopherol was analysed using mass spectrometry to check the similarity with a spectrum of  $\alpha$ -tocopherol from the spectral library (NIST). As shown in the Figure 2.13 that there was considerable similarity between the mass-spectrum of extracted  $\alpha$ -tocopherol (upper) and the spectrum of  $\alpha$ -tocopherol from the spectral library (lower). The similarity will be illustrated further in detail in the Chapter 3.

It is known that the list of most commonly used SPE stationary phases for the purification of tocopherol from biological samples or vegetable oil, and for clean-up before HPLC analysis include following adsorbents: C8,<sup>41</sup> C18,<sup>13</sup> aminopropyl,<sup>42</sup> XAD,<sup>13</sup> florisil,<sup>35</sup> cyclohexyl,<sup>34</sup> Sephadex LH-20<sup>17</sup> or silica gel<sup>19</sup>

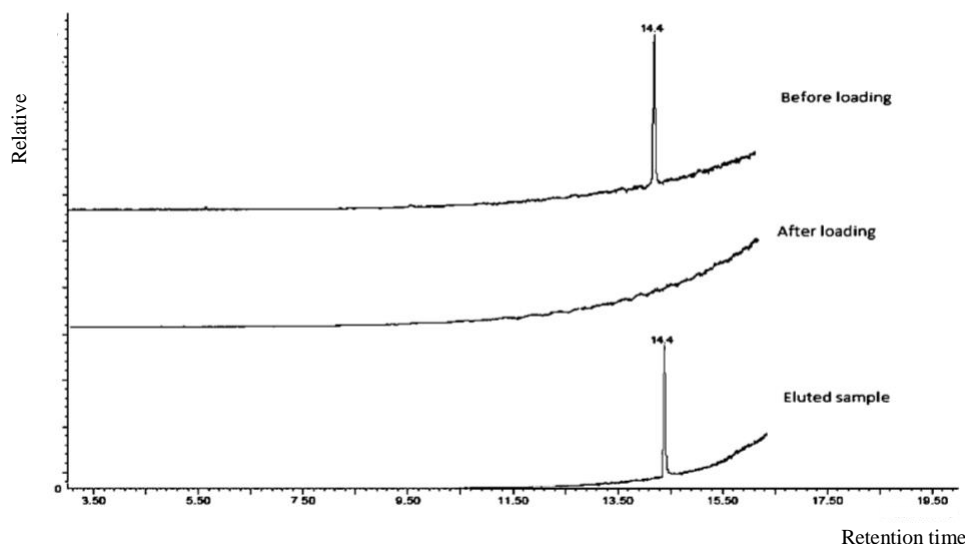


Figure 2.12: The GC/MS chromatogram of a standard solution of  $\alpha$ -tocopherol.

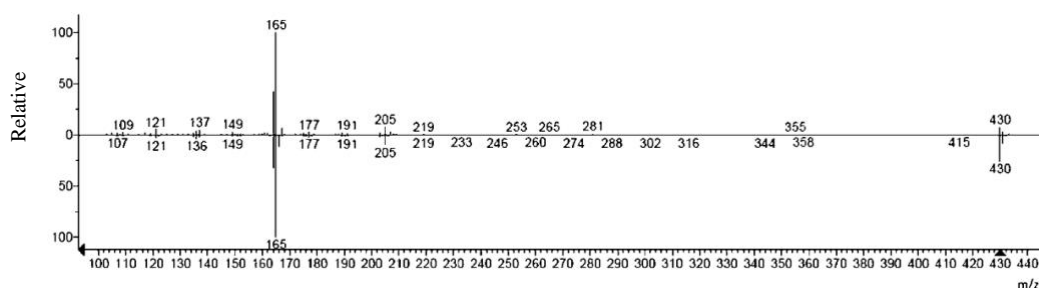


Figure 2.13: The similarity between the mass-spectrum of extracted  $\alpha$ -tocopherol (upper) and the spectrum of  $\alpha$ -tocopherol from the spectral library (lower).

However, none of them was reported to be capable of purification of  $\alpha$ -tocopherol from oil, either because the analysis protocols require pre-treatment steps,<sup>34,36</sup> or adjustment of pH<sup>28</sup> or because the percentage recovery was poor ( $\leq 20\%$ ).<sup>43</sup> Although developing RDP with optimised SPE protocol for large scale applications was not a goal of this feasibility study, we are confident that modern technology allows producing the polymer developed here (RDP) in the industrial quantities and use it to extract  $\alpha$ -tocopherol from the oils on a large scale following the optimised extraction protocol that doesn't require any sample pre-treatment or adjustment.

According to the achieved percentage recovery of  $\alpha$ -tocopherol from the model solution, it is evident that the current achievement is comparable with the results from the literature.<sup>23,32,38,44</sup> The benefits of the developed RDP and the optimised SPE protocol

include a minimal dilution of the oil sample, no need in the pre-treatment of the oil and allowed to extract a group of essential minor compounds in a single step.

### 2.3.5 Application of the SPE conditions for the extraction of $\alpha$ -tocopherol and other minor compounds from sunflower oil

After the validation of SPE protocol based on high recovery percentage of  $\alpha$ -tocopherol from the model solution, the developed RDP and the optimised protocol have been used to harvest the minor components directly from sunflower oil. Thus, the conditions of SPE optimised for the model solution of  $\alpha$ -tocopherol were applied to a sample of 20% sunflower oil in heptane spiked with  $300 \mu\text{g mL}^{-1}$  of the compounds which were then purified using RDP, eluted and measured using GC/MS. It was observed that it was possible to process it without pre-treatment, which makes it advantageous due to reduced consumption of organic solvents compared to the current industry standards (1:10 dilution ratio between oil and solvent).<sup>23,44</sup> The standard compounds which were used to spike the oil sample included palmitic, oleic and linoleic acids,  $\alpha$ -tocopherol and mixture of campesterol, stigmasterol and  $\beta$ -sitosterol. The calibration curves were used to calculate the concentration of the eluted compounds from sunflower oil followed by 5-times dilution in heptane, as shown in Table 2.11. The eluted compounds are presented as separate peaks in the GC chromatogram (Figure 2.14).

Table 2.11: Quantities of minor components extracted from sunflower oil in heptane.

Eluted compound	Eluted amount ( $\text{mg kg}^{-1}$ )
Palmitic acid	$2400 \pm 600$
Linoleic and Oleic acids	$17250 \pm 333$
$\alpha$ -tocopherol	$1138 \pm 144$
Campesterol	$1994 \pm 200$
Stigmasterol	$2705 \pm 77$
$\beta$ -sitosterol	$5394 \pm 38$

The eluted compounds were identified using the suggested identifications of the NIST library of mass-spectra. Each peak was analysed by comparison to standard solutions of the compound present in the mass-spectroscopy library (Figure 2.14(a)).

It was found that the  $\alpha$ -tocopherol and phytosterols recovered from the sunflower oil (Figure 2.14 (b)) using developed RDP are comparable or even superior to other published reports. For example, the concentration of the  $\alpha$ -tocopherol extracted from sunflower oil was more than  $485 \text{ mg g}^{-1}$  which was reported by Gonzalez *et al.*<sup>45</sup>

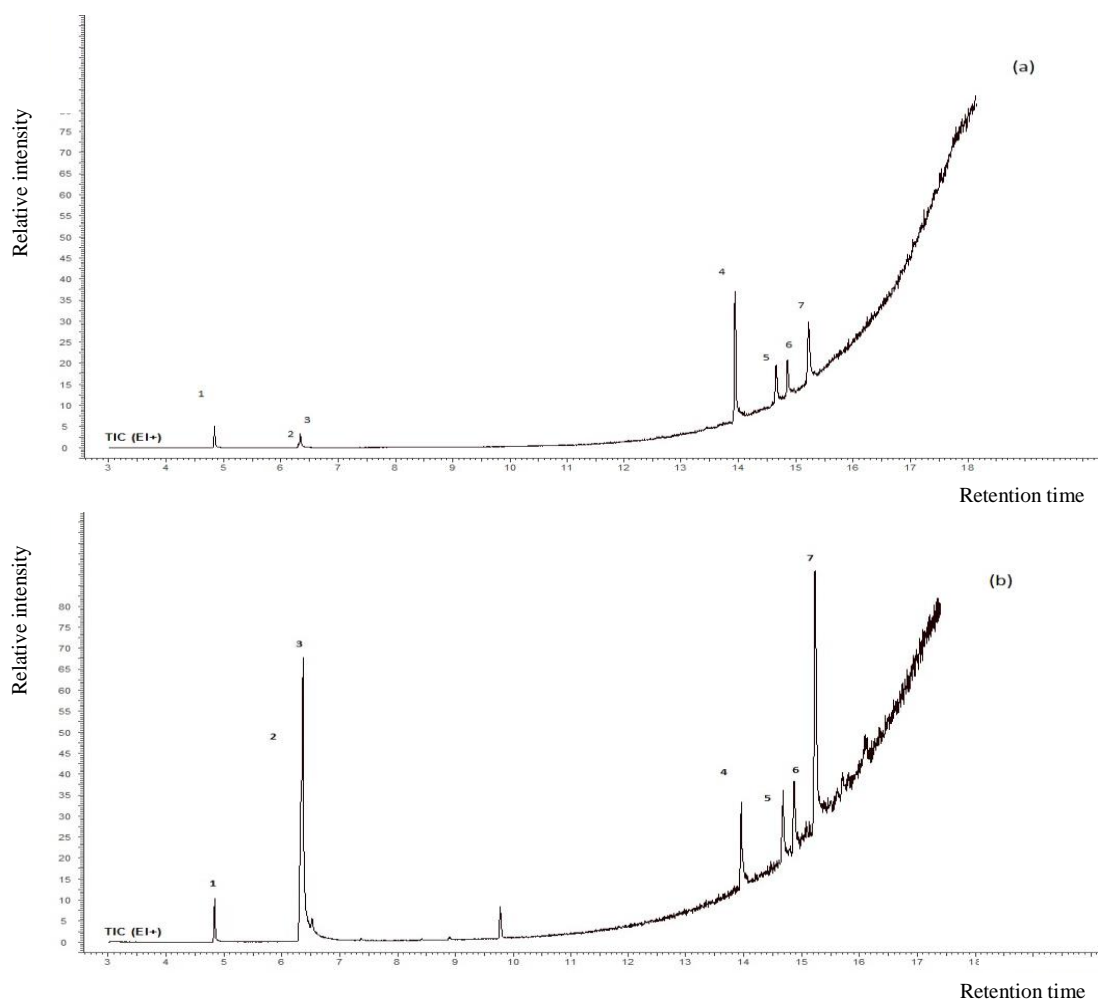


Figure 2.14: The GC/MS chromatogram for the eluted samples.

A mixture of standards solutions (a), eluted sample from 20% of sunflower oil (b),  
1) palmitic acid, 2) oleic acid, 3) linoleic acid, 4)  $\alpha$ -tocopherol, 5) campesterol, 6)  
stigmasterol and 7)  $\beta$ -sitosterol.

In addition, the content of  $\alpha$ -tocopherol in spiked unrefined sunflower oil was found to be close to the published range measured in sunflower seeds by Galea *et al.* (416 mg kg<sup>-1</sup>)<sup>23</sup> and Ballesteros *et al.* (473 mg kg<sup>-1</sup>)<sup>46</sup> indicating the efficiency of the developed method. Similarly, the concentrations of phytosterols extracted were in good correlation with the concentrations reported by Lechner *et al.* who has recovered 325 mg kg<sup>-1</sup> of campesterol, 198 mg kg<sup>-1</sup> of stigmasterol and 1868 mg kg<sup>-1</sup> of  $\beta$ -sitosterol.<sup>47</sup> The phytosterols extracted from sunflower oil by Schwartz *et al.* were reported as campesterol (68 mg kg<sup>-1</sup>), stigmasterol (280 mg kg<sup>-1</sup>) and  $\beta$ -sitosterol (2060 mg kg<sup>-1</sup>).<sup>8</sup>

## 2.4 Conclusions

An effective protocol for the extraction and purification of  $\alpha$ -tocopherol beside other minor components from sunflower oil, based on a bespoke RDP, has been developed. The optimised SPE method resulted in the increased recovery of the valuable natural product,  $\alpha$ -tocopherol from a complex matrix of the sunflower oil. Another important advantage of using the developed polymer over traditional methods of extraction included a two-fold reduction in the volume of solvent required. The protocol reported here for the extraction of a group of components involved only 5 times dilution of the sunflower oil with heptane. This dilution rate is twice improved by comparison with the 10-fold dilution applied in the industrial protocol, representing a reduction in waste and saving in the resources and time.

It was also demonstrated that the combination of the optimised SPE protocol and developed RDP allowed a quantitative extraction of minor components from sunflower oil to be performed without any additional pre-treatment. It is important to highlight that the optimised protocols and proposed strategy could be used as blueprints for the development of extraction procedures for different groups of compounds from other natural oil-containing biomasses.

The relatively high percentage recovery of the minor components from sunflower oil has encouraged the research to be directed to evaluate the possibility of applying the proposed protocol to other vegetable oils and report to what extent that is going to be potential, which is going to be demonstrated in the next chapter.

## References

- 1) Lechner M.; Reiter B.; Lorbeer E. Determination of tocopherols and sterols in vegetable oils by solid-phase extraction and subsequent capillary gas chromatographic analysis. *J Chromat A*. **1999**, *857*, 231-238.
- 2) Ashleya, J.; Shahbazia M.; Krishna K.; Aaydha V.; Wolff A.; Bangb D.; Sun Y. Molecularly imprinted polymers for sample preparation and biosensing in food analysis: Progress and perspectives. *Biosens Bioelectron*. **2017**, *91*,606–615.
- 3) Madikizelaa L.; Tawanda, N.; Chimuka L. Applications of molecularly imprinted polymers for solid-phase extraction of non-steroidal anti-inflammatory drugs and analgesics from environmental waters and biological samples. *J Pharm Biomed Anal*. **2018**, *147*, 624–633.
- 4) Regal P.; Barreiro R.; Cepeda A.; Fente C. Application of molecularly imprinted polymers in food analysis: clean-up and chromatographic improvements. *Cent Eur J Chem*. **2012**, *3*,766-784.
- 5) Madikizela L.; Mdluli P. Experimental and theoretical study of molecular interactions between 2-vinyl pyridine and acidic pharmaceuticals used as multi-template molecules in a molecularly imprinted polymer. *React Funct Polym*. **2016**, *103*, 33–43.
- 6) Lolić A.; Paíga P.; Santos L.; Ramos S.; Correia M.; Delerue-Matos C. Assessment of non-steroidal anti-inflammatory and analgesic pharmaceuticals in seawaters of North of Portugal: Occurrence and environmental risk. *Sci Total Environ*. **2015**, *508*,240-250.
- 7) Lindqvist N.; Tuhkanen T.; Kronberg L. Occurrence of acidic pharmaceuticals in raw and treated sewages and in receiving waters. *Water Res*. **2005**, *39*, 2219-2228.
- 8) Stolker A.; Brinkman U.; Analytical strategies for residue analysis of veterinary drugs and growth-promoting agents in food-producing animals - a review. *J Chromatogr A*, **2005**, *1067*,15-53.
- 9) Yiyan L.; Edward C.; Extraction of 17 $\beta$ -estradiol in water using non-imprinted polymer submicron particles in membrane filters. *J Environ Sci*. **2010**, *22*,1820–1825.

- 10) Duan Y.; Dai C.; Zhang Y.; Ling C. Selective trace enrichment of acidic pharmaceuticals in real water and sediment samples based on solid-phase extraction using multi-templates molecularly imprinted polymers. *Anal Chim Acta*. **2013**, 758, 93-100.
- 11) Meischl F.; Schemeth D.; Harder M.; Köpfle N.; Tessadri R.; Rainer M. Synthesis and evaluation of a novel molecularly imprinted polymer for the selective isolation of acetylsalicylic acid from aqueous solutions. *J Environ Chem Eng*. **2016**, 4, 4083-4090.
- 12) Boulanouar S.; Combès A.; Pichon S.; Mezzacheb V. Synthesis and application of molecularly imprinted polymers for the selective extraction of organophosphorus pesticides from vegetable oils. *J Chromat A*. **2017**, 1513, 59–68.
- 13) Guerreiro A.; Soares A.; Piletska E.; Mattiasson B.; Piletsky S. Preliminary evaluation of new polymer matrix for solid-phase extraction of nonylphenol from water samples. *Anal Chim Acta*. **2008**, 612, 99-104.
- 14) Qiao F.; Sun H.; Yan H.; Row K. Molecularly Imprinted Polymers for Solid Phase Extraction. *Chromatographia*. **2006**, 64, 625-634.
- 15) Herrero-Latorre C.; Barciela-García J.; García-Martín S.; Crecente R. Graphene and carbon nanotubes as solid phase extraction sorbents for the speciation of chromium : A review. *Anal Chim Acta J*. **2017**, 1002, 1-17.
- 16) Wackerlig J.; Schirhagl R. Applications of Molecularly Imprinted Polymer Nanoparticles and Their Advances toward Industrial Use: A Review. *Anal Chem*. **2016**, 88, 250-261.
- 17) Melchert H.; Pollok D.; Pabel E.; Rubach K.; Stan H. Determination of tocopherols, tocopherolquinones and tocopherol hydroquinones by gas chromatography-mass spectrometry and pre separation with lipophilic gel chromatography. *J Chromatogr A*. **2002**, 976, 215-220.
- 18) Shakerian F.; Kim K., Kwon E.; Szulejko J.; Kumar P.; Dadfarnia As.; Mohammad A. Advanced polymeric materials: Synthesis and analytical application of ion imprinted polymers as selective sorbents for solid phase extraction of metal ions. *Trends Anal Chem*. **2016**, 83, 55-69.

- 19) Bakas I.; Oujji N.; Moczko E.,; Georges I.; Piletsky S.; Piletska E.; Ait-Addi E.; Ait-I.; Noguier T.; Rouillon R. Computational and experimental investigation of molecularly imprinted polymers for selective extraction of dimethoate and its metabolite omethoate from olive oil. *J Chromatogr A*. **2013**, *1274*, 13-18.
- 20) Piletsky S.; Karim K.; Piletska E.; Day C.; Freebairn K.; Legge C. Turner A.; Piletsky S.; Recognition of ephedrine enantiomers by molecularly imprinted polymers designed using a computational approach. *Analyst*. **2001**, *126*, 1826–1830.
- 21) Piletska E.; Kumir J.; Sergeyeva T. Rational design and development of affinity adsorbents for analytical and biopharmaceutical. *JCAM*. **2013**, *1*, 229-244.
- 22) Pyka A.; Pyka a.; Sliwiok J. Chromatographic separation of tocopherols. *J Chromatogr A*. **2001**, *935*,71-76.
- 23) Beldean-Galea M.; Horga C.; Coman M. Separation and determination of tocopherols in vegetable oils by solid phase extraction on porous polymers SPE cartridges and capillary gas chromatography analysis. *Cent Eur J Chem*. **2010**, *8*, 1110-1116.
- 24) Bramley P.; Elmadfa I.; Kafatos A.; Kelly F.; Manios Y.; Roxborough H.; Schuch W.; Sheehy P.; Wagner K. Vitamin E. *J Sci Food Agric*. **1999**, *80*, 913-938.
- 25) Azzi A.; Stocker A. Vitamin E: non-antioxidant roles. *Prog lipid research*. **2000**, *39*, 321-255.
- 26) Chianella I.; Karim K.; Piletska E.; Preston C.; Piletsky S. Computational design and synthesis of molecularly imprinted polymers with high binding capacity for pharmaceutical applications-model case: Adsorbent for abacavir. *Anal Chim Acta*. **2006**, *559*, 73-78.
- 27) Luo M.; Ross A.; Morgan M.; Day A. Effects of pH on the ability of flavonoids to act as Pickering emulsion stabilizers. *Colloids Surf B Biointerfaces*. **2012**, *92*, 84-90.
- 28) Piletsky S.; Piletska E.; Karim K.; Foster G.; Legge C.; Turner A. Custom synthesis of molecular imprinted polymers for biotechnological application: Preparation of a polymer selective for tylosin. *Anal Chim Acta*. **2004**, *504*, 123-130.

- 29) Mijangos I.; Navarro-Villoslada F.; Guerreiro A.; Piletska E.; Chianella I.; Karim K.; Turner A.; Piletsky S. Influence of initiator and different polymerisation conditions on performance of molecularly imprinted polymers. *Biosens Bioelectron.* **2006**, *22*, 381-387.
- 30) Muhammad T.; Nur Z.; Piletska E.; Piletsky S. Rational design of molecularly imprinted polymer: the choice of cross-linker. *Analyst.* **2012**, *137*, 2623-2628.
- 31) Breton F.; Rouillon R.; Piletska E.; Karim K.; Guerreiro A.; Chianella I. Virtual imprinting as a tool to design efficient MIPs for photosynthesis-inhibiting herbicides. *Biosens Bioelectron.* **2005**, *22*, 1948-1954.
- 32) Gimeno E.; Castellote A.; Lamuela-Ravent R.; Torre M.; López-Sabater M. Rapid determination of vitamin E in vegetable oils by reversed-phase high-performance liquid chromatography. *J Chromatogr A.* **2000**, *881*, 251-254.
- 33) Piacham T.; Nantasenamat C.; Isarankura-Na-Ayudhya C.; Prachayasittikul V. Synthesis and computational investigation of molecularly imprinted nanospheres for selective recognition of alpha-tocopherol succinate. *EXCLI J.* **2013**, ; *12*, 701-718.
- 34) Garbaras A.; Masalaite A.; Garbariene I.; Ceburnis D.; Krugly E.; Remeikis V.; Puida E.; Kvietkus K.; Martuzevicius D. Stable carbon fractionation in size-segregated aerosol particles produced by controlled biomass burning. *J Aerosol Sci.* **2015**, *79*, 86-96.
- 35) Horváth C.; Wayne R. Theory of chromatography. In: *J Chromat Library.* **1983**, *22*, A27-A135.
- 36) Klejn D.; Luliński P.; Maciejewska D.; Klejn D.; Luliński P.; Maciejewska D. Desorption of 3,3'-diindolylmethane from imprinted particles: An impact of cross-linker structure on binding capacity and selectivity. *Mater Sci Eng.* **2015**, *56*, 233-240.
- 37) Ariffin M. The application of novel extraction and analytical techniques in forensic toxicology. PhD Thesis, University of Glasgow, 2006.
- 38) Puoci F.; Cirillo G.; Curcio M.; Iemma F.; Spizzirri U. Molecular imprinted SPE of selective HPLC determination of  $\alpha$ -tocopherol in bay leave. *Anal Chim Acta.* **2007**, *593*, 164-170.

- 39) Dai C.; Zhang J.; Zhang Y.; Zhou X.; Duan Y.; Liu S. Selective removal of acidic pharmaceuticals from contaminated lake water using multi-templates molecularly imprinted polymer. *Chem Eng J.* **2012**, *211*, 302-309.
- 40) Dai C.; Zhou X.; Zhang Y.; Liu Z. Synthesis by precipitation polymerization of molecularly imprinted polymer for the selective extraction of diclofenac from water samples. *J Hazard Mater.* **2011**, *198*, 75-181.
- 41) Chatzimichalakis P.; Samanidou V.; Papadoyannis I. Development of a validated liquid chromatography method for the simultaneous determination of eight fat-soluble vitamins in biological fluids after solid-phase extraction. *J Chromat B Anal Technol Biomed Life Sci Appl.* **2004**, *805*, 289-296.
- 42) Touchstone J. Thin-layer chromatographic procedures for lipid separation. *J Chromat B Biomed Sci Appl.* **1995**, *671*, 169-195.
- 43) Fernández-Cuesta Á.; Aguirre-González M.; Ruiz-Méndez M.; Velasco L. Validation of a method for the analysis of phytosterols in sunflower seeds. *Eur J Lipid Sci Technol.* **2012**, *114*, 325-331.
- 44) Feng S.; Gao F.; Chen Z.; Grant E.; Kitts D.; Wang S.; Lu, X. Determination of  $\alpha$ -Tocopherol in Vegetable Oils Using a Molecularly Imprinted Polymers – Surface-Enhanced Raman Spectroscopic Biosensor. *J Agric Food Chem.* **2013**, *61*, 10467-10475.
- 45) Gonzalez M.; Ballesteros E.; Gallego M.; Valcarcel M. Continuous-flow determination of natural and synthetic antioxidants in foods by gas chromatography. *Anal Chim Acta.* **1998**, *359*, 47-55.
- 46) Ballesteros E.; Gallego M.; Valcárcel M. Gas chromatographic determination of cholesterol and tocopherols in edible oils and fats with automatic removal of interfering triglycerides. *J Chromat A.* **1996**, *719*, 221-227.
- 47) Lenchner M.; Reiter B. Determination of tocopherols and sterols in vegetable oils by SPE and subsequent capillary chromatographic. *J Chromatogr A.* **1999**, *857*, 231-238.

48) Schwartz H.; Ollilainen V.; Piironen V.; Lampi A. Tocopherol, tocotrienol and plant sterol contents of vegetable oils and industrial fats. *J Food Compos Anal.* **2008**, *21*, 152-161.

# Chapter three

# **Applications of the optimised SPE protocols to extract selected physiologically-active compounds from the vegetable oils**

## **3.1 Introduction**

Vegetable oils consist of 95 to 98% of triacylglycerol and 2 to 5% of different groups of minor components such as hydrocarbons, tocopherols, phytosterols and their esters.<sup>1-3</sup> The typical raw materials for biodiesel production are vegetable oils, such as rapeseed, canola, soybean, sunflower and palm oils. “The cost of biodiesel can be lowered by increasing feedstock yields, developing novel technologies, and increasing economic return”<sup>4</sup> (p.S111), described by Demirbas (2009) to highlight the importance of encouraging this industry to protect our planet. Triglycerides are the target components of vegetable oils which are used as reactants with methanol or ethanol in the transesterification reaction in the presence of the alkali catalyst to produce biodiesel (Figure 3.1).<sup>1-7</sup> Therefore, the minor components of vegetable oils, most of which are physiologically active, are lost during the biodiesel production process.

Free fatty acids are the main group of minor compounds in the vegetable oils that are desirable to be separated or treated before biofuel production process. One of the reactions used for producing the biofuel is transesterification. Transesterification is the reaction of a fat or oil with an alcohol to yield esters and glycerol. The reaction should be controlled by an alkali catalyst. This equilibrium reaction requires a great amount of alcohol to keep the reaction equilibrium in the forward direction and produce more methyl esters, not the opposite.<sup>1,2</sup> It was observed that the presence of free fatty acids has a negative effect on the biodiesel production from vegetable oils due to their reaction with the alkali catalyst to form soap and water, thus inhibiting the separation and purification processes of the biodiesel as demonstrated in Figure 3.2.<sup>2,3</sup> Hence, free fatty acids represent a potential problem in biodiesel production. The most common fatty acids in vegetable oils are palmitic, oleic and linoleic acids. Palmitic acid is the main saturated fatty acid that has numerous food and industrial applications. According to Mancini *et al.*, palmitic acid is an important constituent in industrial products

such as ice cream, toothpaste, candles and cosmetic products.<sup>4</sup> The main mono-unsaturated fatty acid is oleic acid which can reduce blood sugar and protect the heart.<sup>5</sup> Linoleic acid as the main di-unsaturated fatty acid can lower the triglyceride and cholesterol in the human body which leads to reduce the chances of cardiovascular diseases.<sup>6</sup>

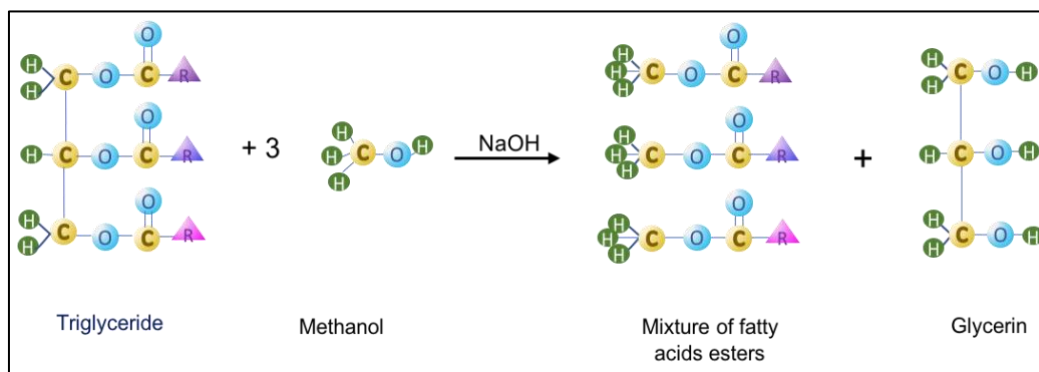


Figure 3.1: The equation of esterification (biofuel production).

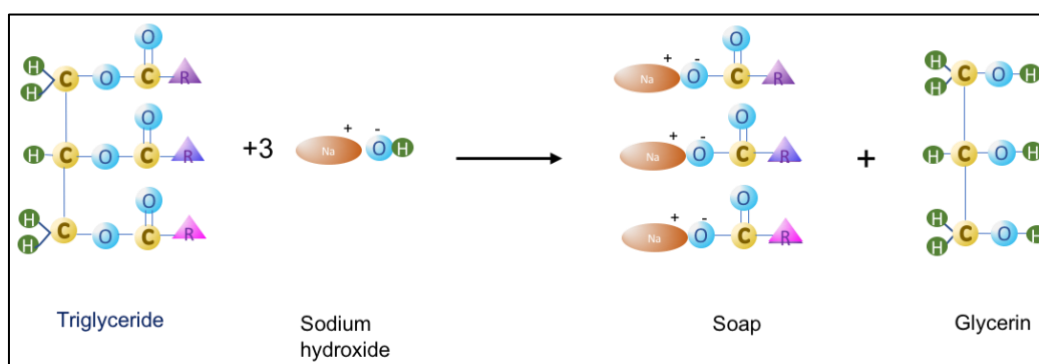


Figure 3.2: The formation of soap during the esterification (undesirable interference by free fatty acids in the reactants).

Tocopherols are minor components of vegetable oils that represent some of the vitamin E family of compounds. Vitamin E compounds are associated with antioxidant activity in the human body. Thus far,  $\alpha$ -tocopherol has attracted much attention as a potential protective and palliative agent among this group of compounds,<sup>7-11</sup> however, recent studies have indicated the importance of  $\gamma$ -tocopherol.<sup>16,17</sup> The main role of vitamin E in the body is the reduction of peroxy radicals, and it was proved practically that the presence of  $\gamma$ -tocopherol with  $\alpha$ -tocopherol leads to increase the bioavailability of  $\gamma$ -tocopherol.<sup>12</sup> Additionally,

vitamin E is widely used in industrial applications like medicine, cosmetics, agriculture and the food industry.<sup>13,14,15</sup>

Other minor components of vegetable oils are comprised of phytosterols (plant sterols) a type of triterpenes which have drawn the attention of many researchers due to their bioactivity. They are available in plants in their free and conjugated forms with fatty acids or glycosylated with hexose. It is known that phytosterols have the potential to reduce total serum cholesterol as well as LDL-cholesterol in the human body through the inhibition of the absorption of dietary cholesterol and the reabsorption of excreted cholesterol in the bile in the enterohepatic cycle.<sup>16-18</sup>

Many published studies suggested several protocols to purify and extract the minor components from vegetable oils separately or simultaneously.<sup>19,20</sup> However, all of these methods require either pre-treatment of the oil sample or consuming a lot of chemical solvents to dilute the oil sample and using developed technologies for separation such as HPLC and supercritical fluid extraction.<sup>21,22</sup> Thus, applications of these methods in the industry are limited.

In this study, the proposed protocol presented here was based on an optimised method which allows to “harvest” some physiologically-active compounds in a single step, from the vegetable oils with a minimum of organic solvents in an environmentally-safe process using an earlier developed bespoke adsorbent.

## **3.2 Materials and methods**

### **3.2.1 Chemicals and reagents**

The unrefined and cold pressing oils including sunflower and sesame oil were purchased from Activecare. Palm oil was obtained from KTC and olive oil, wheatgerm and soybean oil were all bought from the Food Marketplace through Amazon.com. Standards were originated from vegetable oil including  $\alpha$ -tocopherol that was purchased from Santa Cruz Biotechnology (UK). In addition to the  $\alpha$ -tocopherol, mixtures of phytosterols, containing 46%  $\beta$ -sitosterol, 24% campesterol and 16% stigmasterol, were also purchased from Santa Cruz Biotechnology (UK). Ethylene glycol dimethacrylate (EGDMA), azobis (cyclohexane carbonitrile), methacrylic acid (MAA) and free fatty acids including palmitic, oleic and linoleic acids were purchased from Aldrich (UK). Methanol, ethyl acetate, heptane, acetonitrile, n-hexane, dichloromethane and acetic acid were obtained from Fisher Chemicals (UK). All solvents were used without any purification and they were all HPLC-quality grade. 1, 1'-azobis (cyclohexane carbonitrile), methacrylic acid (MAA) and ethylene glycol dimethacrylate (EGDMA) were purchased from Aldrich (UK). Dimethylformamide (DMF) was obtained from Acros Organics (UK).

### **3.2.2 Equipment and analysis techniques**

1 mL SPE columns were packed with 200 mg of the RDP and used in SPE supported with a vacuum manifold (Supelco, UK). Gas Chromatography-Mass Spectrometry (Perkin Elmer, TurboMass, UK) was used for the analysis and quantification of the extracted components in the eluted samples during SPE protocol. Gas Chromatography was performed using a 30 m X 250  $\mu$ m, 0.25 mm I.D., ZB-5 capillary column (Phenomenex, UK). To carry the sample, helium gas was used as a mobile phase with a flow-rate of 1 mL min<sup>-1</sup> at 200 °C. The temperature of the GC oven was raised after a sample injection by 10 °C min<sup>-1</sup> to 350 °C and held for 3 min.

### **3.2.3 Investigation the affinity of RDP towards minor components**

In order to justify the potential of the synthesised RDP in the previous chapter, modelling process has been applied again (though using different templates) to demonstrate specific recognition to some minor components, such as fatty acids and phytosterols in vegetable oils. The molecular modelling software capable to illustrate the hydrogen bonds between each of these minor components with the same functional monomers as presented in the previous chapter.

The main goal of doing the modelling for the extracted minor components was to be able to predict the possible molecular interactions contributing to the formation of the template: monomer interactions among the RDP. Molecular modelling was performed using a workstation from Research Machines running the CentOS 5 GNU/Linux operating system. The workstation was configured with a 3.2GHz core 2 duo processor, 4 GB memory and a 350 GB fixed drive. Molecular modelling was conducted using the software packages SYBYL 7.0 (Tripos Inc., St. Louis, Missouri, USA).<sup>23</sup> The LEAPFROG screening of the library of functional monomers for their potential interactions with the template resulted in tables of functional monomers with the binding energy to each template. Each modelling process was repeated for all the minor components as a template in this study including palmitic, oleic, linoleic acids, campesterol, stigmasterol and  $\beta$ -sitosterol.

### **3.2.4 Applications of the optimised SPE protocol to the vegetable oils**

The optimised protocol that has been applied to all types of oil was based on the optimised protocol in the previous chapter, which has been published<sup>24</sup> (Appendix1), as follows:

#### **3.2.4.1 Preparation of the samples**

Dissolved the oils (20%) and the standards of each minor components in heptane. Further, used these standards to spike 1 mL of each oil (sunflower, sesame, soybean, olive, palm and wheat germ) solution in heptane with 0.3 mg of each standard.

### 3.2.4.2 The SPE protocol conditions

The SPE cartridges were packed with 200 mg of synthesised RDP and conditioned with 1 mL heptane. Further, two separate cartridges were loaded, one with 1 mL of spiked oil sample and other with 1 mL of oil without spiking, for each type of oils. After that, the cartridges were washed with 1 mL of 60% methanol, subsequently, 3 mL of methanol with 5% acetic acid was used for the elution of the adsorbed compounds from the cartridges. The eluted samples were evaporated and reconstituted in hexane (1 mL) to be analysed with GC/MS. The quantitative measurements were performed using the integration values of the area under peaks in GC chromatogram which is directly proportional to the concentration of the analysed samples. The concentration of compounds was calculated in  $\text{mg g}^{-1}$  of oil using calibration curves of the pure standards. The mass spectra of each compound were analysed to match the fragmentation pattern in the NIST library and the literature with the obtained fragments. In addition, IR was used to distinguish between fatty acids and their esters in the eluted samples.

### 3.2.4.3 Calibration curves

Calibration curves were made using the integration of the peaks corresponding to the series of concentrations of the standards solution in hexane for the minor components involved in this study, in GC/MS chromatogram. Hence integration values of these peaks were directly proportional to the concentration of analysed samples. The calibration curve was generated from plotting the relationship between the integration of series of known concentration solutions and their concentration. The straight line resulted follow the equation  $y=mx$  where  $x$  is the concentrations and  $y$  is the corresponding integration. Then, simply replaced the integration ( $y$ ) of the unknown concentration into the equation, where the  $m$  is known from the resulted equation produced from calibration curve, to calculate the unknown concentration.

The calibration curves were made for each fatty acid: palmitic acid, oleic acid and linoleic acid. Calibration curve for  $\alpha$ -tocopherol was presented in the previous chapter. Phytosterols standard sample contained naturally 24% of campesterol and

16% of stigmasterol. Therefore, the calibration curve was made from a series of the mixture to each sterol alone as shown in the results section.

### **3.2.5 Saponification the fatty acids**

For comparison in GC/MS between the fatty acids and their esters, methyl esters were synthesised from each fatty acid individually. The saponification was carried out by following the method described by Fallon *et al.*<sup>25</sup> Briefly, 0.7 mL of 10 N KOH in water was added to 40  $\mu$ L of liquid fatty acid or 0.5 mg of solid fatty acid in 125x16 mm screw-cap Pyrex tubes. Then, 5.3 mL of methanol was added before heating at 55°C for 1.5 hours with the mixture being shaken by hand every 20 minutes. The mixture was cooled to room temperature before adding 0.58 mL of sulfuric acid (24 N) in water. The mixture was heated again at 55°C with it being shaken 3 min every 20 min. Next, the mixture was vortex shaken after cooling it to room temperature and adding 3 mL of hexane. Finally, the mixture was centrifuged for 5 min at 4000 rpm. The layer of hexane contained the ester of fatty acids, which was separated and analysed using GC/MS.

### **3.2.6 Method validation**

Method reliability and matrix effects were investigated using the published method in Flakelar *et al.* 1 mL of heptane was spiked with the mixed standards.<sup>26</sup> 1 mL of the spiked solution was analysed with GC/MS with the same used conditions of this study. Using the calibration curve and the integration of peaks, it was possible to calculate the percentage of each standard compound in the spiked sample as shown in Table 3.8 in results section. Further matrix effects were examined by comparing the weight of the eluted sample from 20% sunflower oil in heptane with weight of the eluted sample after subtracting the calculated weight of the natural compounds quantified using GC/MS. The calculations of the concentrations of eluted compounds were performed using the integration of peaks and the calibration curve.

### 3.3 Results and discussion

The main objective of this chapter was to determine the possibility of applying the optimised protocol to other vegetable oils. Before presenting the results of these experiments, it is important to highlight the properties of the RDP that provided specificity towards these minor components. In order to explain the common molecular interaction between the minor compounds, which were extracted in the current study, and the synthesised polymer, a molecular modelling has been conducted using the SYBYL software as it was described in the previous chapter for  $\alpha$ -tocopherol.

#### 3.3.1 Molecular modelling:

The RDP has been synthesised based on  $\alpha$ -tocopherol as a template. However, after applying the optimised method to the sunflower oil sample, it was found that the polymer has demonstrated recognition to not only  $\alpha$ -tocopherol but also to other minor compounds. The used polymer has been synthesised based on the 3D chemical structure of  $\alpha$ -tocopherol, therefore, the investigation of the modelling for other minor compounds was focused on the same functional monomers in the top of the LEAPFROG list in terms of their binding energy with each template. The functional monomers include MAA, EGDMA, AMPSA, EGMP, IA and UA. The results of the modelling were presented initially together in Figure 3.3 for the purpose of justification the affinity of these minor compounds to the same functional monomers. In general, it was found that AMPSA showed the highest binding energy then, EGMP with a little exception in some phytosterols, then MAA and EGDMA (cross-linker) and, finally, IA and UA with some exceptions. In the next part, each group of minor compounds was presented with these functional monomers and was explained in more detail.

RDP was applied in this study as a resin or a stationary phase which retained the analytes based on binding to the organic moieties of some available compounds from the different groups of vegetable oil components. To explain the capacity of RDP and the excellent efficiency of RDP towards the fatty acids in the vegetable oils a comparison has been made between the different chromatographic separation

mechanisms to justify the common features that led to the separation of the group of compounds in this study.

In the solid phase extraction, the retentive properties and the selectivity of certain analytes are affected mainly by the stationary phase and the mobile phase.<sup>27</sup> There are six different modes of stationary phases which were presented in details in the fourth chapter. In this chapter, the stationary phases that have common features with RDP have been demonstrated to understand the retention mechanism of RDP. Firstly, in normal-phase separation, the analytes are separated according to their polar moieties (e.g. the hydroxyl group, amine group or ester bonds). Therefore, the retentive properties of silica gel as stationary phase are due to the interactions between silanol groups, to which hydroxyl groups are linked, and the polar moieties from analytes. Thus, the separation depends on the nature and the number of the polar functional groups of the analytes.<sup>28</sup>

In the reversed-phase the stationary phase retains the compounds by attractive dispersion interactions. Moreover, shape and size of molecules have an effect on the retentive properties.<sup>29</sup> The third separation mode could be used in the explanation of the RDP selectivity is the ion-exchange separation. Ion-exchange separation modes are based on the competition between the analyte ion and counter ion comes from the mobile phase in certain site with opposite charge on the sorbent. The separation is performed by controlling the concentration of ion or pH of the elution solvent (the mobile phase).<sup>28,29</sup>

RDP has some common features with the three above mentioned separation modes. RDPs are particles contain functional groups such as carboxylic (come from MAA), imidazole rings (come from urocanic acid) or phosphoric (come from EGMP). These functional groups interact with polar intermolecular interactions such as hydrogen bonds or non-polar intermolecular interactions such hydrophobic interactions depending on the nature of the analytes and the functional groups on the surface of the polymer particles. In the polymer particles, the orientation of functional monomers was fixed using cross-linker (EGDMA), which contributed as well to the retentive properties of the polymer particles via the electron-withdrawing and electron-donor properties of alkoxy and carbonyl groups. Furthermore, the

mobile phase was the solvent that was miscible with these compounds at optimal pH sufficient to disturb the intermolecular interactions and elute the compounds of interest.

The results of the molecular modelling have been presented for all separated compounds in one Figure 3.3 to have an overview of the chosen functional monomers by SYBYL software. Then, the binding energies were presented for each group in the current chapter. It was found that MAA was among the functional monomers possessing the highest binding energy towards the extracted compounds, which was in accordance with the experimental results.

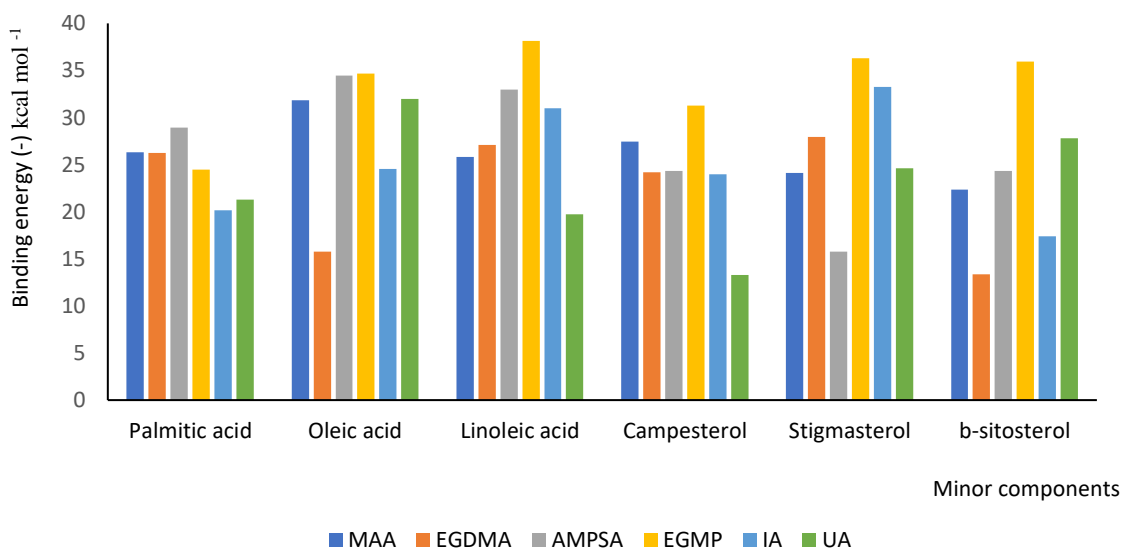


Figure 3.3: The relative binding energy of common functional monomers towards minor components.

### 3.3.1.1 Study the molecular modelling of fatty acids

The chemical structure of each fatty acid was downloaded and minimised. Then, all of the modelling processes was applied to it as mentioned in the previous chapter. The SYBYL software has the potential to demonstrate the hydrogen bond interactions only (Figures 3.4, 3.5 and 3.6). However, the other types of molecular interactions can be predicted by looking at the type of atoms or measuring the distances between the template and functional monomer atoms.

According to Christie, the fatty acids have several organic moieties, by which fatty acids were separated using different types of stationary phases.<sup>27</sup> The lipid compounds were separated in the normal-phase mode based on the chain-length moieties and the degree of saturation. In reversed-phase chromatography the alkyl moieties, carboxyl moieties and the number and configuration of the fatty acids were contributing to the separation process. The used mobile phase was methanol with 5% acetic acid that disturbed the interactions between the fatty acids with the functional monomers on the RDP surface. The potential moieties by which the intermolecular interactions occur include two double bonds in linoleic acid, a carboxylic group and 18 carbon chain-length. In case of oleic acid, only one double bond with the carboxylic group and 18 carbon chain-length participated in the retentive properties. Palmitic acid has no double bond and the contributed moieties to the retention on the stationary phase included the 16 carbon chain-length and carboxyl group.

The fatty acids were interacting using London forces and Van der Waals with the alkyl moiety or double bonds on fatty acid and methyl groups on the polymer surface.<sup>27,29</sup> Moreover, hydrogen bonds, polar dipole-induced dipole, dipole-dipole and proton donor-proton acceptor interactions have also participated in the retention process. Therefore, it was suggested that the difference in the preference of these types of interactions could lead to the preferential binding of the functional monomers towards different fatty acids. For example, since AMPSA has carbonyl group, nitrogen and sulfur atoms as proton acceptors and hydrogen linked to a sulfonic group could act as a proton donor, it could provide an explanation why this functional monomer could prefer interacting through polar intermolecular interactions with polar moieties. On the other hand, UA and IA have alkyl moieties that could show more non-polar intermolecular interactions such as van der Waals with the alkyl chain and double bonds. Moreover, EGMP was at the beginning of oleic and linoleic acids and in the middle of the list in palmitic acid. This could be explained through the preference of oleic and linoleic to interact with EGMP with van der Waals since it has methyl and methylene moieties.

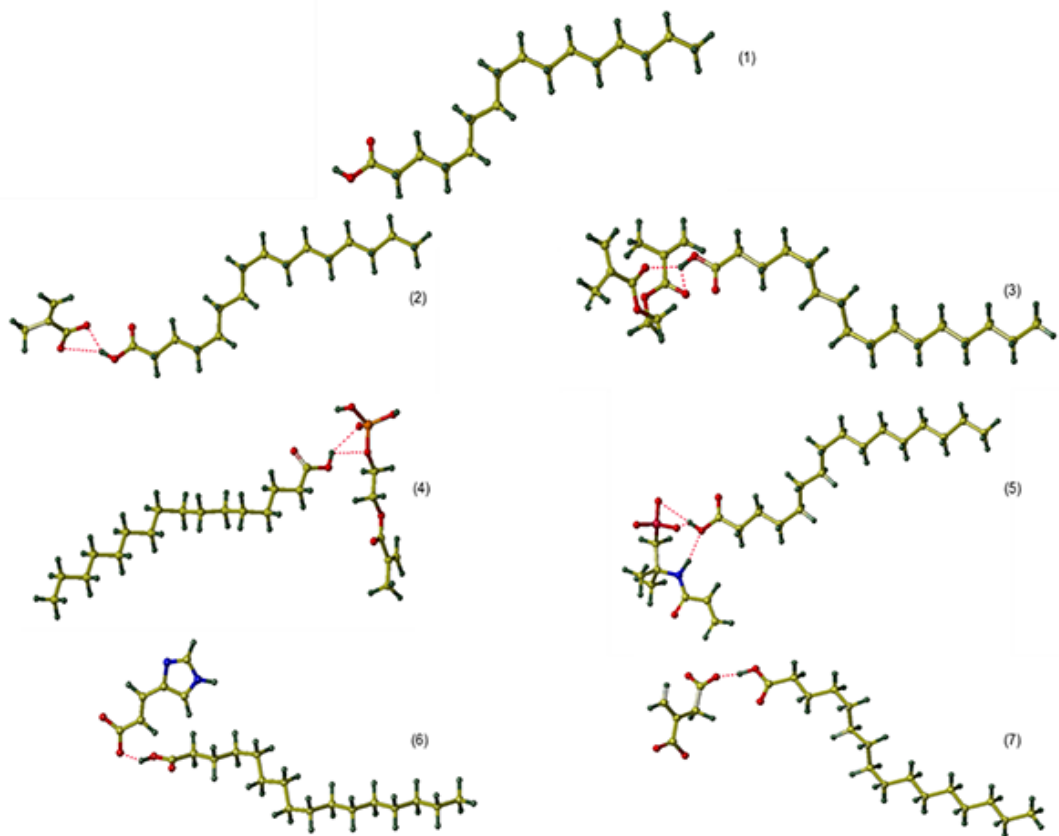


Figure 3.4: The 3D structures of palmitic acid (1), the hydrogen bonds between palmitic acid and the functional monomers: MAA (-) (2), EGDMA(cross-linker) (3), AMPSA (4), EGMP (-) (5), UA (-) (6) and IA (-) (7).

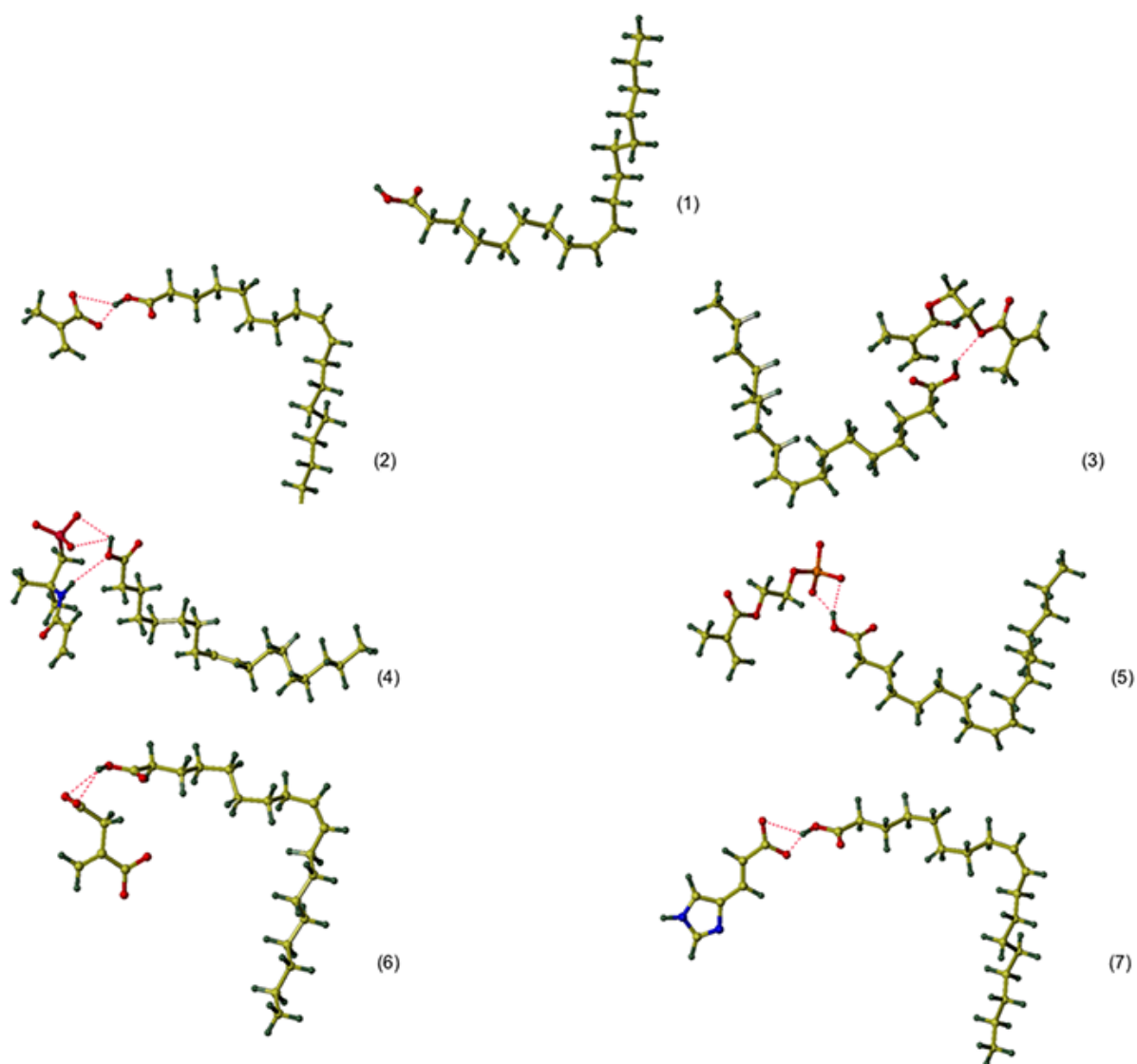


Figure 3.5: The 3D structures of oleic acid (1), the hydrogen bonds between palmitic acid and the functional monomers: MAA (-) (2), EGDMA(cross-linker) (3), EGMP (-) (4), AMPSA (5), IA (-) (6) and UA (-) (7).

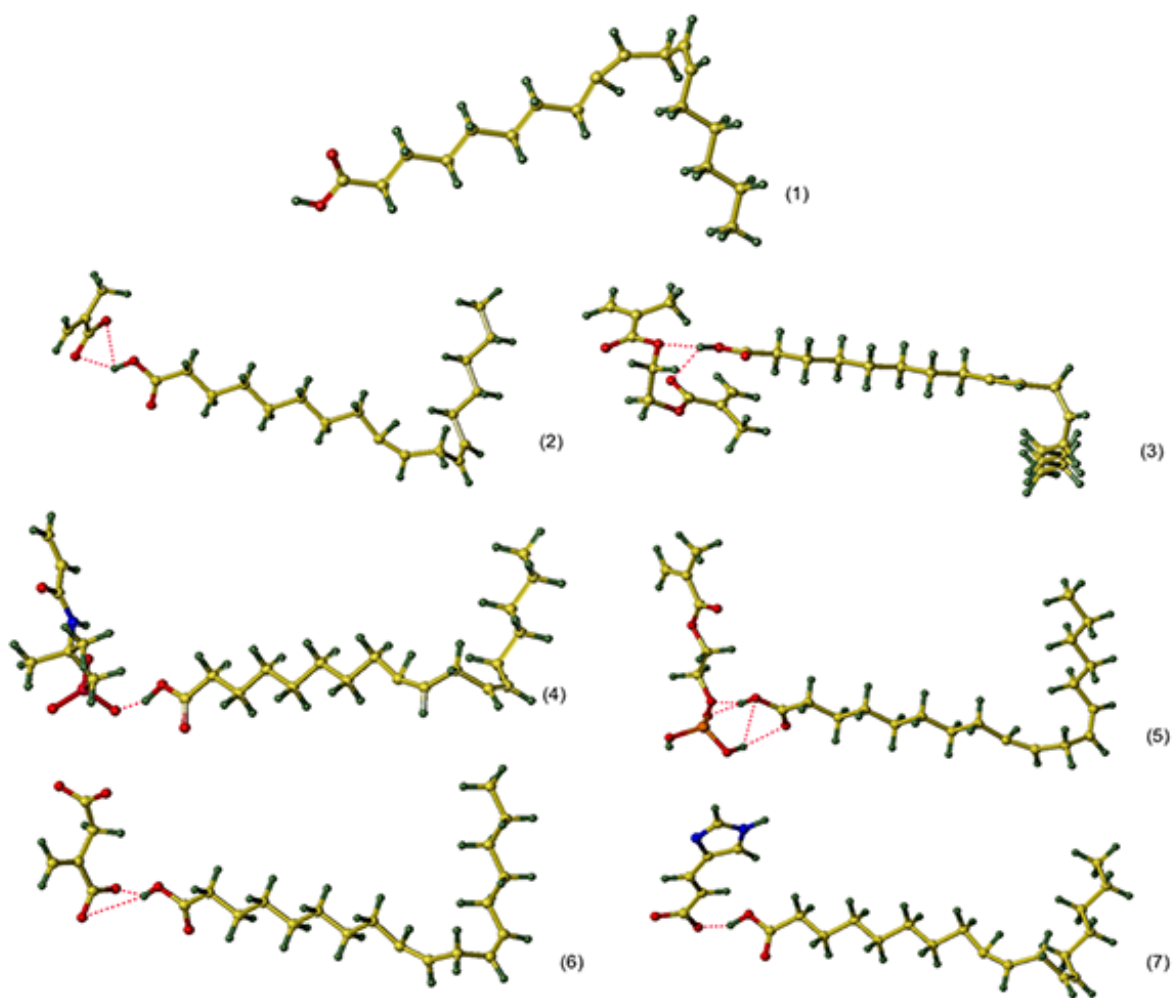


Figure 3.6: The 3D structures of linoleic acid (1), the hydrogen bonds between palmitic acid and the functional monomers: MAA (-) (2), EGDMA(cross-linker) (3), EGMP (-) (4), AMPSA (5), IA (-) (6) and UA (-) (7).

The molecular modelling software SYBYL as was mentioned above provided 3D pictures of the hydrogen bonds may be formed between the fatty acids and the functional monomers as shown in Figures 3.4, 3.5 and 3.6. Fatty acids have common features which are carboxyl groups that could act as either donor or acceptor for the hydrogen bonds with the different functional monomers. In addition, the alkyl chain is another common feature that may contribute to the non-polar

intermolecular interactions involving, for example, van der Waals and London forces.<sup>28</sup>

### **3.3.1.2 Study the molecular modelling of phytosterols**

Phytosterols molecules consist of four rings with standard carbon numbering. The three are six carbon atoms in a non-linear arrangement and are attached to one 5-carbon atom ring. The different phytosterols extracted from plants vary in the number of carbon atoms in the side chain and the position and number of double bonds in the ring and side chain. The structure of phytosterols determines the chromatographic properties of them. It has been demonstrated that phytosterols interacted with the chromatographic surfaces with hydrophilic and hydrophobic interactions due to the presence of polar and non-polar moieties in the same molecule.<sup>30-32</sup> According to Demel *et al.*, phytosterols could participate in polar intermolecular interactions via 3-hydroxy group in the meanwhile of making non-polar interactions through the alkyl side chain.<sup>32</sup>

The binding energy of intermolecular interactions between the three types of phytosterol in the current study (campesterol, stigmasterol and  $\beta$ -sitosterol) and six types of functional monomers that were calculated by SYBYL software.

The SYBYL software demonstrated the hydrogen bonds between the six types of functional monomers and the three phytosterols only through the 3b-hydroxy group as shown in Figures 3.7, 3.8 and 3.9.

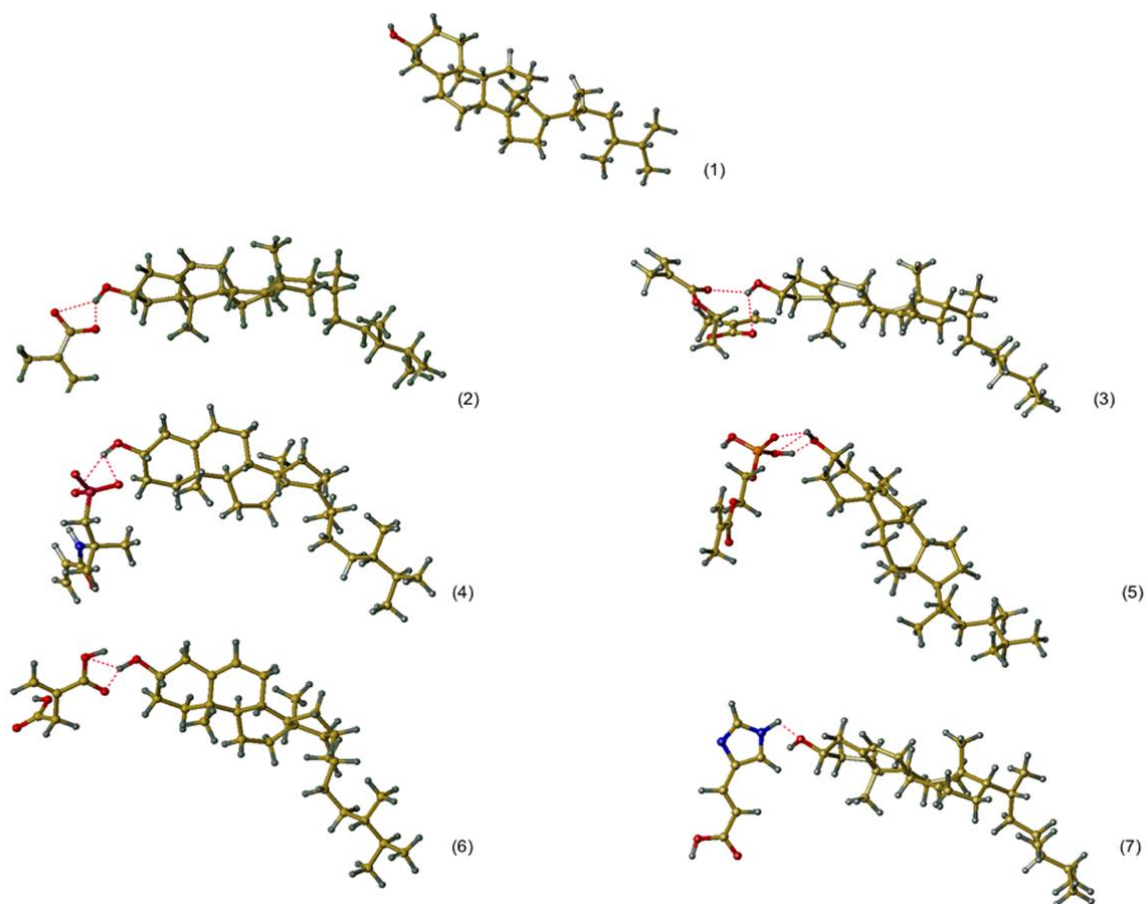


Figure 3.7: The 3D structures of campesterol (1) and the hydrogen bonds between campesterol and the functional monomers: MAA (2), EGDMA(cross-linker) (3), EGMP (-) (4), AMPSA (5), IA (-) (6) and UA (-) (7).

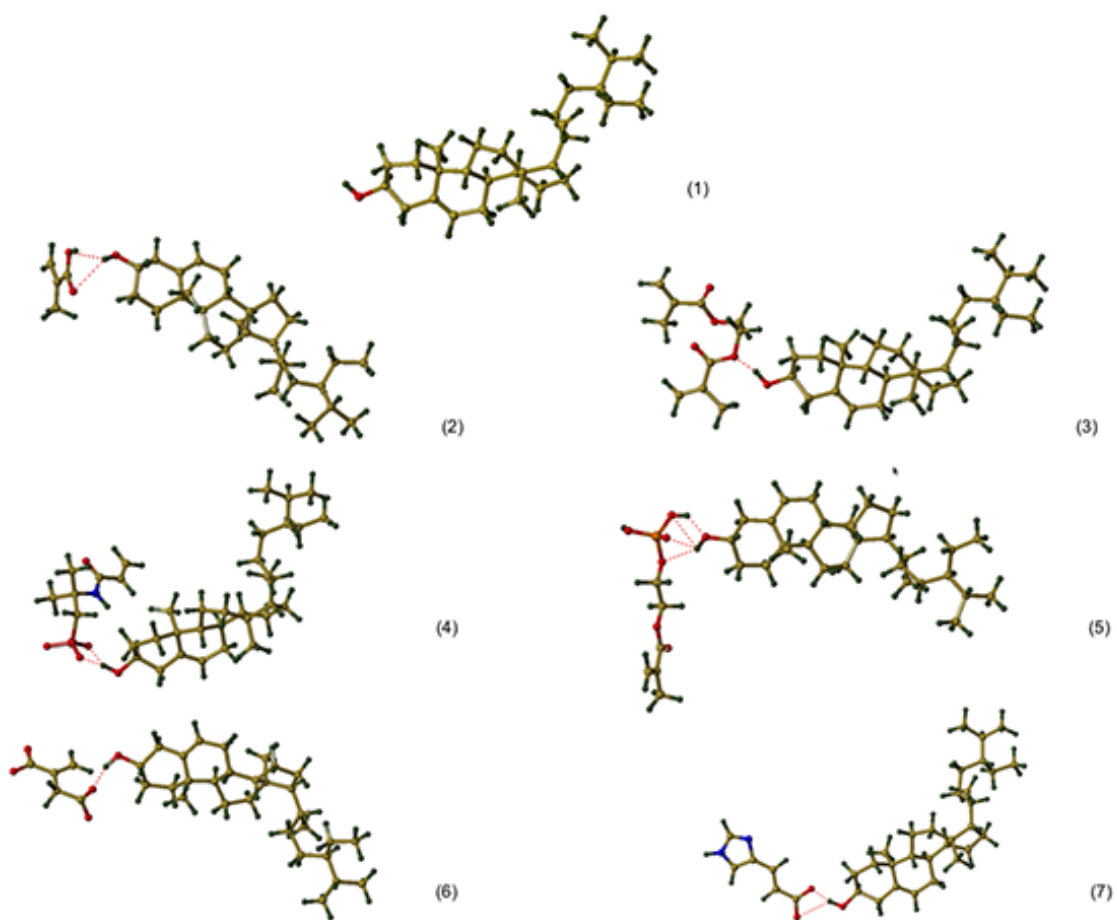


Figure 3.8: The 3D structures of stigmasterol (1) and the hydrogen bonds between stigmasterol and the functional monomers: MAA (2), EGDMA (cross-linker) (3), EGMP (-) (4), AMPSA (5), IA (-) (6) and UA (-) (7).

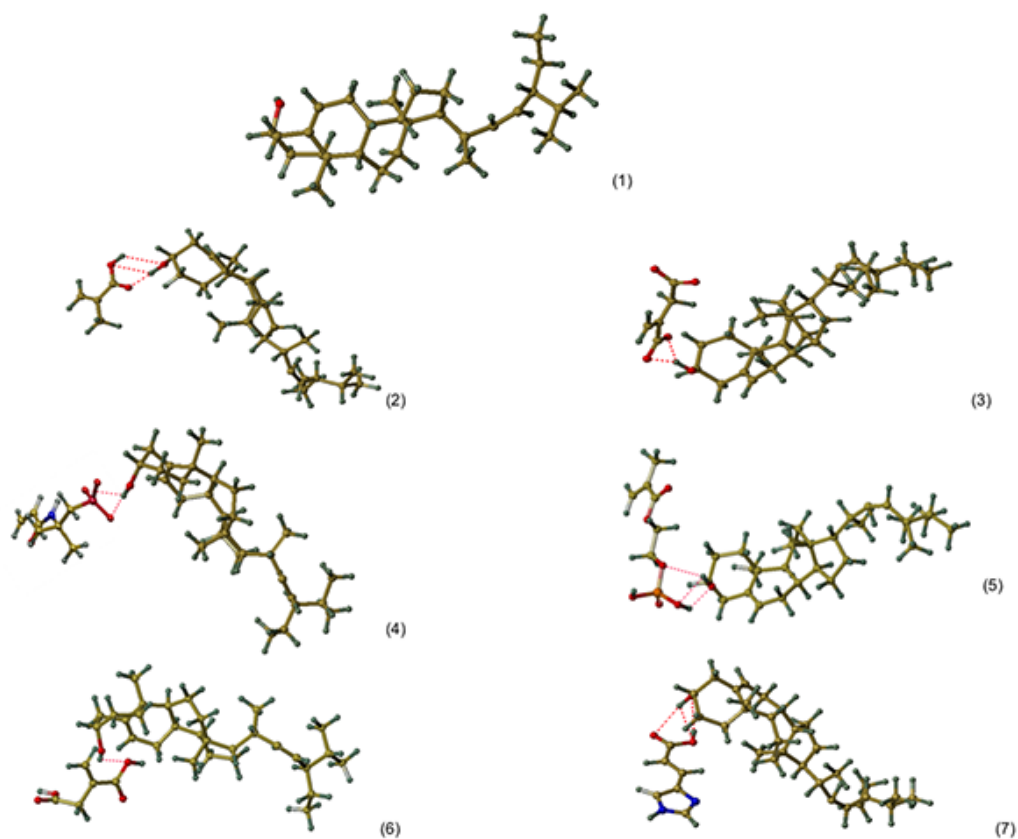


Figure 3.9: The 3D structures of  $\beta$ -sitosterol (1) and the hydrogen bonds between  $\beta$ -sitosterol and the functional monomers: MAA (2), EGDMA(cross-linker) (3), EGMP (-) (4), AMPSA (5), IA (-) (6) and UA (-) (7).

### 3.3.2 Quantification of the minor components in the vegetable oils

#### 3.3.2.1 Calibration curves

Calibration curves of the minor components in the current study facilitated the quantification of the components in all of these experiments (Table 3.1). The minor components included palmitic, oleic, linoleic acids, campesterol, stigmasterol,  $\beta$ -sitosterol and sesamin (observed in sesame oil only). It is important to highlight here that  $\alpha$ -tocopherol was quantified along with these minor components in the vegetable oils, but its calibration curve was showed in the previous chapter.

Table 3.1: Summarised the calibration curve equations and R-squared values were produced from calibration curves (Appendix 2) for all the minor compounds.

Minor compound	Calibration curve equations	R <sup>2</sup> value
Palmitic acid	$y = 0.4527x - 21.111$	R <sup>2</sup> = 0.99183
Oleic acid	$y = 0.4501x - 7.3577$	R <sup>2</sup> = 0.9984
Linoleic acid	$y = 0.4599x - 10.138$	R <sup>2</sup> = 0.99651
$\alpha$ -tocopherol	$y = 0.4991x - 6.7026$	R <sup>2</sup> = 0.99902
Campesterol	$y = 0.6204x - 23.724$	R <sup>2</sup> = 0.99325
Stigmasterol	$y = 0.5852x - 25.821$	R <sup>2</sup> = 0.99237
$\beta$ -sitosterol	$y = 1.4715x - 67.776$	R <sup>2</sup> = 0.99085
Sisamen	$y = 0.7617x - 17.122$	R <sup>2</sup> = 0.99556

### 3.3.3 Investigation the minor components

As discussed in Chapter 2, the optimised protocol was applied to sunflower oil. In this chapter, the optimised method has applied to sesame oil, soybean oil, wheat germ oil, olive oil and palm oil. The proposed method, as aforementioned, involved using RDP as arisen in the SPE cartridge and applied the optimised solvents with appropriate optimised quantities in SPE steps to the oil samples separately. The data obtained in this experiment was recorded as the mean of triplicate determinations and standard deviation (SD).

It is important to point out that in this chapter, the listed quantities (in sections from 3.3.3.1 to 3.3.3.5) consisted of the amount of extracted minor compounds using the optimised method sorted in two columns for each component. One of them showed the extracted amount from oil in heptane. The other column was referring to the extracted amount from the spiked oil with  $0.3 \text{ mg mL}^{-1}$  of the standard solution of each minor components. The most noticeable point was that the difference between the two columns varied from the spiked amount by a value of  $\pm 0.3 \text{ mg mL}^{-1}$ . This difference in the extracted quantities led to the conclusion that spiking the oil with the standards improved the extracting process as has been

concluded in previous studies.<sup>32</sup> One possible explanation is using the intermolecular attractive forces theory. Increasing the initial concentration of the minor component by spiking. It seems that more concentration of these compounds encourage the extraction process and leading to more yield. The Figure 3.10 displayed the chromatogram of each oil individually. This allowed to compare each minor component in all vegetable oils. In the next section, each minor component was discussed individually in all oils.

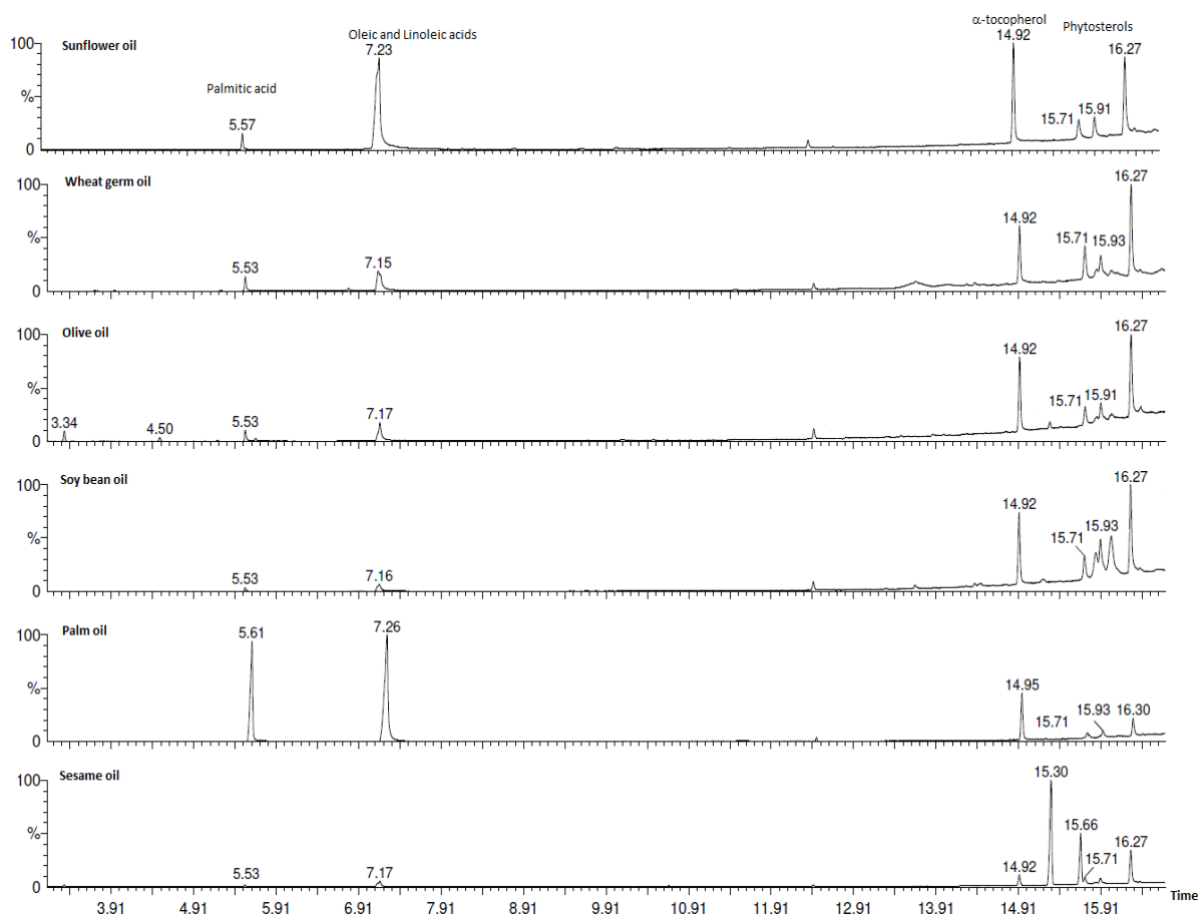


Figure 3.10: GC chromatograms of the eluted samples from the six different vegetable oils spiked with the seven standards (this experiment was repeated three times).

### 3.3.3.1 Extraction and analysis of palmitic acid (16:0)

The first common extracted compound at the retention time around 5 min is palmitic acid (a saturated fatty acid). Palmitic acid is found in vegetable oils either in free form or in conjugated form as an ester.<sup>13,21,34</sup> The presence of palmitic acid was proved using the classical analysis method of lipids by comparing the retention time, pattern of fragmentation in mass spectra and IR spectra of free acid and methyl ester forms.<sup>35</sup> Free fatty acids and ester have been quantified in several studies such as those reported in Eisenmenger *et al.*, and Ghafoor *et al.*, where free fatty acids comprised of 0.5 to 22%<sup>13</sup> and 0.2 to 7.9 %<sup>35</sup> respectively from a total component of fatty acids in wheat germ oil.<sup>13,37</sup> It was found that free fatty acids did not exceed 60 g kg<sup>-1</sup>, however this number could be amplified in the case of extracting the oil by cold pressing to reach 23.46 mg g<sup>-1</sup> thus all the used vegetable oils in this study are either unrefined or obtained by cold pressing to extract relatively measurable levels from the minor components.<sup>13</sup>

The extracted fatty acids in this research are in their free form only (Table 3.2) which were confirmed by three ways:

- 1) Comparing the following peaks in GC chromatogram with their standards.
- 2) IR spectra.
- 3) The mass spectra of each fatty acid and its corresponding ester.

Table 3.2: The concentrations of palmitic acid in different vegetable oils.

Vegetable oils	Quantities (mg/g)	Spiked quantities (mg/g)
Wheat germ	1.14 ± 0.51	1.73 ± 0.09
Soybean	0.004 ± 0.01	1.22 ± 0.13
Sunflower	0.942 ± 0.09	1.82 ± 0.8
Sesame	0.366 ± 0.14	0.62 ± 0.06
Palm	15.6 ± 0.87	16.28 ± 0.43
Olive	1.19 ± 0.13	2.16 ± 0.12

Standard solution of palmitic acid in heptane and the methyl ester of palmitic acid were analysed using GC/MS and IR to determine the differences between them. Firstly, GC chromatogram has shown a peak related to the ester form before the acid form as shown in Figure 3.11, the upper plot represented the GC/MS chromatogram for palmitic acid and the lower one represented methyl palmate. Therefore, under the current conditions of GC, the difference in time of separation of ester from its corresponding acid is very short in the GC column.

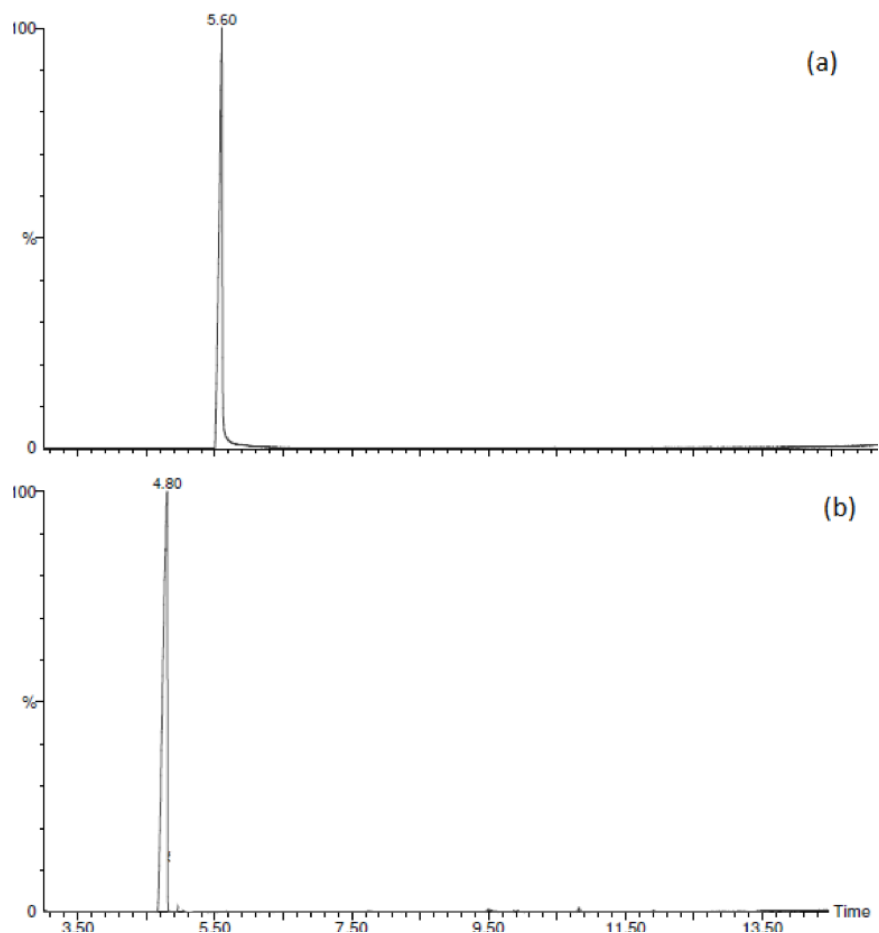


Figure 3.11: GC chromatogram for (a) palmitic acid and (b) methyl palmate solutions in hexane.

By comparing the mass spectra of the peak at 5.5 min in the GC/MS to the NIST library mass spectrum of palmitic acid, it was found that the fragmentation patterns were identical. It has been reported that free fatty acids were hardly found in research analysed by GC/MS without derivatisation, however, the mass spectra

could be compared with the corresponding methyl ester of these acids.<sup>37</sup> By looking at mass spectra in Figure 3.12 (a,b), it was possible to confirm that spectrum (a) refers to palmitic acid and the molecular ion was seen at  $m/z$  256. In addition, specifying fragment was at  $m/z$  239 produced from loss the  $\text{OH}^-$  ion. Other fragments at  $m/z$  101, 115, 129, 143, 157, 171, 185 were representing fragmentations between methylene groups of the form  $[\text{HOOC}(\text{CH}_2)_n]^+$ .<sup>36</sup> Another fragment was at  $m/z$  213  $[\text{M}-43]^+$  was produced from complicated rearengment to loos of  $\text{C}_2$  to  $\text{C}_4$ . On the other hand, mass spectra (b) shows the fragments of methyl palmate. The baseline is the fragment at  $m/z$  270, then the fragment at  $m/z = 239$  that refers to the loss of the methoxyl group  $[\text{M}-31]^+$ . The other distinguished ion is the one at  $m/z = 227$ , which is formed by losing  $\text{C}_3$  unit (carbons 2 to 4). Then, the homologous series of fragments at  $m/z = 101, 115, 129, 143, 157$  and  $199$  refer to the general formula  $[\text{CH}_3\text{OCO}(\text{CH}_2)_n]^+$ , which indicated to the absence of functional groups in the chain.<sup>37</sup>

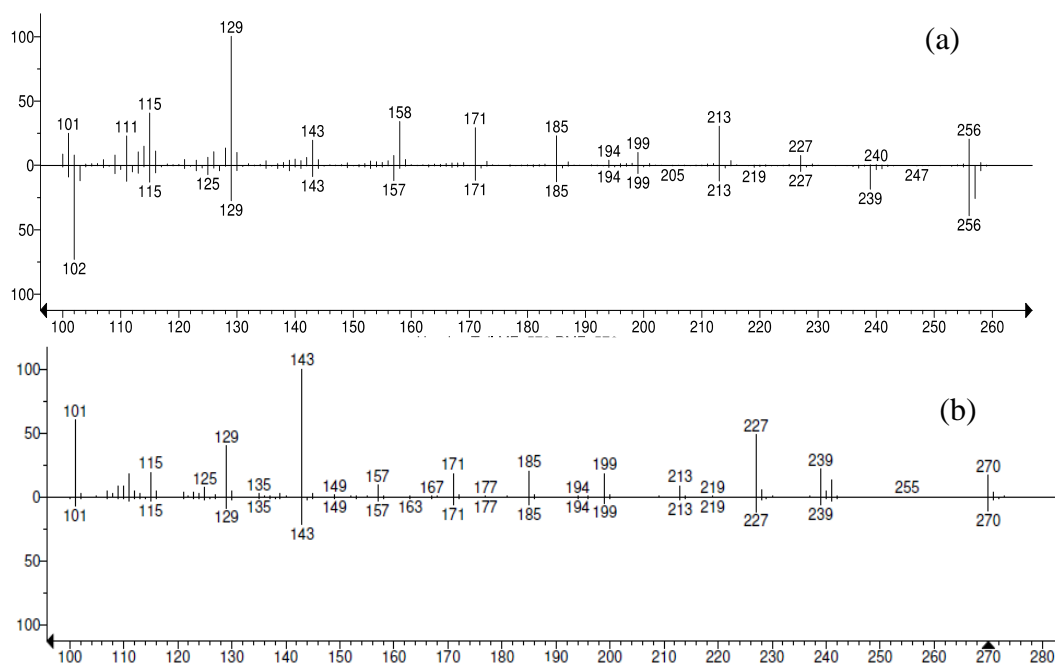


Figure 3.12: Mass spectrum of (a) palmitic acid and (b) methyl palmate.

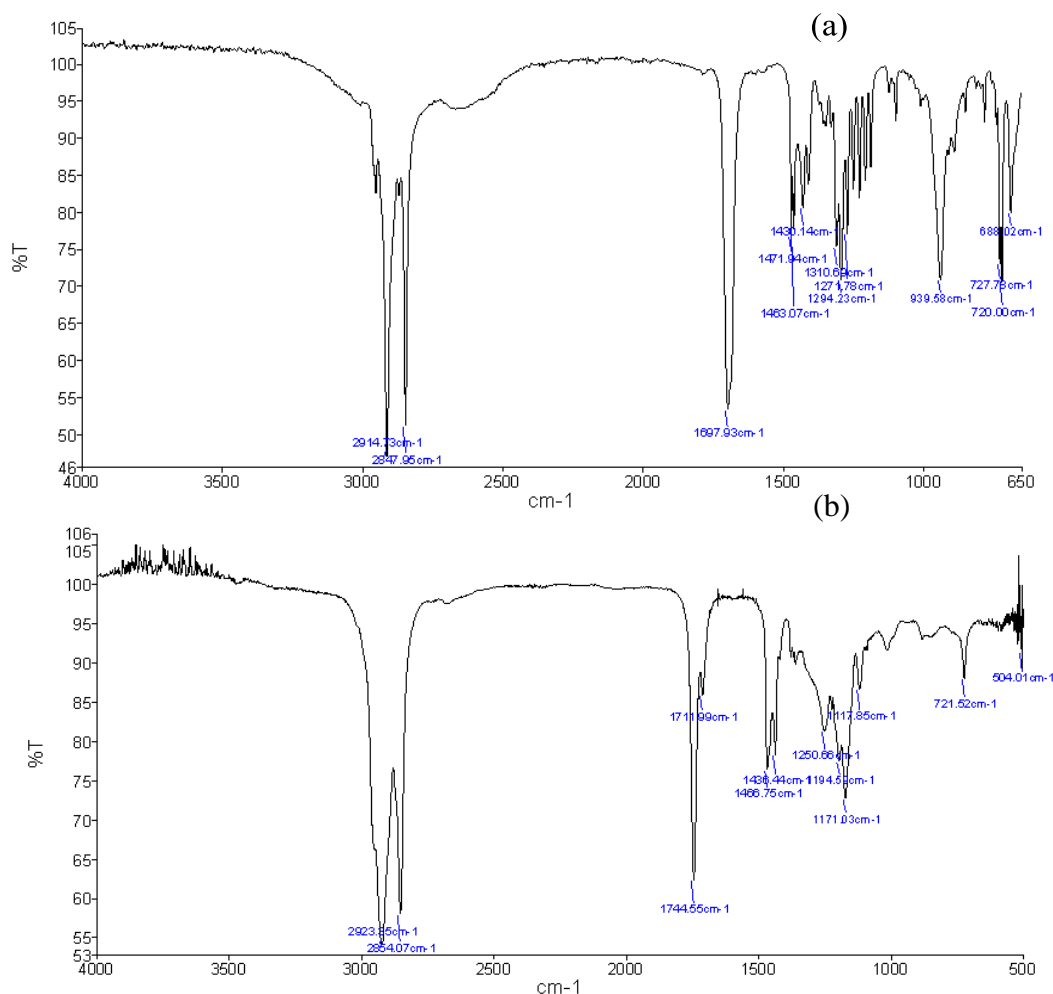


Figure 3.13: IR spectrum for (a) palmitic acid and (b) methyl palmate

In addition, IR spectra were used to support the outcomes. There are substantial differences in peaks of carboxylic acid and its ester which are noticed in Figures 3.13 (a, b). The first difference appeared on the C-H bond stretch, in spectrum (a), this peak started broadly between 2800 and 3000  $\text{cm}^{-1}$  due to the presence of O-H stretching vibration. This broadness disappeared in the spectrum (b) that refers to methyl palmate ester. The second difference related to the carbonyl bond stretch band, it was a broader peak that appears at a lower wave number (1697  $\text{cm}^{-1}$ ) in the spectrum (a) of fatty acid, relative to a sharp band observed at 1744  $\text{cm}^{-1}$  in the corresponding ester. These differences in the two IR spectra indicate the presence of carbonyl group in carboxylic acid in the spectrum (a) and an ester in the spectrum (b), as carbonyl group in carboxylic acid participates in hydrogen bond

leading to reduce the strength of the double bond C=O comparing to the same bond in the ester, spectrum (b).

The majority of the published data measured the percentage of each fatty acid relative to the sum of free fatty acid and its ester after chemical esterification.<sup>4,13,35,38-42</sup> This could be due to the difficulty of determination of fatty acids in a free form using GC/MS for analysis at low temperature. By comparing the GC conditions in the current study, it was found that it is possible to analyse the fatty acids in a free form using GC/MS at the current temperature conditions where the analysis in GC/MS oven started at a relatively high temperature 200°C.

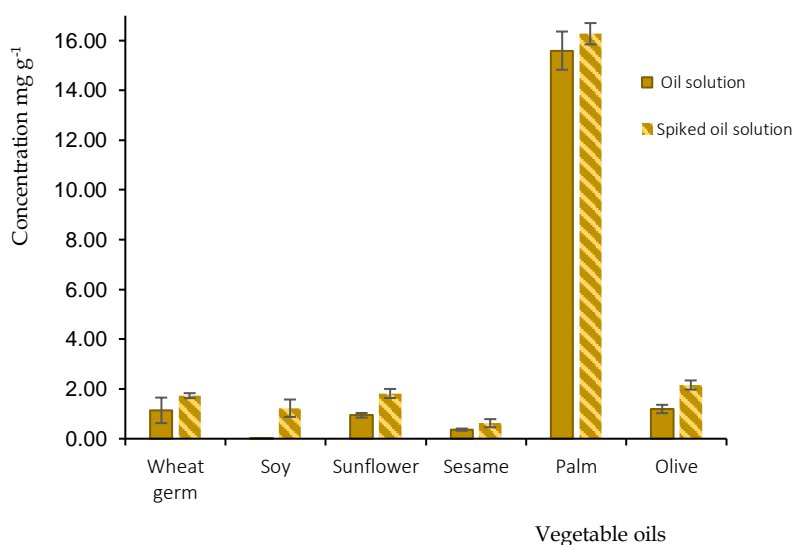


Figure 3.14: The relative quantities of palmitic acid in different vegetable oils.

To compare the quantities (percentages) of palmitic acid or any other fatty acids with the published work, these percentages should be converted to weight, then, compared to the quantities (measured weight) in the current research. Even though, the far difference between the quantities in the published data and what was extracted in this study, the order of the palmitic acid in some vegetable oils in the current study is similar to what mentioned in Ramos *et al.*, where palm oil was found to be the highest source of saturated free fatty acid (palmitic acid) followed by olive oil, then sunflower oil (Figure 3.14).<sup>42</sup>

### 3.3.3.2 Extraction and analysis of oleic (18:1) and linoleic (18:2) acids

The second peak around 7 min in GC/MS represented both mono-unsaturated fatty acid (oleic acid) and di-unsaturated fatty acid (linoleic acid) which eluted almost at the same time, thus appear as one peak. Therefore, the difference between the oil samples spiked and non-spiked are more than in other compounds in this study because here the oil samples were spiked with two compounds (oleic and linoleic acids) (Table 3.3).

Table 3.3: The concentrations of oleic and linoleic acid in different vegetable oils.

Vegetable oils	Quantities (mg g <sup>-1</sup> )	Spiked quantities (mg g <sup>-1</sup> )
Wheat germ	7.181 ± 1.31	10.41 ± 4.3
Soy bean	0.088 ± 0.12	2.719 ± 0.77
Sunflower	16.425 ± 7.8	28.411 ± 15.7
Sesame	2.407 ± 0.12	6.246 ± 2.19
Palm	34.496 ± 8.4	38.914 ± 7.5
Olive	1.325 ± 0.87	3.823 ± 1.19

However, the presence of each one of them has been examined individually by spiking the oil sample, and calibration curves were drawn separately for each fatty acid. In addition, each peak of oleic and linoleic acids and their esters on the GC chromatogram (Figure 3.15 and 3.16) were analysed individually to find out the similarity with the mass spectra available in the NIST library (Figure 3.17 and 3.19). Starting with the GC chromatogram of the acid forms and the corresponding ester forms of oleic and linoleic acids displayed similar results that were represented in the case of palmitic acid. The peak in case of esters (Figure 3.18, b and 3.20, b) in the two esters are separated slightly earlier than the carboxylic acids.

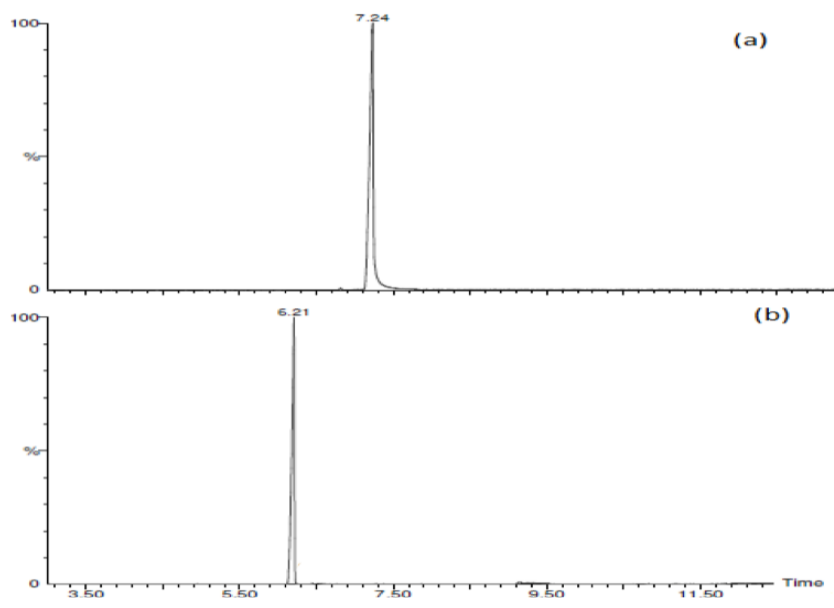


Figure 3.15: GC chromatogram for (a) oleic acid and (b) methyl oleate solutions in hexane.

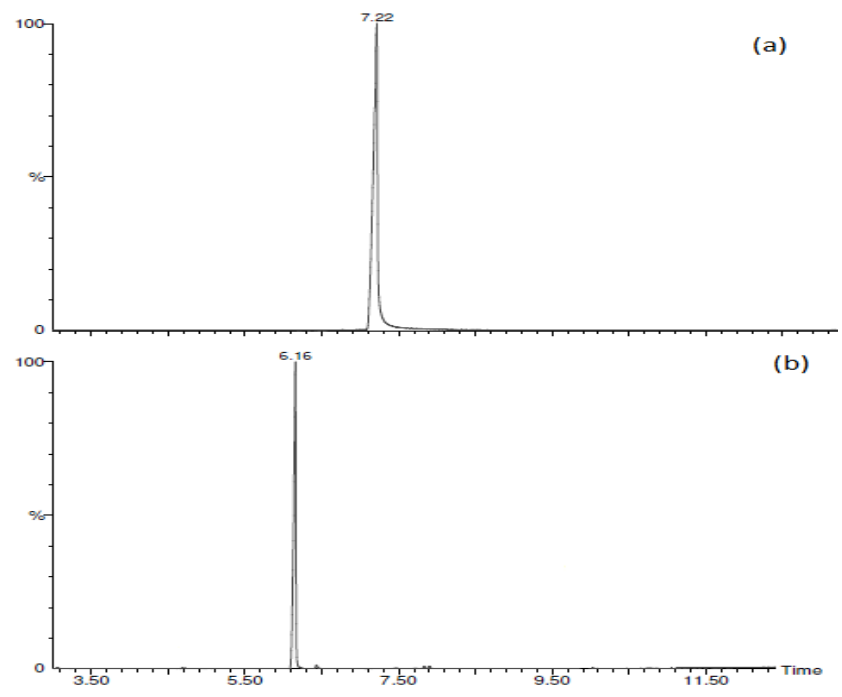


Figure 3.16: GC chromatogram for (a) linoleic acid and (b) methyl linoleate solutions in hexane.

Regarding the mass spectrum of oleic acid (Figure 3.17, a), the molecular ion was observed at  $m/z$  282 with a lower abundance than  $[M-18]^+$  at  $m/z$  264 representing the loss of a molecule of water from the carboxyl group of oleic acid. The most abundant fragments were in the low mass region representing the hydrocarbon ions with their general formula  $[C_nH_{2n-1}]^+$  at  $m/z$  111, 123, 137...

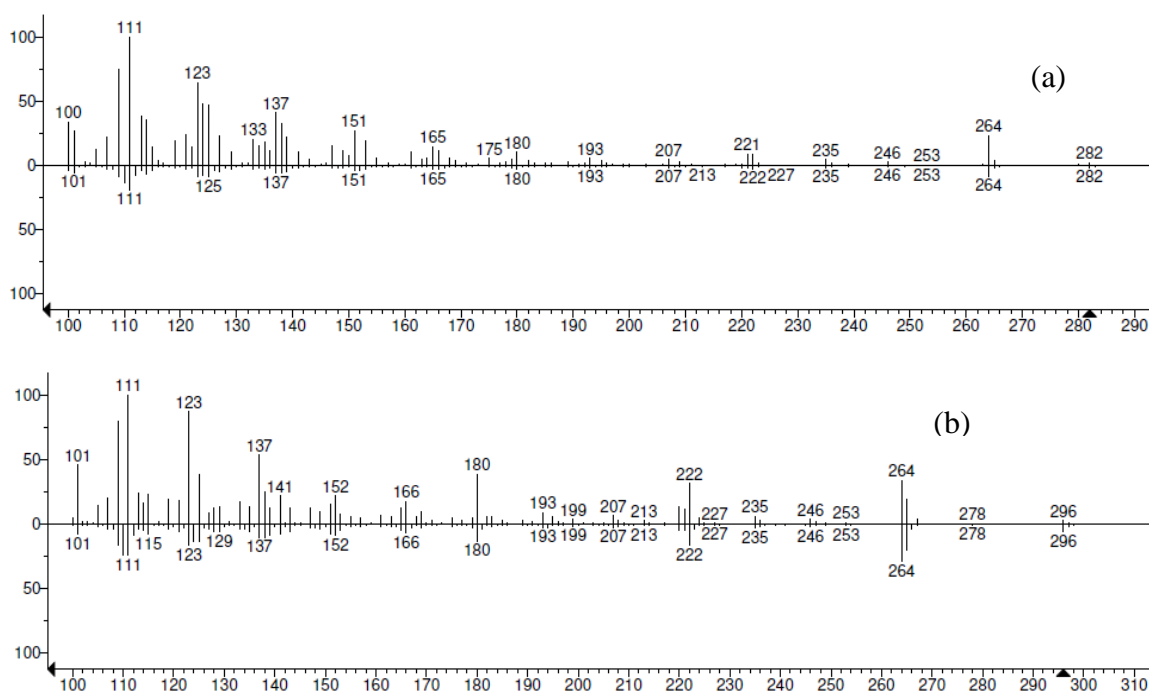


Figure 3.17: Mass spectrum of oleic acid (a) and methyl oleate (b).

In the mass spectrum of methyl oleate ester (Figure 3.17, b), the molecular ion was observed at  $m/z = 296$ , along with a daughter ion at  $m/z = 264$  that referred to the loss of the methanol molecule  $[M-32]^+$ . The next distinguished ion seen at  $m/z = 222$  represented the McLafferty ion rearrangement. Characteristic fragments at  $m/z = 180, 166, 152$ , etc were also diagnostic. They were formed by the loss of a fragment containing the carboxyl group by cleavage between carbons 5 and 6 with the addition of a rearranged hydrogen atom.

By looking at IR of oleic acid and methyl oleate (Figure 3.18 (a and b)), the main differences in the two spectra occurred due to the transference of the carboxylic acid in oleic acid to methyl ester group. First, the strong broad band of

O-H stretch in spectrum 3.42 (a) changed to a strong narrow band related only to the C-H stretch in the spectra (b). Second, the carbonyl (C=O) stretch at  $1712\text{ cm}^{-1}$  in the spectrum (a) (acid) changed into a sharp band at a slightly longer wavelength ( $1745.9\text{ cm}^{-1}$ ) in the spectrum (b). These differences were confirmation of the formation of methyl oleate ester from oleic acid.

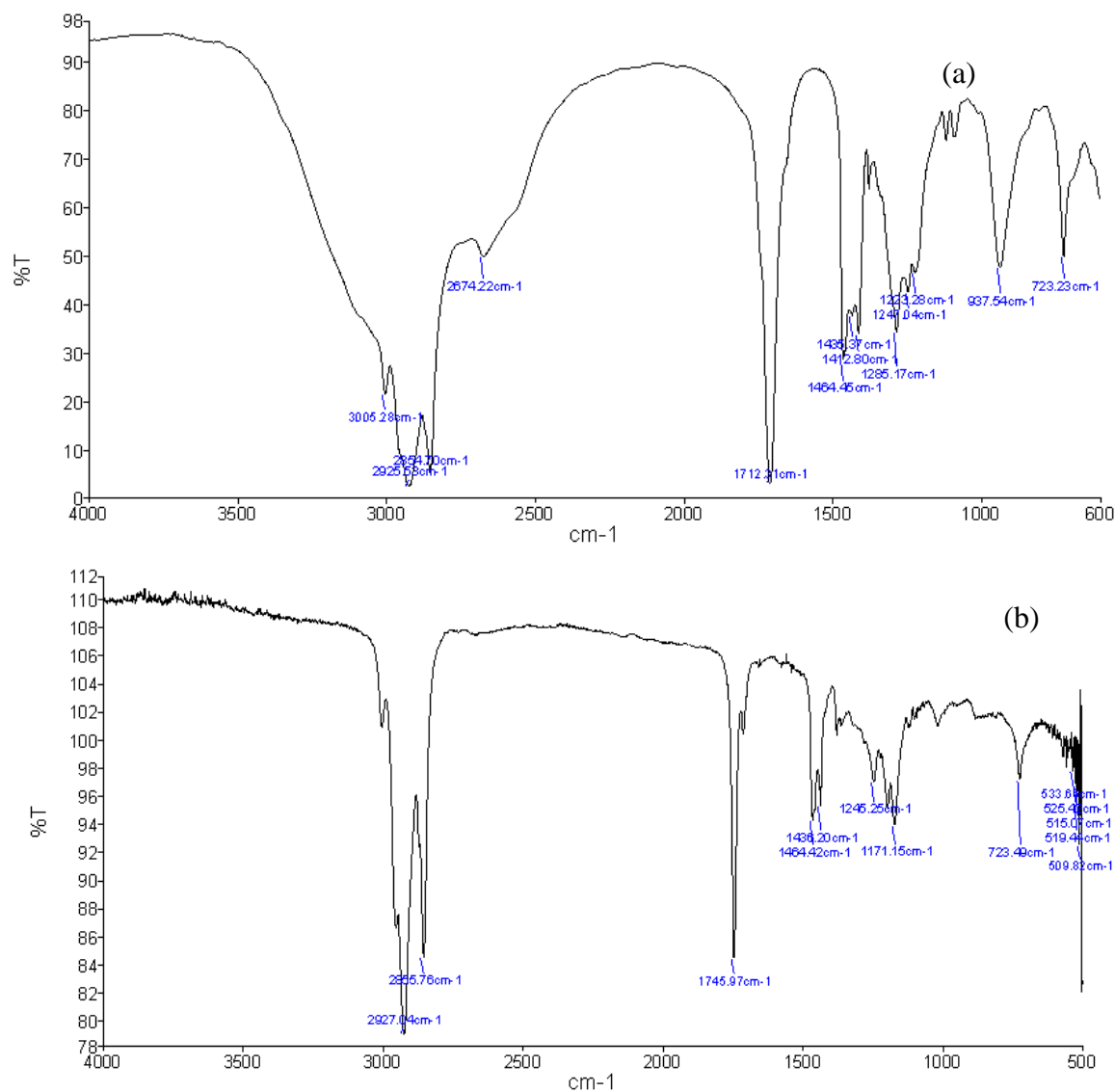


Figure 3.18: IR spectrum for (a) oleic acid and (b) methyl oleate.

Similarly, the mass spectrum of linoleic acid (Figure 3.19 (a)) is dominated by the hydrocarbon ions of the general formula  $[C_nH_{2n-3}]^+$  in the low mass range at  $m/z$  109, 123, 135, 149, 163 etc. The molecular ion was observed at  $m/z$  280 with an abundance greater than  $[M-18]^+$  at  $m/z$  262 which in accordance with published studies.<sup>34, 44</sup> In the mass spectrum of methyl linoleate (Figure 3.19, b), the abundant

molecular ion is seen at  $m/z = 294$ , and the ion for the loss of the McLafferty ion appears at  $m/z = 220$ . Then, the ion that represented  $[M-31]^+$  is more abundant than that of  $[M-32]^+$ . Hydrocarbon ions of the general formula  $[C_nH_{2n-3}]^+$  dominate in the lower mass range ( $m/z = 109, 121, 135, 149$  etc).

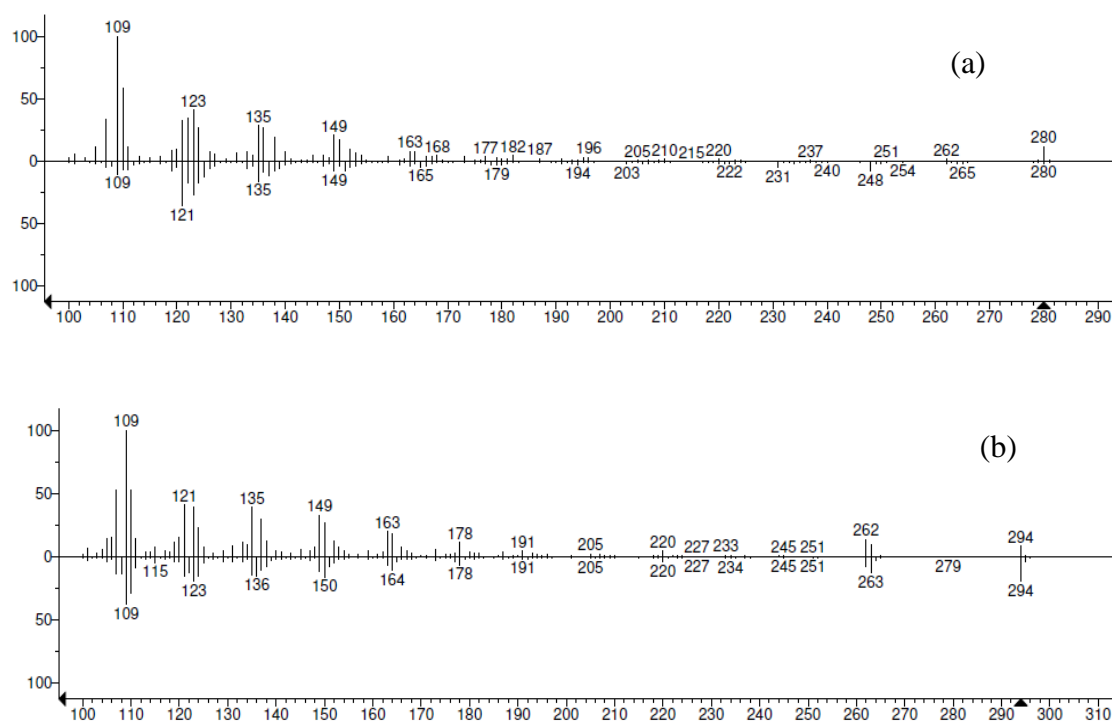


Figure 3.19: Mass spectrum of (a) linoleic acid and (b) methyl linoleate.

Similar to the previous fatty acids, IR analysis has been carried out for the linoleic acid before and after esterification to confirm the transformation of the carboxylic group to methyl ester group. Figures 3.20 (a and b) show the difference between the two forms by the differences in their peaks. O-H strong broad band of the linoleic acid in the spectrum (a) disappeared in the corresponding ester spectrum (b). Moreover, the peak corresponding to the carbonyl stretching in the IR spectrum of acid was seen as wider, stronger and at a shorter wavelength than in the ester form.

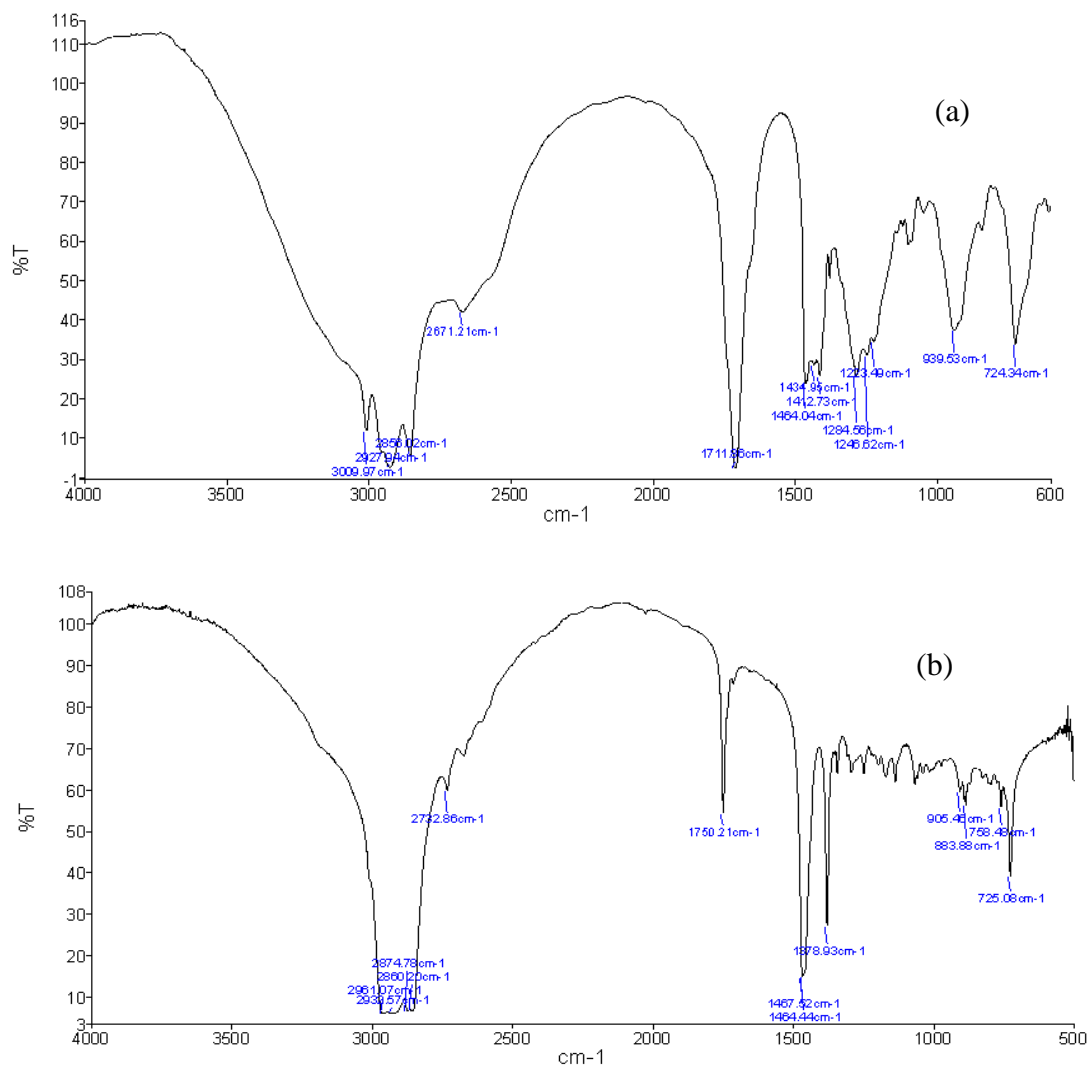


Figure 3.20: IR spectrum of linoleic acid (a) and methyl linoleate (b).

Most published work focussed on calculating the percentage of each fatty acid to the total content of fatty acids after its conversion to the ester form for all of them (free and conjugated forms) as illustrated in the palmitic acid.<sup>13,36,38–41,35,43,45,46</sup> A study by Eisenmenger *et al.*, quantified the free fatty acid in the wheat germ oil within a range between 0.2 to 7.9 mg g<sup>-1</sup> which included the extracted amount of these acids in that study.<sup>35</sup> It is important to emphasise that the spiking of the oil sample with standards of minor components encouraged the separation of the fatty acids by the effect of intermolecular attractive forces as mentioned in subtitle 3.3.3. The difference between the concentrations of extracted oleic and linoleic acids together from vegetable oils and spiked extracted amount with 0.3 mg mL<sup>-1</sup> from

standards solutions of minor components is not equal in all types of oils (Figure 3.21).

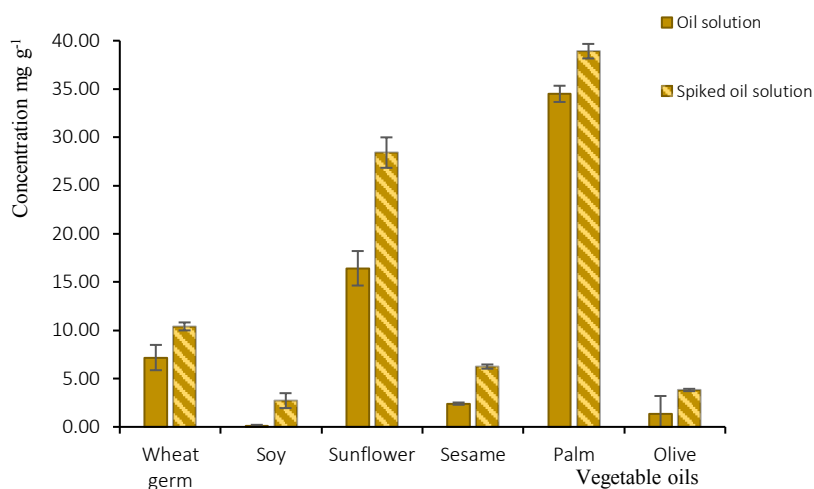


Figure 3.21: The relative quantities of oleic and linoleic acids together in different vegetable oils.

### 3.3.3.3 Extraction and analysis of $\alpha$ -tocopherol

One of the common peaks among the GC/MS investigations of the studied vegetable oils in this research was proved to be to  $\alpha$ -tocopherol. Table 3.4 summarises the extracted  $\alpha$ -tocopherol from the vegetable oils in this study in the first column and from the spiked oils with  $0.3 \text{ mg mL}^{-1}$  of a standard solution of  $\alpha$ -tocopherol.

The mass spectrum of the peak at 14.9 min seen in the GC referred to  $\alpha$ -tocopherol. According to Nagy *et al.*,<sup>50</sup> the presence of  $\alpha$ -tocopherol in the sample could be demonstrated using mass spectra Figure 3.22. The marker ions for detecting and confirming the presence of  $\alpha$ -tocopherol were the molecular ion at  $m/z$  430 and the dominated fragment of  $[\text{C}_{10}\text{H}_{13}\text{O}_2]^+$  was observed at  $m/z$  165, which was representing the ion after opening the ether bond and loss of the side chain 2,6,10,14-tetramethylpentadec-1-ene.<sup>41-45</sup>

Table 3.4: The concentrations of  $\alpha$ -tocopherol in different vegetable oils.

Vegetable oils	Quantities (mg/g)	Spiked quantities (mg/g)
Wheat germ	$0.298 \pm 0.06$	$1.357 \pm 0.34$
Soy bean	$0.233 \pm 0.11$	$1.313 \pm 0.60$
Sunflower	$0.277 \pm 0.08$	$1.035 \pm 1.27$
Sesame	nd	$0.876 \pm 0.28$
Palm	$0.148 \pm 0.01$	$0.946 \pm 0.81$
Olive	$0.256 \pm 0.36$	$1.027 \pm 0.72$

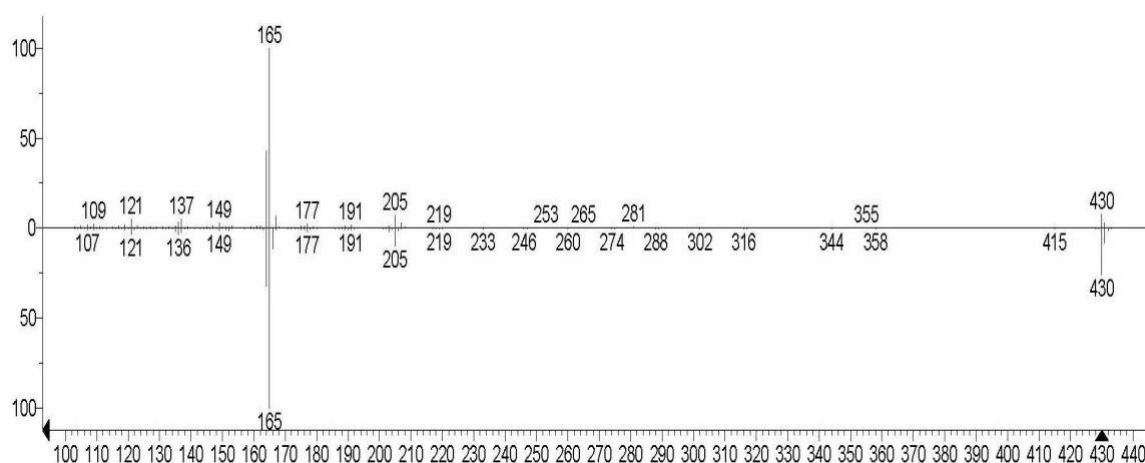


Figure 3.22: Mass spectrum of extracted  $\alpha$ -tocopherol (upward) and NIST mass spectrum (down).

It was observed that this component showed a wide difference between the extracted quantities with spiking and without spiking the oil sample with a known concentration of the standard solution of  $\alpha$ -tocopherol. This had been observed in a report by Feng *et al.*, who carried out the extraction of  $\alpha$ -tocopherol using a molecularly imprinted polymer that was synthesised from MAA as a functional monomer and EGDMA as a cross-linker.<sup>34</sup> Feng *et al.* observed that the increase of

the initial concentration of  $\alpha$ -tocopherol led to the increase of the adsorption capacity of the molecularly imprinted polymer (Table 3.4).<sup>34</sup>

Although the extracted amounts of  $\alpha$ -tocopherol from oils without spiking was very small compared to the extracted amount from the spiked samples, the ratio between the extracted amounts from the spiked oil samples are in agreement with the published results of Schwartz *et al.* on some of these oils including: wheat germ (1.92 mg g<sup>-1</sup>), sesame (0.079 mg g<sup>-1</sup>), sunflower (0.59 mg g<sup>-1</sup>) and olive oil (0.24 mg g<sup>-1</sup>).<sup>16</sup> The highest extracted amount was from wheat germ oil and the lowest was from sesame oil (Figure 3.23). The extracted amount of  $\alpha$ -tocopherol from unspiked wheat germ oil is close to the extracted amount of it reported by Gonzalez *et al.*, which was 0.384 mg g<sup>-1</sup> from wheat germ oil and 0.485 mg g<sup>-1</sup> from sunflower oil.<sup>51,52</sup> In addition, the content of  $\alpha$ -tocopherol was found to be the highest in wheat germ oil (1.357 mg g<sup>-1</sup>) which was consistent with the published data reported by Ghafoor *et al.* (2017) (1.3 - 2.5 mg g<sup>-1</sup>) and in Kumar and Krishna (2013) (1.6 mg g<sup>-1</sup>).<sup>13,35</sup> Sunflower oil is the second highest source of  $\alpha$ -tocopherol (0.277 mg g<sup>-1</sup>) in non-spiked oil and 1.035 mg g<sup>-1</sup> in spiked oil which is close to the published range in unsaponifiable matter reported by Galea *et al.* (0.416 mg g<sup>-1</sup>),<sup>53</sup> and Ballesteros *et al.* (1996) (0.473 mg g<sup>-1</sup>).<sup>54</sup> Similarly, in olive oil the extracted amount (0.256 mg g<sup>-1</sup>) of  $\alpha$ -tocopherol was found to be close to the published quantities reported by Ballesteros *et al.* (0.175 mg g<sup>-1</sup>),<sup>54</sup> Grigoriadou *et al.* (2007) (0.161 - 0.222 mg g<sup>-1</sup>)<sup>55</sup> and Galea *et al.* (2010) (0.530 mg g<sup>-1</sup>).<sup>53</sup>

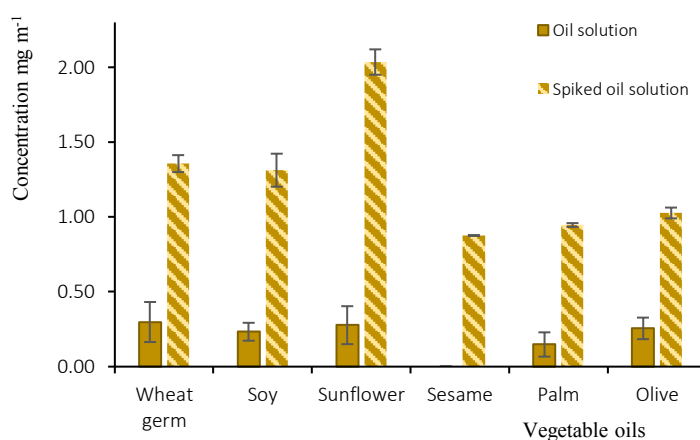


Figure 3.23: The relative quantities of  $\alpha$ -tocopherol in different vegetable oils.

However, the extracted  $\alpha$ -tocopherol is higher than the reported quantity by Ballestsros *et al.* (0.409 mg g<sup>-1</sup>), Hegde (0.12 mg g<sup>-1</sup>) and Gharby *et al.* (0.010 mg g<sup>-1</sup>) from wheat germ oil.<sup>45,54,40</sup> Regarding the other types of vegetable oils such as soybean and palm oils, the extracted level of  $\alpha$ -tocopherol (0.233 mg g<sup>-1</sup>) is slightly higher than of those recorded in the previous work. For example,  $\alpha$ -tocopherol has been extracted from soybean oil ranged between 0.0109 - 0.0143 mg g<sup>-1</sup> in the reports produced by Lee *et al.* and Dijkstra and Kim.<sup>38,56,57</sup> In palm oil,  $\alpha$ -tocopherol quantified in the current study at (0.148 mg g<sup>-1</sup>), while it was reported at lower concentration (0.0202 mg g<sup>-1</sup>) in Gibon *et al.* which could be referred to the difference of the extraction method and conditions.<sup>58</sup>  $\alpha$ -tocopherol is available at low content in sesame oil; therefore, it has not been detected without spiking the oil sample and detected at the lowest amount compared to the other vegetable oils in this study. By comparing this to the previous studies on  $\alpha$ -tocopherol content in sesame oil, it was found that  $\alpha$ -tocopherol was detected at a very low concentration (0.03 – 0.7 mg g<sup>-1</sup>) in Schwartz *et al.* which could be below the detection level of  $\alpha$ -tocopherol in this study which was determined at 0.04 mg g<sup>-1</sup>.<sup>16</sup>

#### **3.3.3.4 Extraction and study of phytosterols**

The next group of compounds are among the phytosterols family which are available in free and esterified forms.<sup>16,18,59</sup> As the current method was applied only to the oil solution without any pre-treatment, the extracted phytosterols are in free forms only.

#### **Campesterol**

This is the first free phytosterol separated within GC/MS at a retention time of 15.7 min. Table 3.5 shows the extracted campesterol from each vegetable oil and spiked with 0.3 mg mL<sup>-1</sup> of phytosterol mixture of standard solution.

Table 3.5: The concentrations of campesterol in different vegetable oils.

Vegetable oils	Quantities (mg/g)	Spiked quantities (mg/g)
Wheat germ	0.489 ± 0.36	0.573 ± 0.06
Soy bean	0.251 ± 0.03	0.344 ± 0.04
Sunflower	0.058 ± 0.03	0.186 ± 0.21
Sesame	0.317 ± 0.11	0.457 ± 0.21
Palm	0.074 ± 0.01	0.131 ± 0.01
Olive	0.075 ± 0.11	0.242 ± 0.01

The mass spectrum of this peak was compared with the NIST library that suggested the peaks corresponding to campesterol (Figure 3.24). In the mass spectrum, the molecular ion  $[M]^+$  is observed at  $m/z$  400. The typical fragments of campesterol are observed at  $m/z$  385 for the ion  $[M-CH_3]^+$ ,  $m/z$  382 for the ion  $[M-H_2O]^+$  and  $m/z$  367 for the fragment  $[M-CH_3-H_2O]^+$ .<sup>59</sup> It was observed that spiking the oil samples lead to optimise the separation of phytosterols and obtain a great amount of them. The quantitative data is comparable with the results reported by Eisenmenger *et al.* for wheat germ, sunflower, sesame and olive oils and Purcaro *et al.* for palm oil.<sup>16,36,61,62</sup>

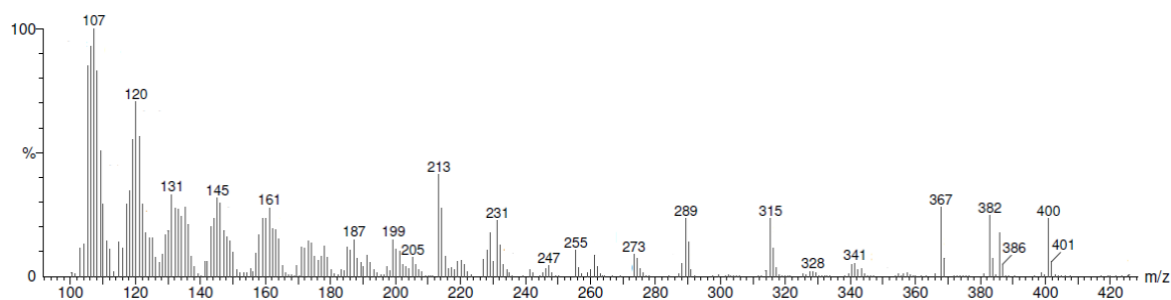


Figure 3.24: The mass spectrum of campesterol.

The quantitative amounts of campesterol in vegetable oils reported in literature were found to be close to the obtained values in this research. For example, the quantities of campesterol reported in literature are 0.074 mg g<sup>-1</sup> in palm oil (Purcaro *et al.*)<sup>63</sup>, 0.068 mg g<sup>-1</sup> in sunflower oil and 0.059 mg g<sup>-1</sup> in olive oil (Schwartz *et al.*)<sup>16</sup>, and from wheat germ oil the amount ranged between 0.5 to 1.7 mg g<sup>-1</sup> as

reported by Eisenmenger *et al.*<sup>36</sup> All of these mentioned amounts are in accordance with the extracted amounts of campesterol from the oils in this study.

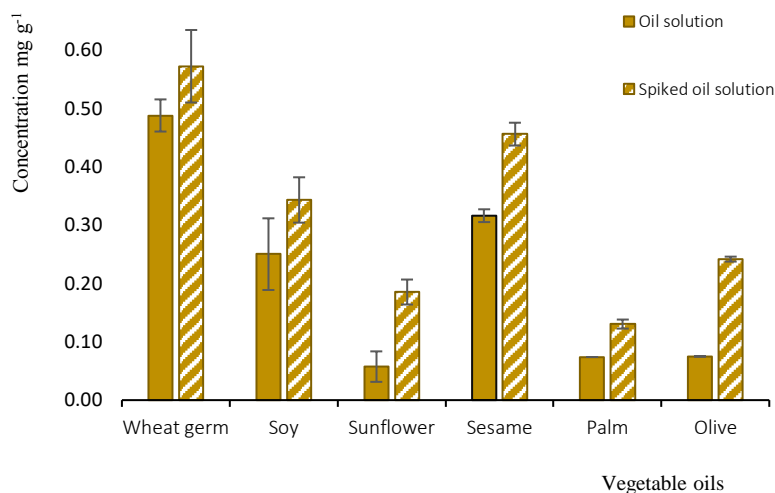


Figure 3.25: The relative quantities of campesterol in different vegetable oils.

Campesterol is typically available at low concentrations in vegetable oils compared to other phytosterols, and it was quantified at the lowest amount in olive oil and the highest concentration was found in wheat germ oil (Figure 3.25).

### Stigmasterol

The next type of common phytosterol in the vegetable oils is stigmasterol. Table 3.6 represents the quantities of stigmasterol in the oil sample alone and the spiked oil samples with 0.3 mg mL<sup>-1</sup> of standard solution of phytosterol mixture.

Table 3.6: The concentrations of stigmasterol in different vegetable oils.

Vegetable oils	Quantities mg g <sup>-1</sup>	Spiked quantities mg g <sup>-1</sup>
Wheat germ	0.307 ± 0.34	0.631 ± 0.06
Soy bean	0.517 ± 0.13	0.956 ± 0.29
Sunflower	0.146 ± 0.03	0.289 ± 0.06
Sesame	0.220 ± 0.09	0.331 ± 0.05
Palm	0.125 ± 0.03	0.266 ± 0.10
Olive	0.008 ± 0.01	0.409 ± 0.28

The NIST library proposed that the peak at 15.9 min in the GC chromatogram (Figure 3.10) referred to stigmasterol and that was evidenced by mass fragmentation pattern. The molecular ion  $[M]^+$  was observed at  $m/z$  412, then the distinctive fragments included the ion at  $m/z$  397 for  $[M-CH_3]^+$ , the ion at  $m/z$  394 for  $[M-H_2O]^+$ , the ion at  $m/z$  369 for  $[M-C_3H_5]^+$ , the ion at  $m/z$  351 for  $[M-C_3H_5-H_2O]^+$  and the ion at  $m/z$  314 for  $[M-C_7H_{14}]^+$ .<sup>59</sup>

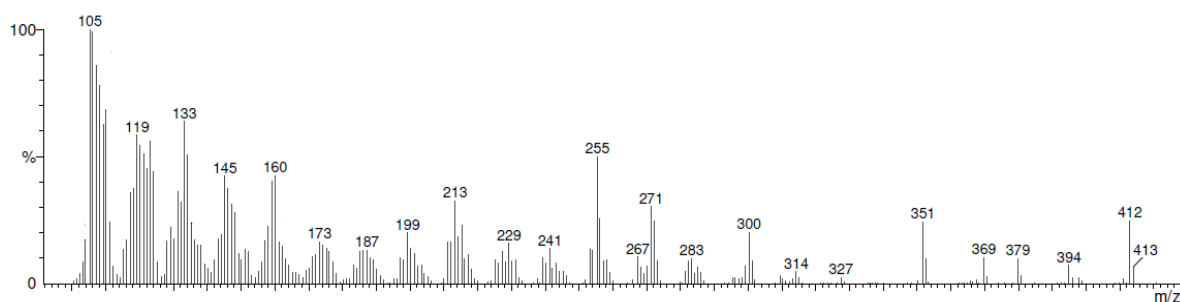


Figure 3.26: Mass spectrum of stigmasterol.

It was observed that the ratio between stigmasteol in wheat germ, sesame, sunflower and olive oil (Figure 3.27) are in accordance with the values mentioned by Schwartz *et al.*<sup>16</sup>

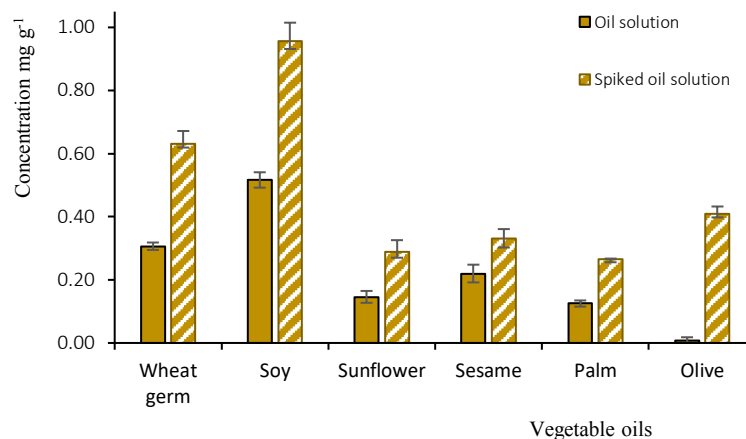


Figure 3.27: The relevant concentrations of stigmasterol in different vegetable oil.

In addition, the extracted amount of stigmasterol in the current study is comparable with published data in Schwartz *et al.*<sup>16</sup>, Eisenmenger *et al.*<sup>36</sup> for wheat germ, with Lechner *et al.*<sup>2</sup> for sunflower and with Schwartz *et al.*<sup>16</sup> for sunflower, sesame and olive oils.<sup>16</sup>

### **$\beta$ -sitosterol**

This is the major sterol in vegetable oils and has been extracted at the highest amounts relative to the other phytosterols. The extracted quantities in Table 3.7 in all type of oils in the current study are in accordance with the previously published quantitative data.<sup>16,18,36,38, 61</sup>

Table 3.7: The concentrations of  $\beta$ -sitosterol in different vegetable oils.

Vegetable oils	Quantities mg g <sup>-1</sup>	Spiked quantities mg g <sup>-1</sup>
Wheat germ	1.903 ± 0.12	2.285 ± 0.41
Soy bean	1.398 ± 0.24	1.684 ± 0.59
Sunflower	0.741 ± 0.19	1.446 ± 0.37
Sesame	2.177 ± 0.28	2.380 ± 0.30
Palm	0.299 ± 0.10	0.575 ± 0.02
Olive	0.760 ± 0.01	0.894 ± 0.24

By analysing the data of GC chromatogram (Figure 3.10), peak at 16.2 min of the eluted samples was designated to  $\beta$ -sitosterol as suggested by the NIST library. The marked fragments in the mass spectrum (Figure 3.28) included the molecular ion  $[M]^+$  at m/z 414, the ion  $[M-CH_3]^+$  at m/z 399, the ion  $[M-H_2O]^+$  at m/z 396, the ion for  $[M-CH_3-H_2O]^+$  at m/z 381, the ion for  $[M-C_6H_{13}]^+$  at m/z 329 and the ion for  $[M-C_7H_{11}O]^+$  at m/z 303.<sup>60</sup>

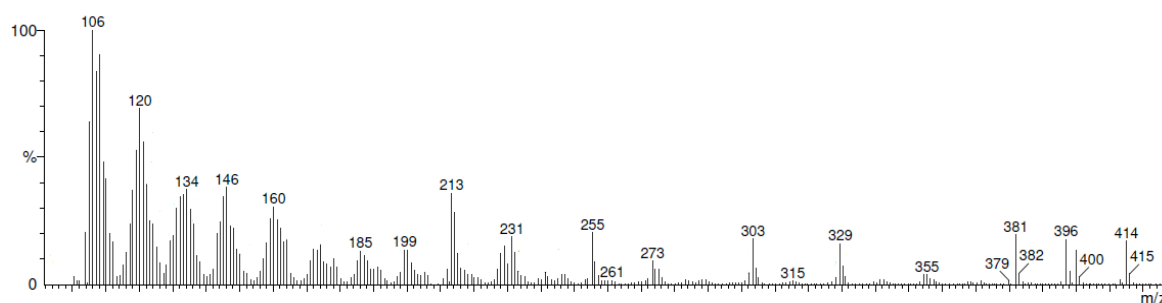


Figure 3.28: The mass spectrum of  $\beta$ -sitosterol.

The conventional method to analyse this group of compounds from vegetable oils is to transform the free form of sterols to ester form and then quantify the total amount of sterols in ester form.<sup>60,62</sup> The RDP as an adsorbent in the SPE allows to selectively adsorb those compounds in their free form to be eluted eventually.

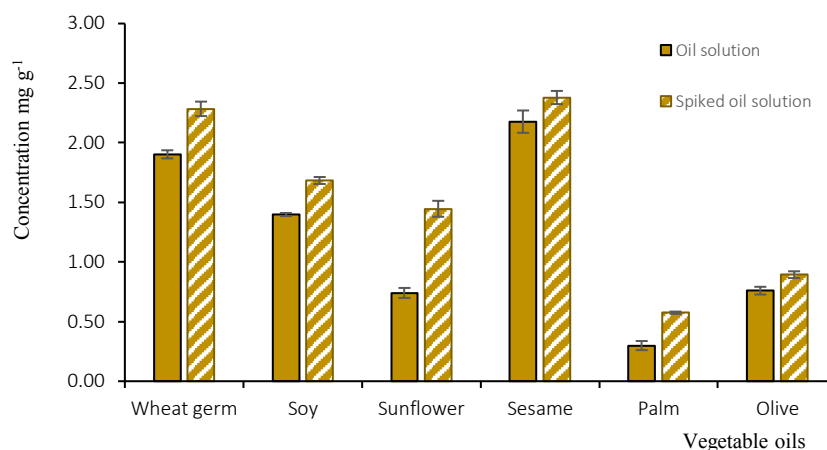


Figure 3.29: The relative concentrations of  $\beta$ -sitosterol in different vegetable oils.

The comparison between the current measurements to the previous studies has suggested that the quantities of  $\beta$ -sitosterol extracted from sunflower ( $1.44 \text{ mg g}^{-1}$ ) and wheat germ ( $2.28 \text{ mg g}^{-1}$ ) oil are close to the reported amounts of the free phytosterols,  $\beta$ -sitosterol particularly as described by Lechner *et al.* ( $1.86$  and  $1.75 \text{ mg g}^{-1}$ ) and Eisenmenger *et al.* ( $2.5$  to  $2.6 \text{ mg g}^{-1}$ ) respectively.<sup>19,36</sup> In addition, there is an agreement between the current quantitative measurements extracted from soybean oil ( $1.68 \text{ mg g}^{-1}$ ), palm oil ( $0.57 \text{ mg g}^{-1}$ ), and olive oil ( $0.89 \text{ mg g}^{-1}$ ), and the published quantities stated by Dijksra *et al.* ( $1.37 \text{ mg g}^{-1}$ ), Lechner *et al.* ( $1.75 \text{ mg g}^{-1}$ ) in soybean oil, Purcaro *et al.* ( $0.304 \text{ mg g}^{-1}$ ) in palm oil and Longbardi *et al.* in olive oil ( $0.83 \text{ mg g}^{-1}$ ).<sup>19,39,61,63</sup> Moreover, the current amounts of  $\beta$ -sitosterol were close to the published quantities as stated by Schwartz *et al.* for sunflower, olive and sesame oil (Figure 3.29).<sup>16</sup>

### 3.3.3.5 Further minor components extraction

#### Sesamin:

At a retention time of 15.3 min in the GC chromatogram (Figure 3.10) of the eluted sample from sesame oil, there is a noticeable peak that showed a component at a very high concentration. The NIST library suggested that this compound is sesamin and further, it was confirmed by the mass spectrum Figure 3.30. The main characteristic peaks are similar to the documented fragments of the mass spectrum of sesamin in several published research papers<sup>64,65</sup>. The baseline is observed at

$m/z$  149 corresponding to  $[1,3\text{-dioxymethylenepheryl-CO}]^+$ , the molecular ion was seen at  $m/z$  354  $[M]^+$ . Other fragment ions were observed at  $m/z$  121 for  $[1,3\text{-dioxymethylphenyl}]^+$ , at  $m/z$  135 for  $[1,3\text{dioxymethylenepheryl-CH}_2]^+$ , at  $m/z$  161 for  $[1,3\text{-dioxymethylenepheryl-CHCH}_2]^+$ , at  $m/z$  203 for  $[M-(1,3\text{dioxymethylenepheryl-CHO-H})]^+$ , and 336  $[M-H_2O]^+$ .<sup>65-67</sup>

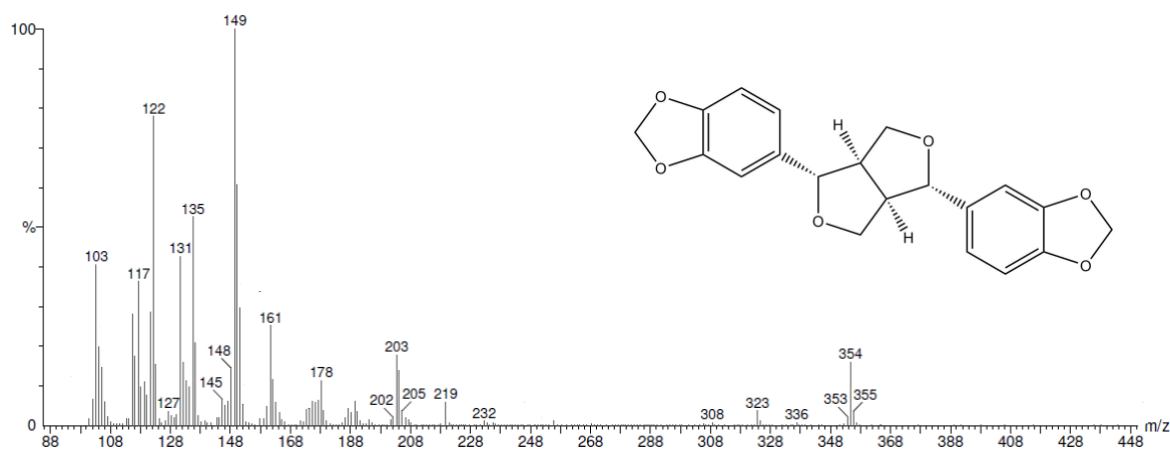


Figure 3.30: The mass spectrum of sesamin.

The presence of sesamin was approved eventually by spiking the sesame oil with 0.3 mg of sesamin and comparing the retention time with the peak of sesamin solution which appeared identical. The standard solution of sesamin in hexane was used to produce a calibration curve that was used for calculating the eluted amount of sesamin from sesame oil using the optimised protocol in this study.  $3.122 \pm 0.877$   $\text{mg g}^{-1}$  in sesame oil and  $3.566 \pm 0.455$   $\text{mg g}^{-1}$  in spiked sesame oil was extracted in the current study. These measurements are in accordance with the published quantities in Jin *et al.* at ( $4.30 \text{ mg g}^{-1}$ ), Wu *et al.* (2007) at ( $3.36$  to  $4.9 \text{ mg g}^{-1}$ ), Moazzami *et al.* at ( $4.44$  to  $16.01 \text{ mg g}^{-1}$ ) in unrefined oil and ( $1.18$  to  $4.01 \text{ mg g}^{-1}$ ) in refined sesame oil and in Dachtler *et al.* at ( $4.74 \text{ mg g}^{-1}$ ).<sup>66-69</sup>

Also, two more peaks were noticed in the GC chromatogram at 3.34 and 4.5 min in case of olive oil. The integrations of these peaks were low; therefore the suggestions of the NIST library of mass spectra were not enough to speculate them. However, it is more likely to be one of the common free saturated fatty acids with molecular weight less than the molecular weight of palmitic acid such as tridecanoic

acid (13:0), myristic (14:0) or pentadecanoic acid (15:0) as published in previous studies.<sup>70,71</sup>

### 3.3.4 Method validation

The proposed method to measure the determine matrix effects was performed by examining the percentage of the spiking standards (palmitic, oleic, linoleic acids,  $\alpha$ -tocopherol, campesterol, stigmasterol and  $\beta$ -sitosterol. Satisfactory recoveries were determined for these solutions, with values ranging from 94–99% as shown in Table 3.8 The purification percentage was evaluated by comparing the dry weight of the 20% oil sample before SPE ( $200 \pm 5$  mg) and a dry weight of the eluted sample after SPE ( $21.45 \pm 4.8$  mg). Considering that  $18.52 \pm 5.2$  mg of the eluted sample constitutes a weight of the natural compounds which were quantified using GC/MS, only 2.93 mg of the matrix is remained which is equivalent of 1.4%. Therefore, a very high level of purification of 98.6% was achieved.

Blank samples were run to check the possibility of memory effect from the analysis of high concentration in the calibration curve. No signal has been given that interfered with the peaks, confirming no memory effect in the chromatographic run.

Analysis of minor fat-soluble compounds in vegetable oils can be challenging due to the interference from the oily matrix.<sup>17, 72</sup> The challenging is presenting in the requirement of complex pre-treatment of the sample to make the hydrophobic sample suitable for the reverse phase (RP) HPLC. Therefore, there is a demand to develop new extraction methods to overcome these challenges and optimise simple and efficient methods. Several published studies suggested simultaneous separation and quantification protocols of some minor components from vegetable oils.<sup>73,74</sup> Almost of these studies depended on optimised chromatographic separation with appropriate detecting techniques to extract tocopherols and carotenoids from different types of vegetable oils. However, all these methods required sample preparation and did not include the phytosterols.

Table 3.8: The matrix effects of spiking 1 mL heptane with standards solutions at known concentrations. (percentage of recovery is average of triplicates  $\pm$  SD).

Standards of minor components	Spiked concentration ( $\mu\text{g mL}^{-1}$ )	Percentage of recovery
Palmitic acid	120	96 $\pm$ 1
Oleic and linoleic acid	240	98 $\pm$ 0.6
$\alpha$ -tocopherol	120	99 $\pm$ 0.5
Campesterol	19.2	74.6 $\pm$ 2
Stigmasterol	28.8	87.8 $\pm$ 1.5
$\beta$ -sitosterol	55.2	91 $\pm$ 1.6

Further analysis methods have emerged to include the separation of phytosterols beside tocopherols and other minor components such as squalene or carotenoids.<sup>17,72–76</sup> However, the pre-treatment processes of oil samples to separate such compounds needed more complex processes such as methylation or saponification, purification and derivatisation which led to loss of phytosterols.

The advantages of the developed RDP and optimised SPE protocol in the current research over the traditional methods of extraction included the separation of the minor compounds with 5 times dilution of the vegetable. This dilution rate was twice improved by comparison with the 10-fold dilution applied in the industrial protocol, leading to decrease the organic solvents waste and saving in the resources and time. It was also exhibited that the combination of the optimised SPE method and synthesised RDP enabled a quantitative extraction of minor compounds from six types of vegetable oils to be performed without any additional pre-treatment. It is important to underline that the optimised protocols and suggested strategy could be used as proposals for the development of extraction procedures for different groups of compounds from other natural oil-containing biomasses.

### 3.5 Conclusions

An eco-friendly, economical and simple method has been developed to extract a group of minor compounds from oil samples in heptane without any pre-treatment of the oil sample. The proposed method has been optimised in the previous chapter using sunflower oil, and in the current research this method was applied to five more types of vegetable oils using spiked oil samples in heptane with the standard solutions of the seven minor components expected to be extracted from the oil samples. With the proposed protocol, it was possible to harvest those physiologically-active components and then GC/MS was used for their identification and quantification. The optimised method involved the RDP synthesis which was used as an adsorbent in the optimised SPE protocol. The method has successfully extracted a group of free fatty acids,  $\alpha$ -tocopherol and three free phytosterols from six types of vegetable oils, despite of the variability of the content of the minor components in each one of these oils. This happened due to the pre-customised selectivity of the polymer which was designed on the basis of common structural features of these compounds. The quantitative results of this study were compared to the published results from different studies using variable methods and techniques to extract these minor components from the same vegetable oils and it was found they were in accordance.

It can be concluded that this protocol is useful to reduce the use of organic solvents and save the cost and time compared to the previously published methods because there is no need for any pre-treatment or derivatisation of the free fatty acids,  $\alpha$ -tocopherol or free phytosterols before the extraction. Finally, the proposed method opened a wide field for future work on the synthesis of the customised polymer with wide selectivity options which could have great applications in different fields.

## References

- 1) Aransiola F, Ojumu V, Oyekola O, Madzimbamuto T, Ikhu-Omoregbe D. A review of current technology for biodiesel production: State of the art. *Biomass Bioenergy*. **2014**,*61*, 276-297.
- 2) Freedman B.; Pryde E.; Mounts T. Variables affecting the yields of fatty esters from transesterified vegetable oils. *J Am Oil Chem Soc*. **1984**, *61*, 1638-1643.
- 3) Van Gerpen J. Biodiesel processing and production. *Fuel Process Technol*. **2005**, *86*, 1097-1107.
- 4) Mancini A.; Mancini A.; Nigro E.; Montagnese C.; Daniele A.; Orrù S.; Buono P. Biological and Nutritional Properties of Palm Oil and Palmitic Acid: Effects on Health. *Molecules* **2015**, *20*, 17339–17361.
- 5) Kris-Etherton P.; Pearson T.; Wan Y.; Hargrove R.; Moriarty K.; Fishell V.; Etherton T. High–Monounsaturated Fatty Acid Diets Lower Both Plasma Cholesterol and Triacylglycerol Concentrations 1 – 3 Experimental Design. *Am. J. Clin. Nutr*. **1999**, *70*, 1009–15.
- 6) Yi J.; WenXue Z.; HaiLe M. Optimization on ultrasonic-assisted extraction technology of oil from *Paeonia suffruticosa* Andr. seeds with response surface analysis. *the Chinese Soc Agric Mach*. **2009**, *40*, 103-110.
- 7) Pająk P.; Socha R.; Gałkowska D.; Rożnowski J.; Fortuna T. Phenolic profile and antioxidant activity in selected seeds and sprouts. *Food Chem*. **2014**, *143*, 300-306.
- 8) Luo Z.; Murray B.; Ross A.; Povey M.; Morgan M.; Day A. Effects of pH on the ability of flavonoids to act as Pickering emulsion stabilizers. *Colloids Surf B Biointerfaces*. **2012**, *92*, 84-90.
- 9) Puoci F.; Cirillo G.; Curcio M.; Iemma F.; Spizzirri U. Molecular imprinted SPE of selective HPLC determination of  $\alpha$ -tocopherol in bay leave. *Anal Chim Acta*. **2007**, *593*, 164-170.
- 10) Azzi A.; Stocker A. Vitamin E: non-antioxidant roles. *Prog lipid researc*. **2000**, *39*, 321-255.
- 11) Lemaire-Ewing S.; Desrumaux C.; Néel D.; Lagrost L. Vitamin E transport, membrane incorporation and cell metabolism: Is alpha-tocopherol in lipid rafts an oar in the lifeboat? *Mol Nutr Food Res*. **2010**, *54*, 631-640.

- 12) Moazzami A.; Kamal-Eldin A. Sesame Seed Oil. *Gourmet Heal Spec Oils*. **2009**, 267-282.
- 13) Ghafoor K.; Ozcan M.; Al-Juhaimi F.; Babiker E.; Sarker Z.; Ahmed I. Nutritional Composition, Extraction, and Utilization of Wheat Germ Oil: A Review. *Eur. J. Lipid Sci. Technol.* **2017**, 1600160, 1–9.
- 14) Yang Y.; Fang J.; Ma W.; Guo D.; Mohammat A. Large-scale pattern of biomass partitioning across China's grasslands. *Glob Ecol Biogeogr.* **2010**, 19, 268-277.
- 15) Naureen R.; Tariq M.; Yuosoff I.; Chowdhury A. Synthesis, spectroscopic and chromatographic studies of sunflower oil biodiesel using optimizes base catalyzed methodlysis. *Saudi J Biol Sci.* **2015**; 3, 1-8.
- 16) Schwartz H.; Ollilainen V.; Piironen V.; Lampi M. Tocopherol, tocotrienol and plant sterol contents of vegetable oils and industrial fats. *J Food Compos Anal.* **2008**, 21, 152-161.
- 17) Abidi S.; Thiam S.; Warner I. Elution behavior of unsaponifiable lipids with various capillary electrochromatographic stationary phases. *J Chromatogr A.* **2002**, 949, 195-207.
- 18) Reiter B.; Lechner M.; Lorbeer E.; Aichholz R. Isolation and characterization of wax esters in fennel and caraway seed oils by SPE-GC. *HRC J High Resolut Chromatogr.***1999**, 22, 514-520.
- 19) Lechner M.; Reiter B.; Lorbeer E. Determination of tocopherols and sterols in vegetable oils by solid-phase extraction and subsequent capillary gas chromatographic analysis. *J Chromat A.* **1999**, 857, 231-238.
- 20) Iqbal M. Trans fatty acids - A risk factor for cardiovascular disease. *Food Chem.* **2014**, 16, 194-197.
- 21) Cert A.; Moreda W.; Pérez-Camino M. Chromatographic analysis of minor constituents in vegetable oils. *J Chromatogr A.* **2000**, 88, 131-148.
- 22) Cocero M. Super critical fluid extraction of sunflower seed oil with CO<sub>2</sub>-ethanol mixtures. *JAOCS.* **1996**, 73, 1573-1578.
- 23) Piletska E.; Stavroulakis G.; Larcombe L.; Whitcombe M.; Sharma A.; Primrose S.; Robinson G.; Piletsky S. Passive Control of Quorum Sensing: Prevention of *Pseudomonas Aeruginosa* Biofilm Formation by Imprinted Polymers. *Biomacromolecules* **2011**, 12, 1067–1071.

- 24) Alghamdi E.; Whitcombe M.; Piletsky S.; Piletska E. Solid phase extraction of  $\alpha$ -tocopherol and other physiologically active components from sunflower oil using rationally designed polymers. *Anal Methods*. **2018**, *10*, 1-8.
- 25) O'Fallon J.; Busboom J.; Nelson M.; Gaskins C. A direct method for fatty acid methyl ester synthesis: Application to wet meat tissues, oils, and feedstuffs. *J Anim Sci*. **2007**, *85*, 1511-1521.
- 26) Flakelar C.; Prenzler P.; Luckett D.; Howitt J.; Doran G. A rapid method for the simultaneous quantification of the major tocopherols, carotenoids, free and esterified sterols in canola (*Brassica napus*) oil using normal phase liquid chromatography. *Food Chem*. **2017**, *214*, 147–55
- 27) Turowski M.; Morimoto T.; Kimata K.; Monde H.; Ikegami T.; Hosoya K.; Tanaka N. Selectivity of Stationary Phases in Reversed-Phase Liquid Chromatography Based on the Dispersion Interactions. *J. Chromatogr. A* **2001**, *911*, 177–190.
- 28) Christie, W. *Lipid Analysis. Isolation, Separation, Identification and Lipidomic Analysis I*, **2012**, Woodhead Publishing Limited: Cambridge, UK.
- 29) Andrade-Eiroa A. Reverse-High Performance Liquid Chromatography Mechanism Explained by Polarization of Stationary Phase. *CheM* **2011**, *1*, 62–79.
- 30) Courtois C.; Allais C.; Constantieux T.; Rodriguez J.; Caldarelli S.; Delaurent C. Cholesteric Bonded Stationary Phases for High-Performance Liquid Chromatography: Synthesis, Physicochemical Characterization, and Chromatographic Behavior of a Phospho–Cholesteric Bonded Support. A New Way to Mimic Drug/Membrane Interactions? *Anal. Bioanal. Chem*. **2008**, *392*, 1345–1354.
- 31) Simpsó N. *Solid Phase Extraction Principles, 2000, Techniques and Applications*; Marcel Dekker, Inc.:New York, USA.
- 32) Demel R.; Bruckdorfer K.; van Deenen L. Structural Requirements of Sterols for the Interaction with Lecithin at the Air-Water Interface. *Biochim. Biophys. Acta BBA - Biomembr*. **1972**, *255*, 311–320.
- 33) Feng S.; Gao F.; Chen Z.; Grant E.; Kitts D.; Wang S.; Lu X. Determination of  $\alpha$ -Tocopherol in Vegetable Oils Using a Molecularly Imprinted Polymers–Surface-Enhanced Raman Spectroscopic Biosensor. *J. Agric. Food Chem*. **2013**, *61*, 10467–75.

- 34) Moreau R.; Whitaker B.; Hicks K. Phytosterols, phytostanols, and their conjugates in foods: Structural diversity, quantitative analysis, and health-promoting uses. *Prog Lipid Res.* **2002**, *41*, 457-500.
- 35) Kumar G.; Krishna A. Studies on the nutraceuticals composition of wheat derived oils wheat bran oil and wheat germ oil. *J Food Sci Technol.* **2013**, *52*, 1145-1151.
- 36) Eisenmenger M.; Dunford N. Bioactive components of commercial and supercritical carbon dioxide processed wheat germ oil. *JAOCS, J Am Oil Chem Soc.* **2008**, *85*, 55-61.
- 37) Christie W. The Lipid Web <http://www.lipidhome.co.uk/ms/others/ffa-tms/index.htm> (accessed Oct 1, 2017).
- 38) Nill K. Changes in the contents and profiles of selected phenolics, soyasapogenols, tocopherols, and amino acids during soybean-rice mixture cooking: Electric rice cooker vs electric pressure rice cooker. *En cycl Food Heal.* **2016**, *100*, 58-63.
- 39) Longobardi F.; Ventrella A.; Casiello G.; Sacco D.; Catucci L.; Agostiano A.; Kontominas, M. Instrumental and Multivariate Statistical Analyses for the Characterisation of the Geographical Origin of Apulian Virgin Olive Oils. *Food Chem.* **2012**, *133*, 579–584.
- 40) Koushki M.; Nahidi M.; Cheraghali F. Physico-chemical properties, fatty acid profile and nutrition in palm oil. *J Paramed Sci Summer.* **2015**, *6*, 2008-4978.
- 41) Xu B.; Han J.; Zhou S.; Wu Q.; Ding F. Quality Characteristics of Wheat Germ Oil Obtained by Innovative Subcritical Butane Experimental Equipment. *J Food Process Eng.* **2016**, *39*, 79-87.
- 42) Kan A. Chemical and elemental characterization of wheat germ oil (*Triticum* spp. L.) cultivated in Turkey. *African J Agric Reseach.* **2012**, *7*, 4979-4982.
- 43) Ramos M.; Fernandez C.; Casas A.; Rodriguez L.; Perez A. Influence of fatty acid composition of raw materials on biodiesel properties. *Bioresour Technol.* **2009**, *100*, 261-268.
- 44) Guttman C M. *Mass Spectrometry Principles and Applications.* **2001**. 3rd Edit. (Edmond H, Vincent S, eds.). West Sussex: JohnWiley & Sons Ltd.
- 45) Hegde D. Sesame, in Peter K.V., Editor. *Handbook of Herbs and Spices*, 2012, pp. 267-28239.

- 46) Gharby S.; Harhar H.; Bouzoubaa Z.; Asdadi A.; El Yadini A.; Charrouf Z. Steam explosion technology based for oil extraction from sesame (*Sesamum indicum* L.) seed. *Food Chem.* **2014**, *7*, 194-197.
- 47) Bartosińska E.; Buszewska-Forajta M.; Siluk D. GC–MS and LC–MS approaches for determination of tocopherols and tocotrienols in biological and food matrices. *J Pharm Biomed Anal.* **2016**, *127*, 156-169.
- 48) Fiorentino A.; Mastellone C.; D'Abrosca B.; Pacifico S.; Scognamiglio M.; Cefarelli G.; Caputo R.; Monaco P.  $\alpha$ -Tocomonoenol: A New Vitamin E from Kiwi (*Actinidia Chinensis*) Fruits. *Food Chem.* **2009**, *115*, 187–192.
- 49) Nair P.; Luna Z. Identification of  $\alpha$ -tocopherol from tissues by combined gas-liquid chromatography, mass spectrometry and infrared spectroscopy. *Arch Biochem Biophys.* **1968**, *127*, 413-418.
- 50) Nagy K.; Courtet-Compondu M.; Holst B.; Kussmann M. Comprehensive Analysis of Vitamin E Constituents in Human Plasma by Liquid Chromatography–Mass Spectrometry. *Anal Chem.* **2007**, *79*, 7087-7096.
- 51) Zou L.; Akoh C. Identification of tocopherols, tocotrienols, and their fatty acid esters in residues and distillates of structured lipids purified by short-path distillation. *J Agric Food Chem.* **2013**, *61*, 238-246.
- 52) Gonzalez M.; Ballesteros E.; Gallego M.; Valcarcel M. Continuous-flow determination of natural and synthetic antioxidants in foods by gas chromatography. *Anal Chim Acta.* **1998**, *359*, 47-55.
- 53) Galea M.; Horga C. Separation and Determination of tocopherols in vegetable oil by SPE. *Cent Eur J Chem.* **2010**, *8*, 110-116.
- 54) Ballesteros E.; Gallego M.; Valcárcel M. Gas chromatographic determination of cholesterol and tocopherols in edible oils and fats with automatic removal of interfering triglycerides. *J Chromatogr A.* **1996**, *719*, 221-227.
- 55) Grigoriadou D.; Androulaki A.; Psomiadou E.; Tsimidou M. Solid phase extraction in the analysis of squalene and tocopherols in olive oil. *Food Chem.* **2007**, *105*, 675-680.
- 56) Lee Y.; Park H.; Lee C.; Kim S.; Hwang T. Comparing Extraction Methods for the Determination of Tocopherols and Tocotrienols in Seeds and Germinating Seeds of Soybean Transformed with OsHGGT. *J. Food Compos. Anal.* **2012**, *27*, 70–80.

- 57) Kim H.; Salem N. Extraction Thermospray LC-MS analysis. *J Lipid Res.* **1990**, *31*, 2285-2289.
- 58) Gibon V.; Dijckmans P.; Greyt W. Future prospects for palm oil refining and modifications. *Innov Technol.* **2009**, *16*, 193-200.
- 59) Koistinen V. Hanhineva K. Mass spectrometry-based analysis of whole-grain phytochemicals. *Crit Rev Food Sci Nutr.* **2017**, *57*, 1688-1709.
- 60) Suttiarporn P.; Chumpolsri W.; Mahatheeranont S.; Luangkamin S.; Teepsawang S.; Leardkamolkarn V. Structures of phytosterols and triterpenoids with potential anti-cancer activity in bran of black non-glutinous rice. *Nutrients.* **2015**, *7*, 1672-1687.
- 61) Purcaro G.; Barp L.; Beccaria M.; Conte L. Characterisation of minor components in vegetable oil by comprehensive gas chromatography with dual detection. *Food Chem.* **2016**, *212*, 730-738.
- 62) Dutta P. Phytosterols as Functional Food Components and Nutraceuticals. **2004** Marcel Dekker, INC New York, USA.
- 63) Dijkstra A J, Soybean Oil. in: B. Catalcro, P. Finglas, F. Toldra, Editor. *Encyclopedia of Food and Health*, **2016**, pp.58–63.
- 64) Yan G.; Li Q.; Huarong T.; Ge T. Electrospray ionization ion-trap time-of-flight tandem mass spectrometry of two furofurans: sesamin and gmelinol. *Rapid Commun Mass Spectrom.* **2007**, *21*, 3613-3620.
- 65) Lee J.; Choe E. Extraction of lignan compounds from roasted sesame oil and their effects on the autoxidation of methyl linoleate. *J Food Sci.* **2006**, *71*, 430-436.
- 66) Dachtler M.; Van De P.; Stijn F.; Beindorff C.; Fritsche J. On-line LC-NMR-MS characterization of sesame oil extracts and assessment of their antioxidant activity. *Eur J Lipid Sci Technol.* **2003**, *105*, 488-496.
- 67) Kim J.; Seo W.; Lee S.; Lee Y.; Park C.; Ryu, H.; Lee J. Comparative Assessment of Compositional Components, Antioxidant Effects, and Lignan Extractions from Korean White and Black Sesame (*Sesamum Indicum* L.) Seeds for Different Crop Years. *J. Funct. Foods* **2014**, *7*, 495–505
- 68) Wu W. The contents of lignans in commercial sesame oils of Taiwan and their changes during heating. *Food Chem.* **2007**, *104*, 341-344.
- 69) Moazzami A.; Haese S.; Kamal-Eldin A. Lignan contents in sesame seeds and products. *Eur J Lipid Sci Technol.* **2007**, *109*, 1022-1027.

- 70) Monfreda M.; Gobbi L.; Grippa A. Blends of olive oil and sunflower oil: Characterisation and olive oil quantification using fatty acid composition and chemometric tools. *Food Chem.* **2012**, *134*, 2283-2290.
- 71) Wabaidur S.; AlAmmari A.; Aqel A.; AL-Tamrah S.; Alothman Z.; Ahmed A. Determination of free fatty acids in olive oils by UPHLC–MS. *J Chromatogr B.* **2016**, *1031*, 109-115.
- 72) Psomiadou E.; Tsimidou M. Simultaneous HPLC Determination of Tocopherols, Carotenoids, and Chlorophylls for Monitoring Their Effect on Virgin Olive Oil Oxidation. *J. Agric. Food Chem.* **1998**, *46*, 5132–8.
- 73) Carrasco-Pancorbo A.; Navas-Iglesias N.; Cuadros-Rodríguez L. From lipid analysis towards lipidomics, a new challenge for the analytical chemistry of the 21st century. Part I: Modern lipid analysis. *Trends Analyt Chem.* **2009**, *28*, 263–78.
- 74) Fromm M.; Bayha S.; Kammerer D.; Carle R. Identification and Quantitation of Carotenoids and Tocopherols in Seed Oils Recovered from Different Rosaceae Species. *J Agric Food Chem.* **2012**, *60*,10733–42.
- 75) Abdallah I.; Tlili N.; Martinez-Force E.; Rubio A.; Perez-Camino M.; Albouchi A.; Boukhchina S. Content of carotenoids, tocopherols, sterols, triterpenic and aliphatic alcohols, and volatile compounds in six walnuts (*Juglans regia* L.) varieties. *Food Chem.* **2015**, *15*, 972–8.
- 76) Li C.; Yao Y.; Zhao G.; Chen Y.; Liu H.; liu C.; Shi Z.; Chen Y.; Wang S. Comparison and analysis of fatty acids, sterols, and tocopherols in eight vegetable oils. *J Agric Food Chem.* **2011**, *59*, 12493–8.

# Chapter four

# **Comparison between the developed RDP and commercial SPE adsorbents for the extraction of minor compounds from sunflower oil**

## **4.1 Introduction**

The development of efficient analytical procedures is one of the most important scientific objectives. SPE is a widely used analytical process to perform analyte separation and improve the performance of analysis. SPE provides several analysis processes such as clean-up, preconcentration and preparation of samples, which are some of the most laborious steps during the analytical techniques, consuming in average 61% of the total time required to execute analytical procedures.<sup>1-5</sup> SPE has been used for more than 20 years as an alternative to liquid-liquid extraction for sample preparation in analysis of organic compounds in industry, bioanalysis, food safety and nutrition and environmental applications.<sup>2-4</sup> SPE usually combined to other analytical technique or preparation method to provide a selective, cheap, quick, and environmentally friendly separation.<sup>5</sup>

### **4.1.1 SPE definition**

SPE is an analytical method applied for the preparation of a certain sample for quantitative or qualitative detection.<sup>1,6</sup> In the SPE process, the analyte is dissolved in a suitable solvent and removed from the solution potentially containing many interfering compounds. The main common goals to be achieved by SPE is either one or more of these of four purposes:

- 1) Concentrating the compound of interest;
- 2) Removal of undesirable interferences from the sample (clean-up);
- 3) Transform the analytes into a group of fractions;
- 4) Alternative storage method for the compound unstable in liquid medium.

In the SPE process, the sample is applied to one of the common formats such as cartridge devices or discs packed with SPE sorbents or magnetic nanoparticles.<sup>7</sup>

The different SPE sorbents are classified in terms of their separation mode, similarly to the classification of the chromatographic stationary phases.<sup>2,8-10</sup> There are several reviews in the literature attempted to separate the SPE sorbents into groups possessing common features, which represent a well-defined classification for the SPE resin that help to enhance the analytes separation and preparations processes.<sup>1,11,12,13</sup> The main types of SPE sorbents are reversed-phase, normal phase, ion exchange resins and customised resins based on functionalised polymers.<sup>1,2,8</sup> Table 4.28 summarised the main features of each approach.

There are some reviews in the literature which suggest adding another group to the sorbents types listed in Table 4.1 is known as mixed mode phases (ion exchange and reversed phase). These group of sorbents are applicable for wide selections of analytes as they are involved the modified reverse-phase with anionic or cationic functional groups such as the silica-based modified resin SDB or the polymeric resin modified with carboxylic or sulfonic acid groups.<sup>1</sup> Moreover, the functionalised resins included a new group of the SPE resins based on molecularly imprinted polymers (MIPs). MIPs offer selectivity, high capacity, regeneration capability, relatively short time for preparation and low-cost extraction and purification applications of different compounds in sustainable, natural/biological matrices, especially if these compounds are present at trace levels.<sup>14-17</sup>

Table 4.1: Characteristics of the main chromatographic separation approaches.<sup>14-17</sup>

Separation approaches	Bed sorbents	Analyte nature	Dissolve solvent	Elution solvent	Common feature/s
Reversed-phase sorbents	C18, C8, C2, Phenyl	Nonpolar or slightly polar	Methanol/water, acetonitrile/water	Hexane, chloroform, methanol	Affected negatively by presence of silanol residual. Effective only in pH= 2-8
Normal-phase sorbents	CN, NH <sub>2</sub> , COH, SiOH, Al <sub>2</sub> O <sub>3</sub>	Slightly polar or strongly polar	Hexane, chloroform, acetonitrile	methanol	
Ion exchange sorbents	Cation exchange: NH <sub>2</sub> , (NH/NH <sub>2</sub> ), Anion exchange: (CH <sub>2</sub> ) <sub>3</sub> N <sup>+</sup> (CH <sub>3</sub> ), COOH, SO <sub>3</sub> H	Negatively or positively charged analytes or biological fluids	Anion exchange: buffer (pH=pKa+2) Cation exchange: buffer (pH=pKa-2)	Anion exchange: buffer (pH=pKa+2), Cation exchange: buffer (pH=pKa-2) pH for high ionic or neutral analyte	Affective in remove polar compounds from nonpolar matrix by the hydrophilic interactions
Functionalised polymers	SAX, SDB, MIP....etc	Wide range of samples: polar, nonpolar, hydrophobic, hydrophilic...	Determined by the nature of analyte and the sorbent	Determined by the nature of analyte and the sorbent	High capacity, stability, no pH limitation

It is clear that the type of SPE sorbent has had a remarkable influence on the separation process, however, Turowski and co-workers highlighted the importance of other elements of the SPE process. For example, in case of the reversed-phase mode, the analyte adsorbed on the sorbent was due to the hydrophobic interactions, which are considered as weak interactions. However, the polar solvent are the dominant effect on the interactions between the solute and the sorbent. This was due to reduction of the surface area of the non-polar area in contact with polar sites by the repulsion forces between the polar and non-polar molecules.<sup>18</sup>

Moreover, the nature of the compound of interest has an important effect on the choice of SPE resins. Courtois *et al.* reported that the reversed-phase separation is mainly affected by the size and the shape of the solute, while normal-phase separation depends on the selectivity interactions of the polar functional groups of solute with polar sorbent.<sup>19</sup>

During the SPE, the analyte of interest is partitioned between a solid phase and a liquid matrix. The analyte/s that has/have higher affinity to the solid phase than towards the sample matrix will be retained on the stationary phase. This process is called retention or adsorption, which is opposite of the other process called elution or desorption. In elution, the retained compound/s on the stationary phase will leave the stationary phase to eluent if it/they has/have a higher affinity towards the eluting solvent than towards the stationary phase.<sup>19,20</sup>

#### **4.1.2 Main steps of SPE**

The SPE process is performed in four steps, namely: condition, loading, washing and elution.

##### **4.1.2.1 Condition**

This step involves the conditioning of the cartridge with a solvent to wet the sorbent. An appropriate solvent is passed over the stationary phase that activates the stationary phase particles. The importance of the conditioning process varies from one to another type of SPE sorbents. For example, in reversed-phase separation systems the stationary phase should be kept wet by the conditioning solvent,<sup>11</sup>

however, functionalised polymers are less sensitive to being dry before the loading step.<sup>8</sup> Simpson explained the importance of the conditioning of C18 sorbent through the comparison between loading a polar sample such as urine or drinking water on dry C18 and after conditioned with polar solvent such as water or methanol.<sup>13</sup> It was found that the environment surrounding the organic moieties of the sorbent became highly polar which in turn led to a more efficient SPE process.

#### **4.1.2.2 Loading (retention)**

The loading step is adding a certain amount of the analyte matrix that contains the compound of interest to be retained in the cartridge that is packed with a specific amount of the stationary phase. Preferably, the analyte and some impurities (in some cases) are retained on the sorbent. The retention is the process by which the analyte is retained in its solid state on the surface of the stationary phase after applying the solution of the sample matrix.<sup>8,21</sup> The analyte retains on the stationary phase by several types of intermolecular interactions, which is determined by the characteristics of the sample matrix, the binding types and strengths between the compound/s of interest and the surface of the stationary phase and its affinity towards solvent molecules.<sup>8,18</sup>

##### **4.1.2.2.1 Mechanisms of retention on SPE stationary phases**

To determine the appropriate SPE sorbent, it is useful to have knowledge about the compound of interest in terms of the analyte matrix, pH, solubility, chemical structure including the functional group/s and the ionic strength to speculate the forces that possibly bind this compound to the solid surface.<sup>1,8,20</sup> The retentive properties of the sorbent of SPE are due to the intermolecular interactions between the analyte molecules and the stationary phase particles with forces such as van der Waal and Coulombic. There are several types of intermolecular interactions including electrostatic, hydrogen bonding and hydrophobic interactions as demonstrated in Figure 4.1. Each type of interaction includes one or more sub-type/s. The retention of the adsorbent on the surface of the sorbent could be occurred due to one or more of these forces in the same time.<sup>8,11,22</sup> The recent tendency of separation research is directed to develop the sorbent that could provide more than

one type of interactions by modifying them with polar and nonpolar moieties, thus, providing an applicable sorbent that could be used in wide range of analytes.<sup>13,23</sup>

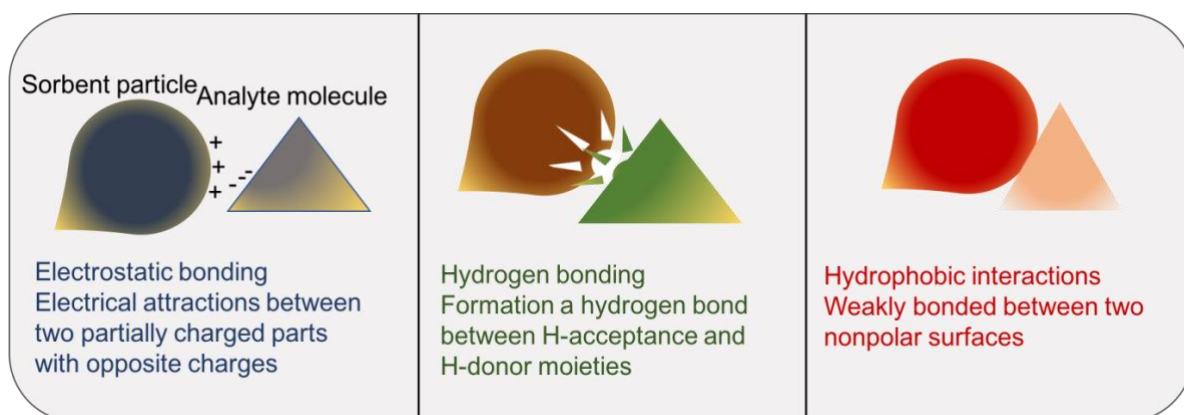


Figure 4.1: Illustration of the possible intermolecular interactions between the analyte and surface of the stationary phase in SPE.

Buszewski *et al.* and Dmitrienko *et al.* reported that the most commonly used are silica-based sorbents. However, considerable effort has been made to develop the stationary phases with high retentive properties, high capacities, excellent efficiencies and performed hydrophilic/hydrophobic balances.<sup>6,9-11,21,24</sup> MIPs are the most common example of the development of the SPE sorbent that has exhibited distinguished successful achievements in the sample preparation science.<sup>25-29</sup> The retention process in this type of SPE sorbent is based on the pre-synthesis of the polymer using the target molecule as a template. The synthesis of MIP includes the polymerisation of functional monomers and cross-linkers around the target molecule (template) and the subsequent elimination of the template molecules leaving cavities with specific recognition sites that are complementary in shape, size, and spatial arrangement to the template molecule.<sup>7,30</sup> Therefore, the retention process of the target is determined by the type of functional monomers and cross-linkers that have been used in the polymerisation.

The strength of intermolecular interactions varies from 1 to 200 k cal mol<sup>-1</sup> as is shown in Figure 4.2 and in one type of resin one or more types of intermolecular interaction could bind the analyte to the stationary phase.

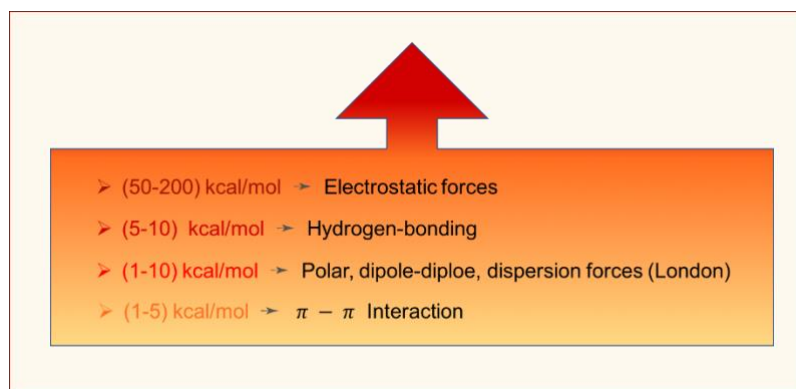


Figure 4.2: Binding energy of different types of intermolecular interactions.

There is a continuous development of the stationary phases for SPE that exhibit sufficient capacity and excellent selectivity. The most commonly used SPE sorbents are among the four types: silica-based types, oxides of metals, carbon-based types or polymer-based sorbents. Qureshi *et al.* suggested that polymer based sorbents have an advantage over silica-based and oxides of metal sorbents due to being less sensitive to drying out after conditioning and have less impact of variation of pH.<sup>21</sup> These polymer based sorbents show enhanced retention of highly polar analytes such as phenols. In addition, these sorbents with a high surface area exhibit a high degree of hydrophobicity that leads to large capacity. On the other hand, the silica active and oxides of metals have limitations by the condition of that the sorbents must be wet with the conditioning solvent before applying the sample (loading step), effective in the limited range of pH and the presence of highly active sites that cause the secondary interaction leading to reduce the efficiency.

#### 4.1.2.3 Washing

To reduce the interferences that may be adsorbed on the stationary phase at the same time as the compound of interest is retained during loading step, it is essential to wash the SPE cartridge with an appropriate solvent that has a greater affinity for the co-retained compounds to desorb and leave the SPE cartridge. Meanwhile, this solvent should not disrupt the interactions between the compound of interest and the resin to allow it to be eluted in the next step.

#### 4.1.2.4 Elution:

The step by which the extraction of the compound of interest is carried out from a mixture using an appropriate solvent is called as elution, which makes the compounds more suitable for analysis. When a liquid mobile phase (eluent) provides more affinity for the analyte than the solid stationary phase, then the compound of interest leaves the solid surface to this liquid. Subsequently, the compound of interest can be collected in the liquid as it exits the SPE device. Recent studies have shown that silica based SPE sorbents, oxides of metals, carbon-based sorbents and polymer-based sorbents are the most commonly used.<sup>1,2,4</sup> In the literature, a range of attempts and methods has been mentioned to develop the silica based stationary phases to improve the quality of the separation and the variety of the purified samples. It was done by modification of the silica surface by immobilising functional groups to enable either hydrophobic or hydrophilic interactions between the analyte and the solid surface. As an example, Qureshi *et al.* presented Oasis HLB as a polymer-based sorbent that was produced by polymerisation of lipophilic DVB and hydrophilic N-vinylpyrrolidone, making a hydrophilic–lipophilic balance. The Oasis HLB sorbent has been applicable in SPE for many polar or apolar analytes.<sup>21</sup>

The principles of the relationships between the main elements of the SPE process are shown in the Figure 4.3. Silica-based sorbents have advantage of the large surface area and versatility to be derivatised. However, they suffer from some drawbacks, such as being unable to be used in pH outside the range 2-8, as silica dissolves in high pH. Moreover, silanol groups are easily ionised causing highly active sites on the silica particles.

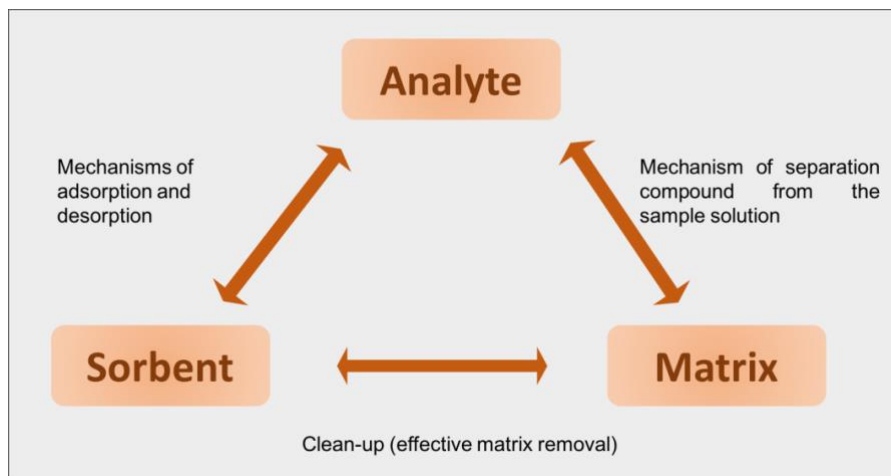


Figure 4.3: The relationships between the main elements of SPE.

In some extraction processes, the silica should be kept wet before applying the sample of the analyte. Therefore, there is an inevitable demand to develop a cost-effective sorbent that combined the selectivity and diversity of purified samples. The polymer-based sorbents have gained more attention for improvement as their development overcame all the difficulties associated with silica-based sorbents. In this chapter, a study has been presented which demonstrates a comparison between the optimised SPE polymer (RDP), which was exhibited in the second chapter, and some commercially available resins in terms of their retention properties and their recovery under the proposed SPE protocol suggested in the second chapter of this thesis.

## 4.2 Materials and methods

### 4.2.1 Chemicals and reagents

Unrefined sunflower oil was purchased from Activecare through Amazon.com. The commercial names of the SPE sorbent used in this study are PAH (Isolute, UK), Vac (Waters, Ireland) Phenyl, SAX and SDB (Phenomenex, UK). The synthesis of adsorbent RDP was described in the second chapter. Methanol, heptane, n-hexane and acetic acid were obtained from Fisher Scientific (UK). All solvents were of HPLC quality grade and used without any purification.

#### 4.2.2 Equipment and analysis techniques

Three-mL SPE cartridges were each packed with 100 mg of all SPE sorbents and used in combination with a vacuum manifold (Supelco, UK). All SPE experiments were repeated three times. The quantification of the minor components was performed using the Gas Chromatography-Mass-spectrometry (GC/MS) set-up (Perkin Elmer, TurboMass, UK) using a 30 m x 250  $\mu\text{m}$ , 0.25 mm I.D., ZB-5 capillary column (Phenomenex, UK). Helium gas was used as the mobile phase to carry the sample at a flow-rate of 1 mL min<sup>-1</sup> at 200 °C. After injection of 10  $\mu\text{L}$  of the sample at 200 °C, the temperature of the GC oven was raised by 10 °C min<sup>-1</sup> to 350 °C and held for 3 min.

To assess the performance of RDP, 100 mg of six different types of commercially available sorbents were packed in SPE cartridge.<sup>25</sup> The commercial names of the SPE sorbent in this study are C18, PAH, Phenyl, SAX, SDB, Vac and RDP. The optimised SPE protocol included following steps: a conditioning 100 mg of adsorbent packed in a 3mL cartridge with 1 mL of hexane, loading of 1 mL of 20% sunflower oil in heptane, washing the cartridge with 1 mL of 60% methanol and then, elution using 3 mL of methanol with 5% acetic acid. The collected eluent from each cartridge was evaporated to dryness and reconstituted in 1 mL of hexane to be analysed with GC/MS. Using calibration curves for each of the minor components (Table 3.1 in the chapter 3 and Appendix 2), it was possible to calculate the concentrations from the integration of each peak in GC/MS chromatogram corresponding to each component. Subsequently, calculation of the loading capacity and percentage of recovery for each sorbent.

### **4.3 Results and discussion**

The goal of the experiments described in this chapter was to compare the performance of the synthesised RDP resin with a group of commercially-available SPE cartridges. An examination of the optimised SPE protocol with different SPE sorbents was carried out. The comparison was made by packing 100 mg of each sorbent in 3-mL SPE cartridges and applying the optimised SPE process in the second chapter. The samples, which were collected from each cartridge and after the three steps of SPE namely: loading (unbounded sample), washing (interferences) and elution (eluted sample), were evaporated and reconstituted in hexane to be analysed with GC/MS. The integration of each peak was converted to concentration using the calibration curves of the minor compounds of sunflower oil and was presented in the second chapter. The results were presented for each step to all sorbents as follows:

#### **4.3.1 After loading**

The loaded sample in each cartridge was 1 mL of 20% of sunflower oil in heptane. It was passed through the cartridge under vacuum using the manifold device. The concentration of the minor components in the collected samples indicated the unabsorbed amount of these compounds. The concentrations of these samples indicated the retentive properties of the sorbents in this study (Table 4.2, Figure 4.4).

Table 4.2: Concentration of the minor components in the samples lost during loading (mg g<sup>-1</sup>).

SPE steps	Stationary phase	Palmitic acid	Oleic and linoleic acids	$\alpha$ -tocopherol	Campesterol	Stigmasterol	$\beta$ -sitosterol	Total (mg)
After loading	C18	0.302 $\pm$ 0.02	1.080 $\pm$ 0.05	0.093 $\pm$ 0.03	0	0	0	1.475
	PAH	0	0	0	0	0	0.056 $\pm$ 0.03	0.056
	PHENYL	0.056 $\pm$ 0.004	0.162 $\pm$ 0.03	0.043 $\pm$ 0.02	0	0	0	0.225
	SAX	0	0	0	0	0	0	0
	SDB	0.011 $\pm$ 0.02	0.915 $\pm$ 0.03	0.083 $\pm$ 0.03	0	0	0	1.009
	Vac	0	0	0.055 $\pm$ 0.02	0.010 $\pm$ 0.004	0	0.017 $\pm$ 0.02	0.082
	RDP	0	0	0	0	0	0	0

It was noticed that the most retention has occurred in SAX and RDP where GC/MS detected no compounds in the collected samples from these cartridges. Further, PAH has shown only 0.056 mg g<sup>-1</sup> from  $\beta$ -sitosterol that was passed through the cartridge. On the other hand, the least retentive sorbent was C18, which allowed the largest amount (total sum as 1.5 mg) of the minor compounds to leave the cartridge. By comparing the sum of the amount of unabsorbed minor compounds, it was found that their order from the least to the highest is as follows: C18 < SDB < Phenyl < Vac < PAH < SAX < RDP. It was found that the resins C18, Phenyl, SAX and SDB were presented in the literature as silica-based sorbents. C18, SDB and Phenyl showed poor retention comparing to the rest of the resins. However, Phenyl and C18 have been used effectively for lipid extraction under different conditions.<sup>8,23,24</sup> Therefore, the reason for the poor performance of these sorbents could be due to that the SPE conditions were inappropriately for them.

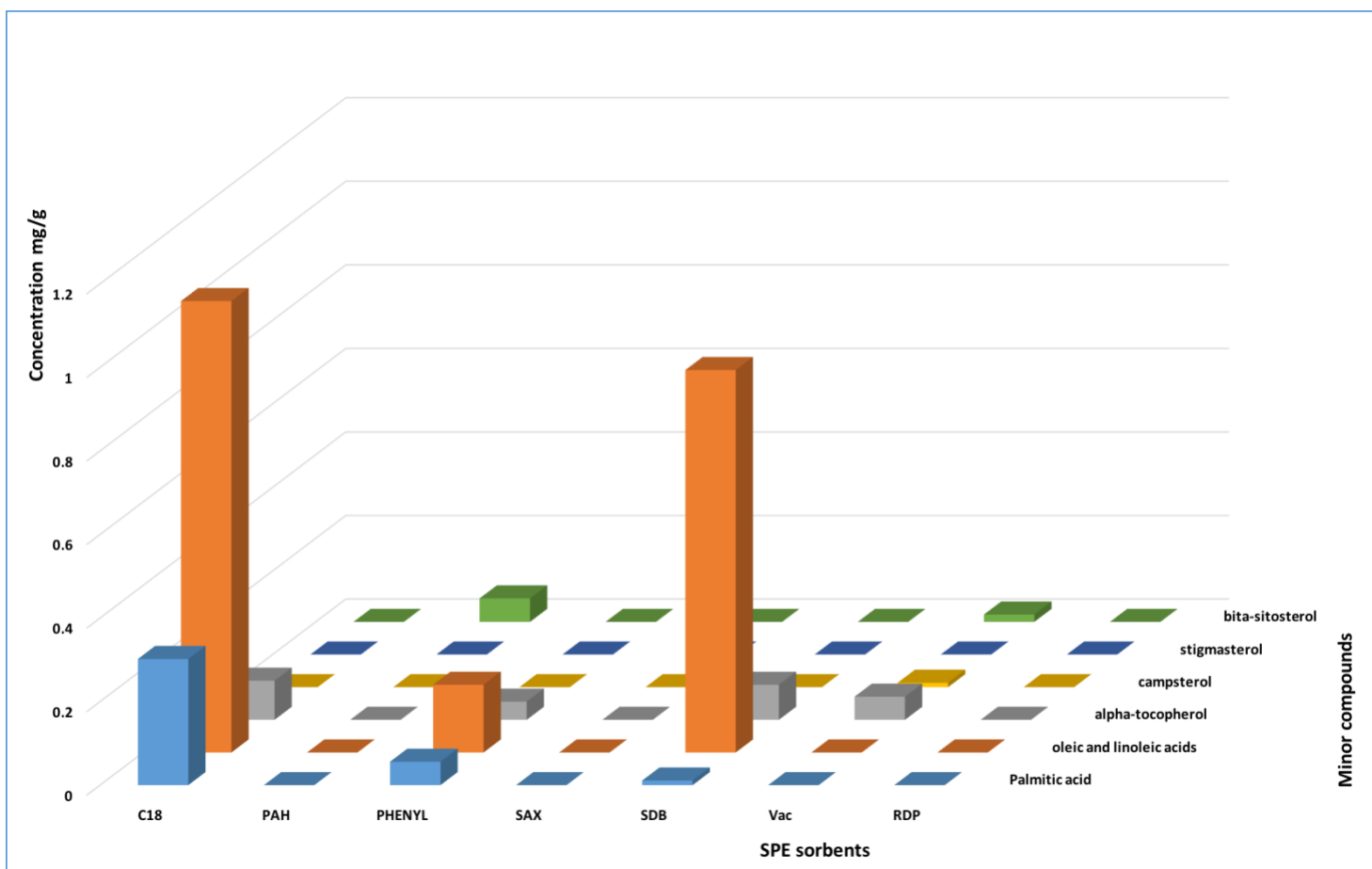


Figure 4.4: Statistical demonstration of the concentration of the compounds which were not absorbed during loading.

### 4.3.2 After washing

The optimised solvent (i.e. 60% methanol in water) for washing out the interferences was based on the proposed method as described in the second chapter.<sup>25</sup> Applying this solvent for the washing step resulted in good outcomes as the cartridges SDB, Vac and RDP in this study retained all the compounds of interest as shown in Table 4.3, Figure 4.5. Moreover, the sorbents C18, PAH, Phenyl and SAX lost small concentrations of the heaviest group of compounds ( $\alpha$ -tocopherol and phytosterols) with exception of Phenyl that lost some of the fatty acids with  $\alpha$ -tocopherol.

The result showed in table 4.3 indicated that 60% methanol was a suitable washing solvent for the sorbents SDB, Vac and RDP, where none of the minor compounds were desorbed. The sorbents C18 and SAX lost some of  $\beta$ -sitosterol. However, 60% methanol was not suitable as a washing solvent for Phenyl, as a considerable amount of the fatty acids and  $\alpha$ -tocopherol were desorbed. Alongside, it proved to be an inappropriate solvent for the sorbent PAH, which lost  $\alpha$ -tocopherol and some of the phytosterols.

Table 4.3: Concentration of the minor components in the samples after washing (mg g<sup>-1</sup>).

<b>SPE steps</b>	<b>Stationary phase</b>	<b>Palmitic acid</b>	<b>Oleic and linoleic acids</b>	<b>α-tocopherol</b>	<b>Campesterol</b>	<b>Stigmasterol</b>	<b>β-sitosterol</b>	<b>Total (mg)</b>
After washing	C18	0	0	0	0	0	0.084±0.03	0.084
	PAH	0	0	0.229±0.04	0.113±0.02	0.056±0.04	0.267±0.02	0.665
	PHENYL	0.013± 0.03	1.31±0.02	0.088±0.01	0	0	0	1.411
	SAX	0	0	0	0	0	0.180±0.02	0.180
	SDB	0	0	0	0	0	0	0
	Vac	0	0	0	0	0	0	0
	RDP	0	0	0	0	0	0	0

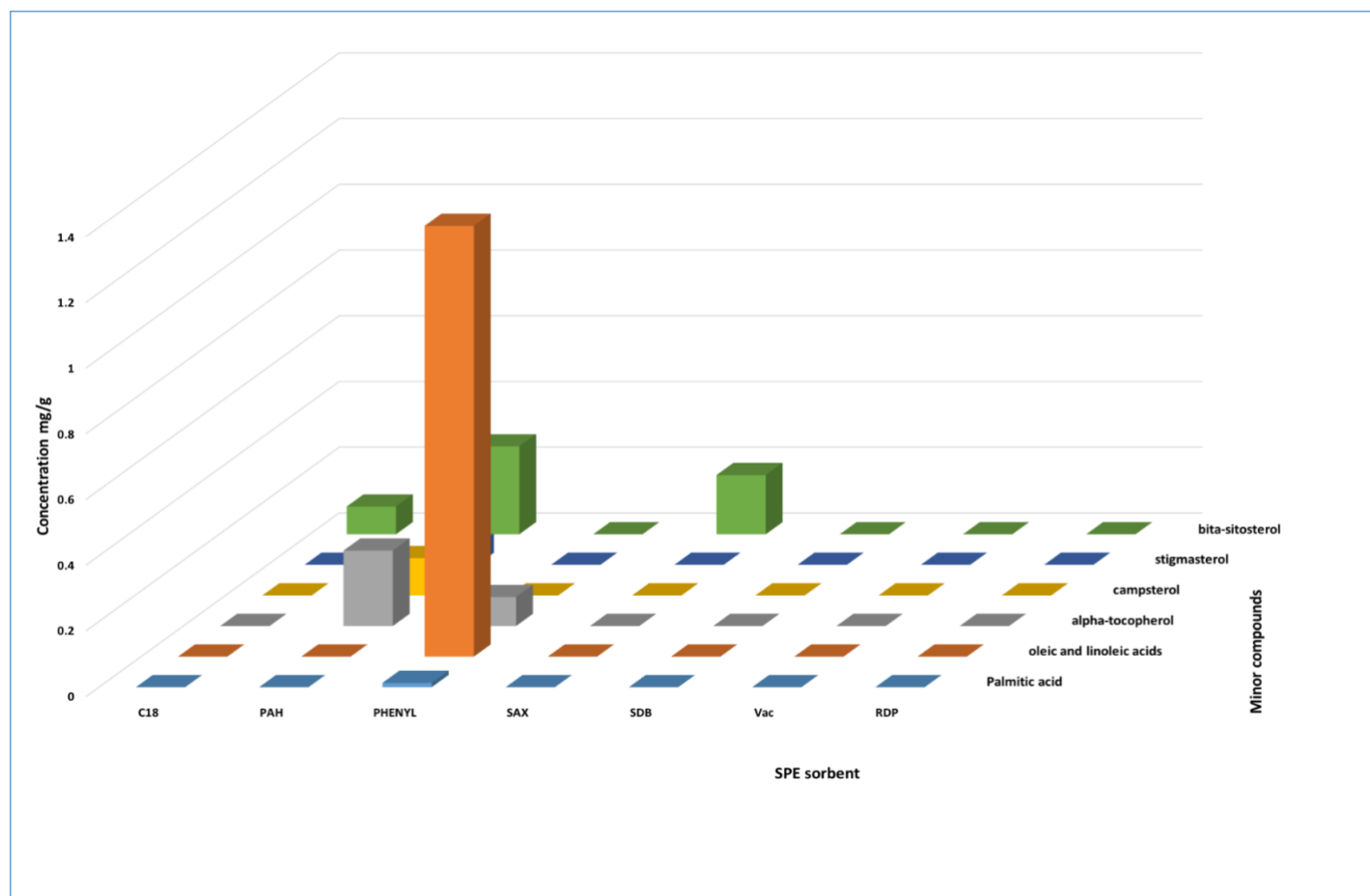


Figure 4.5: Statistical demonstration of the concentration of the compounds which were lost during washing.

### 4.3.3 After elution

The elution step was carried out by adding 3 mL of methanol with 5% acetic acid to the SPE cartridges, then collecting the eluent after passing the sorbents. Afterwards, the solvent was evaporated and the residues were reconstituted in hexane to be analysed using GC/MS. It was possible to calculate the concentrations using the integration of the peaks and the calibration curve for each compound (Table 4.4, Figure 4.6).

To compare the recovery of SPE from the seven types of sorbents in the current study, it was essential to consider the total amount of the separated compounds and the types of eluted compounds in Table 4.4. Regarding the diversity and quantity of the extracted minor compounds, RDP and PAH were far superior to other SPE sorbents with 6.759 and 5.095 mg g<sup>-1</sup>, respectively of the separated minor compounds from the sunflower oil solution. The purification using these adsorbents resulted in the largest number of the compounds under the study that were identified using GC/MS. Moreover, Phenyl and Vac showed the various range of the extracted compounds with less of the total compounds extracted. Purification using SAX and SDB resins allowed to purify fewer variety of the extracted compounds, in general it was only the fatty acids and  $\alpha$ -tocopherol which were extracted in even lower quantities that when other resins were used. C18 showed the least amount of extraction including only fatty acids and  $\alpha$ -tocopherol and this is expected (in terms of the quantity) as this adsorbent has shown the highest loss of unadsorbed compounds after loading.

Table 4.4: Concentration of the minor components in the samples after elution (mg g<sup>-1</sup>).

<b>SPE steps</b>	<b>Stationary phase</b>	<b>Palmitic acid</b>	<b>Oleic and linoleic acids</b>	<b>α-tocopherol</b>	<b>Campesterol</b>	<b>Stigmasterol</b>	<b>β-sitosterol</b>	<b>Total (mg)</b>
After elution	C18	0.004± 0.003	0.319± 0.02	0.011±0.002	0	0	0	0.334
	PAH	0.129± 0.03	4.589±1.02	0.022±0.004	0	0	0.355±0.04	5.095
	PHENYL	0.005±0.002	1.188±0.3	0.033±0.002	0	0.011±0.005	0.035±0.005	1.272
	SAX	0	0.997±0.04	0.141± 0.03	0	0	0	1.138
	SDB	0.016±0.003	0.710±0.03	0.028±0.001	0	0	0	0.754
	Vac	0	1.509±0.05	0.046± 0.004	0.016±0.003	0	0.003±0.003	1.794
	RDP	0.286±0.02	5.749± 0.5	0.121±0.002	0.054±0.005	0.291± 0.02	0.258±0.021	6.759

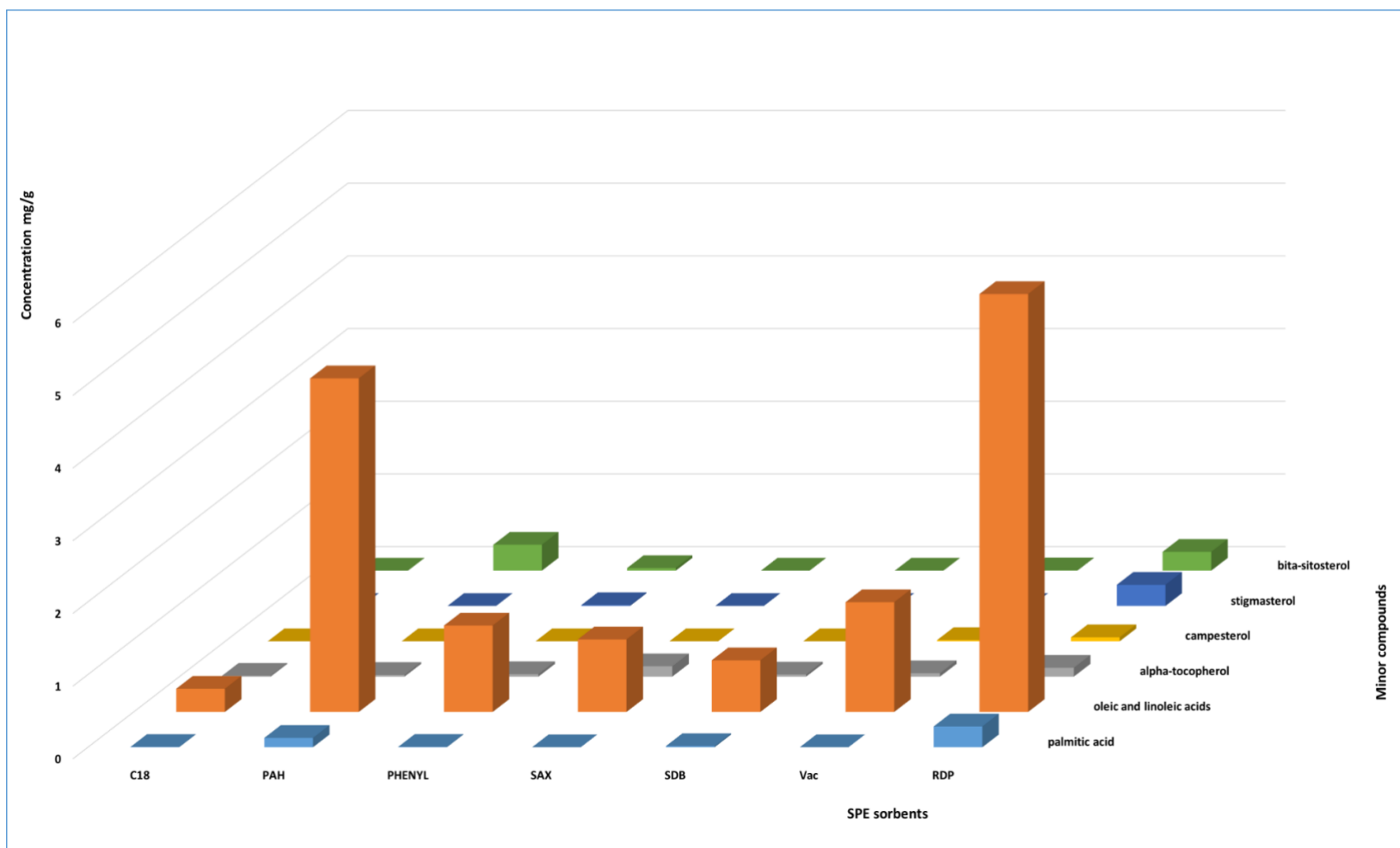


Figure 4.6: Statistical demonstration of the concentration of the eluted compounds.

#### **4.4 Conclusion:**

Based on the time of this research, limited comparison between RDP and some commercially available cartridges was made. Using optimised SPE protocol, the comparison between six commercially available resins and RDP has shown distinguished efficiency of RDP to extract the group of minor components from 20% sunflower oil in heptane with minimum of organic solvents. Moreover, the optimised protocol has enabled to achieve an almost similar and good result with carbon-based polymer PAH. Despite the possibility to extract some of the minor component using the other sorbents they were not as effective as developed RDP.

## References

- 1) Andrade-Eiroa A.; Canle M.; Leroy-Cancellieri V.; Cerdà V. Solid-phase extraction of organic compounds: A critical review (Part I). *Trends Anal. Chem.* **2016**, *80*, 641–654.
- 2) Augusto F.; Hantao L.; Mogollón, N.; Braga, S. New materials and trends in sorbents for solid-phase extraction. *Trends Anal. Chem.* **2013**, *43*, 14–23.
- 3) Płotka-Wasyłka J.; Szczepańska N.; de la Guardia, M.; Namieśnik J. Miniaturized solid-phase extraction techniques. *Trends Anal. Chem.* **2015**, *73*, 19–38.
- 4) Gilart N.; Borrull F.; Fontanals N.; Marcé R. Selective materials for solid-phase extraction in environmental analysis. *Trends Environ. Anal. Chem.* **2014**, *1*, e8–e18. *Trends Anal. Chem.* **2016**, *80*, 12–29.
- 5) Xu C.; Chen G.; Xiong Z.; Fan Y.; Wang X.; Liu Y. Applications of solid-phase microextraction in food analysis. *Trends Anal. Chem.* **2016**, *80*, 12–29.
- 6) Huck C.; Bonn G. Recent developments in polymer-based sorbents for solid-phase extraction. *J. Chromatogr. A* **2000**, *885*, 51–72.
- 7) Song X., Xu S.; Chen L.; Wei Y.; Xiong H. Recent advances in molecularly imprinted polymers in food analysis. *J. Appl. Polym. Sci.* **2014**, *131*, 1–18.
- 8) Buszewski B.; Szultka M. Past, Present, and Future of Solid Phase Extraction: A Review. *Crit. Rev. Anal. Chem.* **2012**, *42*, 198–213.
- 9) Dmitrienko S.; Kochuk E.; Tolmacheva V.; Apyari V.; Zolotov Y. Comparison of adsorbents for the preconcentration of sulfanilamides from aqueous solutions prior to HPLC determination. *J. Anal. Chem.* **2013**, *68*, 871–879.
- 10) Kimata K.; Hirose T.; Moriuchi K.; Hosoya K.; Araki T.; Tanaka N. High-Capacity Stationary Phases Containing Heavy Atoms for HPLC Separation of Fullerenes. *Anal. Chem.* **1995**, *67*, 2556–2561.

- 11) Turowski M.; Morimoto T.; Kimata K.; Monde H.; Ikegami T.; Hosoya K.; Tanaka N. Selectivity of stationary phases in reversed-phase liquid chromatography based on the dispersion interactions. *J. Chromatogr. A* **2001**, *911*, 177–191.
- 12) Christie W. The Lipid Web <http://www.lipidhome.co.uk/ms/others/ffa-tms/index.htm> (accessed Oct 1, 2017).
- 13) Simpson N. *Solid phase extraction principle, techniques and applications*. **2000**, Marcel Dckker, Inc. New York, USA.
- 14) Piletsky S.; Karim K.; Piletska E.; Day C.; Freebairn K.; Legge C. Turner A. Recognition of ephedrine enantiomers by molecularly imprinted polymers designed using a computational approach. *Analyst* **2001**, *126*, 1826–1830.
- 15) Piletska E.; Burns R.; Terry L.; Piletsky S. Application of a molecularly imprinted polymer for the extraction of kukoamine a from potato peels. *J. Agric. Food Chem.* **2012**, *60*, 95–9.
- 16) Piletsky S.; Piletska E.; Karim K.; Foster G.; Legge C.; Turner A. Custom synthesis of molecular imprinted polymers for biotechnological application: Preparation of a polymer selective for tylosin. *Anal. Chim. Acta* **2004**, *504*, 123–130.
- 17) Guerreiro A.; Soares A.; Piletska E.; Mattiasson B.; Piletsky S. Preliminary evaluation of new polymer matrix for solid-phase extraction of nonylphenol from water samples. *Anal. Chim. Acta* **2008**, *612*, 99–104.
- 18) Horváth C.; R.Melander W.; Molnar I. Solvophobic interactions in liquid chromatography with nonpolar stationary phase. *J. Chromatogr.* **1976**, *1269*, 129–156.
- 19) Courtois C.; Allais C.; Constantieux T.; Rodriguez J.; Caldarelli S.; Delaurent C. Cholesteric bonded stationary phases for high-performance liquid chromatography: synthesis, physicochemical characterization, and chromatographic behavior of a phospho–cholesteric bonded support. A new way to mimic drug/membrane interactions? *Anal. Bioanal. Chem.* **2008**, *392*, 1345–1354.

- 20) Ashley, J.; Shahbazi M.; Kant K.; Chidambara V.; Wolff A.; Bang D.; Sun Y. Imprinted polymers for sample preparation and biosensing in food analysis: Progress and perspectives. *Biosens. Bioelectron.* **2017**, *91*, 606–615.
- 21) Qureshi M.; Stecher G.; Huck C.; Bonn G. Preparation of polymer based sorbents for solid phase extraction of polyphenolic compounds. *Cent. Eur. J. Chem.* **2011**, *9*, 206–212.
- 22) Andrade-Eiroa A.; Canle M.; Leroy-Cancellieri V.; Cerdà V. Solid-phase extraction of organic compounds: A critical review. part ii. *Trends Anal. Chem.* **2016**, *80*, 655–667.
- 23) Christie, W. W. *Advance in lipid methodology*. **2013**, Woodhead Publishing Limited, Cambridge. UK.
- 24) Thomas J.; Donnelly C.; Lloyd E.; Mothershead R. Miller M. Development and validation of a solid phase extraction sample cleanup procedure for the recovery of trace levels of nitro-organic explosives in soil. *Forensic Sci. Int.* **2018**, *284*, 65–77.
- 25) Alghamdi E.; Whitcombe M.; Piletsky S.; Piletska E. Solid phase extraction of  $\alpha$ -tocopherol and other physiologically active components from sunflower oil using rationally designed polymers. *Anal. Methods* **2018**, *10*, 1–8.
- 26) Alghamdi E.; Piletsky S.; Piletska E. Application of the bespoke solid-phase extraction protocol for extraction of physiologically-active compounds from vegetable oils. *Talanta* **2018**, *189*, 157–165.
- 27) Munawar H.; Smolinska-Kempisty K.; Cruz A.; Canfarotta F.; Piletska E.; Karim K.; Piletsky S. A Molecularly imprinted polymer nanoparticle-based assay (MINA): application for fumonisin B1 determination. *The Analyst* **2018**, *143*, 3481–3488.
- 28) Smolinska-Kempisty K.; Ahmad, O.; Guerreiro A.; Karim K.; Piletska E.; Piletsky S. New potentiometric sensor based on molecularly imprinted nanoparticles for cocaine detection. *Biose Bioelectronics*, **2017**, *96*, 49-54.
- 29) Musile, G.; Cenci L.; Piletska E.; Gottardo R.; Bossi A.; Bortolotti F. Development of an in-house mixed-mode solid-phase extraction for the

determination of 16 basic drugs in urine by High Performance Liquid Chromatography-Ion Trap Mass Spectrometry. *J. Chromatogr. A* **2018**, *1560*, 10–18.

30) Piletska E.; Kumir J.; Sergeyeva T.; Rational design and development of affinity adsorbents for analytical and biopharmaceutical. *JCAM* **2013**, *1*, 229-244.

31) Nabarlantz D.; de Celis J.; Bonelli P.; Cukierman A. Batch and dynamic sorption of Ni(II) ions by activated carbon based on a native lignocellulosic precursor. *J. Environ. Manage.* **2012**, *97*, 109–115.

32) Fu, M.; Xing H.; Chen X.; Zhao R.; Zhi C.; Wu C. Boron nitride nanotubes as novel sorbent for solid-phase microextraction of polycyclic aromatic hydrocarbons in environmental water samples. *Anal. Bioanal. Chem.* **2014**, *406*, 5751–5754.

# Chapter five

# Comparison of the selectivity and capacity of the three different formats of molecularly imprinted polymers

## 5.1 Introduction

Molecular imprinting technology is a widely accepted synthetic approach to produce pre-designed polymeric materials with memory to a specific template (or its analogues) presented during polymer preparation.<sup>1,2</sup> The main attractive feature of the molecularly imprinted polymers that makes them applicable in separation studies is the selectivity.<sup>1,3</sup> MIPs have been applied in different research fields based on the capability to recognise the specific structure and three dimensional shape of the functional groups.

According to Koesdjojo *et al.*, there are a number of successful examples of using MIPs in separation science<sup>4</sup> and sample preparation or concentration before the analysis. MIPs have been used as stationary phases for SPE.<sup>5,6</sup> There are many successes examples that have been reported in the pharmaceutical, cosmetic, and nutraceutical industries where selective MIPs have been used to these compounds. For example, selective microparticles MIPs have been reported to extract kukoamine from potato peel, the antibiotic tylosin andephedrine.<sup>7-9</sup>

More than 40 years ago, many published studies attributed to the development of molecularly imprinted technology under the same simple concept of using the molecular template to create recognition sites. Although the great number of successful applications of these materials, several reviews have suggested that bulk MIPs have some limitations that require more research and improvements. One of the main drawbacks of MIP is an irregular shape of the resultant bulk MIPs particles produced after grinding and sieving.<sup>1,3,10,11</sup> MIPs are highly stable materials and can withstand high pressure, temperatures, organic solvents and different ranges of pH, which made them relevant for the chromatographic applications.<sup>1,12,13</sup> However, it is claimed that the physical appearances (polydispersity) of MIPs have a significant impact on the efficiency of their chromatographic performance.<sup>3,10,11</sup> The irregular shape of the MIP microparticles, obtained by grinding of the bulk polymer, hinders the complete removal of the template molecules that are located in the interior area of the particles due to the high cross-linking nature of the MIP particles. Therefore, the difficulties of removing the template molecules from internal binding sites contribute to the reduction of the rebinding capacity and cause

poor site accessibility to target molecules.<sup>11</sup> Therefore, there are many studies that have introduced alternative synthetic processes such as those based on the surface imprinting approaches to generate uniform polymer particles,<sup>4</sup> for example, suspension,<sup>14</sup> precipitation,<sup>15</sup> emulsion<sup>16</sup> and dispersion<sup>17</sup> polymerisations.

MIP synthesis has been developed to overcome these limitations through the new generation of the molecularly imprinted polymers. Synthesis MIP in nano-structured can be one of the attempts to controlling the position of the templates to be only on the surface of the particles, offering the thorough removal of template molecules. The original initiative to enhance the MIPs nanostructure was to optimise the uniformity of the polymeric materials by increasing the surface area-to-volume ratio, leading to better separation performance and to minimise the variation of the produced polymer particles.<sup>1,11</sup> However, the synthesis of MIP nanoparticles does not have the same degree of simplicity of preparing bulk MIPs that can be prepared in any moderately equipped lab.<sup>18</sup> Various approaches were developed for the synthesis of molecularly imprinted polymer nanoparticles (MIP NPs) such as core-shell approaches, precipitation polymerisation, emulsion polymerisation, and living radical polymerisation processes.<sup>3,19</sup>

The main goal of this chapter was to compare the main characteristics of the microparticles RDP and MIP and magnetic nanoparticles (MIP NPs) and discuss their advantages for particular separation and purification needs. In addition, to complete the framework of this thesis, this chapter includes an optimised protocol of solid-phase synthesis of molecularly imprinted polymer nanoparticles (MIP NPs) specific for  $\alpha$ -tocopherol based on the procedure recently developed by Leicester Biotechnology Group.

## 5.2 Materials and methods

### 5.2.1 Chemicals and reagents

Ethylene glycol dimethacrylate (EGDMA), 1,1'-azobis (cyclohexane carbonitrile), methacrylic acid (MAA), tri-methylolpropane tri-methacrylate (TRIM) and methanol were purchased from Sigma-Aldrich, UK.  $\alpha$ -tocopherol was purchased from Santa Cruz Biotechnology (UK). Acetonitrile, iron (II, III) oxide, ethyl acetate, heptane, n-hexane, dry toluene, 3-(trimethyloxysilyl) propyl methacrylate and acetic acid were obtained from Fisher Scientific (UK). Dimethylformamide was obtained from Acros Organics (UK). All solvents were of HPLC-quality grade and used without any purification. N, N-diethyldithiocarbamic acid benzyl ester (iniferter) was synthesised in the lab by a member of the group. Glass beads (diameter, 70 - 100  $\mu\text{m}$ ) (Potters, Spheringlass A-Glass cat. no. 2429, CP 00), Blagden Chemicals, UK. Phosphate buffered saline (PBS), N, N'-diisopropylethylamine (DIPEA), (3-glycidyloxypropyl) trimetoxysilane (GOPTS), N-ethyl-diisopropylamine (EIPA), Sodium hydroxide (NaOH) and sulfuric acid ( $\text{H}_2\text{SO}_4$ ) were purchased from Sigma-Aldrich, UK

### 5.2.2 Equipment and analysis techniques

The quantification of the  $\alpha$ -tocopherol in the different experiments was performed using the Gas Chromatography-Mass-spectrometry (GC/MS) set-up (Perkin Elmer, TurboMass, UK) using a 30 m x 250  $\mu\text{m}$ , 0.25 mm I.D., ZB-5 capillary column (Phenomenex, UK). Helium gas was used to carry the sample at a flow-rate of 1  $\text{mL min}^{-1}$  at 200  $^\circ\text{C}$ . After injection of 10  $\mu\text{L}$  of the sample at 200  $^\circ\text{C}$ , the temperature of the GC oven was raised by 10  $^\circ\text{C min}^{-1}$  to 350  $^\circ\text{C}$  and held for 3 min.

Surface Area Analyser and Porosimeter (Quantachrome, UK) was used for the measurement of the surface area of bulk microparticles (MIP and RDP). The size of the nanoparticles was analysed using a Zetasizer Nano (Nano-S) from Malvern Instruments Ltd (Malvern, UK) in a glass cuvette at 25  $^\circ\text{C}$ .

UHPLC/DAD/MS was used for analysing the samples of  $\alpha$ -tocopherol in the experiment of incubation with MIP NPs. It consists of UHPLC (Waters Acquity UPLC), UV detector (DAD) (Waters PDA  $e\lambda$  detector), MA (Waters Xevo G2XS QToF), (+ESI)

ionisation and C18 column, 1.7 $\mu$ m, 2.1 mm  $\times$  50 mm (Waters UPLC BEH) with solvent system 100% acetonitrile for 2 min run and 1  $\mu$ L injection of the sample.

### **5.2.3 Synthesis of the microparticles of bulk polymer (RDPs and MIP)**

The bulk polymers RDP and MIP were prepared using the same monomeric composition that was mentioned in the second chapter for synthesis of the RDP. The synthesis of the polymer has started with the molecular modelling that has been presented in the second chapter as well. Then, synthesis of MIP involved adding  $\alpha$ -tocopherol as a template in the polymerisation mixture, while it was not included in the synthesis RDP.

### **5.2.4 Preparation of the bulk MIP**

The bulk MIP was prepared based on the optimised formulation that was mentioned in the second chapter with some modification associated with the presence of the template in the case of MIPs as follows:

MIP was prepared using the free radical polymerisation to produce the polymers in a bulk form. The used ratio of monomer: cross-linker by mass was 1:9, then the addition of the template was 5% of the monomer mixture, which was included in the amount of the cross-linker as follows: the polymer was prepared by weighing all the components of polymerisation mixture. Firstly, 1 g of MAA (10%) and 0.5 gm of  $\alpha$ -tocopherol with 8.5 g of EGDMA (90%) were dissolved in an equal weight of dimethylformamide (10 g), then, 0.1 g of the initiator 1,1' azobis (cyclohexane carbonitrile) was added. All the components were dissolved using an ultrasonic bath for 5 min. Then, the monomeric mixture was deoxygenated by purging it with the nitrogen for 10 min. The vial with the monomeric mixture was tightly closed with cap, additionally secured using parafilm and thermo-polymerised at 80  $^{\circ}$ C for 24 h. After 24 hours, the polymer was removed from the vial and ground using electrical mortar. The resulting particles were sieved and the polymer fraction with a size between 63 to 125  $\mu$ m was collected. The prepared polymer fraction was washed for 36 hours using Soxhlet extraction with methanol: acetic acid (9:1 v/v). The MIP was further washed with methanol in order to remove the remaining acetic acid. Then, the polymer was dried in the oven at 70  $^{\circ}$ C. To test the complete wash of MIP and removal of  $\alpha$ -tocopherol from imprinted cavities, the polymer was packed in SPE cartridges and eluted with the solvent (ethanol containing 5% acetic acid). No  $\alpha$ -

tocopherol was detected in the elution sample that was analysed using the UV-Vis spectrophotometer. All experiments were repeated three times.

### **5.2.5 Characterisation of the MIP particles**

#### **Surface area**

As it was done with RDP, the surface area of MIP was measured using the multi-point Brunauer, Emmett and Teller (BET) method using the Surface Area and Pore Volume Analyser (Quantachrome, UK).<sup>8,20</sup> The total pore volume and average pore diameter were evaluated using the 45-point isotherm curve.

### **5.2.6 Recognition of MIP towards $\alpha$ -tocopherol**

Three different amounts of MIP (50, 100, 500 mg) were incubated in 2 mL of 2 mg mL<sup>-1</sup> of  $\alpha$ -tocopherol in heptane for 4 hours. Then,  $\alpha$ -tocopherol analytes were filtered and dried under nitrogen, then, dissolved in hexane before measuring the unbounded  $\alpha$ -tocopherol. Then, the concentration of  $\alpha$ -tocopherol was measured by using UV spectroscopy and compared to the calibration curve of  $\alpha$ -tocopherol in hexane to measure to the concentration of adsorbed  $\alpha$ -tocopherol was calculate as follows:

$$\begin{aligned} [\text{bound } \alpha\text{-tocopherol}] &= [\text{Initial concentration of } \alpha\text{-tocopherol}] - [\text{unbound } \alpha\text{-} \\ \text{tocopherol}] & \text{ Adsorption \%} = ([\text{bound } \alpha\text{-tocopherol}] / [\text{Initial concentration of } \alpha\text{-} \\ \text{tocopherol}]) \times 100 \end{aligned}$$

### **5.2.7 Comparison between the microparticles MIP and RDP**

This comparison between the performance of the two polymers was made by comparing the loading capacity and the recovery from each of them. The loading capacity was measured by weighing 100 mg from each of RDP and MIP and transferring them to 3 different vials for each polymer including 1 mL of three different concentrations: 1, 2, 3 mg mL<sup>-1</sup>. After 4 hours, the polymers were filtered. The filtrates were dried under nitrogen and dissolved in hexane to quantify the unbounded  $\alpha$ -tocopherol using GC/MS, then, the loading capacity was calculated as follows:

Loading capacity= [bound template (mg)]/weight of the polymer (g)

After filtering from the incubation solution, recovery of  $\alpha$ -tocopherol was quantified by filtering the solution and placing the polymer into 3mL of methanol containing 5% acetic acid. The eluted solution was then filtered and evaporated to the dryness. The obtained residues were solvated in hexane and analysed using GC/MS. The recovery of the eluted  $\alpha$ -tocopherol was calculated as follows:

Recovery % = ([eluted analyte]/ [ bound template]) $\times$ 100

### **5.2.8 Application of the optimised SPE protocol to sunflower oil solution to MIP**

The same solvent system of the SPE process to extract the minor components from vegetable oils which was described in the second chapters was applied here to examine the difference in the performance of MIP and RDP towards 20% sunflower oil in heptane. 100 mg of MIP and RDP were incubated in 2 vials, each of them contained 1 mL of 20% of sunflower oil in heptane. Then, each millilitre was filtered through the polymer and filtrates were collected, evaporated and dissolved in hexane to be analysed with GC/MS. The experiment was repeated three times.

### **5.2.9 Exploration the Selectivity and capacity of MIP NPs**

#### **Synthesis of MIP NPs**

The synthesis of MIP NPs was performed based on the protocol developed by Leicester Biotechnology Group.<sup>21</sup> The protocol consisted of three parts: (1) the preparation of the glass beads (GB) as a solid phase with an immobilised template ( $\alpha$ -tocopherol); (2) the synthesis of molecularly imprinted polymer nanoparticles (MIP NPs); (3) the purification and characterisation of the MIP NPs.

#### **5.2.9.1 Functionalisation of the glass beads (GB)**

Starting with the glass beads with diameters between 70 to 100  $\mu$ m (Potters, Spherglass A glass) that were activated and modified to have an epoxy group on their surface as a preamble to immobilise the template on them. 500 g of glass beads (75-100  $\mu$ m) were placed in a flask with an aqueous of sodium hydroxide solution (4 M) and boiled for 15 mins. Solution was kept 2 cm above the solids. Then, the glass beads were washed with deionised water 3 times. After washing the glass beads, they were incubated in a

solution of 50% H<sub>2</sub>SO<sub>4</sub> for (60 min). Subsequently, the glass beads were washed again 3 times with deionised water. Further, PBS was used for washing and neutralisation, and then the beads were washed three times with deionised water to remove the potential salt residues. pH of the beads solution was tested to ensure that the base has been completely removed (pH 6 –7). Next, rinsed the glass beads with acetone (twice with 200 mL) and dried it at 80 °C for 3 h.

### 5.2.9.2 Silanisation of the glass beads

The template in this polymerisation was  $\alpha$ -tocopherol. The functional group as is shown in Figure (5.1. a) is the hydroxyl group linked to the unsaturated ring, therefore,  $\alpha$ -tocopherol was classified as a template bearing –OH group which could be covalently coupled to the solid phase. In this case the glass beads were activated and modified to have epoxy groups on their surface. It is known that the epoxy groups under basic catalysis are attacked by hydroxide or alkoxide to the least sterically hindered epoxide carbon in an S<sub>N</sub>2 displacement (Figure 5.1, b).

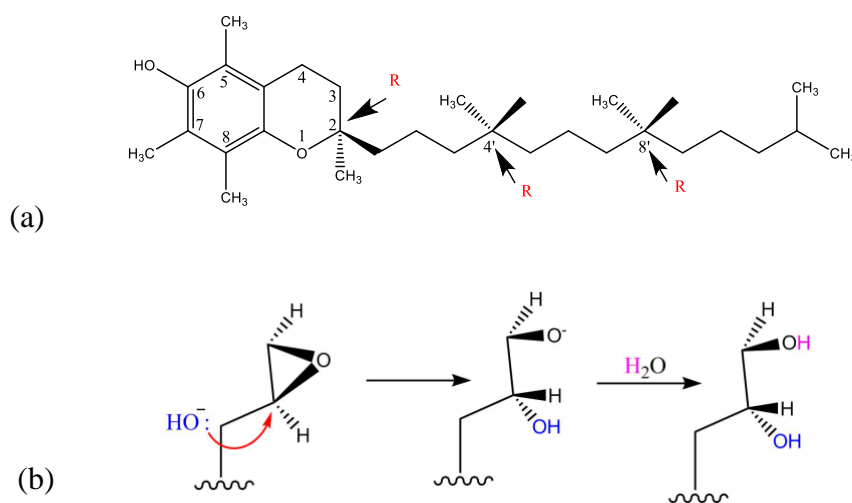


Figure 5.1: The chemical structure of  $\alpha$ -tocopherol (a), the mechanism for breaking the epoxy ring under basic conditions (b).

The addition of the epoxy group to the glass beads was executed by placing the 500 g of activated glass beads from the previous step in a flask containing 3% (v/v) (6 mL) solution of (3-glycidyloxypropyl-trimethoxysilane) (GOPTS) (Figure 5.2) in dry toluene with 400 mg of EIPA as a catalyst. Then, the glass beads were heated at 70°C for 10 hours. Afterward, the glass beads were washed with acetone 6 times and then, dried at 70°C in a sieve for 30 min.

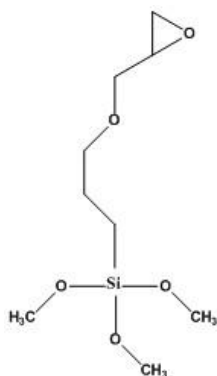


Figure 5.2: Chemical structure of GOPTS used in the immobilisation.

### 5.2.9.3 Immobilisation of $\alpha$ -tocopherol on the surface of the glass beads

38 g of modified glass beads with epoxy groups were weighed and added to 30 mL of  $2 \text{ mg mL}^{-1}$  of  $\alpha$ -tocopherol in acetonitrile. Then, the base catalyst DIPEA (N-ethyl-diisopropylamine) was added by weight (60 mg) to make 1 M. The mixture was incubated in the shaker overnight at  $40^\circ\text{C}$  for 150 rpm. The immobilisation was stopped the next day by blocking the rest of epoxy groups by adding 1 M of 2-amino methanol (by weight 18.5 mg). After one hour, the glass beads were filtered and washed using 1 L of acetonitrile at room temperature. The glass beads on the sintered glass filter were dried using vacuum pump, and then stored at  $4^\circ\text{C}$  until use.

### 5.2.9.4 Salinisation the iron oxide nanoparticles

Iron particles were added to the polymer mixture to give the magnetic properties to the nanoparticles which simplified the separation process using the magnet. The iron particles were salinised to be more capable to participate in the polymerisation process. The salinisation of the iron nanoparticles was performed by placing 1 g of iron oxide particles in 45 mL of dry toluene and adding 5 mL of 3-(trimethoxysilyl)propyl methacrylate in a glass bottle. This mixture was sonicated for 10 min (stopped sonication every 2 mins and washed the glass bottle from outside with cold water to avoid increase the temperature to prevent the polymerisation of the double bond. Next, the mixture was left on the shaker overnight. The iron NPs were washed 10 times using fresh toluene on the next following day. The particles were flushed with nitrogen for 20 min to evaporate toluene and stored at room temperature.

### 5.2.9.5 Solid-phase synthesis of MIP NPs in organic solvent

To prepare the polymerisation mixture 0.50 g of PETMP (chain transfer agent), 0.75 g of iniferter, 3.44 g of MAA (0.40 mmol), 0.40 g of EGDMA and 0.40 g of TRIM (0.10 mmol) were weighed in a glass bottle. 5 g of acetonitrile was added to this mixture, and all of these components were mixed by shaking the bottle vigorously. Subsequently, 100 mg of the silanised iron particles from step 5.2.9.4 were added to the mixture and sonicated for 3 min. This mixture was deoxygenated by purging with a stream of N<sub>2</sub> (Figure 5.3, a). Afterwards, 38 g of  $\alpha$ -tocopherol-derivatised glass beads were weighed in a 200-ml flat-bottomed glass container and deoxygenated with a continuous stream of N<sub>2</sub>. Next, the polymerisation mixture was added to the solid phase (Figure 5.3, b). Then, the flat glass container containing solid phase and monomeric mixture was placed between two UV-lamps (Philips HB/171/A, each with 4  $\times$  15 W tubes, one above and one below) for 90 s (Fig. 5.3, c).

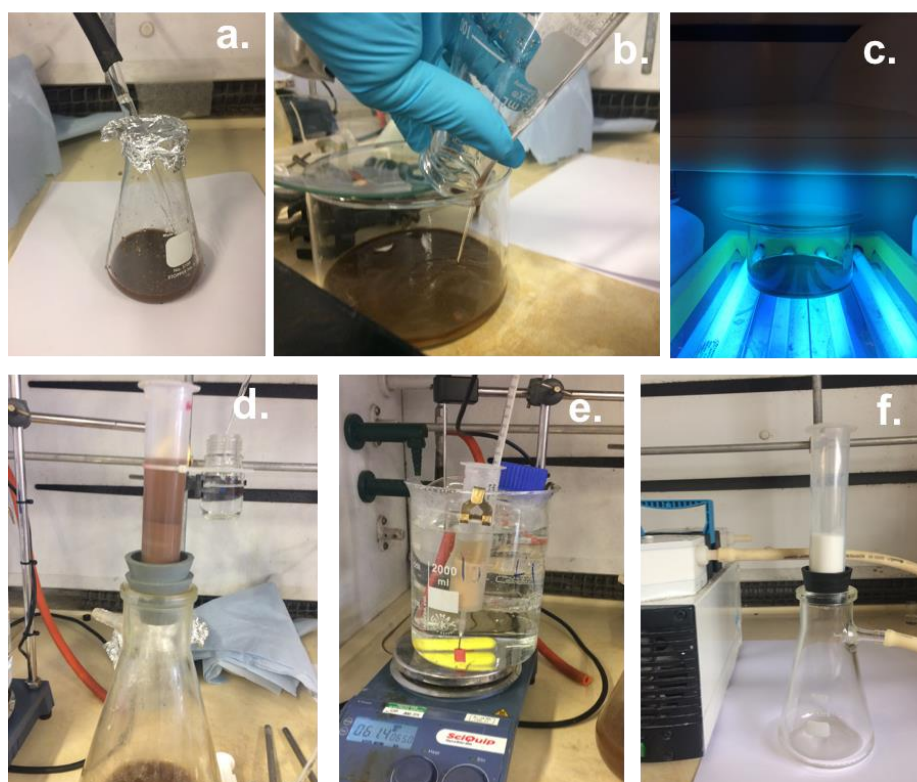


Figure 5.3: The steps of solid phase synthesis (deoxygenate the polymerisation mixture by purging with a stream of N<sub>2</sub> (a), addition of the polymerisation mixture to the solid phase (b), UV polymerisation (c), cooled washing (d), hot washing (e) and colour of glass beads after last hot wash (f).

### **5.2.9.6 The elution of MIP NPs**

To collect the MIP NPs the content of the flat glass container after UV polymerisation was transferred into a 10 mL SPE cartridge blocked with polyethylene frit (Figure 5.3, d). Then, the SPE cartridge was cooled in an ice bath at 0°C for 10 min. To remove the un-react monomers and low-affinity MIP NPs, cold acetonitrile at 4 °C was used for washing out the SPE content for 10 times. Next, the SPE cartridge was placed into a water bath at 60 °C. To monitor and maintain the temperature at 60 °C, a thermometer was placed inside the cartridge (Figure 5.3, e). To collect the nanoparticles, the SPE content was washed with pre-warmed acetonitrile at 60 °C until the glass beads turned white in colour (Figure 5.3, f). The acetonitrile from each wash was collected to finish up with 100 mL of acetonitrile that enclosed the high affinity nanoparticles. The solution was left at the room temperature to cool down and then, stored them in the fridge at 4°C.

In order to determine the yield of the MIP NPs, the solution of nanoparticles was reduced to 20 mL using magnet to collect the nanoparticles and remove the solvent. The yield and total MIP NPs concentration in the stock solution was calculated by transferring 1 mL of nanoparticles solution to the pre-weighed small vial. The vial weight was also measured after the complete evaporation of solvent and yield of MIP NPs was calculated by subtracting original weight of the vial.

## **5.2.10 Physical characterisation of magnetic nanoparticles (MIP NPs)**

### **5.2.10.1 Dynamic Light Scattering (DLS) size analysis**

The characterisations of MIP NPs which have been done in the current study were analysis of the nanoparticles by DLS to determine the average hydrodynamic diameter ( $d_h$ ) and the PDI of the MIP NPs. To evaluate the size of the synthesised MIP nanoparticles, Nano-S Zetasizer Particle Size Analyser (Malvern Instruments, UK) was used to measure the particle size as an average of the hydrodynamic diameter and the polydispersity index (PDI). These measurements were used as an indicator of the success of the synthesis.<sup>29</sup> DLS measures are based on the interaction between a laser source and the particles to be measured. The particles were in constant movements (Brownian motion) which was based on their size. The Brownian motion change by exposing the particles to laser light that in turn scattered by the nanoparticles. The result of this interaction is fluctuations in the

intensity of the scattered light. The DLS apparatus measures the timing of the fluctuations to define the rate of Brownian motion that was related to the diffusion coefficient (D).  $d_h$  (hydrodynamic diameter) can be calculated using the Stokes-Einstein equation:

$$d_h = kT / 3\pi\eta D$$

$k$  = Boltzmann's constant,  $\eta$  = viscosity,  $T$  = absolute temperature.

**Equation 5.1:** Stokes-Einstein equation.

DLS measurements were done at 25 °C in a glass cuvette (1 cm path length) for MIP NPs in acetonitrile. 1 mL of MIP NPs in acetonitrile was placed in a vial and sonicated for 2 min to remove any aggregations and the measurements under similar conditions were taken again. Then, the same measurements were repeated for MIP NPs with a dilution of 10 and 20 times. Further, the MIP NPs were transferred to the glass cuvette and analysed in the DLS. Six readings were averaged to obtain the measurements.

#### **5.2.10.2 Investigating the sorption property of MIP NPs**

In order to investigate the possibility of the produced MIP nanoparticles to rebind  $\alpha$ -tocopherol molecules, known amounts of these particles were incubated overnight in the different concentrations of  $\alpha$ -tocopherol solution. 0.5 mL of MIP NPs solution containing 1.3 mg of nanoparticles was placed in four different concentrations of a standard solution of  $\alpha$ -tocopherol in acetonitrile (40, 60, 80, 100  $\mu\text{g mL}^{-1}$ ). Subsequently, the incubated solutions were separated from MIP NPs using a magnet. Then, acetonitrile with 5% acetic acid was added and sonicated to disturb the intermolecular binding between  $\alpha$ -tocopherol and surface of the nanoparticles. After 30 mins, the eluting solution was collected using a magnet. This solution was evaporated and then, the residues were reconstituted in acetonitrile and analysed using UHPLC/MS/DRD. Each concentration was repeated two times and each measurement was repeated five times to take the average.

A calibration curve was made based on the range of  $\alpha$ -tocopherol concentrations that were used in the incubation. The concentrations of  $\alpha$ -tocopherol before and after incubation with MIP NPs were calculated using the calibration curve equation. Consequently, calculating the percentage of adsorbed  $\alpha$ -tocopherol.

### 5.3 Results and discussion

Vegetable oils are a rich source for valuable physiological-active compounds that have many benefits in the health and pharmaceutical industry. However, there are several obstacles make this type of research challenging.<sup>22,23</sup> Most of the physiologically-active compounds which are considered as minor components of oil (about 2%) belong to the polar fraction of vegetable oils. Besides the health importance of this fraction, it has been considered as an indicator of the quality of the oil measured by the international regulations. Therefore, there is a demand for improving a reliable method to separate and analyse the minor components from vegetable oils.  $\alpha$ -tocopherol is one of the minor components in vegetable oils that has been drawing researchers' attention. Several studies have been reported that analysed  $\alpha$ -tocopherol directly from oil solution without processing the oil through the chemical reactions such as saponification that reduced the yield of separated  $\alpha$ -tocopherol. For example, using SPE based on a silica cartridge, it was possible to extract 225 mg kg<sup>-1</sup> from olive oil.<sup>22</sup> Similarly, another report by Lechner, *et al.*, highlights that  $\alpha$ -tocopherol was extracted directly from the olive oil solution using a silica cartridge which yielded 200 mg kg<sup>-1</sup>.<sup>23</sup> However, these studies were conducted using relatively large amount of solvents or performing multistep pre-treatment of the oil sample before the SPE using silica gel sorbents.

As has been shown in Chapters 2 and 3 of this thesis,  $\alpha$ -tocopherol was extracted from vegetable oils using an optimised SPE protocol and a developed resin together with several minor components. For example, from olive oil  $\alpha$ -tocopherol was extracted at level 265 mg kg<sup>-1</sup> and this amount was maximised to 1.03 g kg<sup>-1</sup> by spiking the oil sample with (27 $\times$ 10<sup>-5</sup>) mg kg<sup>-1</sup>. In the previous work in this thesis, GC/MS was applied to analyse the samples, identify the extracted compounds and measure their quantities. Nevertheless, it became more challenging to use GC/MS to analyse the samples after extracting using MIP NPs. This directed the research to explore a more sensitive technique that was capable of detecting much smaller amounts of  $\alpha$ -tocopherol in the several experiments in this work. Fortunately, UHPLC/DAD/MA was available, and kindly the analysis of this part was conducted by Michael Lee within the Department of Chemistry.

### **5.3.1 Synthesis of microparticles MIP**

As mentioned above, MIP was synthesised using the optimised method in the second chapter with one modification. 5% of  $\alpha$ -tocopherol was added as a template which correspond the percentage of template optimised and the commonly used by imprinting community. Therefore, it was expected that the resulted polymer will have the specificity towards  $\alpha$ -tocopherol. Moreover, it was assumed that the quantity of  $\alpha$ -tocopherol extracted will be equal to 0.5 mg (the added amount of the template) or less, in contrast to RDP that extracted  $\alpha$ -tocopherol with other minor compounds with no restrictions to the added amount of the template.

#### **5.3.1.1 Characterisation of the MIP**

MIPs are synthesised by copolymerisation of functional monomers and cross-linkers in the presence of template molecules. The synthesis of the polymer underwent to grinding and sieving, and then, Soxhlet was applied with methanol: acetic acid (9:1) for 36 hours to wash the template molecule out of the polymer. After removal of the template molecules, cavities with specific recognition to  $\alpha$ -tocopherol were formed in the highly cross-linked polymer matrix. Therefore, the bulk polymer differed from the RDP in terms of the addition of the template ( $\alpha$ -tocopherol) in the polymer mixture.

To ensure that the template was completely washed out from the MIP, 30 mg of the polymer particles were placed in methanol with 5% acetic acid for 4 hours. Then, filtered the eluting solution, evaporated and dissolved the residue in hexane to analysis with UV-Vis spectrophotometer. No  $\alpha$ -tocopherol was detected as evidence for complete washing out of the template from the polymer particles.

#### **5.3.1.2 Rebinding of $\alpha$ -tocopherol towards the MIP**

The rebinding of  $\alpha$ -tocopherol towards the MIP was assessed by calculating the percentage of adsorbed  $\alpha$ -tocopherol on the polymer particles from the standard solution in heptane. In the beginning, 100 mg of MIP was packed in a 1 mL SPE cartridge to be used as RDP in the current research. However, under the same SPE conditions mentioned in the third chapter, MIP did not show sufficient binding of  $\alpha$ -tocopherol as it was assessed using GC/MS. This could be because that 100 mg of MIP was insufficient to extract  $\alpha$ -tocopherol that in the range of GC/MS detection range. Therefore, to keep the

research focused on the main goal, which is comparing the performance of RDP to MIP under the same optimum conditions that showed the best performance of RDP, this test was performed using different conditions. The comparison between the performance of RDP and MIP towards separating  $\alpha$ -tocopherol from its standard solution of heptane was made based on the published method in Lashini *et al.* as follows:<sup>24</sup> the different amounts of MIP particles were incubated in 1 mL of  $\alpha$ -tocopherol in heptane (the optimised loading solvent) as displayed in Table 5.1. After 4 hours, the polymer particles were filtered and the filtrate was evaporated to dryness. The unbound  $\alpha$ -tocopherol was dissolved in hexane and measure with GC/MS. The calibration curve of  $\alpha$ -tocopherol in hexane was plotted to calculate the percentage of adsorption.

Table 5.1: The percentage of adsorbed  $\alpha$ -tocopherol on MIP particles.

Concentration (mg mL <sup>-1</sup> )	Amount of MIP (mg)	Concentration of unbound $\alpha$ -tocopherol (mg ml <sup>-1</sup> )	Adsorption %
2	500	n.d*	100
2	100	0.8 ± 0.1	60
2	50	0.95 ± 0.07	52.5

\* n.d not detected

The percentages of adsorption indicated that MIP is capable to adsorb  $\alpha$ -tocopherol as no  $\alpha$ -tocopherol was detected after incubation with 500 mg of MIP. Further analysis was made to compare the performance of MIP to RDP in terms of the loading capacity and the specificity.

### 5.3.2 MIP vs. RDP

#### 5.3.2.1 Physical characteristic of polymers

The measurements of the surface areas and total pore size of microparticles of MIP and RDP are to investigate whether the different adsorption showed by the polymer particles of  $\alpha$ -tocopherol molecules were due to differences in the physical characteristics of the polymers' particles such the surface area and pore size, or because of the presence of template- specific cavities in MIP, which are not present in RDP. This procedure was performed by a defined amount of MIP or RDP (0.03–0.05 g), which was degassed at 100

°C for 2 hours before analysis to remove the adsorbed gases and moisture. Then, the polymer surface areas from multi-point N<sub>2</sub> adsorption isotherms were determined using the multi-point Brunauer, Emmett and Teller (BET) method by Surface Area and Pore Volume Analyser (Quantachrome, UK).

Table 5.2: The physical characteristics (surface area and pore size) of MIP and RDP particles.

polymer	Surface area (m <sup>2</sup> g <sup>-1</sup> )	Pore size (cm <sup>3</sup> g <sup>-1</sup> )
RDP	276	0.349
MIP	215	0.0487

Table 5.2 showed that MIPs and RDPs have different surface areas and different total pore volumes. However, the differences between the physical characteristics were still in the expected range and the differences were less than to be the cause of the difference in adsorption performance. This could be explained as the differences in the observed performance between MIPs and RDPs were due to the difference in the quantity of the specific binding sites. Golker *et al.* investigated the influence of the morphology of the polymer on its chromatographic properties.<sup>25</sup> It was concluded that there is no apparent relationship between morphology (surface areas, pore volumes) and template recognition. Additionally, it was found that a porous polymer structure was not necessary for effective chromatographic performance. Another study by Mahony *et al.* has confirmed the same findings, when the performance of the quercetin MIP was described having chromatographic behaviour that was independent of differences in surface area between the MIPs and the control polymers NIPs that were synthesised with the same compositions and under the same conditions with the absence of the template molecule.<sup>26</sup>

### 5.3.2.2 Loading capacity

The loading capacity of a certain polymer is defined as the amount of the template that is retained on 1 g of the polymer under given conditions<sup>27</sup>. It was possible to demonstrate the difference between the performance of the microparticles of the two bulk polymers - RDP and MIP by calculating the loading capacity of  $\alpha$ -tocopherol on RDP and MIP. The experiment was executed by incubating 100 mg of polymers separately with

three different concentrations of  $\alpha$ -tocopherol in heptane 1, 2, 3 mg mL<sup>-1</sup> for 4 hours. It was possible to measure the difference between the performance of the two polymers only in the case of 3 mg mL<sup>-1</sup> since in the case of 1 and 2 mg mL<sup>-1</sup> of  $\alpha$ -tocopherol solution RDP adsorbed  $\alpha$ -tocopherol completely thus only the last concentration (3 mg mL<sup>-1</sup>) was presented in Table 5.3. The experiments were conducted three times and the calculations were presented with the standard deviations. The presented results are based on three repetitions.

After 4 hours, the solution was filtered from the polymers and analysed by GC/MS to measure the difference between the concentration of  $\alpha$ -tocopherol before and after incubation and calculate the concentration using the integration of peaks and calibration curves. The peaks corresponding to  $\alpha$ -tocopherol before and after incubation in each polymer are shown in Figures 5.4.

Table 5.3: The loading capacity of MIP and RDP calculated from the recovery percentage of  $\alpha$ -tocopherol.

<b>Polymer</b>	<b>Unbound <math>\alpha</math>-tocopherol concentration (mg mL<sup>-1</sup>)</b>	<b>Bound <math>\alpha</math>-tocopherol concentration (mg mL<sup>-1</sup>)</b>	<b>Adsorption (%)</b>	<b>Loading capacity (mg g<sup>-1</sup>)</b>
RDP	0.7 ± 0.4	2.29 ± 0.46	77%	22.9
MIP	2.1 ± 0.08	0.84 ± 0.07	28%	8.4

Table 5.3 shows the results of this experiment. It was found that both polymers have shown an affinity towards  $\alpha$ -tocopherol. Nevertheless, there was a remarkable difference in the percentage of the adsorption which resulted in a considerable difference in the loading capacity between the two polymers, which could be illustrated based on the difference of the mechanism of adsorption of each polymer. In the case of RDP, the polymer performance relied on the abundance of functional groups on the surface of the polymer partials with formed hydrogen bonds with  $\alpha$ -tocopherol and separated it from the solution. On the other hand, it appears that MIP had only a limited number of the cavities with specific recognition towards  $\alpha$ -tocopherol which resulted in lower binding in comparison with RDP. Therefore, the amount of adsorbed  $\alpha$ -tocopherol was restricted to the available cavities on the polymers surface.

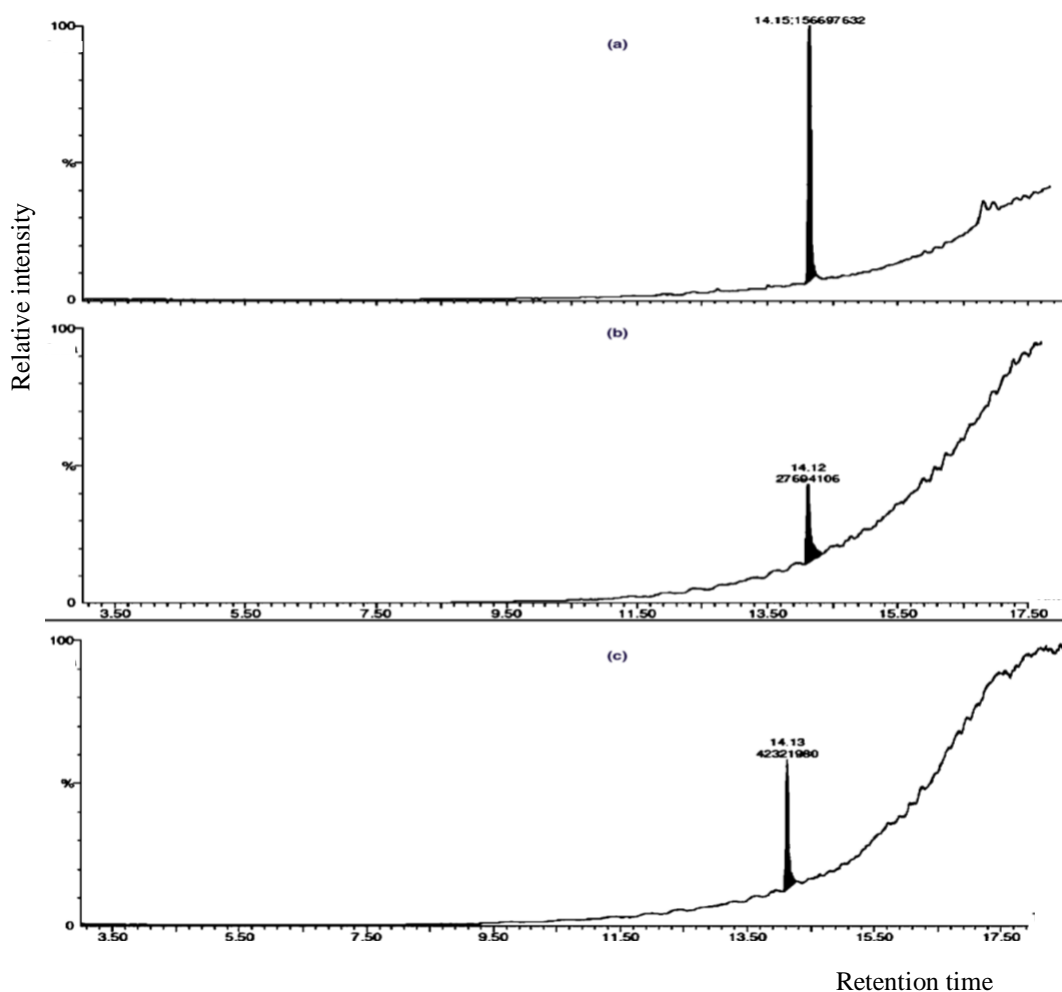


Figure 5.4: GC/MS chromatograms with the integration of the peaks.

$\alpha$ -tocopherol before incubation (a), after incubation with RDP (b) and after incubation with MIP particles (c).

### 5.3.2.3 Recovery of $\alpha$ -tocopherol

After the incubation in the previous experiment, the polymers were eluted using optimised eluting solutions (methanol with 5% acetic acid). The polymer particles were placed in the eluting solvent for 4 hours. Then the eluent solution was removed and evaporated. The residue was dissolved in hexane to be analysed with GC/MS. The concentrations were calculated using the integration of the peaks and then the concentration and finally the percentage of recovery was calculated using the calibration curves (Table 5.4). The experiment was repeated three times and then the standard deviation was calculated.

Table 5.4: The percentage of recovery  $\pm$  standard deviation from RDP and MIP.

Polymer	Recovery (%)
RDP	20.7 $\pm$ 1.2
MIP	0.8 $\pm$ 0.1

It is important to point out the difference in the percentage of recovery that demonstrated a superior performance of RDP over MIP under applied conditions. Elution using methanol acidified with 5% acetic acid resulted in the higher recovery of the adsorbed  $\alpha$ -tocopherol using RDP microparticles than MIP. MIP required more optimisation for the eluting solvent to increase the percentage of recovery. MIP has been approved in an enormous number of studies as selective adsorbent with high specificity to a wide range of compounds in various types of the sample matrixes as presented in the previous chapters. However, due to the cost implications MIPs are still limited to the analytical applications conducted on small scales only. On the other hand, RDP seems to be a promising sorbent because it is suitable to re-use, reducing of the cost of extraction process. In addition, it could be used on large scales with considerable efficiency in the applications that require harvesting a compound or a group of compounds possessing similar moieties.

#### 5.3.2.4 SPE from 20% sunflower using bulk MIP and RDP

The same protocol of measuring the rebinding of  $\alpha$ -tocopherol from heptane solution was used to compare the performance of RDP and MIP towards 20% of sunflower solution in heptane. 100 mg of MIP and RDP were placed overnight separately with 1 mL of 20% of sunflower solution in heptane. Then, the polymer particles were separated and the residues of oil samples were evaporated to dryness and reconstituted in 1 mL of hexane before being analysed with GC/MS.

Table 5.5: Concentration (mg mL<sup>-1</sup>) of the non-adsorption minor components to MIP and RDP after incubating overnight with 20% sunflower oil in heptane.

Minor components	Concentration of non-adsorption on RDP	Concentration of non-adsorption on MIP
Palmitic acid	0.147 ± 0.2	0.404 ± 0.03
Oleic and linoleic acids	0.206 ± 0.1	0.734 ± 0.2
α-tocopherol	0.184 ± 0.03	0.400 ± 0.02
Campesterol	0.358 ± 0.02	0.472 ± 0.1
Stigmasterol	0.179 ± 0.01	0.170 ± 0.04
β-sitosterol	0.189 ± 0.03	0.408 ± 0.2

As mentioned in the previous subtitle (5.3.2.3 recovery of α-tocopherol), 5% of acetic acid with methanol was not the best eluting solvent for MIP microparticles. Therefore, the difference of the performance of RDP and MIP towards the sunflower oil solution was measured through checking the difference of the concentration of the minor compounds after incubation with the two microparticles (figure 5.5). The concentrations of non-adsorption minor compounds were calculated using calibration curves of these compound, which were presented in the second chapter. The concentrations were presented in Table 5.5 as the average of triplicate with standard deviation.

These results indicated to the fact that the functional monomers located on the surface of the polymer were responsible about the binding to the minor components from the oil solution. The difference between performances of the two polymers existed due to the difference between the shape of the surface area of RDP's and MIP's. MIP has cavities that remained after removing α-tocopherol molecules in comparison with RDP that is covered with the functional groups which were desirable for the interactions with other minor components.

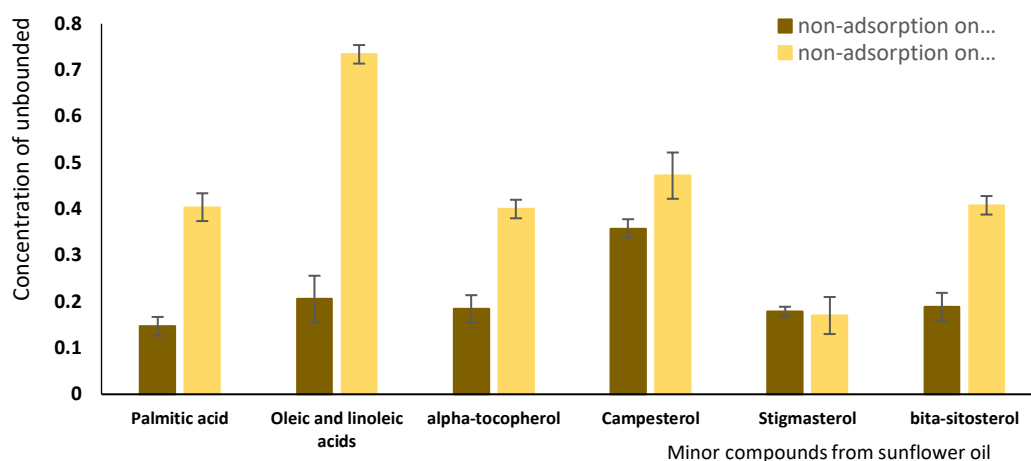


Figure 5.5: Statistical analysis of the concentrations of non-adsorption of the minor components to MIP and RDP particles after the incubation with 20% sunflower oil in heptane.

RDP has shown a higher loading capacity compared to bulk MIP, this could be due to the incomplete removal of the template from the MIP microparticles which resulted in a lower capacity. Other reason to consider that the rebinding of template by MIPs is limited by the number of binding sites generated during imprinting, typically created by up to 5% of template molecules used in the polymer preparation. Therefore, the resultant RDP microparticles are capable to perform the extraction depending on optionally larger concentration of the functional groups available on their surface without any limit to the amount of the template used in the synthesis steps. It is important to point out the selectivity of RDPs is expected to be much lower than observed in MIPs. However, RDPs are suitable for all types of pre-concentration, cleaning or separation tasks which benefit from group specificity and relatively low cost.

To complete the story of this thesis, it was necessary to explore the latest enhancement protocol to synthesis the molecularly imprinted polymer nanoparticles (MIP NPs) with recognition to  $\alpha$ -tocopherol that could be applicable in the analysis field.

### 5.3.3 Synthesis of MIP NPs

Recently, the extraction using MIPs in combination with magnetic particles (the core-shell technique) has considerably simplified sample handling and pre-treatment procedures.<sup>3,4,19</sup> This approach of imprinting has been based on the formation of a spherical core nanostructure presented as magnetic nanoparticles ( $\text{Fe}_3\text{O}_4$ ) followed by the

synthesis of MIP on these pre-formed nanostructures. The imprinting sites have situated either on the surface of the cores or on the shells of nanoparticles.<sup>4,19</sup>

The synthesis protocol as reported in Canfarotta *et al.* and Poma *et al.* has been started with the activation of the glass beads with diameters between 70 to 100  $\mu\text{m}$  by boiling with an aqueous 4 M of sodium hydroxide solution to allow the number of silanol groups (Si-OH) be formed on the surface to increasing the reactivity.<sup>21,28</sup> Subsequently, the activated glass beads were silanised with an epoxy silane 3-glycidoxypropyltrimethoxysilane (GOPTS) to link the glass beads to surfaces containing hydroxide groups (Figure 5.6). The remaining epoxy group subsequently reacted with 2-amino methanol.

Consequently, the template ( $\alpha$ -tocopherol) was covalently attached (immobilised) to the modified solid phase (glass beads). The reaction of the epoxide with a hydroxyl group of  $\alpha$ -tocopherol forms an ether bond linking between  $\alpha$ -tocopherol and the modified glass beads as shown in Figure 5.7. The aim of the post-polymerisation modification of the glass beads and the functionalisation process was to add an outer layer on the glass beads in order to manipulate their properties such as solubility or surface reactivity without affecting the binding sites of the polymerisation reactants.

The next stage was the formation of the polymer nanoparticles. The immobilised template on the surface of the solid phase participated to the shape of the cavities that have been formed during the polymerisation as follows: the polymerisation mixture including the functional monomers (MAA), cross-linkers (TRIM and EGDMA), silanised iron particles, iniferter and chain transfer agents were added to the glass beads that strongly attached to  $\alpha$ -tocopherol (template). The polymers particles were formed by photo-polymerisation (Figure 5.8).

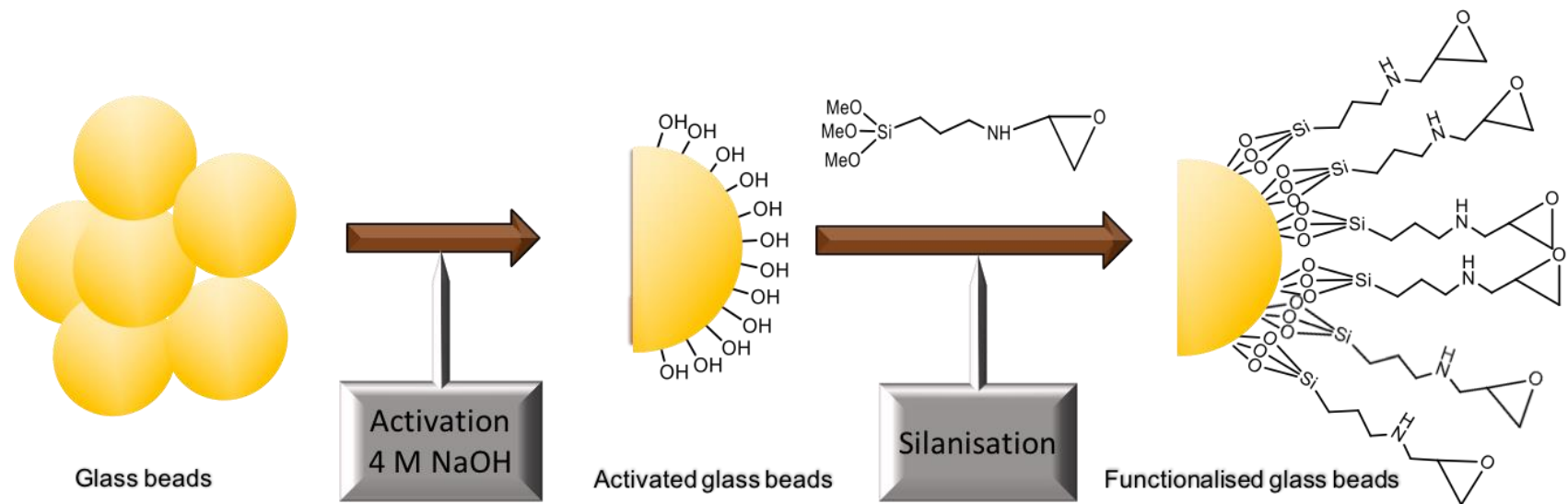


Figure 5.6: Salinisation with epoxy derivative for the activated glass beads.

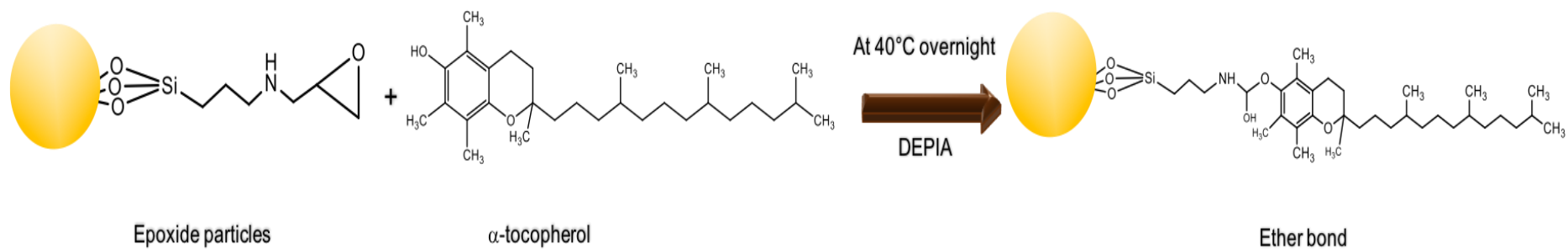


Figure 5.7: The immobilisation of  $\alpha$ -tocopherol on the modified glass beads.

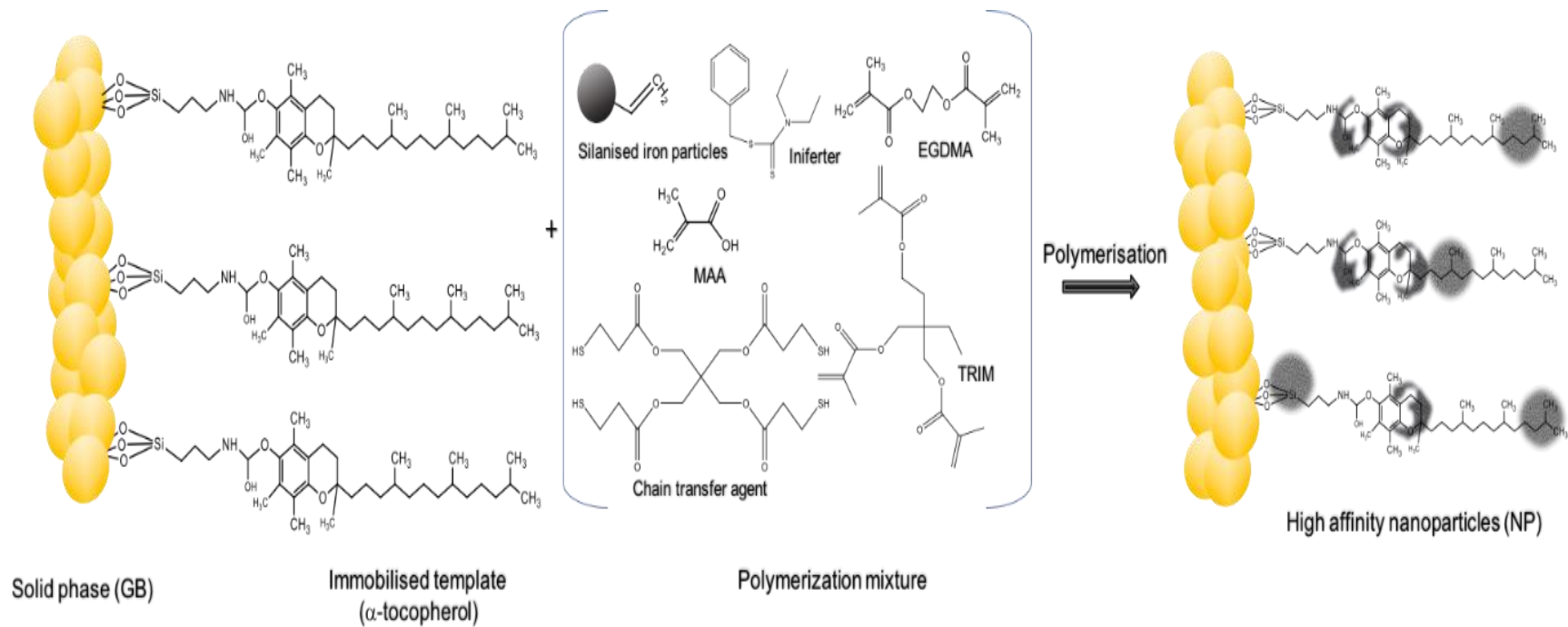


Figure 5.8: The polymerisation of magnet MIP NPs specific to  $\alpha$ -tocopherol.

Followed the above mentioned of polymerisation, the process in organic solvents has been recommended due to the advantage of imprinting of small molecules (MW<500 Da) in the organic solvents over the aqueous polymerisation.<sup>21</sup> Since the molecular weight of  $\alpha$ -tocopherol is 430 Da, acetonitrile was used as the solvent of the polymerisation. In addition, the use of methacrylic acid (MAA) as functional monomers has been commonly involved with the UV-triggered polymerisation in organic chemistry that successfully and non-covalently reacted with hydroxyl groups on  $\alpha$ -tocopherol. With regards to the cross-linkers, it has been recommended to combine two of them: trimethylolpropane trimethacrylate (TRIM) and ethylene glycol dimethacrylate (EGDMA), which resulted in increasing the recognition properties compared to using only one.<sup>19</sup> A radical initiator was recommended to be replaced by iniferter (benzyl diethyldithiocarbamate) due to the living nature of the process. The iniferter-based polymerisation yielded to a better control over the particle size, as the polymer chains grew at a more constant rate compared to non-controlled radical polymerizations (without iniferter). In addition, the presence of a small amount of chain transfer agent (e.g., alkyl thiols) also contributed to controlling the polymerization process.<sup>21</sup>

After the polymerisation of the low affinity nanoparticles, the unreacted monomers should have been separated from the MIP NPs before collecting them. The covalent bonds (ether bond) between  $\alpha$ -tocopherol and the epoxide groups that were formed in the template immobilisation step are strong enough not to be affected by washing with cold acetonitrile (4 °C) to remove unreacted monomers and low-affinity polymers, then, using hot acetonitrile (60 °C) to extracted only the high-affinity MIP NPs from the solid phase by breaking the non-covalent interaction between the formed polymer and the template to obtain MIP NPs as demonstrated by Figure 5.9.

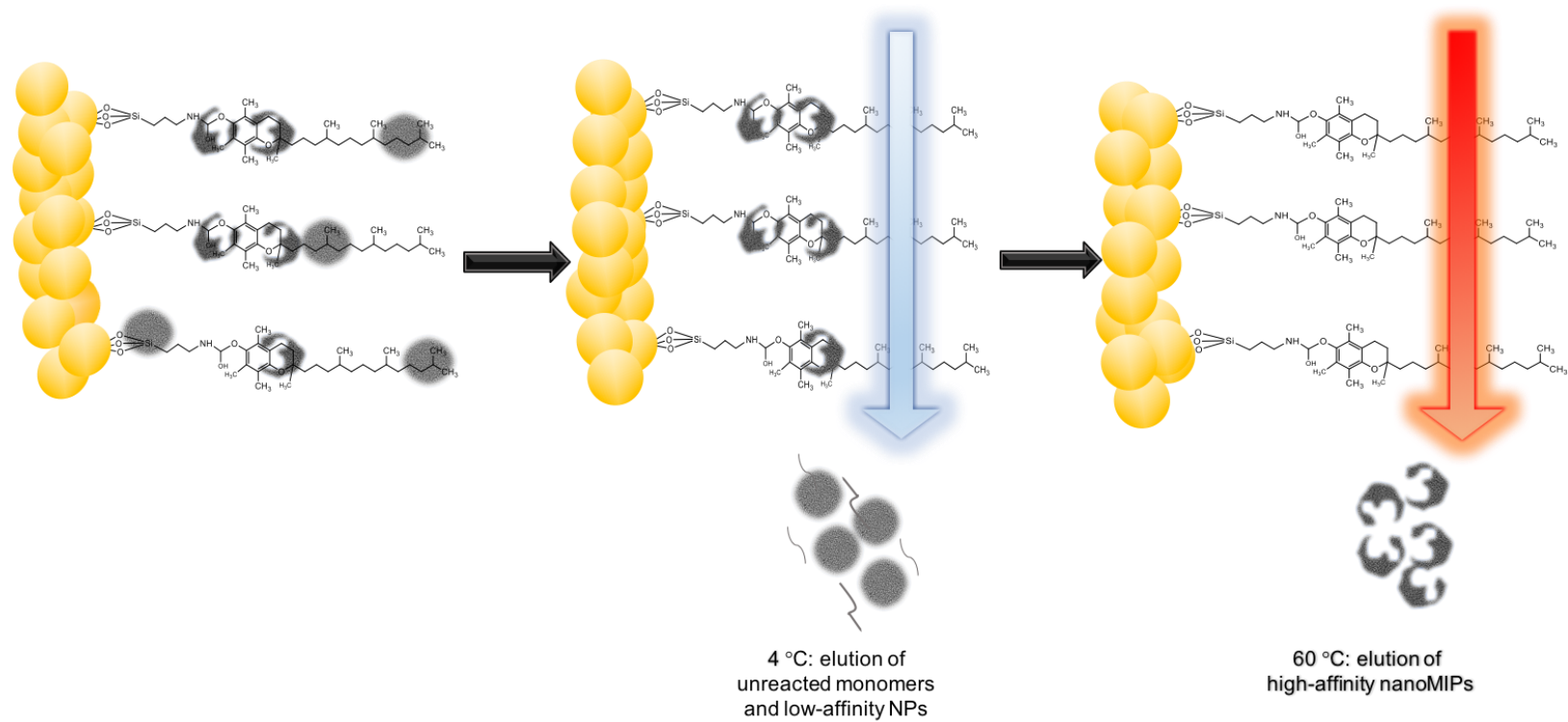


Figure 5.9: The process of collection of MIP NPs.

It was expected that because of the nature of the protocol, the binding sites will be generated in very small numbers (typically just one) per each nanoparticle. Thus, the yield of MIP NPs was lower than in other molecularly imprinted polymerisation approaches. The magnetic MIP NPs (Figure 5.10) were concentrated down to 20 mL using a magnet as demonstrated by Figure 5.11. The weight of the magnet MIP NPs was measured as 2 mL by evaporating the solvent under N<sub>2</sub> then, calculated of the total yield of the magnetic MIP NPs.



Figure 5.10: The image of the eluted MIP NPs obtained in one synthesis cycle.

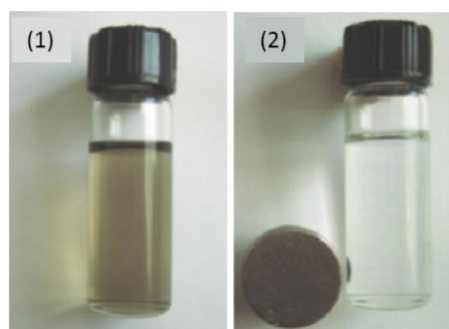


Figure 5.11: The method of separating magnetic MIP NPs from solution using the magnet.

Physical characteristics of MIP NPs have been done in the current study by analysis of the nanoparticles by DLS to determine the average hydrodynamic diameter ( $d_h$ ) and the PDI of the MIP NPs. PDI was used as an indicator to the heterogeneity of the particle sizes in the sample. Moreover, the PDI in the monodisperse sample tended to 0 value, and it is acceptable between the range from 0 to 0.7.

The results of these measurements were presented in Table 5.6 that showed the size distribution of the nanoparticles in different concentrations. As shown in Table 5.6, there were no significant differences in the average hydrodynamic diameter of the nanoparticles even with dilution. In addition, PDI measurements showed values between 0.21 and 0.24 which were within the acceptable range.

Table 5.6: The physical characterisations of MIP NPs.

Characteristics	5x concentrated	10x diluted	20x diluted
$d_h$ (nm)	$214 \pm 2$	$186 \pm 1$	$209 \pm 12$
PDI	$0.24 \pm 0.008$	$0.21 \pm 0.01$	$0.22 \pm 0.04$
MIP NPs ( $\text{mg mL}^{-1}$ )	2.6	-	-

Analysing the size distribution by intensity graphs as presented in Figure 5.12 showed that the size distribution was quite homogenous. Regarding the correlation curves (Figure 5.12), the extracted information from them was related to the concentration of the nanoparticles. The correlation coefficient had a value between 0.5 to 1.0 if measured shortly after the sonication. Moreover, the MIP NPs at the highest dilution (1:20) tended to aggregate as shown in the correlation curves (Figure 5.12, c), the correlation coefficient at high delay times arise from the baseline giving small fluctuations movements. This phenomenon occurred due to increasing the Brownian movements of the particles. All the physical measurements indicated the successful synthesis of MIP NPs.

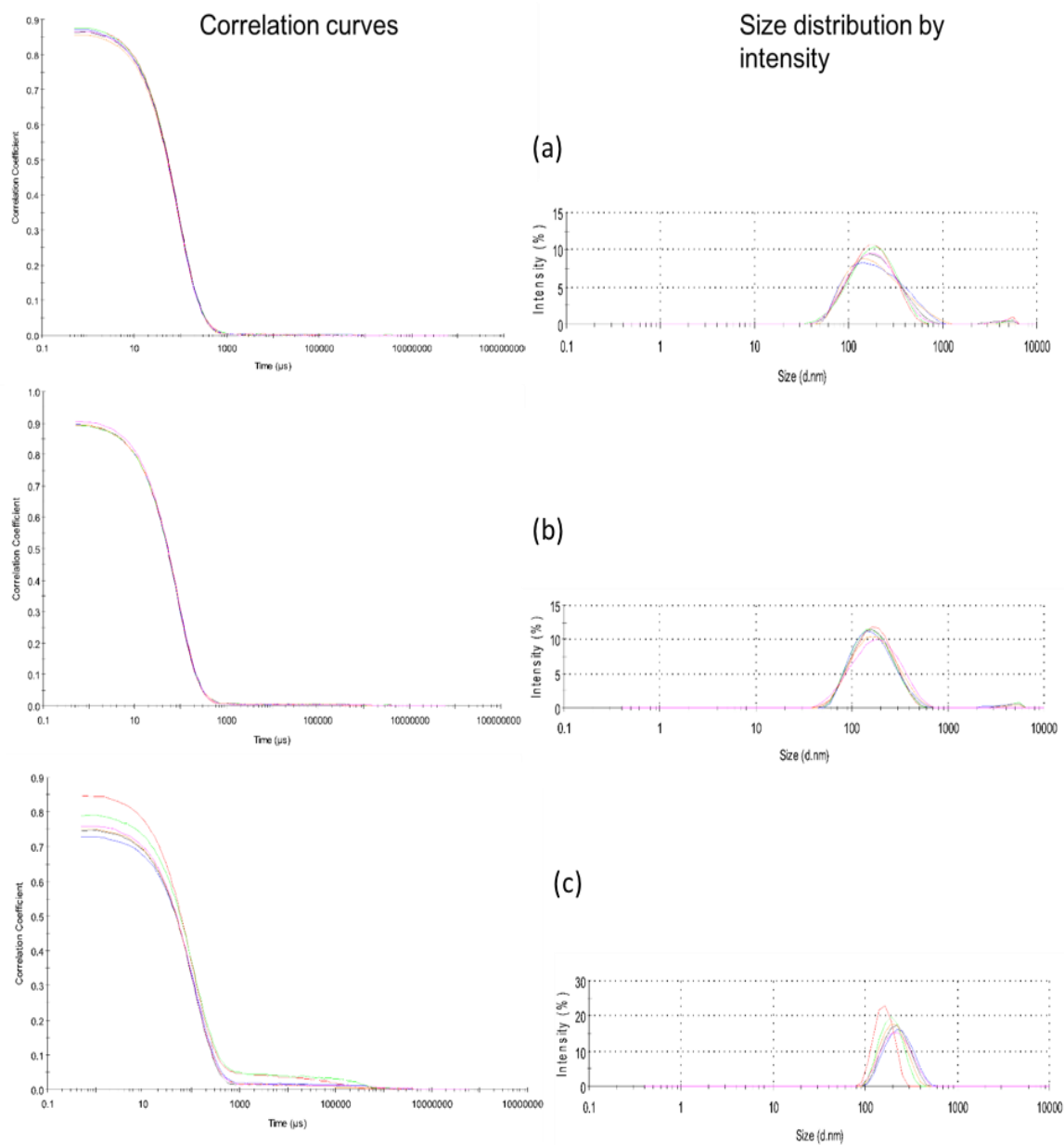


Figure 5.12: The DLS graphs for three different concentrations of MIP NPs solutions.

concentrated 5 times (a), 10x dilution (b), 20x dilution (c).

#### 5.3.4 The affinity properties of MIP NPs

To analyse  $\alpha$ -tocopherol binding and follow the change in its concentration in the next part of this research, it was important to find sensitive analytical method compatible with low concentrations of analysed samples and very small changes which happen after its binding with the nanoparticles. From the literature review, it was found that  $\alpha$ -tocopherol has been analysed with several sensitive techniques. According to Schwarts *et al.* the usual analysis of  $\alpha$ -tocopherol was performed using GC/MS, GC/FID and NP-HPLC.<sup>30</sup> However, these techniques required pre-treatment of the sample before conducting the analysis which differed depending on the nature of the sample. The researcher added that in the case of vegetable oils, it was possible to analyse  $\alpha$ -tocopherol from the low concentration of the vegetable oil directly because  $\alpha$ -tocopherol is presented mainly in the unconjugated form in these oils.

Other suggestion has been presented by several studies that recommended the reverse phase (RP) HPLC for analysis of  $\alpha$ -tocopherol, which is effective more than normal phase (NP).<sup>31-35</sup> By comparing the results of RP-HPLC and NP-HPLC, it was noticed that RP did not distinguish between  $\gamma$  and  $\beta$ -tocopherol which were not available in the vegetable oils or available at a very low levels according to literature.<sup>34</sup> This contributed to minimising the error of the quantification process. In addition, RP-HPLC has the advantage of short equilibrium and analysis time and high reproducibility of the retention time. On the other hand, NP-HPLC presented better separation for all isomers of  $\alpha$ -tocopherol, but during longer time and with more variable retention time.

The examination of the affinity of the synthesised nanoparticles towards  $\alpha$ -tocopherol was performed by incubation the same amount of MIP NPs solution in three different concentrations of the standard solution of  $\alpha$ -tocopherol in acetonitrile as demonstrated in figure 5.13.

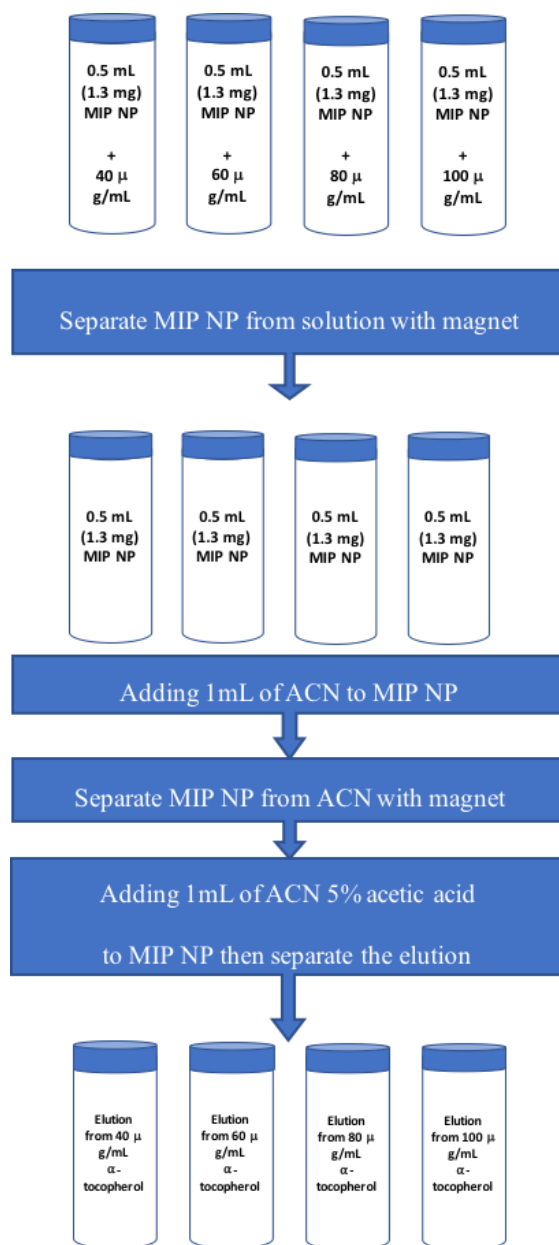


Figure 5.13: The steps of the optimised protocol of separation of  $\alpha$ -tocopherol by incubation with MIP NPs.

The analysis of  $\alpha$ -tocopherol samples before and after incubation and after elution was conducted using HPLC/ DAD / MS to measure the linked and eluted amount of  $\alpha$ -tocopherol from the nanoparticles.

Before measuring  $\alpha$ -tocopherol in the affinity experiment, it was necessary to plot a calibration curve for  $\alpha$ -tocopherol under the same conditions and using the same technique. Figure 5.14 shows calibration curve of the range of  $\alpha$ -tocopherol that including the concentrations have been incubated with MIP NPs.

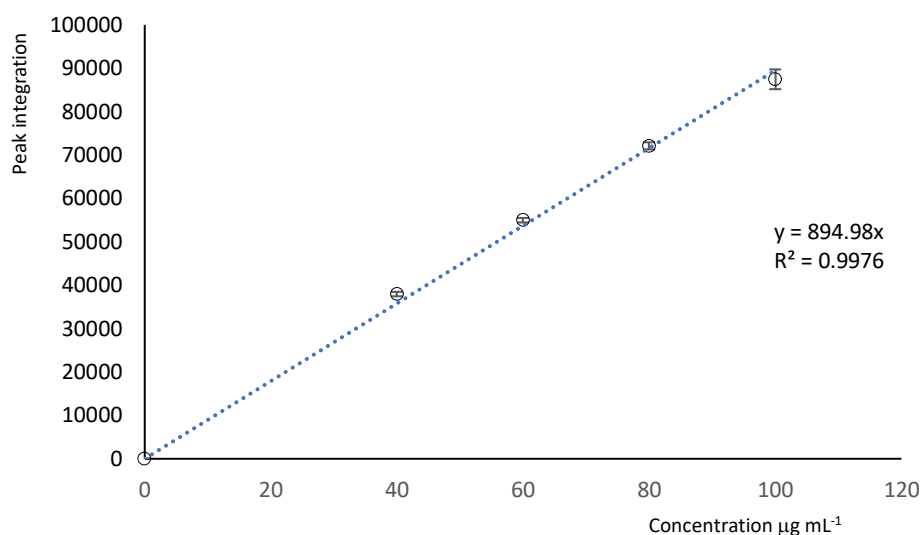


Figure 5.14: The calibration curve  $\alpha$ -tocopherol using UHPLC/DAD/MS.

The experiment of incubation has been repeated twice for each concentration and each sample was tested five times to present the average of them and the standard deviation of the duplicates as shown in Table 5.7. The results of this experiment calculated using the integration of the peak of  $\alpha$ -tocopherol before and after incubation. In addition, it was possible to use the calibration curve to calculate the bound  $\alpha$ -tocopherol to MIP NPs from the difference between the integrated peak values.

Table 5.7: The concentration and percentage of  $\alpha$ -tocopherol bound by the MIP NPs from different concentration of standard solution.

$\alpha$ -tocopherol, ( $\text{mg mL}^{-1}$ )	Unbound $\alpha$ -tocopherol ( $\mu\text{g mL}^{-1}$ )	% unbound $\alpha$ -tocopherol	% bound $\alpha$ -tocopherol
40	$32 \pm 1$	78.7	21.3
60	$43 \pm 0.5$	71.6	28.3
80	$57 \pm 0.9$	71.3	28.7
100	$71 \pm 0.2$	70	30

The next step was the elution of the adsorbed  $\alpha$ -tocopherol which was performed by washing the separated nanoparticles on the magnet by cold acetonitrile, then, placing these particles in acetonitrile containing 5% acetic acid for 20 min before separation and evaporating the solvents and reconstituted in acetonitrile to be analysed using UHPLC/DAD/MS. In the case of 40 and 60  $\mu\text{g mL}^{-1}$  nothing was detected in the eluted samples; however,  $\alpha$ -tocopherol concentration was measurable in 80 and 100  $\mu\text{g mL}^{-1}$  (Table 5.8).

Table 5.8: The concentration and percentage of eluted  $\alpha$ -tocopherol from the MIP NPs from different concentration of standard solution.

<b><math>\alpha</math>-tocopherol (<math>\text{mg mL}^{-1}</math>)</b>	<b>Eluted <math>\alpha</math>-tocopherol (<math>\mu\text{g mL}^{-1}</math>)</b>	<b>% eluted <math>\alpha</math>-tocopherol</b>
40	n.d	-
60	n.d	-
80	0.95	4%
100	1.75	6%

n.d (not detected)

## 5.4 Conclusion

Molecular imprinting technology has been attractive field to investigate owing to the specificity offered by this technology towards valuable compounds in various fields. However, different aspects of this research could be improved. Currently, the promising material is the nanoparticles that could be obtained by different methods of polymerisation. In the current research, different methods were followed to develop materials that have selectivity to the group of compounds and higher capacity. In this chapter, a comparison has been presented between the molecularly imprinted polymers (MIP) and the optimised RDP by applying the SPE protocol which was optimised in previous chapter (2) in this thesis. MIP has shown affinity towards  $\alpha$ -tocopherol, however, RDP extracted not only  $\alpha$ -tocopherol but also other compounds in higher concentration under the mild conditions of SPE. It seems that RDP has a distinguish features that make them suitable for the pre-concentration or fractionation of larger amount like in industrial sector.

On the other hand, this chapter describes the synthesis of magnetic MIP NPs performed accordingly to the recently developed method of solid phase synthesis of MIP NPs. The produced MIP NPs demonstrated affinity and specificity towards  $\alpha$ -tocopherol which allowed to separate it specifically from the complex mixture of other compounds purified using RDP developed in the frame of this project. However, due to the limited time of this studentship no further investigation of the synthesis and application of magnetic MIP NPs was made. In general, magnetic MIP NPs still need more development before being considered for purification application. It is possible to state that in existing state of development the magnetic MIP NPs, similarly to MIP microparticles, are more appropriate for the analytical purposes. The feasibility study which has been done in this research will open various investigations to be conducted in the future.

## References

- 1) Huiqi Z. Application of Controlled “Living” Radical Polymerization Techniques in Molecular Imprinting. In *Molecular Imprinting Principles and Applications of Micro-and Nanostructured Polymers*; Ye, L., Editor. **2013**; pp 105–160.
- 2) Alexander C.; Andersson S.; Andersson I.; Ansell J.; Kirsch N.; Nicholls A.; O’Mahony J.; Whitcombe J. Molecular Imprinting Science and Technology: A Survey of the Literature for the Years up to and Including 2003. *J. Mol. Recognit.* **2006**, *19*, 106–180.
- 3) Poma A.; Turner A.; Piletsky S. Advances in the Manufacture of MIP Nanoparticles. *Trends Biotechnol.* **2010**, *28*, 626–639.
- 4) Koesdjojo Y.; Tennico V.; Remcho T. 18 Molecularly Imprinted Polymers as Sorbents for Separations and Extraction/Separation Science Technology. *Sep. Sci. Technol.* **2007**, *8*, 479–503.
- 5) Cheong, H.; McNiven S.; Rachkov A.; Levi R.; Yano K.; Karube I. Testosterone Receptor Binding Mimic Constructed Using Molecular Imprinting. *Macromolecules* **1997**, *30*, 1317–1322.
- 6) Sajonz P.; Kele M.; Zhong G.; Sellergren B.; Guiochon G. Study of the Thermodynamics and Mass Transfer Kinetics of Two Enantiomers on a Polymeric Imprinted Stationary Phase. *J. Chromatogr. A* **1998**, *810*, 1–17.
- 7) Piletska E.; Burns R.; Terry L.; Piletsky S. Application of a Molecularly Imprinted Polymer for the Extraction of Kukoamine A from Potato Peels. *J. Agric. Food Chem.* **2012**, *60*, 95–99.
- 8) Piletsky S.; Piletska E.; Karim K.; Foster G.; Legge C.; Turner A. Custom Synthesis of Molecular Imprinted Polymers for Biotechnological Application: Preparation of a Polymer Selective for Tylosin. *Anal. Chim. Acta* **2004**, *504*, 123–130.
- 9) Piletsky S.; Karim K.; Piletska E.; Day C.; Freebairn K.; Legge C.; Turner A.; Recognition of Ephedrine Enantiomers by Molecularly Imprinted Polymers Designed Using a Computational Approach. *Analyst* **2001**, *126*, 1826–1830.

- 10) Tokonami S.; Shiigi H.; Nagaoka T. Micro- and Nanosized Molecularly Imprinted Polymers for High-Throughput Analytical Applications. *Anal. Chim. Acta* **2009**, *641*, 7–13.
- 11) Gao D.; Zhang Z.; Wu M.; Xie C.; Guan G.; Wang D. A Surface Functional Monomer-Directing Strategy for Highly Dense Imprinting of TNT at Surface of Silica Nanoparticles. *J Am. Chem. Soc* **2007**, *129*, 7859–7866.
- 12) Kempe M.; Mosbach K. Direct Resolution of Naproxen on a Non-Covalently Molecularly Imprinted Chiral Stationary Phase. *J. Chromatogr. A* **1994**, *2*, 276–279.
- 13) Remcho V.; Tan Z. MIPs as Chromatographic Stationary Phases for Molecular Recognition. *Anal. Chem.* **1999**, *71*, 248A-255A.
- 14) Mayes A.; Mosbach K. Molecularly Imprinted Polymer Beads: Suspension Polymerization Using a Liquid Perfluorocarbon as the Dispersing Phase. *Anal. Chem.* **1996**, *68*, 3769–3774.
- 15) Ye L.; Weiss R.; Mosbach K. Synthesis and Characterization of Molecularly Imprinted Microspheres. *Macromolecules* **2000**, *33*, 8239–8245.
- 16) Masci G.; Aulenta F.; Crescenzi V. Uniform-sized Clenbuterol Molecularly Imprinted Polymers Prepared with Methacrylic Acid or Acrylamide as an Interacting Monomer. *J. Appl. Polym. Sci.* **2002**, *83*, 2660–2668.
- 17) Sellergren B. Imprinted Dispersion Polymers: A New Class of Easily Accessible Affinity Stationary Phases. *J. Chromatogr. A* **1994**, *673*, 133–141.
- 18) Sellergren B.; Hall A. Synthetic Chemistry in Molecular Imprinting. In *Molecular Imprinting Principles and Applications of Micro-and Nanostructured Polymers*; **2013**; pp 25–70.
- 19) Wackerlig J.; Schirhagl R. Applications of Molecularly Imprinted Polymer Nanoparticles and Their Advances toward Industrial Use: A Review. *Anal. Chem.* **2016**, *88*, 250–261.
- 20) Mijangos I.; Navarro-Villoslada F.; Guerreiro A.; Piletska E.; Chianella I.; Karim K.; Turner A.; Piletsky S. Influence of Initiator and Different Polymerisation Conditions on

Performance of Molecularly Imprinted Polymers. *Biosens. Bioelectron.* **2006**, *22*, 381–387.

21) Canfarotta F.; Poma A.; Guerreiro A.; Piletsky S. Solid-Phase Synthesis of Molecularly Imprinted Nanoparticles. *Nat. Protoc.* **2016**, *11*, 443–455.

22) Grigoriadou D.; Androulaki A.; Psomiadou E.; Tsimidou M. Solid Phase Extraction in the Analysis of Squalene and Tocopherols in Olive Oil. *Food Chem.* **2007**, *105*, 675–680.

23) Lechner M.; Reiter B.; Lorbeer E. Determination of Tocopherols and Sterols in Vegetable Oils by Solid-Phase Extraction and Subsequent Capillary Gas Chromatographic Analysis. *J. Chromat A* **1999**, *857*, 231–238.

24) Lahsini R.; Louhaichi M.; Adhoum N.; Monser L. Preparation and Application of a Molecularly Imprinted Polymer for Determination of Glibenclamide Residues. *Acta Pharm.* **2013**, *63*, 265–275.

25) Golker K.; Karlsson B.; Wiklander J.; Rosengren A.; Nicholls I. Hydrogen Bond Diversity in the Pre-Polymerisation Stage Contributes to Morphology and MIP-Template Recognition – MAA versus MMA. *Eur. Polym. J.* **2015**, *66*, 558–568.

26) O’Mahony J.; Molinelli A.; Nolan K.; Smyth M.; Mizaikoff B. Anatomy of a Successful Imprint: Analysing the Recognition Mechanisms of a Molecularly Imprinted Polymer for Quercetin. *Biosens. Bioelectron.* **2006**, *21*, 1383–1392.

27) Lahsini R.; Louhaichi M.; Adhoum N.; Monser L. Preparation and application of a molecularly imprinted polymer for determination of glibenclamide residues. *Acta Pharm.* **2013**, *63*, 265-75.

28) Poma A.; Guerreiro A.; Whitcombe M.; Piletska E.; Turner A.; Piletsky S. Solid-Phase Synthesis of Molecularly Imprinted Polymer Nanoparticles with a Reusable Template–“Plastic Antibodies.” *Adv. Funct. Mater.* **2013**, *23*, 2821–2827.

29) Hansen S. DLSanalysis.Org: A Web Interface for Analysis of Dynamic Light Scattering Data. *Eur. Biophys. J.* **2018**, *47*, 179–184.

- 30) Schwartz H.; Ollilainen V.; Piironen V.; Lampi A. Tocopherol, Tocotrienol and Plant Sterol Contents of Vegetable Oils and Industrial Fats. *J. Food Compos. Anal.* **2008**, *21*, 152–161.
- 31) Cert A.; Moreda W.; Pérez-Camino M. Chromatographic Analysis of Minor Constituents in Vegetable Oils. *J. Chromatogr. A* **2000**, *881*, 131–148.
- 32) Andersson, L.; Paprica A.; Arvidsson T. A Highly Selective Solid Phase Extraction Sorbent for Pre-Concentration of Sameridine Made by Molecular Imprinting. *Chromatographia* **1997**, *46*, 57–62.
- 33) Victor R.; Watson R. *The Encyclopedia of Vitamin E*; CABI, 2007, UK
- 34) Grilo E.; Costa P.; Santos C.; Gurgel S.; Fernanda A.; Beserra D.; Niéce F.; Almeida D.; Dimenstein R. Alpha-Tocopherol and Gamma-Tocopherol Concentration in Vegetable Oils. *Food Sci. Technol.* **2014**, *34*, 379–385.
- 35) Aturki Z.; D’Orazio G.; Fanali S. Rapid Assay of Vitamin E in Vegetable Oils by Reversed-Phase Capillary Electrochromatography. *Electrophoresis* **2005**, *26*, 798–803.

# Chapter six

## Conclusions and future work

### 6.1 Conclusions

An effective protocol for the extraction and purification of seven minor compounds (free fatty acids,  $\alpha$ -tocopherol and three free phytosterols) from the six vegetable oils (sunflower oil, soy bean oil, sesame oil, wheat germ oil, palm oil and olive oil) using heptane without any pre-treatment for the oil samples was developed. It was shown that it was possible to harvest those physiologically-active components in their free forms as it was confirmed using GC/MS, despite the variability of the content of the minor components in each of these oils. The optimised SPE protocol was performed using the rationally designed polymer (RDP) which was capable of recognising  $\alpha$ -tocopherol and other minor components in vegetable oils.

The quantitative results of this study were comparable with published data that used various methods and techniques to extract these minor components from the vegetable oils. Application of the developed polymer was advantageous over traditional methods of extraction which included the possibility of a two-fold reduction in the volume of solvent required and ability to extract the physiologically active free forms of the compounds without saponification. The protocol of the extraction of a group of components involved only 5 times dilution of the vegetable oils with heptane which was twice improved by comparison with the 10-fold dilution applied in the industrial protocol, representing a reduction of waste and a saving in resources and time. It is important to highlight that the optimised protocols and proposed strategy could be used as blueprints for the development of extraction procedures for different groups of compounds from other natural oil-containing biomasses. Analysis of the matrix presence before and after purification using developed SPE protocol and RDP, suggested that the 98.6%-pure  $\alpha$ -tocopherol has been extracted. Moreover, a direct correlation was found between the quantitative results of this study and results published from different studies that employed various methods and techniques commonly used to extract these minor components from the same vegetable oils.

The optimised solid-phase extraction protocol was compared with the performance of several commercial adsorbents, particularly in relation to the retention properties and recovery of the minor components explored in this study. The comparison was performed

between six commercially available resins and RDP using optimised SPE protocol. It has shown the distinguished efficiency of RDP to extract the group of minor components from 20% sunflower oil in heptane with the minimum of organic solvents. Despite the possibility to extract some of the minor component using the other sorbents, they were not as effective as developed RDP.

Subsequently, in the purpose of presenting the similarity and difference between the traditional molecularly imprinted polymer (MIP) and the optimised RDP, the SPE protocol was also applied to MIP that was synthesised using similar components and under similar conditions as RDP. Even though developed MIP has shown affinity and specificity towards  $\alpha$ -tocopherol, RDP extracted not only  $\alpha$ -tocopherol but also other compounds in higher concentration under the mild conditions of SPE. The developed RDP has a superior capacity towards  $\alpha$ -tocopherol and other minor oil compounds including palmitic acid, oleic acid, linoleic acid, campesterol, stigmasterol and  $\beta$ -sitosterol, which make it capable to pre-concentrate or fractionate of the larger quantities of the compounds making it suitable for industrial application. 1140mg kg<sup>-1</sup> of palmitic acid, 7181 mg kg<sup>-1</sup> of oleic and linoleic acids, 298 mg kg<sup>-1</sup>  $\alpha$ -tocopherol 489 mg kg<sup>-1</sup> of campesterol, 307 mg kg<sup>-1</sup> of stigmasterol and 1903 mg kg<sup>-1</sup> of  $\beta$ -sitosterol have been extracted from wheat germ oil, 4 mg kg<sup>-1</sup> of palmitic acid, 88 mg kg<sup>-1</sup> of oleic and linoleic acids, 233 mg kg<sup>-1</sup>  $\alpha$ -tocopherol 251 mg kg<sup>-1</sup> of campesterol, 517 mg kg<sup>-1</sup> of stigmasterol and 1398 mg kg<sup>-1</sup> of  $\beta$ -sitosterol have been extracted from soy bean oil, 942 mg kg<sup>-1</sup> of palmitic acid, 16425 mg kg<sup>-1</sup> of oleic and linoleic acids, 277 mg kg<sup>-1</sup>  $\alpha$ -tocopherol 58 mg kg<sup>-1</sup> of campesterol, 146 mg kg<sup>-1</sup> of stigmasterol and 741 mg kg<sup>-1</sup> of  $\beta$ -sitosterol have been extracted from sunflower oil, 366 mg kg<sup>-1</sup> of palmitic acid, 2407 mg kg<sup>-1</sup> of oleic and linoleic acids, 3122 mg kg<sup>-1</sup> sesamin 317 mg kg<sup>-1</sup> of campesterol, 220 mg kg<sup>-1</sup> of stigmasterol and 2741 mg kg<sup>-1</sup> of  $\beta$ -sitosterol have been extracted from sesame oil, 15600 mg kg<sup>-1</sup> of palmitic acid, 34496 mg kg<sup>-1</sup> of oleic and linoleic acids, 148 mg kg<sup>-1</sup>  $\alpha$ -tocopherol 74 mg kg<sup>-1</sup> of campesterol, 125 mg kg<sup>-1</sup> of stigmasterol and 299 mg kg<sup>-1</sup> of  $\beta$ -sitosterol have been extracted from palm oil and 1190 mg kg<sup>-1</sup> of palmitic acid, 1325 mg kg<sup>-1</sup> of oleic and linoleic acids, 256 mg kg<sup>-1</sup>  $\alpha$ -tocopherol 75 mg kg<sup>-1</sup> of campesterol, 8 mg kg<sup>-1</sup> of stigmasterol and 760 mg kg<sup>-1</sup> of  $\beta$ -sitosterol have been extracted from olive oil.

The optimised SPE protocol in this study, in comparison to six commercially available resins, has shown significant efficiency to extract the group of minor components from 20% sunflower oil in heptane with minimum of organic solvents.

Moreover, to complete the framework of molecular imprinting theme of this project, the synthesis of magnetic MIP NPs using the recently developed method was performed. The MIP NPs have shown affinity towards  $\alpha$ -tocopherol which could be used to selectively extract it from the complex mixture eluted using developed SPE protocol.

## **6.2 Future work**

The work in this project has opened a wide field for future work on the synthesis of the customised polymers with group selectivity towards natural physiologically-active compounds present in vegetable oils which could have great applications in different fields.

To broaden the potential interest of commercial and industrial partners for this technology, it would be interesting to cover the following research topics in the future:

Application of the optimised extraction approach to explore the possibility to extract the tocopherols, fatty acids or phytosterols from the extraction of other parts from biomass.

Development of a fractionation protocol based on magnetic MIP NPs which could be applied to extract any particular compound from the complex mixture eluted using optimised RDP-based SPE protocol.

It was demonstrated already in this thesis that MIP NPs have shown an affinity towards  $\alpha$ -tocopherol, further investigation is needed to develop the extraction of  $\alpha$ -tocopherol from other parts of biomass such as extraction of leaves, seeds ... etc.

The application of protocol optimised in this study resulted in extraction of a significant amount from sesamin from sesame oil, which has a great biological activity. This could be a target for a new research as the literature has no studies related to sesamin purification using MIPs.

## Appendix 1

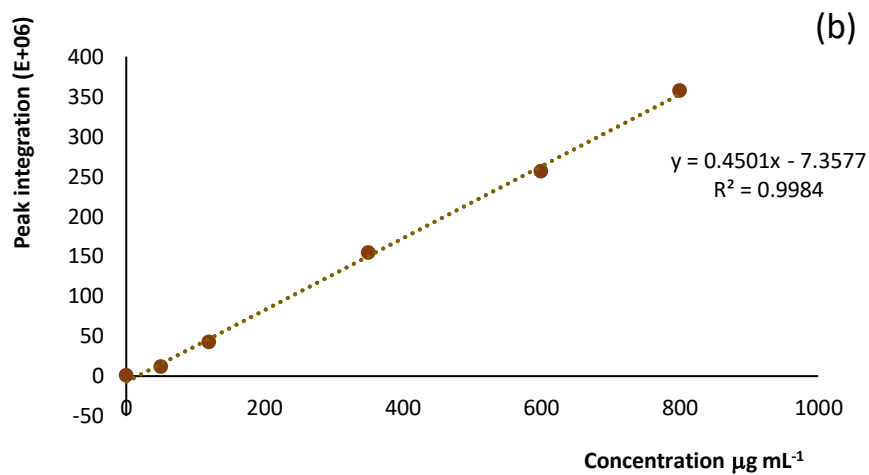
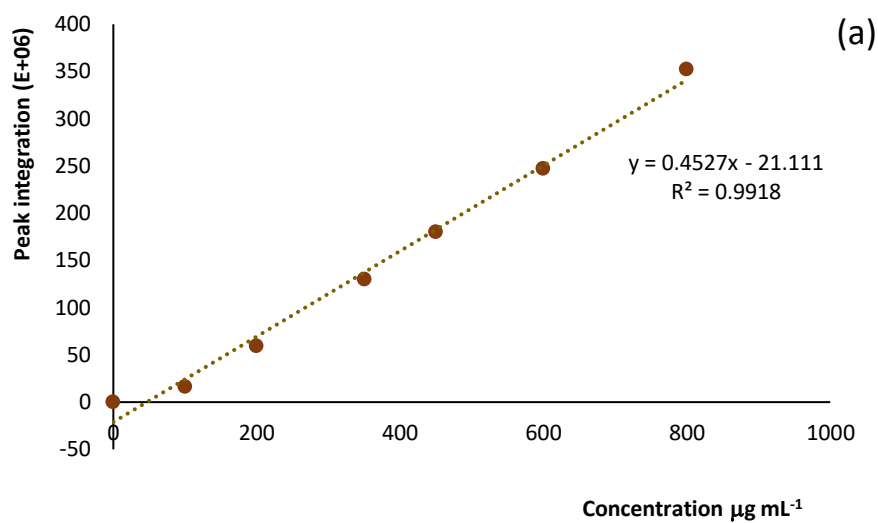
### The published papers:

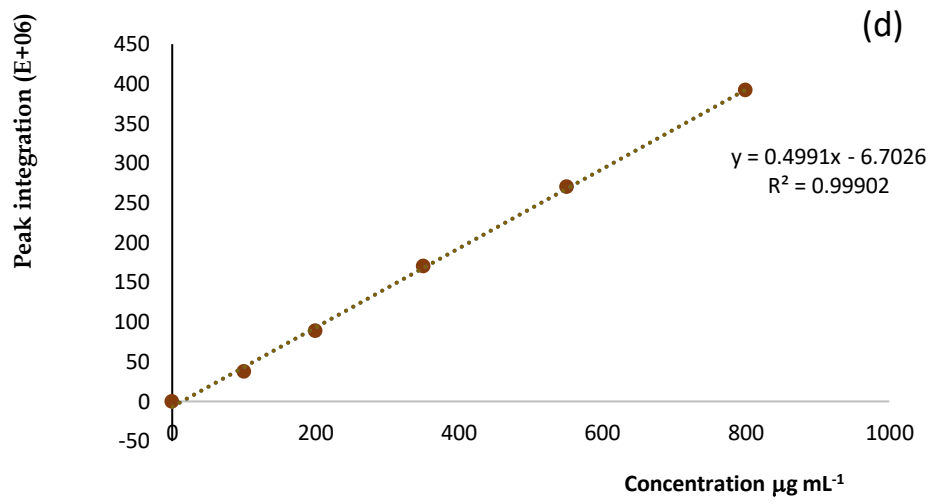
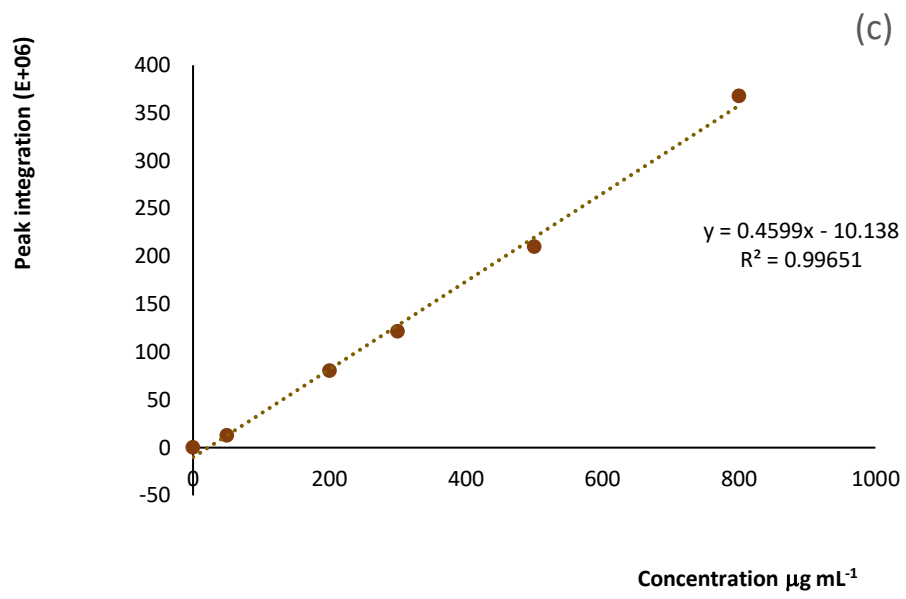
1- Alghamdi E.; Whitcombe M.; Piletsky S.; Piletska E. Solid phase extraction of  $\alpha$ -tocopherol and other physiologically active components from sunflower oil using rationally designed polymers. *Anal. Methods* 2018, 10, 1–8.

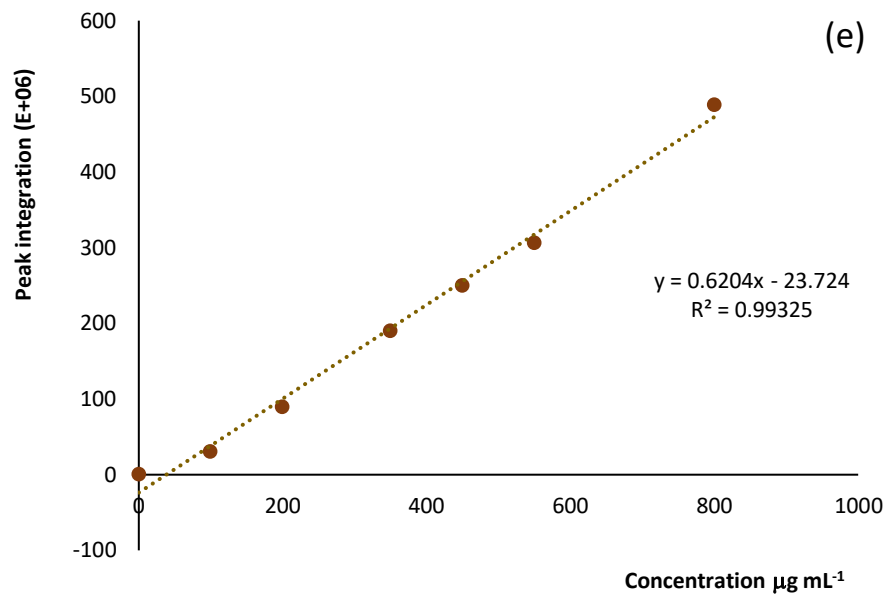
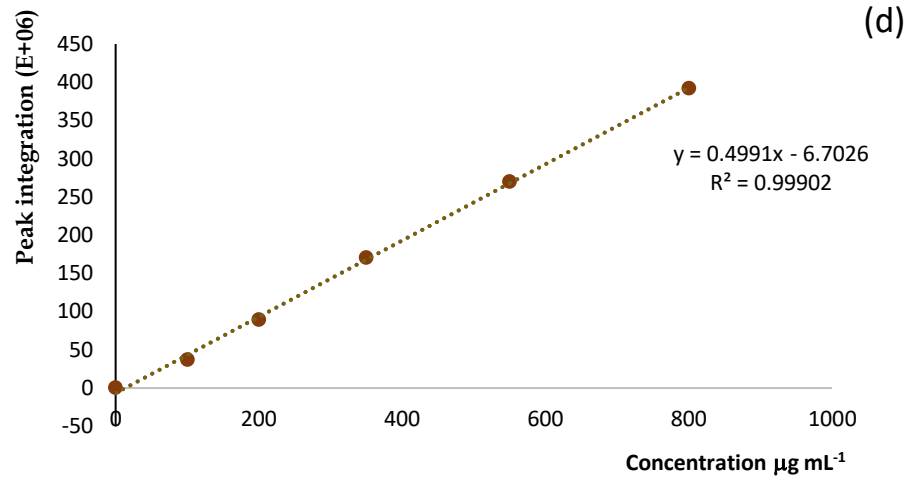
2) Alghamdi E.; Piletsky S.; Piletska E. Application of the bespoke solid-phase extraction protocol for extraction of physiologically-active compounds from vegetable oils. *Talanta* 2018, 189, 157–165.

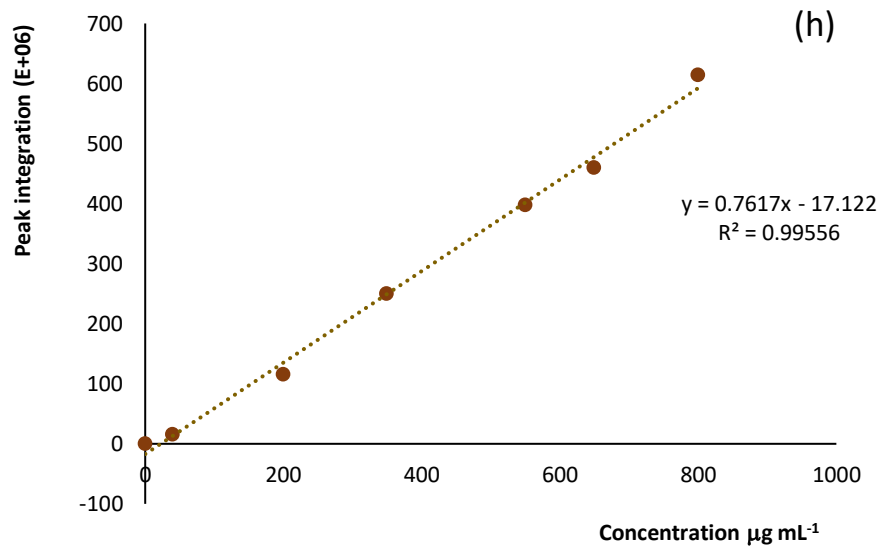
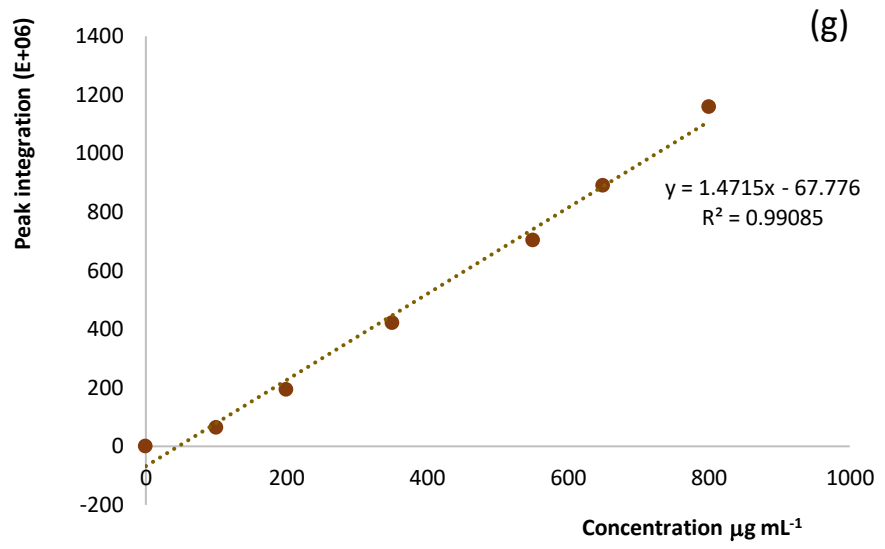
## Appendix 2

The calibration curves of the minor components: (a) palmitic acid, (b) oleic acid, (c) linoleic acid, (d)  $\alpha$ -tocopherol, (e) campesterol, (f) stigmasterol, (g)  $\beta$ -sitosterol, (h) sesamin









## Appendix 3

### **Surface area and total pore volume evaluated by BET theory**